Universität Bremen

Theoretical Aspects of Relativistic Geodesy

Dennis Philipp

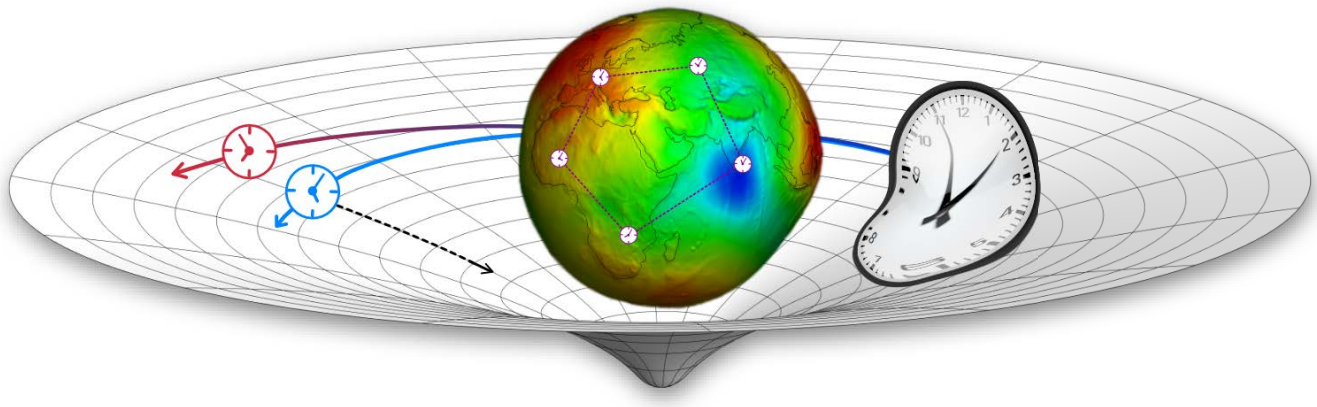

Universität Bremen

Theoretical Aspects of Relativistic Geodesy

Dem Fachbereich Physik und Elektrotechnik der Universität Bremen

zur Erlangung des akademischen Grades
Doktor der Naturwissenschaften (Dr. rer. nat.)
vorgelegte Dissertation

von

MSc. Dennis Philipp

1. Gutachter: Prof. Dr. Claus Lämmerzahl
2. Gutachter: Prof. Dr. Jürgen Müller

Eingereicht am: 12.11.2018
Tag des Kolloquiums: 20.12.2018

Bremen, 2018

"*In a dark place we find ourselves, and a little more knowledge lights our way.*"

Master Yoda

"*If I have seen further it is by standing on the shoulders of Giants.*"

Isaac Newton

Abstract

Theoretical Aspects of Relativistic Geodesy

by Dennis Philipp

In this thesis, I show how fundamental geodetic notions can be defined within a general relativistic framework. Among the concepts that are analyzed there are the relativistic gravity potential, the geoid, the normal gravity field and its potential, as well as the genuinely relativistic definition of chronometric height. Moreover, a simple procedure for the operational preservation of a chosen level surface of the relativistic gravity potential is investigated. For all these concepts, the respective Newtonian notions are recovered in the weak-field limit. In the first-order (parametrized) post-Newtonian expansion the results previously published in the literature are obtained and it is shown how they are embedded into the present framework. Magnitudes of leading-order relativistic corrections to the geoid as well as redshift and acceleration measurements are calculated in a simple gravity field model.

After the most important geodetic notions are introduced, the theory of General Relativity and the mathematical formalism are briefly discussed. Emphasis lies on some exact solutions to Einstein's vacuum field equation. These spacetimes are used in the following to either estimate relativistic effects or generalize geodetic concepts. Proceeding to a relativistic theory of gravity changes the underlying stage on which all physics takes place. The involved mathematical structure, related to the description of a curved spacetime, causes conventional geodetic notions to become ill-defined in the framework of General Relativity. Here, it is shown how relativistic generalizations of these notions can be constructed, working without any kind of weak-field approximation. The approach is mainly based on a so-called redshift potential of which the level sets foliate a stationary spacetime into isochronometric surfaces. It gives rise to the definition of a relativistic gravity potential which is used intensively. In particular, using a parametrized post-Newtonian spacetime for the Earth, the magnitude of relativistic corrections to the geoid is investigated in a simple Earth model. In the last part, the relation between proper time on the geoid and the defining constant L_g in the IAU resolutions is discussed and a consistent relativistic definition for chronometric heights is proposed. Finally, relativistic orbital effects are compared to non-gravitational perturbations of satellite orbits and relativistic gravity gradiometry is investigated to link geodesic deviation to the curvature of spacetime, which is determinable by geodetic measurements.

Acknowledgements

First of all, I want to express my deepest gratitude to my supervisor Claus Lämmerzahl. Without his continuous support, scientific guidance, and patience this thesis would not have been possible. Claus, never before have I met someone who dedicates his life to science in the way you do. Thank you for inspiring me and for guiding me on my way to become a scientist. I am proud to be your student and a member of your research group!

Moreover, the same is true for Volker Perlick, Eva Hackmann and Dirk Pützfeld. Without our insightful discussions and the knowledge you provided I would have been lost. I truly admire the way you teach and pursue science, and I enjoy working with you wholeheartedly.

A special thanks goes to Domenico Giulini and Vojtech Witzany for many enlightening discussions and insightful lunch breaks, and to Pavel Efremov as well as Kris Schroven for our many philosophical discussions way beyond physics. Also, I want to thank Sandro Gödtel for proof reading the manuscript and being a very cool office mate.

To all my collaborators and colleagues of the past years, especially to Florian Wöske, Benny Rievers, Meike List, Felix Finke, Sven Hermann, Enrico Mai, and Liliane Biskupek: Working with you was fun! I learned a lot about so many different things and I am grateful for your support, your ideas, the time we spent together, and I am proud of the work we have done. My sincere thanks also goes to all members of the CRC "geo-Q" and the RTG "models of gravity".

I am deeply indebted to my parents, Anne and Jörg, and my entire family who supported me unconditionally for all my life. None of this would have been possible without you! There are no adequate words to describe how grateful I am.

To Silja: your continuous support, encouragement, and love motivates and drives me to push myself to the limit. I don't know what I would do without you, and you make me the happiest physicist on Earth.

To Thomas, Katrin, Iris, Hartmut, and Bjarne: thank you so much for all the joy you bring into my life. Thomas, I am very glad to be your friend and mud-buddy.

The financial support provided by the DFG within the Collaborative Research Center 1128 "Relativistic Geodesy and Gravimetry with Quantum Sensors (geo-Q)", the Research Training Group 1620 "Models of Gravity" is gratefully acknowledged. Furthermore, I am thankful for hospitality and invited research stays at the UAM and UNAM in Mexico City, the University of Aveiro, and the Nikhef institute at the University of Amsterdam.

Contents

List of Figures

Physical and Geometrical Constants

Speed of light (exact)	$c = 2.997\,924\,58 \times 10^{8}\,\mathrm{m\,s^{-1}}$
Newton's gravitational constant	$G = 6.674\,08 \times 10^{-11}\,\mathrm{m^{3}\,kg^{-1}\,s^{-2}}$
WGS84 semi-major axis	$a_{\mathrm{WGS84}} = 6.378\,137 \times 10^{6}\,\mathrm{m}$
WGS84 semi-minor axis	$b_{\mathrm{WGS84}} = 6.356\,752\,314\,2 \times 10^{6}\,\mathrm{m}$
WGS84 inverse flattening	$(1/f)_{\mathrm{WGS84}} = 298.257\,223\,563$
WGS84 Earth's angular velocity	$\Omega_{\mathrm{WGS84}} = 7.292\,115 \times 10^{-5}\,\mathrm{rad\,s^{-1}}$
WGS84 Earth's gravity constant	$(GM)_{\mathrm{WGS84}} = 3.986\,004\,418 \times 10^{14}\,\mathrm{m^{2}\,s^{-1}}$
Earth's quadrupole moment (GRS80)	$J_2 = -1.082\,63 \times 10^{-3}$
Earth's mean radius	$R_{\oplus} = 6.371\,000\,8 \times 10^{6}\,\mathrm{m}$
Earth's mean density	$\rho_{\oplus} = 5.515 \times 10^{3}\,\mathrm{kg\,m^{-3}}$
Geopotential value defining the geoid	$W_0 = 6.263\,685\,60 \times 10^{7}\,\mathrm{m^{2}/s^{2}}$
Time constant relating TT and TCG	$L_g = 6.969\,290\,134 \times 10^{-10}$

List of Symbols and Abbreviations

Symbols

$(x^\mu) = (x^0, x^1, x^2, x^3)$	General coordinates
$\vec{X} = (X, Y, Z)$	Cartesian coordinates
(R, Θ, Φ)	Spherical coordinates
(h, β, Φ)	Ellipsoidal coordinates
(h, Λ, Φ)	Ellipsoidal (geodetic) coordinates
(u, β, Φ)	Ellipsoidal-harmonic coordinates
(ρ, z, φ)	Weyl's canonical coordinates
(x, y, φ)	Spheroidal coordinates
P, P_0	Points in space / spacetime events
m_i	Mass of object i
R_{ref}	Reference radius
a	Semi-major axis
b	Semi-minor axis
f	Flattening
E	Linear eccentricity
e, e'	First, second eccentricity
$\vec{e}$	Unit vector
$\vec{F}$	Force vector
$\vec{n}$	Surface normal
$\rho(\vec{X})$	Mass density
U	Gravitational potential
V	Centrifugal potential
W	Gravity potential
W_N	Normal gravity potential
W_0	Geopotential value defining the geoid
L_g	Time constant relating TT and TCG
P_l	Legendre polynomial of degree l
C_{lm}, S_{lm}, $\tilde{C}_{lm}$, $\tilde{S}_{lm}$	Newtonian multipole moments
J_l, $\tilde{J}_l$	Axisymmetric Newtonian multipole moments
∂_μ	Partial derivative
$\vec{\nabla}$	Nabla (gradient) operator
Δ	Laplace operator
$\vec{x}$	Position vector
$\vec{v}$	Velocity vector
$\vec{a}$	Acceleration vector
H	Orthometric height
h	Ellipsoid height

H_{N}	Normal height
H_{D}	Dynamic height
H^*	Chronometric height
C	Geopotential number
C^*	Redshift potential number
N	Geoid undulation
$\vec{g}$, g	Gravity
$\vec{\gamma}$, γ	Normal gravity
$\mathrm{d}s$	Invariant line element
$g_{\mu\nu}$	Metric
D_μ	Covariant derivative
$\Gamma^\mu{}_{\nu\sigma}$	Christoffel symbols
$\mathcal{R}^\mu{}_{\nu\rho\sigma}$	Riemann curvature tensor
$\mathcal{R}_{\mu\nu}$	Ricci tensor
$\mathcal{R}$	Ricci scalar
ξ^μ	Killing vector field
ϕ	Redshift potential
z	redshift
$r_s = 2m$	Schwarzschild radius
q_l, $\bar{q}_l$	Quevedo multipoles
c_l	Weyl multipoles
ψ, γ	Weyl's metric functions
$\mathcal{M}_l$	Relativistic (Geroch-Hansen) mass multipoles
$\mathcal{S}_l$	Relativistic (Geroch-Hansen) spin multipoles
a	Kerr rotation parameter
U^*	Relativistic gravity potential
U_N^*	Relativistic normal gravity potential
ψ_N, γ_N	Metric functions of the normal gravity spacetime
$\boldsymbol{R}(t)$	Orthogonal rotation matrix
$\boldsymbol{\omega}(t) = \dot{\boldsymbol{R}}(t)\boldsymbol{R}(t)^{-1}$	Rotation matrix product
u^μ	Four-velocity (field)
$a^\mu = \dot{u}^\mu$	Four-acceleration (field)
$P_{\mu\nu}$	Congruence projection operator
$\omega_{\mu\nu}$	Congruence rotation
$\sigma_{\mu\nu}$	Congruence shear
θ	Congruence expansion
t_{TT}	Terrestrial time
t_{TCG}	Geocentric time
t_{TCB}	Barycentric time
t_{TAI}	International atomic time

Abbreviations

GR	General Relativity
pN	Post-Newtonian
ppN	Parametrized post-Newtonian
GOCE	Gravity field and steady-state Ocean Circulation Explorer
GRACE(-FO)	Gravity Recovery And Climate Experiment (Follow On)

SLR	Satellite Laser Ranging
LLR	Lunar Laser Ranging
GFZ	Geoforschungszentrum
ICGEM	International Centre for Global Earth Models
IERS	International Earth Rotation and Reference Systems Service
IAU	International Astronomical Union
GRS80	Geodetic Reference System 1980
WGS84	World Geodetic System 1984
VLBI	Very Long Baseline Interferometry
ITRS (ITRF)	International Terrestrial Reference System (Frame)
ICRS (ICRF)	International Celestial Reference System (Frame)
LAGEOS	Laser Geodynamics Satellite
LARES	Laser Relativity Satellite
GPA, GPB	Gravity Probe A, Gravity Probe B

Author's Publications

During the time of my PhD studies, I was involved in the peer-reviewed publications and conference proceedings papers listed below.

- Ref. [145]: Dennis Philipp, Volker Perlick, Dirk Puetzfeld, Eva Hackmann, and Claus Lämmerzahl: *"Definition of the relativistic geoid in terms of isochronometric surfaces"*. In: Phys. Rev. D 95 (10 2017), p. 104037. doi: 10.1103/PhysRevD.95.104037.

The paper was published under the lead-authorship of DP, based on the work of and results provided by Volker Perlick on the redshift potential and clock measurements in GR, the work of Claus Lämmerzahl and Dirk Puetzfeld on worldline congruences for continuous media, and contributions of Eva Hackmann on the motion of observers and clock effects. DP was responsible for editing the text, for the main part of the calculations, merging all authors' contributions, clarifying the convention, and the application to spacetime models. The plots and the code for the isometric embedding were generated by DP.

- Ref. [146]: Dennis Philipp, Florian Woeske, Liliane Biskupek, Eva Hackmann, Enrico Mai, Meike List, Claus Lämmerzahl, and Benny Rievers: *"Modeling approaches for precise relativistic orbits: Analytical, Lie-series, and pN approximation"*. In: Advances in Space Research 62.4 (2018), pp. 921 –934. issn: 0273-1177.
doi: 10.1016/j.asr.2018.05.020.

In this work, DP is the main author and was responsible for the communication and for gathering the data and results of all authors as well as editing the paper and mainly writing the chapters on the relativistic and pN equations of motion and the Lie-series application. The figures where generated by DP using the results provided by Florian Woeske. XHPS calculations were performed by Florian Woeske, Meike List, and Benny Rievers. Liliane Biskupek and Enrico Mai contributed calculations for Lie-series solutions and Eva Hackmann provided analytical solutions to the geodesic equation and cross check calculations.

- Ref. [144] Dennis Philipp, Dirk Puetzfeld, and Claus Lämmerzahl: *"On geodesic deviation in static spherically symmetric situations"*. In: The Fourteenth Marcel Grossmann Meeting, pp. 3731–3736. doi: 10.1142/9789813226609_0489.

The conference proceedings paper was edited and mainly written by DP based on the results obtained by calculations of the authors. DP was responsible for the main part of the final calculations and generating the figures.

- Ref. [148] Dennis Philipp, Volker Perlick, Dirk Puetzfeld, Eva Hackmann, and Claus Lämmerzahl: *"The relativistic geoid"*. In: 2017 IEEE International Workshop on Metrology for AeroSpace (MetroAeroSpace). 2017, pp. 114–119.
doi: 10.1109/MetroAeroSpace.2017.7999549.

The paper was edited, mainly written, and presented at the conference by DP. Figures and calculations were generated by DP based on the results of [145] and discussions with all authors who checked the results and the framework.

- Ref. [147] Dennis Philipp, Volker Perlick, Claus Lämmerzahl, and Kaustubh Deshpande: *"On geodesic deviation in Schwarzschild spacetime"*. In: 2015 IEEE Metrology for Aerospace (MetroAeroSpace). 2015, pp. 198–203.
doi: 10.1109/MetroAeroSpace.2015.7180653.

Based on preliminary calculations of Kaustubh Deshpande, DP extended the applications to cover the presented orbital scenarios. Construction of the figures and drafting the text as well presenting the results at a conference was done by DP.

- Ref. [143] D. Philipp, D. Puetzfeld, and C. Lämmerzahl."On the Applicability of the Geodesic Deviation Equation in General Relativity". In: Relativistic Geodesy, Fundamental Theories of Physics. Ed. by D. Puetzfeld and C. Lämmerzahl. 2019, p. 419. doi: 10.1007/978-3-030-11500-5_13.

The paper is based on earlier work on the deviation equation and extends the results to cover more applications. DP was responsible for writing the paper and the calculations as well as the generation of the figures. Dirk Puetzfeld and Claus Lämmerzahl provided theoretical background and consistency checks of the fundamental framework and the employed conventions regarding geodesic equations and their generalizations.

Chapter 1

Introduction

Geodesy and its objectives

Geodesy, a science that is in our modern understanding a combination of physics, applied mathematics, and engineering, is concerned with the description and measurement of the Earth's fundamental properties.

According to Helmert's classical definition, "geodesy is the science of measurement and mapping of the Earth's surface[1]" [88]. Nowadays, this definition can still be regarded as a fundamental description of geodesy. The surface of the Earth is influenced, shaped, and continuously changed by gravitational forces and various other dynamical phenomena. Hence, the determination and description of the (external) gravity field of the Earth must also be an objective of geodesy. Since the mathematical description of the Earth and its properties requires well-defined reference systems, the Earth's orientation and motion in space is a central part of geodetic research. Ref. [188] gives a description of geodesy that summarizes these aspects in a clear way: "The objective of geodesy is to determine the figure and external gravity field of the Earth, as well as its orientation in space, as a function of time, from measurements on and exterior to the Earth's surface."

Typically and for historical reasons, geodesy employs Newtonian physics. In particular, Newton's theory of the gravitational interaction as a force, which is proportional to the involved masses and the square of their inverse distance, is used to great extent. In the following, we will speak of "conventional geodesy" whenever we want to indicate that the associated framework is based on Newtonian mechanics and notions.

[1] Ref. [88] appeared in German. The original statement is "Die Geodäsie ist die Wissenschaft von der Ausmessung und Abbildung der Erdoberfläche."

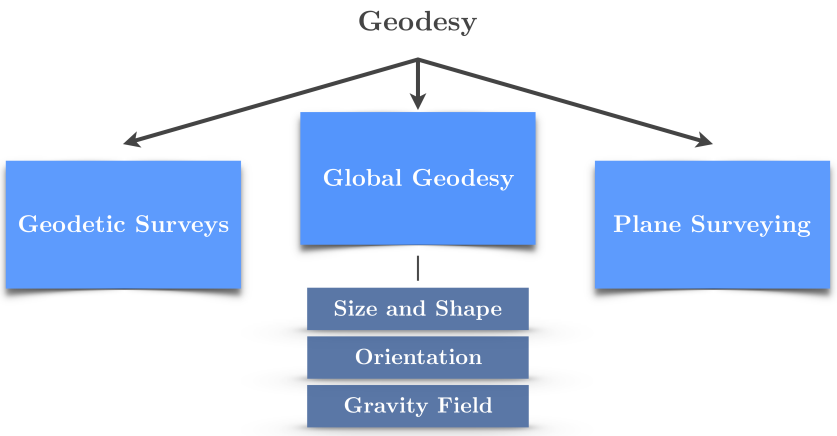

FIGURE 1.1: Sketch of the subdivision of geodesy and involved objectives according to Ref. [188]. For the field of global geodesy, the part to which this work is dedicated, the three main pillars are given as well.

However, the purpose of this work is to develop and refine (some) fundamental geodetic notions and observables within the theory of General Relativity. Therefore, we will make a clear distinction to the former case and use the term "relativistic geodesy" whenever we want to indicate that we work in a general relativistic framework. According to the standard treatment in the textbook [188], geodesy and its objectives might be subdivided into the three branches

- global geodesy,
- geodetic surveys,
- plane surveying.

Global geodesy is furthermore composed of three main pillars that are related to (i) the Earth's shape and size, (ii) the Earth's orientation and motion in space, and (iii) its (external) gravity field. Geodetic surveys are localized investigations of the Earth's surface, shape, size, and gravity field, and are linked to reference frames and conventions established by global geodesy. Usually, countries, groups of countries, or even continents are the regions of interest and on these scales the curvature of the surface and local variations of gravity must be taken into account. Plane surveying on the other hand is used for the development of, e.g., national maps and cadastral systems. The local change of gravity as well as the surface curvature is usually negligible on the involved scales. However, modern high-precision measurements do also enable the investigation of these properties on small local scales, and methods that were developed for global geodesy, such as GNSS, are used for geodetic surveys and plane surveying as well.

The present work can now be classified according to the structural division of geodesy above. We mainly work on the framework of global geodesy in a relativistic spacetime environment around the Earth. Geodetic notions and fundamental concepts

are investigated in General Relativity and this leads to generalizations of well-known definitions and new observables, mainly within the genuinely relativistic field of chronometric geodesy. Figure 1.1 schematically shows the structural subdivision of geodesy and involved objectives for the branch that is to be investigated in this work.

The central object of interest here is the Earth's gravity field and its description in General Relativity. However, it should be mentioned that also other planets and objects in space can be investigated in the same way as the Earth is investigated in geodesy. Modern technological (space-based) developments offer unprecedented possibilities in this respect. There is, e.g., the field of lunar and planetary geodesy, see Refs. [8, 132, 166, 197]. For instance, photogrammetric and other methods have been applied to obtain a general and unified lunar control network [2]. Note that the structure of geodesy, as shown in Fig. 1.1, applies also to these fields. Moreover, methods and notions developed in this work will be applicable in general to the geodesy of arbitrary objects with strong gravitational fields in their vicinity.

The gravitational field of the Earth can be investigated in many ways. On the Earth's surface, (differential) acceleration measurements and leveling give insight into the structure and position dependence of the gravity acceleration. Including space missions and astronomical observations, even more data sources become accessible. Based on the best available results and data fusion, reference system realizations and gravity field models are constructed with ever-increasing accuracy. Usually, such gravity models contain parameters of a multipole expansion of the gravitational potential up to a maximal degree, which is related to the spatial resolution. In Fig. 1.2, we show the distribution of the gravitational acceleration on the Earth's surface. The resolution of the color-coded scale does not matter for now. The figure is composed of three plots: on the top, a plot of the gravitational acceleration as a function of longitude and latitude is shown, which we constructed up to degree 360 according to the EGM96 gravity field model, see [117]. We can see that local structures are not resolved, even though the model data is actually detailed enough. The signal is dominated by a quadrupolar contribution which causes gravity to increase from the equator towards the poles. This behavior is a result of the Earth's oblateness - it is not a perfect sphere but rather squashed to the shape of an ellipsoid. Processing the data gives access to smaller structures: in the middle and bottom plots, we show the gravity acceleration after successively averaging over longitude and latitude values and subtracting the dominant contribution. Thus, adequate data processing is an important part of the interpretation of measurements and the evaluation of gravity models.

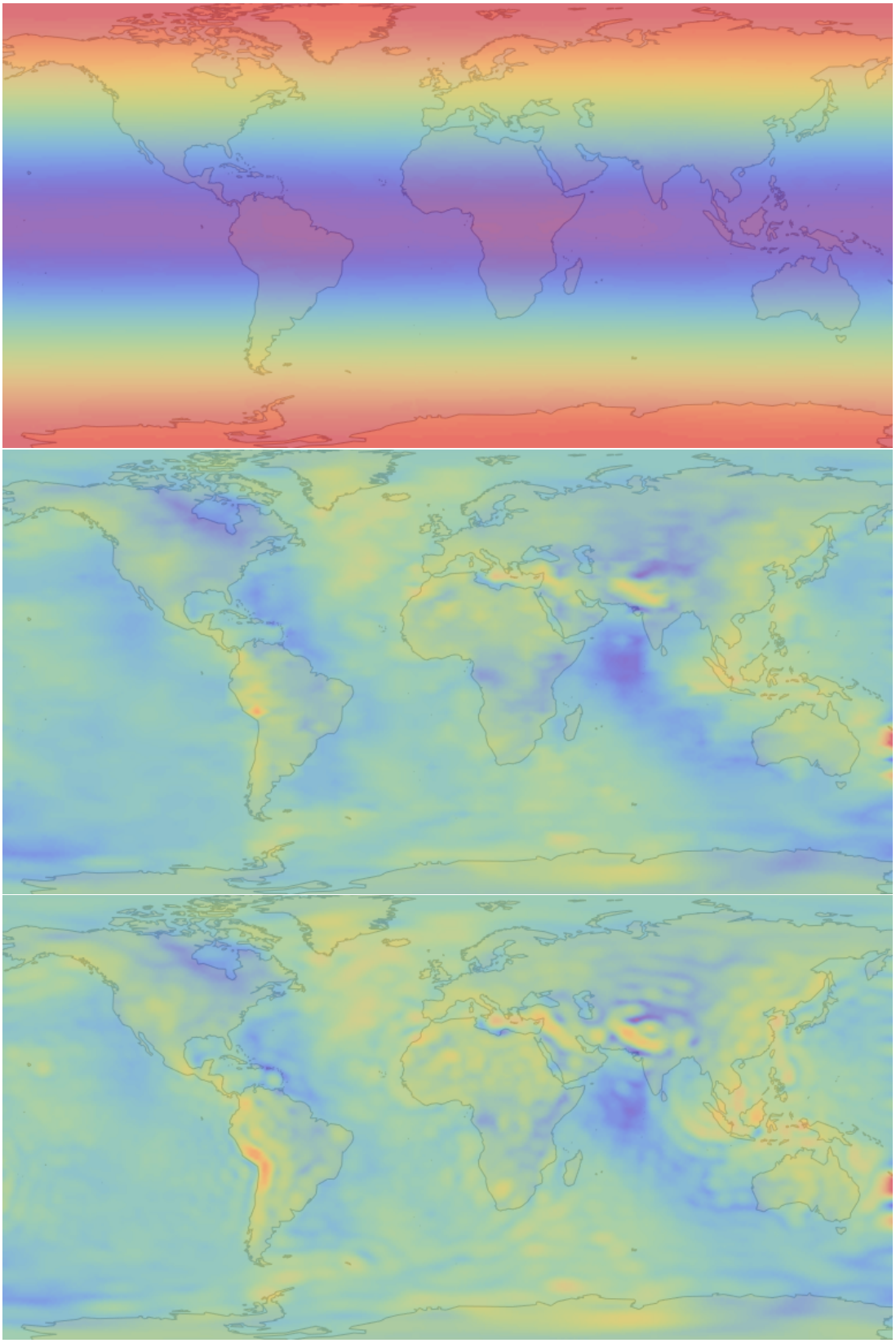

FIGURE 1.2: Gravity on the Earth in the EGM96 model after successive refinements (top to bottom) via longitudinal and azimuthal averaging.

The structure of the Earth's gravity field is extremely complex. Thus, the question arises how a good approximation can be constructed. One possible approximation is to introduce an ellipsoid of rotation as a best fit to a particular level surface of the Earth's true gravity potential, the geoid; see chapter 2. Then, for each gravity field model the difference between the geoid and its ellipsoidal approximation can be calculated and is termed geoid undulation. In Fig. 1.3, we show these geoid undulations for the EGM96 (top). The undulations range from about $-100\,\mathrm{m}$ (blue) to $+100\,\mathrm{m}$ (red). In the second plot (bottom) we show the differences between EGM96 and its successor EGM2008. The differences are about $\pm 10\,\mathrm{m}$; more accurate measurements and inclusion of new data sources lead to improvements over time. Gravity field models also offer information on local scales such as continents or countries. In Fig. 1.4, the variations of the acceleration on the surface is shown for Europe and Germany, respectively. To display the local change, the mean value is again subtracted. Such information is important to, e.g., establish and relate height systems on larger regions of the Earth, see for instance Ref. [188]. Every gravity field model has some maximal degree to which parameters (multipole moments) are integrated and derived quantities, such as the gravity acceleration in a certain region, depend on the chosen maximal degree. To depict this relation, we have calculated the gravity acceleration in Bremen, Germany (WGS84 8.83° longitude, 53.07° latitude) as a function of the maximal degree l, which tells how many terms in the expansion of the model are taken into account. The result is shown in Fig. 1.5.

Measuring the gravity field of the Earth over longer time scales yields information about the temporal change. Via extensive modeling schemes, such changes are translated into mass variations on the surface. The probably most famous space mission to monitor such variations is the GRACE mission [66, 186]. Since 2002, the two GRACE-satellites follow each other in a polar orbit. Due to the inhomogeneity of the gravitational field, the spatial separation of the two spacecraft changes over time, and this distance change is a map of the gravitational field. Based on GRACE data (and other results in data fusion), static gravity field models as well are monthly solutions are calculated, see, e.g., [124] and [98] for a collection of results and further references. Based on the monthly solutions of the gravity field, geodetic modeling allows to translate the data into mass changes and variations. One of the most prominent results is the observed ice mass loss in Greenland, see Fig. 1.6, which is in agreement with all other observations of this region. However, the GRACE result is outstanding in many ways and the ice mass loss was purely derived from changes in the gravitational field, deduced from satellite measurements at a few hundred kilometers above the Earth's surface. Thus, geodetic measurements and climate research are intimately related. Observation of climate change, development of pre-warning systems for, e.g., floods and earthquakes, ocean research, and many others can benefit from accurate geodetic measurements.

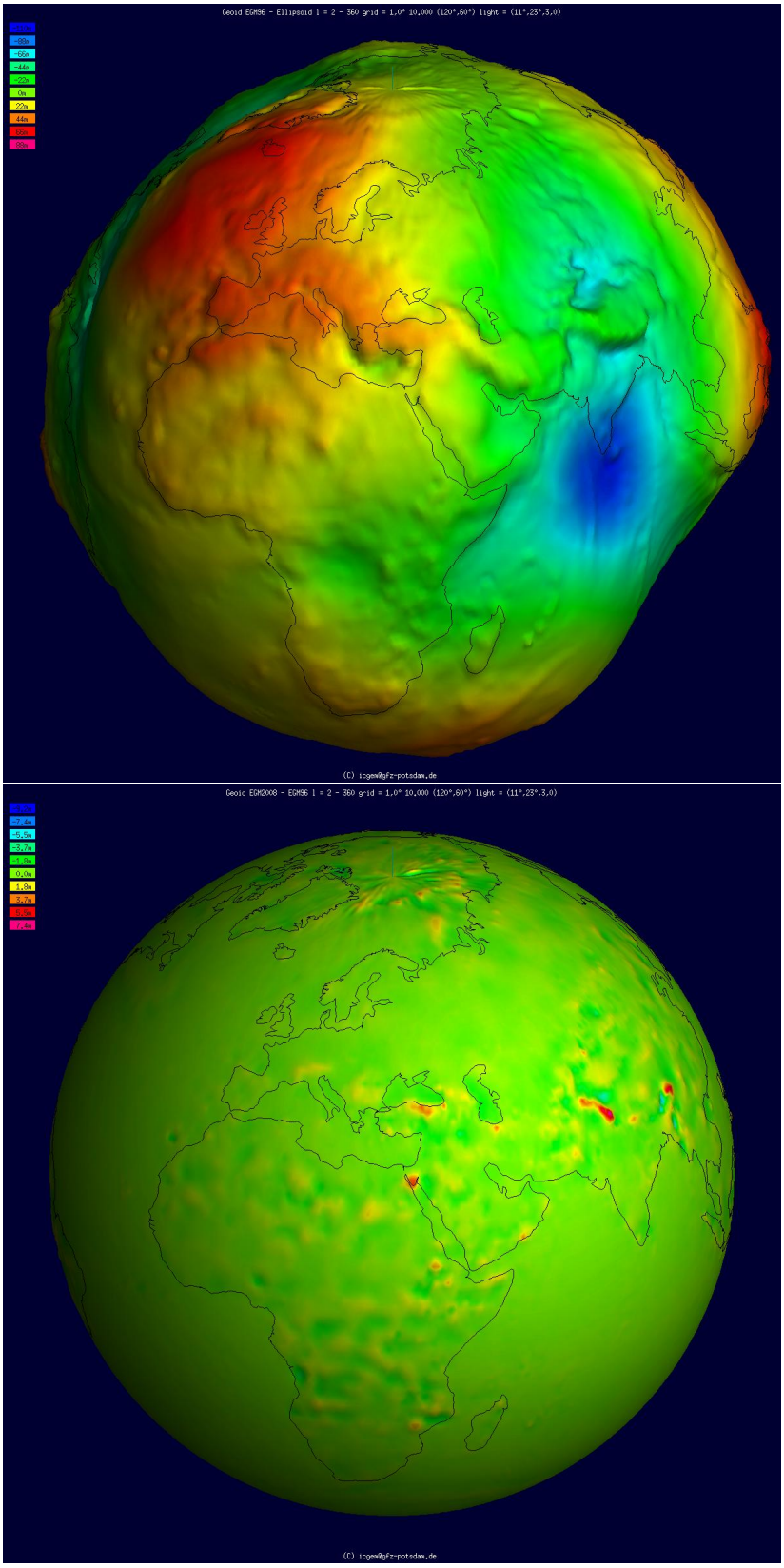

FIGURE 1.3: Geoid undulations in the EGM96 gravity model (top) and differences to the EGM2008 gravity model (bottom). Both plots were calculated using the ICGEM calculation service [98].

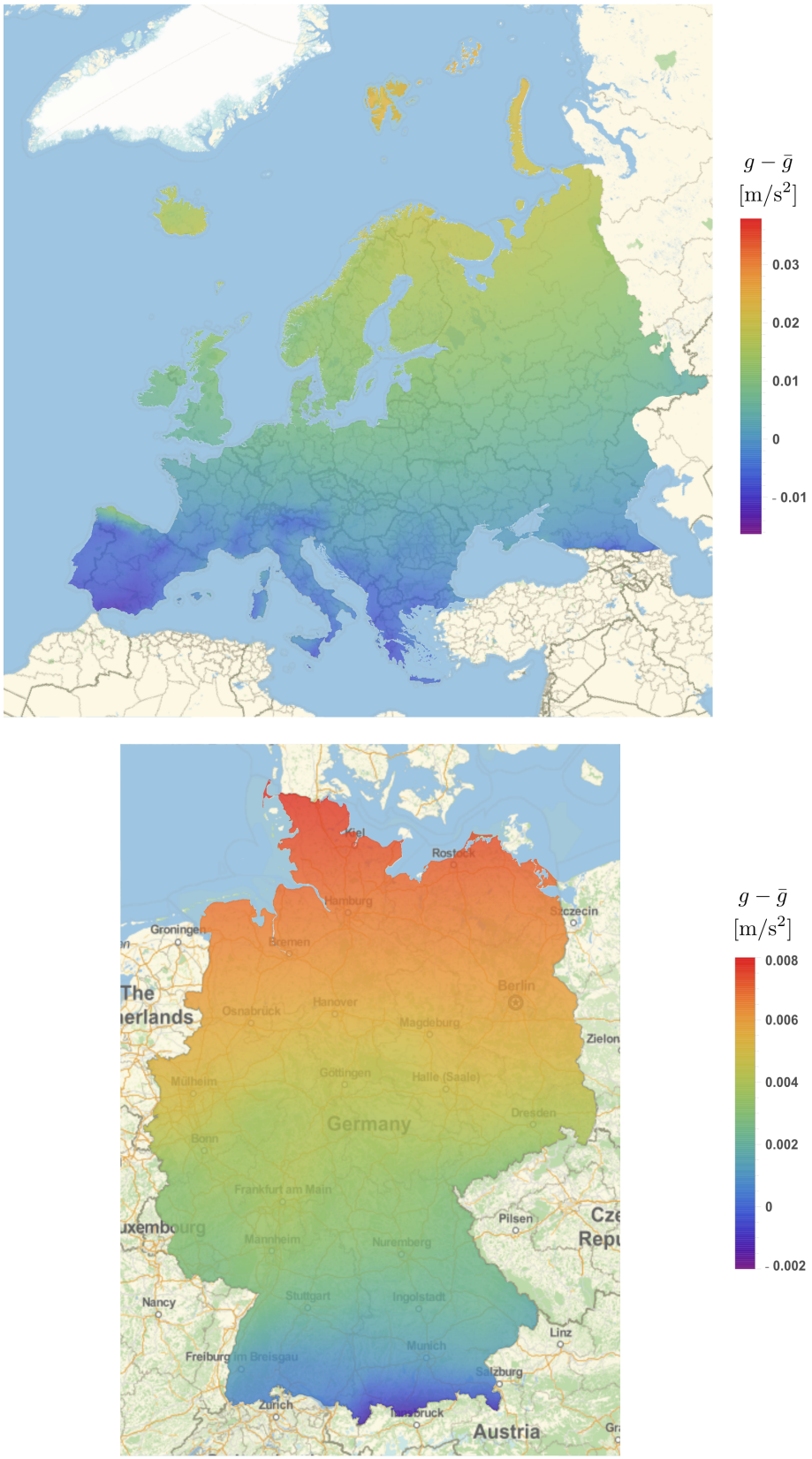

FIGURE 1.4: Gravity on local scales: Europe (top) and Germany (bottom). In either case, we show the deviation from the mean value of gravity $\bar{g} = 9.806\,65\,\mathrm{m\,s^{-2}}$. The data was calculated using the EGM96 gravity field model.

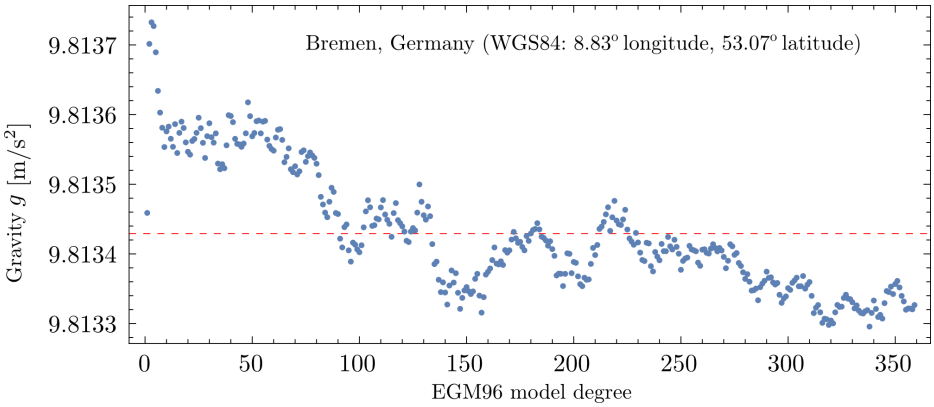

FIGURE 1.5: Gravity on local scales: The gravity acceleration in Bremen depending on the model parameter l in the EGM96 gravity model for $l = 0$ to $l = 360$.

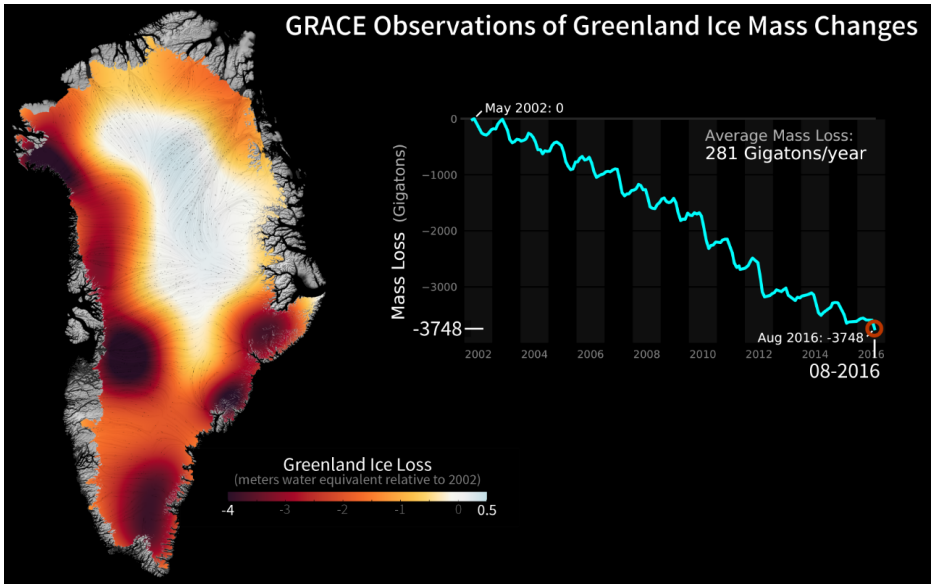

FIGURE 1.6: GRACE result on the ice mass loss in Greenland between 2002 and 2016. The figure is taken from JPL's website on GRACE-FO, see Ref. [70].

Motivation of relativistic geodesy

Unprecedented technological possibilities offer geodetic measurements with ever-increasing precision and accuracy. For example, the successor of the long-lasting GRACE mission, GRACE-FO, is expected to measure the change of the distance between both spacecraft within an accuracy of about 10 nm by means of laser ranging interferometry [52, 67, 122].

However, we know that Newton's theory of gravity is not the most fundamental framework. At a certain observational level, relativistic effects become important and must be considered to deliver an undoubtedly correct interpretation of measurements. Einstein's General Relativity, a theory of gravity and spacetime, comes with a set of new observables but takes away the simplicity of Newtonian linear gravity. Space and time merge to the concept of spacetime and gravity is described as the curvature thereof. To date, General Relativity is in agreement with all observations and conducted experiments [199, 200]. It is motivated by philosophical as well as mathematical arguments and, arguably, one of the most beautiful theories ever created by mankind.

The geometry of spacetime is described by the metric tensor, a symmetric bilinear form, which introduces the notions of, e.g., length, area, and volume on the spacetime manifold. The metric is to be determined from the sources of gravity, i.e. mass, energy, momentum, and their fluxes. In Newtonian gravity, the source is the mass density only, whereas in General Relativity it must be replaced with the energy momentum tensor. Then, Einstein's field equation relates the spacetime geometry to the sources and tells the sources how to move in the curved spacetime, see chapter 3 in this work and the fundamental reference for all relativists, Ref. [127]. Moreover, we recommend the textbooks [165, 170, 184, 195] for detailed introductions to the theory.

The mathematical structure of relativistic gravity becomes much more involved as compared to Newtonian physics. The mathematical tools of differential geometry need to be employed and well known Newtonian concepts lose their meaning. In this work, the implications of General Relativity for applications in geodesy are studied. We develop the relativistic generalizations of fundamental geodetic notions and measurement prescriptions. Among others, we consider the Earth's gravity potential, the geoid, its normal gravity field, height definitions and applications in terms of acceleration measurements and gradiometry in the theoretical framework of Einstein's theory.

One of the major differences between Newton's and Einstein's theory is the notion of time. In contrast to Newton's absolute and universal time, General Relativity tells us that the rate of a clock (its proper frequency), as compared to some reference, depends on the clock's state of motion and position in the gravitational field. This opens a new branch of geodetic research which is called chronometric geodesy. The comparison

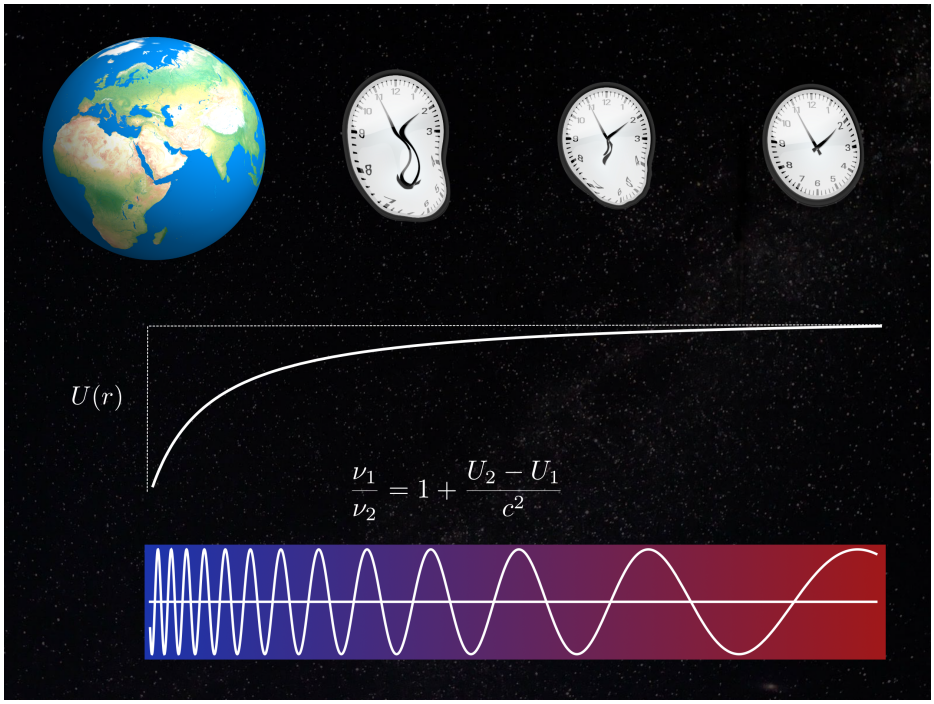

FIGURE 1.7: The redshift of a photon that escapes the Earth's gravity field. The Newtonian potential differences $U_2 - U_1$ are the first order terms for the redshift between two clocks. Note that in our convention $U < 0$ such that the redshift is positive for a signal from smaller to larger distances w.r.t. the Earth.

of clocks at different positions yields their frequency difference, the so-called redshift. Special relativity already introduced Doppler redshifts on signals between emitter and receiver for a non-zero relative velocity. These effects are, of course, contained in the general relativistic description since locally the theory of Special Relativity remains valid and is included in the general framework. For a general idea of how spacetime geometry influences the frequency of signals see Fig. 1.7.

The first experimental verification of the gravitational redshift as the measurement of "the apparent weight of photons" was achieved by Pound and Rebka in 1960 [151]. They used the Mößbauer effect to compare the redshift of photons which were sent in the vertical direction of the Earth's gravity field. Nowadays, for Earth-bound chronometric measurements modern atomic and optical lattice clocks can be compared to resolve height differences at the scale of some centimeters, see Refs. [24, 116, 126, 185]. Moreover, such clocks can be connected by optical fibers and their redshift is obtained over large spatial separations of some 10^3 km via frequency transfer and amplification techniques, see Refs. [40, 76, 118] and references therein. It appears to be that frequency transfer at the 10^{-20} level is feasible (in the near future) using so-called Brillouin amplification [162]. Such experiments will help to establish common international time scales and height systems on large scales [38, 68, 99] and offer the possibility to test the theory of relativity [36]. Last but not least, transportable optical clocks offer

the prospect to obtain many local comparisons in measurements campaigns [75]. Extending clock comparison and chronometric measurements to space yields even more possibilities. Gravity Probe A (GPA) performed a test of the gravitational redshift in space at the 10^{-4} accuracy level by comparing a hydrogen maser on a rocket to another one on ground [191, 192, 193]. With the ACES experiment [22, 91, 92] a test of the equivalence principle with clocks will be conducted and the general relativistic prediction for the redshift will be tested. Furthermore, missions such as RELAGAL [90], in which the clock data of the errant Galileo satellites is analyzed, look for the validity of the gravitational redshift and aim to beat the GPA accuracy, see also Ref. [37]. Another independent mission in this respect is the RadioAstron experiment [121].

In a nutshell, chronometric geodesy in space and on Earth will become one (and probably the most important) cornerstone of high-precision geodetic research in the future. Therefore, a major part of this work is devoted to its theoretical framework and we shall base our definitions on concepts that are accessible by chronometric measurements.

For a general overview of relativistic geodesy, chronometric geodesy, and involved issues we recommend Refs. [129, 130, 35, 38, 75, 126, 179, 4]. Two special science projects in the field of relativistic geodesy are "Relativistic Geodesy and Gravimetry with Quantum Sensors (geo-Q)" [163] and "International Timescales with optical clocks (ITOC)" [101]. The former of which the author of this work has the pleasure to be a member of.

Structure of this work

The main part of this work is divided into five chapters. We start by an introduction of conventional geodetic notions and measurement prescriptions in chapter 2. This includes a brief recapitulation of Newtonian gravity, an introduction to reference systems and frames, and the definition of the Earth's geoid as well as the reference ellipsoid. Normal gravity and the level ellipsoid are defined as an approximation to the complex true gravity field. Thereupon, we introduce geodetic reference systems and end the chapter by defining height measures and related concepts. This chapter allows physicists to get used to the notions and concepts in geodesy, and enables geodesists to recognize our notation.

In chapter 3, we briefly recapitulate the basics of General Relativity and introduce necessary notions and mathematical formulae. The intention of this chapter is to give readers, who are not familiar with Einstein's theory, a chance to catch up with the bare minimum of mathematical structures needed to understand the remainder of this work. Furthermore, the central purpose of this chapter is to introduce spacetime

models which are solutions to Einstein's vacuum field equation. These models will be used to approximate the spacetime around the Earth, to define geodetic concepts in a relativistic framework, and to calculate estimates for relativistic effects in geodetic measurements.

Chapter 4 is devoted to the definition of fundamental notions of geodesy in the mathematical framework of General Relativity. We introduce observer congruences, their kinematical decomposition and properties, the redshift and acceleration potential, isochronometric surfaces, and give a definition of the relativistic geoid as well as the relativistic normal gravity potential in the normal gravity spacetime that is constructed based on the results of the preceding chapter.

The concepts defined so far will be applied to the spacetime models in chapter 5. Important estimates of relativistic effects for the redshift and acceleration measurements of co-rotating observers are obtained and we show how previous results are embedded into our framework. In particular, we investigate the new concepts and notions in a parametrized post-Newtonian spacetime.

The last chapter focusses on some relativistic effects in geodetic measurements on Earth and in space. We calculate the leading order relativistic corrections to the Newtonian geoid and investigate the conceptual problem involved in this comparison. Since the definition (or determination) of the geopotential value W_0, which defines the Newtonian geoid, is involved in some inconsistencies, we try to shed some light on the situation in this chapter. We show how the proper time on the geoid, the constant L_g defined in the IAU resolutions for the transformation between the timescales TAI and TCG, and the potential value W_0 are related in a framework even beyond first-order post-Newtonian approximations. Height definition are re-addressed in the context of chronometric geodesy. We relate the height difference of two observers to the redshift between their standard clocks. A general relativistic definition of chronometric heights is suggested, which coincides with the definition of the familiar orthometric height in the Newtonian limit. Moreover, we outline a procedure of how a certain isochronometric surface (a gravity level surface) can be operationally maintained over time. Finally, relativistic effects on satellite orbits in space are investigated. We determine relativistic corrections and induced accelerations for satellite orbits in a post-Newtonian spacetime model of the Earth. Relativistic contributions are compared to various non-gravitational accelerations, such as solar radiation pressure and atmospheric drag, due to the space environment. Lastly, an introduction to relativistic gravity gradiometry and the gradiometer equation is presented. We apply the concept to the deviation of orbits in a monopolar Newtonian gravity field and investigate the relativistic pendant, the Jacobi equation in a Schwarzschild spacetime.

Chapter 2

Notions in Conventional Geodesy

2.1 Newtonian gravity and the gravitational field

Newton's law of gravitation describes the attraction between point-like particles with given masses. The gravitational force $\vec{F}$ between two point-like masses is proportional to the product of the masses m_1 and m_2, and it is proportional to the inverse of their squared distance r,

$$\vec{F}_{12} = -G\,\frac{m_1 m_2}{r^2}\,\vec{e}_r\,. \tag{2.1}$$

The minus sign in Eq. (2.1) indicates that the gravitational force is attractive. The unit vector $\vec{e}_r$ takes care of the direction and points from m_2 to m_1 when we interpret $\vec{F}_{12}$ as the force exerted on m_1 by m_2. Newton's gravitational constant G appears in the form of a coupling constant that takes care of the units. To describe the gravitational interaction of n particles, a suitable sum over all pairwise interactions must be constructed. The gravitational force is a conservative force. Therefore, it can be represented as the gradient of a gravitational potential U such that

$$\vec{F}/m = -\vec{\nabla}U\,. \tag{2.2}$$

Here, $\vec{\nabla} := (\partial_X, \partial_Y, \partial_Z)$ is the gradient operator in a global Cartesian coordinate system (X, Y, Z) for the three-dimensional Euclidean space $\mathbb{R}^3$. Note that we choose the negative sign convention, in which the potential U is negative and the minus sign appears in equation (2.2). This convention is usually used in physics, whereas in geodesy also the positive sign convention is commonly employed. However, in the end both conventions yield the same force in magnitude and direction.

In Newtonian gravity, the field equation

$$\Delta U\big(\vec{X}\big) = 4\pi G\rho\big(\vec{X}\big) \tag{2.3}$$

allows to determine the Newtonian gravitational potential U of a given source, which might be distributed over some (compact) region. This source of gravitation is to be described by a mass density $\rho(\vec{X})$, and $\Delta := \vec{\nabla}^2 = \partial_X^2 + \partial_Y^2 + \partial_Z^2$ is the Laplace operator that makes Eq. (2.3) a second order linear differential equation for the gravitational potential.

In conventional geodesy, the following distinction between the notions of gravitation and gravity is made. Gravitation is described by the field equation above, of which the solution is the gravitational potential U. Then, one proceeds to describe phenomena on the rotating Earth. For observers who are confined to its surface, centrifugal effects play a significant role in geodetic measurements. The combination of centrifugal and gravitational effects is what these observers feel and is termed "gravity". From the viewpoint of relativistic physics, however, this artificial distinction appears to be somewhat weird – usually both notions are used interchangeably and are related by coordinate transformations and inertial effects. Nevertheless, we will adopt the notation here since we develop concepts in relativistic gravity which shall have a particular well-known limit in conventional geodesy. Therefore, geodesists might develop some intuition for relativistic concepts that generalize known Newtonian counterparts and physicists hopefully excuse the abuse of notions.

We assume that the Earth rotates around the Z-axis of the coordinate system. On the rotating Earth, observers feel and observe centrifugal effects in an Earth-fixed non-inertial reference system. The centrifugal force is conservative and its effects can be described by the centrifugal potential

$$V(\vec{X}) := -\frac{1}{2}\omega^2 d_Z^2 = -\frac{1}{2}\omega^2 R^2 \sin^2\Theta\,, \tag{2.4}$$

where ω is the Earth's angular velocity, d_Z is the distance to the rotation axis, and we introduce spherical coordinates (R, Θ, Φ) by the standard transformation such that Θ is the polar angle, measured from the north pole, and Φ is the azimuthal angle, measured from the X-axis. Now, we combine centrifugal and gravitational effects and define the gravity potential W by[1]

$$W(\vec{X}) = U(\vec{X}) + V(\vec{X})\,. \tag{2.5}$$

[1] In the context of geodesy of the Earth, the potential $W(\vec{X})$ is also called the geopotential.

The force of gravity per unit mass, which observers on the rotating Earth experience, is then given by

$$\vec{g} = -\vec{\nabla} W \,, \tag{2.6}$$

and its magnitude $g := ||\vec{g}||_2$ is simply called gravity. The dimension of g is the dimension of an acceleration, $[g] = \mathrm{m/s^2}$, whereas the potentials have the dimension of a squared velocity, i.e. we have $[U] = \mathrm{m^2/s^2} = [V]$. Note that U is a harmonic function in empty space, whereas V does not share this property. Therefore, all the advantages that harmonic functions offer do not apply to the combined gravity potential W.

In a system of spherical coordinates, the gravitational part U of the gravity potential W can be expanded into spherical harmonics according to[2]

$$U(R,\Theta,\Phi) = -\frac{GM}{R}\sum_{l=0}^{\infty}\sum_{m=0}^{l}\left(\frac{R_{\mathrm{ref}}}{R}\right)^{l} P_l(\cos\Theta)\left[C_{lm}\cos(m\Phi) + S_{lm}\sin(m\Phi)\right] . \tag{2.7}$$

The reference radius R_{ref} is arbitrary and usually chosen to be the Earth's mean radius $R_\oplus$. The expansion coefficients C_{lm}, S_{lm} are referred to as multipole coefficients (multipole moments) and any table for the values of C_{lm} and S_{lm} must also give the values for the gravity constant GM and the reference radius R_{ref}, which are used in the respective analysis. The lowest order moments are set to the values $C_{00} = 1$ and $S_{00} = 0$ such that the parameter M in (2.7) has the interpretation of the total mass of the source.[3] Furthermore, all coefficients S_{l0} do not contribute to the sum and can conventionally be set to zero. If we let the origin of the coordinate system coincide with the Earth's center of mass, all dipole term vanish, i.e. $C_{1m} = 0 = S_{1m}$, $m = 0, 1$. This can easily be proven by working out the explicit relations

$$C_{10} = \frac{1}{R_{\mathrm{ref}}}\int_{\mathrm{Vol}_\oplus}\frac{Z}{M}\mathrm{d}m \,, \tag{2.8a}$$

$$C_{11} = \frac{1}{R_{\mathrm{ref}}}\int_{\mathrm{Vol}_\oplus}\frac{X}{M}\mathrm{d}m \,, \tag{2.8b}$$

$$S_{11} = \frac{1}{R_{\mathrm{ref}}}\int_{\mathrm{Vol}_\oplus}\frac{Y}{M}\mathrm{d}m \,, \tag{2.8c}$$

where $\mathrm{Vol}_\oplus$ is the volume of the Earth, i.e. the integration is to be performed over the region where $\rho(\vec{X}) \neq 0$. The above expressions yield the coordinates of the center of

[2] The expansion is valid in the exterior of the source, i.e. in the region $\rho(\vec{X}) = 0$. Furthermore, we assume boundary conditions such that the potential vanishes at infinity. Formally, Laplace's equation has a symmetry $R \to 1/R$ which generates a second family of solutions that are neglected here.

[3] Without the convention $C_{00} = 1$, the meaning of M in (2.7) is different; the product $C_{00}M$ is the total mass of the gravitating source.

mass, $(X, Y, Z)_{\mathrm{COM}} = (C_{10}, C_{11}, S_{11})$, which proves the point.

Under the assumption of axisymmetry, we can reduce the expansion of the potential to

$$U(R, \Theta) = -\frac{GM}{R} \sum_{l=0}^{\infty} \left(\frac{R_{\mathrm{ref}}}{R} \right)^{l} J_l \, P_l(\cos \Theta) \,, \tag{2.9}$$

where all $m > 0$ terms vanish. The new coefficients J_l are related to the old ones by

$$J_l := C_{l,0} \,. \tag{2.10}$$

Note that the coefficients C_{lm}, S_{lm} and therefore also J_l are dimensionless. We can rewrite the expansion in a more formal way by isolating only the coupling constant G and introducing new moments with physical dimensions as expansion parameters. This yields

$$U(R, \Theta, \Phi) = -G \sum_{l=0}^{\infty} \sum_{m=0}^{l} \frac{P_l(\cos \Theta)}{R^{l+1}} \left[\tilde{C}_{lm} \cos(m\Phi) + \tilde{S}_{lm} \sin(m\Phi) \right] \,, \tag{2.11}$$

which reduces to

$$U(R, \Theta) = -G \sum_{l=0}^{\infty} \tilde{J}_l \, \frac{P_l(\cos \Theta)}{R^{l+1}} \tag{2.12}$$

for the axisymmetric case. The new multipole moments are

$$\tilde{C}_{lm} := C_{lm} R_{\mathrm{ref}}^{l} M \quad \text{and} \quad \tilde{S}_{lm} := S_{lm} R_{\mathrm{ref}}^{l} M \,, \tag{2.13}$$

and their dimension is $[\tilde{C}_{lm}] = \mathrm{kg\,m}^{l} = [\tilde{S}_{lm}]$. Furthermore, the new axisymmetric moments are given by

$$\tilde{J}_l := \tilde{C}_{l0} = R_{\mathrm{ref}}^{l} \, J_l \, M \,, \tag{2.14}$$

and they have the dimension $[\tilde{J}_l] = \mathrm{kg\,m}^{l}$ as well. Now, the lowest order moment, the monopole, is the mass: $\tilde{J}_0 = \tilde{C}_{l0} = M$. Hence, we have a scaling according to $[\tilde{J}_l / \tilde{J}_0] = \mathrm{m}^{l}$.

The problem of determining the external gravity field of the Earth reduces to the determination of the multipole coefficients. Various measurements on ground and in space contribute to combined gravity field models, see, e.g., [188, 98]. Ground based measurement techniques include, e.g., classical spirit leveling and (relative) acceleration measurements. Ground to space and space-based measurements are done, e.g., by satellite laser raging using artificial satellites and dedicated missions such as GRACE

and its successor GRACE-FO [52, 66, 67, 122, 186].

In later parts of this work, we focus on relativistic contributions to geodetic notions and measurements due to the lowest order multipole moments of gravitational fields, see chapter 6. In particular, we analyze configurations which possess a monopole and quadrupole moment only. For such a system, the Newtonian gravitational potential becomes

$$U(R,\Theta) = -\frac{GM}{R} - \frac{G\tilde{J}_2 P_2(\cos\Theta)}{R^3} = -\frac{GM}{R}\left(1 + \frac{J_2 R_{\text{ref}}^2}{2R^2}\left(3\cos^2\Theta - 1\right)\right). \quad (2.15)$$

Thereupon, the gravity potential for the quadrupolar Earth model is

$$W(R,\Theta) = -\frac{GM}{R}\left(1 + \frac{J_2 R_{\text{ref}}^2}{2R^2}\left(3\cos^2\Theta - 1\right)\right) - \frac{1}{2}\omega^2 R^2 \sin^2\Theta\,. \quad (2.16)$$

In Tab. 2.1, we show values for the involved quantities taken from the EGM96 gravity field model [117]. Note that the combination GM, known as the Earth's gravity constant, can be measured to much higher accuracy than each of the individual values for G and M. Furthermore, the factor $\sqrt{5}$ is due to a different normalization and must be applied to match our Eq. (2.16).

TABLE 2.1: Parameters that appear in a quadrupolar Earth model (2.15), taken from the gravity field model EGM96 [117] (tide-free gauge).

Quantity	**Magnitude**	**Dimension**
GM	$3.986004415 \times 10^{14}$	m^3/s^2
R_{ref}	6378136.300	m
J_2	$-\sqrt{5} \times 4.84165371736 \times 10^{-4}$	1

2.2 Reference systems and surfaces

To describe the figure of the Earth and its orientation and motion in space, obviously reference systems are needed. By the figure of the Earth, we understand (i) the Earth's physical surface that is formed by the topography, and (ii) in a more abstract sense the gravitational Earth. In either case, reference systems need to be defined to describe shape, orientation, and dynamical changes.

The irregular shape of the Earth's surface topography can not be investigated in terms of a simple mathematical model. Instead, control stations with coordinates of reference points are interpolated to obtain a global control network [188]. The gravitational (mathematical) Earth on the other hand can be described by a simpler mathematical model. A 'mathematical figure' of the gravitational Earth, which is called the geoid, is introduced and used as a reference surface for height measurements.

This geoid is defined by certain equilibrium conditions and a chosen level surface of the Earth's gravity potential. In the absence of external forces and internal disturbances, it represents the mean ocean surface, thought to be extended underneath the continents as well. As a good approximation to the geoid, an ellipsoidal Earth model is introduced. It serves as the first non-trivial approximation of the geoid's complex geometry and is used for horizontal positioning. Modern positioning systems, such as GPS, use coordinates that are adapted to a reference ellipsoid, see the WGS84 [100] and Ref. [4].

Note that the first reference to the geoid was made by the German scientist Carl Friedrich Gauss: "What in the geometrical sense is called the surface of the Earth, is nothing but the particular surface, which perpendicularly intersects the direction of gravity everywhere and which is part of the oceans surface."[4] [62]. Later, Listing [120] coined the name "geoid" for Gauss' mathematical Earth.

Newton, in his fundamental work [131], proposed an ellipsoidal Earth model. He used a rotating fluid Earth and calculated an ellipsoid with an inverse flattening of $f \approx 230$, which is only 0.6% off compared to todays most accurate measurements, see also the historical remarks in Ref. [188].

The following sections provide details on reference systems and reference surfaces used for various applications and observations. We define the Earth's geoid and investigate its basic properties in a simple model that allows to deduce the dominant contributions and features. Thereupon, the reference and level ellipsoid as well as the normal gravity potential of the Earth are defined. Using these results, height concepts and measurements are described in the last part of this chapter.

2.2.1 Reference systems and frames

This section serves as a brief overview of reference systems, which are used in geodetic observations. Reference systems are obviously necessary to describe the state of motion and position of the Earth, its dynamics, the positions and motions of other celestial objects and artificial satellites which are used for high-precision geodetic measurements.

In geodesy, there is a clear distinction between reference systems and reference frames. According to the International Earth Rotation and Reference Systems Service (IERS) [142] : "A Reference System is a set of prescriptions and conventions together with the modeling required to define at any time a triad of coordinate axes." And furthermore: "A Reference Frame realizes the system by means of coordinates of definite

[4] The original German text is "Was wir im geometrischen Sinn Oberfläche der Erde nennen, ist nichts anderes als diejenige Fläche, welche überall die Richtung der Schwere senkrecht schneidet, und von der Oberfläche des Weltmeers einen Theil ausmacht [...]", see [62].

points that are accessible directly by occupation or by observation." See also Refs. [95, 102, 188].

A simple example for a reference system is the definition of a Cartesian coordinate system consisting of three perpendicular axes, one of which aligned with the Earth's rotation axis, another one into the direction of the Greenwich meridian, and the last one completing the right-handed orthogonal system. A reference frame, as a realization of this system, can consist of a globally distributed set of control network points of which the coordinates are specified. In Ref. [102], the relation between the reference system and a reference frame realizing it is described very well by: "A frame cannot exist without a system, and a system is of no practical value without a frame".

Simple reference systems, usually part of undergraduate lecture series in physics, comprise Cartesian and spherical coordinate systems. The next step in adapting the coordinates to the symmetry of the oblate Earth and its gravity field is to use ellipsoidal coordinate systems, based on a particular reference ellipsoid of revolution, see section 2.2.4 below and appendix A. In Ref. [161] and Ref. [102] tables with historically used reference ellipsoids can be found.

We genuinely distinguish between celestial and terrestrial reference systems and we end this section by introducing the internationally used reference systems for global descriptions. As a general reference, we recommend the IERS and IAU resolutions [125, 142] and [96, 97, 178, 103] as well as the standard literature [95, 102, 188] and references therein.

We shall here also define the commonly used notion of a geodetic datum, which is actually a set of values that define a coordinate system, its orientation, and scale.

Celestial Reference Systems (CRS)

Space-fixed Celestial Reference Systems (CRS) are approximations to inertial systems and well-suited for the description of the ephemerides of solar system objects including artificial satellites. CRS can be dynamical and kinematically defined. Dynamical CRS use solar system bodies' ephemerides and proper motions of stars. Kinematical CRS are defined by positions and motions of distant stars and quasars.

A particular kinematical GRS is the International Celestial Reference System (ICRS). It was finally introduced in the year 2000 and is related to extragalactic radio sources. The ICRS is based on a relativistic framework [108] and its realization, the International Celestial Reference Frame (ICRF) is based on coordinates obtained from VLBI observations [123, 51]. In Fig. 2.1 the distribution of the defining sources of the second realization of the ICRF is shown, see also [51]. The origin of the ICRS is at

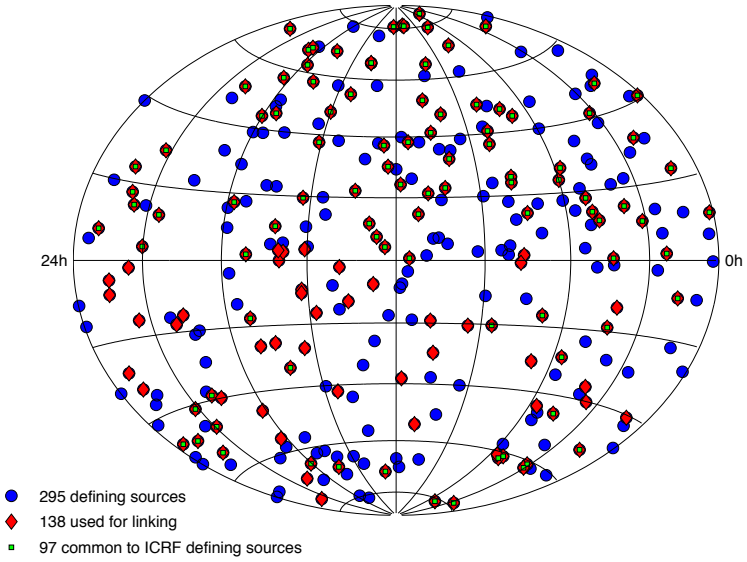

FIGURE 2.1: Distribution of VLBI sources defining the ICRF2 (second realization); taken from IERS Technical Report No. 35 [51].

the barycenter of the solar system, hence it is a Barycentric Celestial Reference System (BCRS). The coordinate time is the barycentric time t_{TCB}, see [178].

To relate celestial to terrestrial reference frames, a Geocentric Celestial Reference Frame (GCRS) is defined. It is non-rotating with respect to the BCRS and moves with the Earth's center of mass. The coordinate time is the geocentric time t_{TCG}. The transformation between the BCRS and the GCRS involves relativistic concepts, Lorentz transformations, in a first-order post-Newtonian approximation.

Terrestrial Reference Systems (TRS)

Terrestrial Reference Systems (TRS) are Earth-fixed and rotate with the Earth. Therefore they are of course non-inertial. The origin coincides with the Earth's center of mass. Due to these properties, TRS are best suited to describe geodetic surveys and dynamics close to the Earth's surface. They are also used for navigation systems such as GPS, Glonass and others. Ellipsoidal reference systems are special kinds of TRS, e.g., the GRS80 and WGS84 are particular examples of such systems [100, 128].

An important international TRS is the International Terrestrial Reference System (ITRS), which is realized by the International Terrestrial Reference Frame (ITRF) provided by the IERS. The coordinate time of the ITRS is the geocentric coordinate time t_{TCG}. A particular solution for the ITRF contains the station coordinates and motions of globally distributed geodetic observing stations, see Ref. [1]. In Fig. 2.2 we show the global distribution of the stations defining the ITRF.

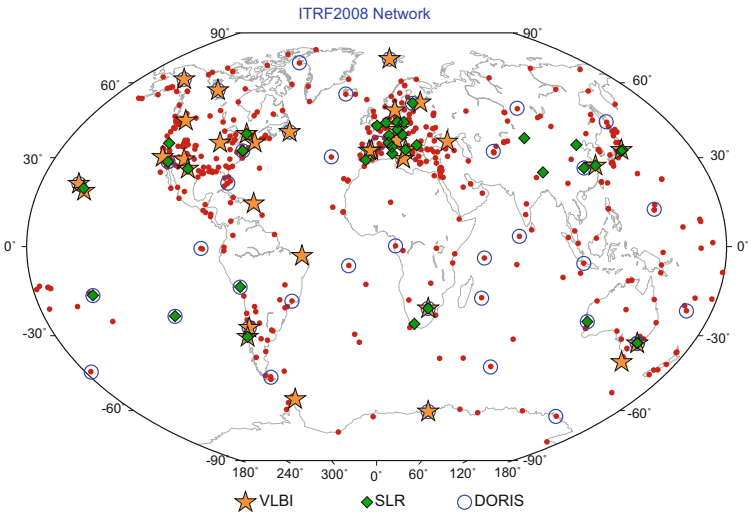

FIGURE 2.2: Distribution of stations defining the ITRF; taken from Ref. [1].

2.2.2 The geoid

Potentials, as scalar functions in space, can be visualized by their level sets. The equipotential surfaces are then always perpendicular to the gradient of the potential. Hence, such surfaces can be determined by interpolation of point-wise measurements of the direction of the gradient - the plumb line in the case of gravity. They might also be determined by a sufficiently detailed model of the scalar field and measurements which determine the model parameters - the Earth's multipole moments.

For observers on the rotating Earth, one particular equipotential surface of the gravity potential is of great importance: the geoid. Following the ideas of Gauss and Listing, we make the following definition:

The Earth's geoid is defined by the level surface of the gravity potential $W(\vec{X})$ which coincides best with the mean sea level, such that

$$-W(\vec{X})\big|_{\text{geoid}} = W_0 = \text{constant} \tag{2.17}$$

with a constant $W_0 = 6.263\,685\,60 \times 10^7\,\text{m}^2\,\text{s}^{-2}$, the numerical value that complies with modern conventions.

Hence, in mathematical terms, the Earth's geoid is the set of all points $\{(R, \Theta, \Phi)\}$ in $\mathbb{R}^3$ for which we have

$$-W(R,\Theta,\Phi) = \frac{GM}{R}\sum_{l=0}^{\infty}\sum_{m=0}^{l}\left(\frac{R_{\text{ref}}}{R}\right)^{l} P_l(\cos\Theta)\left[C_{lm}\cos(m\Phi) + S_{lm}\sin(m\Phi)\right] + \frac{1}{2}\omega^2 R^2\sin^2\Theta = W_0\,. \tag{2.18}$$

Note that the second part of the definition (2.17) above is to some extent inconsistent with the first part, see, e.g., [130]. Nevertheless, this is the modern definition and the nature of the inconsistency is elaborated below.

The force of gravity $\vec{g}$ is always perpendicular to the geoid and its direction is called the plumb line. Ground and space-based measurements such as SLR, GRACE, and GOCE contribute to the determination of the multipole moments C_{lm} and S_{lm}. Thereupon, the geoid surface can be determined as a solution of Eq. (2.18) once the value of W_0 is chosen. However, there is a conceptual difficulty here: on the one hand, the geoid is defined as the level surface where the gravity potential takes the value W_0. On the other hand, the value of W_0 is to be obtained by the evaluation of the gravity potential on the geoid, i.e. closest to mean sea level according to the first part of the definition. Now, we encounter an inconsistency regarding the following statements, see also Refs. [130, 168],

- The geoid is a level surface of the gravity potential W such that this surface is closest to mean sea level.
- The gravity potential W takes the value W_0 on the geoid.
- The value W_0 can be defined to have a fixed value.

Besides the fact that the concept of "mean sea level" must again be clarified using some tide gauges; mean sea level "does not care about" W_0 being a defining constant or not. The following part is dedicated to shed some light on the involved concepts.

On the geopotential value W_0

To determine or define a suitable value for W_0, a variety of strategies can be pursued. The reasons behind any particular choice are mainly of philosophical nature, i.e. they seek to incorporate one or the other fundamental assumptions and differ mainly by the choice of which concepts are time-independent and which are dynamical. The geopotential value W_0 on the geoid

- can be determined by evaluating a gravity potential model on points at the mean sea level and taking a statistical average,

- can be chosen according to fulfill useful requirements and maintained to be constant over certain time scales,
- can be conventionally defined - as it is done nowadays - see, e.g., References [130, 168] for overview and explanations and [73, 74] for contemporary conventional values.

As indicated above, there is an inconsistency when more than one of the listed properties is to be realized. The contemporary agreed-upon value is

$$W_0 = 6.263\,685\,60 \times 10^7\,\mathrm{m^2\,s^{-2}}\,, \tag{2.19}$$

see, e.g., [168]. In Tab. 2.2, we list various best-estimate values for W_0 which were obtained for certain epochs. The corresponding references are given as well.

Before the year 2000, the value of W_0 was derived from various data sets and it was not constant. Multiple observations, including satellite data, were combined and the gravity potential reduced to the mean sea surface, incorporating ocean models and tide gauges, was obtained for a discrete set of points. In a statistical approach, mean sea surface values for the gravity potential allowed best estimates for W_0. In Fig. 2.3, we sketch the general idea: points P on the sea surface, provided by, e.g., satellite altimetry, are reduced by sea surface topography. The resulting points P_0 are assumed to describe the mean sea surface. Then, a gravity potential model is to be evaluated at a distributed set of points P_0 and, e.g., a least square evaluation yields best estimates for W_0. Moreover, at the shore the mean sea level can be obtained by time averaging. Via classical leveling, the geoid surface is used as a reference and coupled into local networks.

In 2000, however, the IAU convention promoted the parameter L_g to be a defining constant [97, 178]. The value

$$L_g = 6.969\,290\,134 \times 10^{-10} \tag{2.20}$$

TABLE 2.2: Conventional values for W_0, the gravity potential value defining the geoid. Data overview taken from Ref. [168] and references therein. The values of W_0 and L_g are linked by $L_g = W_0/c^2$. In the year 2000, the IAU declared L_g to be a defining constant.

Year	W_0 $[\mathrm{m^2\,s^{-2}}]$	**Ref.**	L_g	**Ref.**
1991	$6.263\,686\,0 \times 10^7 \pm 30$	[25]	$6.969\,291 \times 10^{-10} \pm 3 \times 10^{-16}$	[96]
1992	$6.263\,685\,65 \times 10^7 \pm 3$	[18]	$6.969\,290\,2 \times 10^{-10} \pm 3 \times 10^{-17}$	[61]
1995	$6.263\,685\,685 \times 10^7 \pm 1$	[17]	$6.969\,290\,3 \times 10^{-10} \pm 1 \times 10^{-17}$	[125]
1999	$6.263\,685\,60 \times 10^7 \pm 0.5$	[19, 74]	$6.969\,290\,134 \times 10^{-10}$	[97]

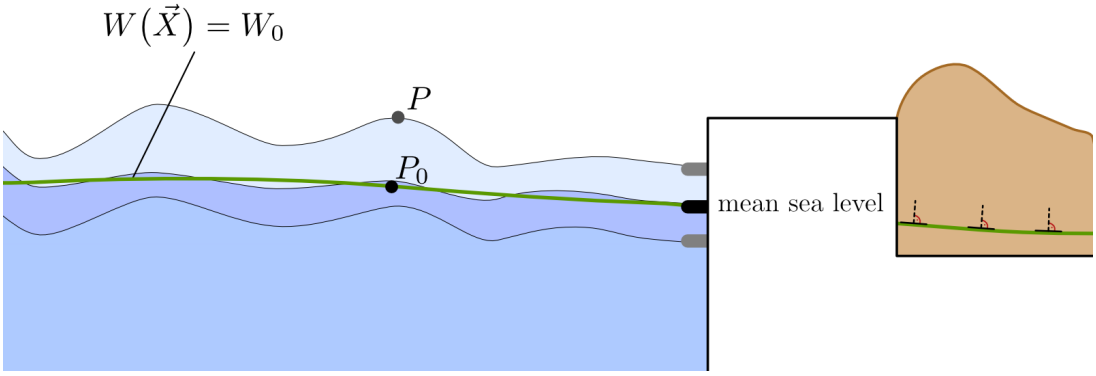

FIGURE 2.3: Determination of the geopotential W_0 defining the geoid.

was adopted in the IAU resolution. Since the relation between L_g and W_0 is given by

$$L_g = \frac{W_0}{c^2}\,, \tag{2.21}$$

the parameter W_0 becomes a derived constant with a value according to (2.19). The parameter L_g is introduced in the IAU conventions due to relativistic effects and it relates timescales of particular reference systems, see [97, 178, 103, 20] and section 6.1.3 in this work. The coordinate time t_{TCG} of the geocentric reference system GCRS is related to the proper time on the geoid by

$$\frac{\mathrm{d}t_{\mathrm{TT}}}{\mathrm{d}t_{\mathrm{TCG}}} =: 1 - L_g\,, \tag{2.22}$$

where the Terrestrial Time t_{TT} (proper time on the geoid) is usually realized by International Atomic Time t_{TAI} based on the SI-second. In sections 6.1 and 6.1.2, we come back this point and show how the relation between L_g and W_0 is embedded in a more general framework. The application to a first-order post-Newtonian setup as used in the IAU resolution is then a special case and yields the relation above.

From the viewpoint of relativistic gravity, however, we regard W_0 as a derived constant once L_g is conventionally defined. However, a self-consistent resolution of the problem, preferably in a general relativistic framework, is still to be worked out. We will come back to this point in later sections, after defining the relativistic geoid and related notions in the framework of General Relativity.

On the existence of a time-independent geoid

As shown in Ref. [145], there are three requirements which guarantee the existence of a time-independent geoid. They are related to the Earth's rigid motion, constant rotation, and absence of external forces and have analogs in the general relativistic

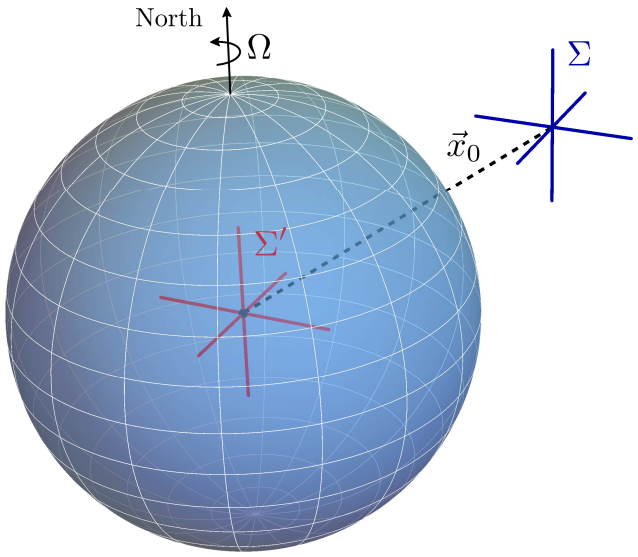

FIGURE 2.4: Reference systems for the definition of the Newtonian geoid. We need two reference systems for a derivation of the conditions for the existence of a time-independent geoid: an inertial reference system Σ and a co-rotating, and therefore non-inertial, Earth-fixed reference system Σ'.

description in terms of isometric congruences and their properties. In the following, we recall and investigate these existence conditions.

Various time-dependent phenomena as well as interior and exterior dynamics cause the Earth and its geoid to be dynamical as well. Hence, the geoid surface in reality is not strictly constant. The same is true for the Earth's angular velocity and rotation axis, see, e.g., the textbook [188] and Ref. [189] for an overview of influences on the dynamical Earth. All temporal variabilities and dynamics should be treated as perturbations of a time-independent (stationary) geoid. Only in this way, the geoid can serve as a constant reference to describe all these phenomena. Physical effects that must be treated in that way include, among others, the intrinsic time dependence of the mass multipoles, tidal effects, anelastic deformations, friction, ocean loading and sea surface dynamics, atmospheric effects, mass variations in the hydrosphere and cryonosphere, postglacial mass variations, interior dynamics of the Earth, and the influence of other solar system objects.

However, for the existence of a time-independent geoid, we make the following three idealizing assumptions:

(A1): The Earth is in rigid motion.

(A2): The Earth rotates with constant angular velocity about a fixed rotation axis.

(A3): There are no external forces acting on the Earth.

Note that the assumption (A3) explicitly excludes the time-independent deformations caused by other gravitating bodies, the so-called "permanent tides", see, e.g., Ref. [188]. Just as the time-dependent variations mentioned above, they may be considered as perturbations at a later stage.

In conventional geodesy, different notions of the geoid are known and commonly used. Their difference is mainly due to the implementation of permanent and time-dependent tidal effects. Three different geoid conventions are

- the mean geoid,
- the non-tidal geoid,
- and the zero-geoid,

see Refs. [21, 46, 47, 161, 188]. Since by assumption (A3), we exclude all the influences of external forces by exterior objects - in particular the sun and moon for the most dominant effects - we refer to the concept of the non-tidal (also called tide-free) geoid. Also, later on in chapter 4, we define a relativistic generalization with respect to this notion. The assumptions (A1), (A2), and (A3) guarantee the existence of the time-independent potential W as given in Eq. (2.17); the geoid is then defined as the time-independent surface $W(\vec{X}) = W_0$ with the constant W_0 chosen by an appropriate convention, as indicated above.

Now, we rewrite the three assumptions in a more mathematical way that allows the comparison with the relativistic versions of these requirements later. Let Σ be an inertial reference system and Σ' another non-inertial reference system attached to a rigidly moving Earth, see Fig. 2.4 for a sketch of the situation. The transformation behavior for the coordinates in both systems can be described as follows

$$\vec{x} = \vec{x}_0(t) + \boldsymbol{R}(t)\,\vec{x}\,', \tag{2.23}$$

where $\boldsymbol{R}(t)$ is an orthogonal rotation matrix that describes the momentary rotation (direction and magnitude) of the Earth about an axis through its center of mass. Furthermore, $\vec{x}_0(t)$ is the position vector of the Earth's center of mass in the reference system Σ.

Since the rotation matrix is orthogonal, $\boldsymbol{R}(t)^{-1} = \boldsymbol{R}(t)^T$, we know that the derived matrix

$$\boldsymbol{\omega}(t) = \dot{\boldsymbol{R}}(t)\,\boldsymbol{R}(t)^{-1} \tag{2.24}$$

is antisymmetric by definition. Using Eq. (2.23), we now find for the velocity

$$\vec{v} = \dot{\vec{x}} = \dot{\vec{x}}_0 + \boldsymbol{\omega}\,(\vec{x} - \vec{x}_0)\,. \tag{2.25}$$

Here, the overdot denotes a derivative with respect to the time t, keeping $\vec{x}\,'$ fixed. Successive differentiation allows to calculate also the acceleration $\vec{a}$ and its change $\dot{\vec{a}}$,

$$\vec{a} = \dot{\vec{v}} = \ddot{\vec{x}}_0 + \dot{\boldsymbol{\omega}}\,(\vec{x} - \vec{x}_0) + \boldsymbol{\omega}\,(\vec{v} - \dot{\vec{x}}_0)\,, \tag{2.26a}$$

$$\dot{\vec{a}} = \dddot{\vec{x}}_0 + \ddot{\boldsymbol{\omega}}\,(\vec{x} - \vec{x}_0) + 2\,\dot{\boldsymbol{\omega}}\,(\vec{v} - \dot{\vec{x}}_0) + \boldsymbol{\omega}\,(\vec{a} - \ddot{\vec{x}}_0)\,. \tag{2.26b}$$

The three assumptions (A1), (A2), and (A3) can now be recast one by one to imply the following conditions

(A1') The velocity gradient $\nabla \otimes \vec{v}$ is antisymmetric.

(A2') The time derivative of the matrix $\boldsymbol{\omega}$ vanishes $\dot{\boldsymbol{\omega}} = 0$.

(A3') The change of the acceleration is purely caused by the rotation $\dot{\vec{a}} = \boldsymbol{\omega}\,\vec{a}$.

Proof: Eq. (2.25) for the velocity means that the assumption of rigid motion implies (A1') by definition. Moreover, assumption (A2) obviously requires $\dot{\boldsymbol{\omega}}$ to be zero; therefore condition (A2') follows directly. Lastly, assumption (A3) implies that $\ddot{\vec{x}}_0(t) = \vec{0}$. This means that we can always choose the inertial system Σ such that the vector relating the origins is the zero-element of the vector space, $\vec{x}_0 = \vec{0}$. Together with Eq. (2.26b) and condition (A2') we finally obtain condition (A3').

The three conditions (A1'), (A2'), and (A3'), which are necessary for defining a time-independent geoid of an isolated Earth model in the Newtonian theory, have natural analogs in the relativistic theory as we will outline in chapter 4.

2.2.3 Lowest order multipole contributions to the geoid

We end this section on the geoid by investigating the lowest order contribution due to the first two multipole moments. Hence, in this simplified model, we stop the summation in Eq. (2.18) at $l = 2$ and consider only the Earth's monopole and quadrupole. Therefore, the gravity potential is

$$\begin{aligned} W(R,\Theta,\Phi) = &- \frac{GM}{R}\sum_{l=0}^{2}\sum_{m=0}^{l}\left(\frac{R_{\text{ref}}}{R}\right)^{l} P_l(\cos\Theta)\,[C_{lm}\cos(m\Phi) + S_{lm}\sin(m\Phi)] \\ &- \frac{1}{2}\omega^2 R^2 \sin^2\Theta\,, \end{aligned} \tag{2.27}$$

and the geoid in this model is given by $\{(R,\Theta,\Phi) : -W(R,\Theta,\Phi) = W_0\}$. However, since we assume that the origin of the coordinate system coincides with the center of mass, we have $C_{10} = 0$, $C_{11} = 0$, and $S_{11} = 0$ in addition to S_{00} and S_{10}, which vanish by convention. Hence, the only parameters left are ($C_{11} = 1$) C_{20}, C_{21}, C_{22} as well as S_{21} and S_{22}. In Tab. 2.3, we show the value of these parameters for two gravity field models: the zero-tide model GOCO05s [124, 135] and the tide-free EGM96 gravity field

TABLE 2.3: Parameters in a simple Earth gravity field model up to $l = 2$. Data taken from the satellite-only gravity field model GOCO05s [124, 135] (zero-tide) and the EGM96 gravity field model [117] (tide-free).

Quantity	**GOCO05s (zero-tide)**	**EGM96 (tide-free)**
GM	$3.9860044150 \times 10^{14}\,\mathrm{m}^3/\mathrm{s}^2$	$3.986004415 \times 10^{14}\,\mathrm{m}^3/\mathrm{s}^2$
R_{ref}	$6378136.3000\,\mathrm{m}$	$6378136.300\,\mathrm{m}$
C_{20}	$-4.841694552725 \times 10^{-4}$	$-4.84165371736 \times 10^{-4}$
C_{21}	$-3.387892504353 \times 10^{-10}$	$-1.86987635955 \times 10^{-10}$
S_{21}	$1.450327268364 \times 10^{-9}$	$1.19528012031 \times 10^{-9}$
C_{22}	$2.439357196868 \times 10^{-6}$	$2.43914352398 \times 10^{-6}$
S_{22}	$-1.400303490705 \times 10^{-6}$	$-1.40016683654 \times 10^{-6}$

model [117]. Note that the combination GM, known as the Earth's gravity constant, can be measured to much higher accuracy than the each of the individual values for G and M. However, we notice two things: firstly, the tide system has a slight influence on the values of the parameters. Transformation equations between the tide systems are known, see [46, 190]. Secondly, these values are fully normalized, i.e. they must be multiplied by a factor

$$\sqrt{\frac{(2l+1)(l-m)!}{n(l+1)!}}\,, \quad n = 1 \;\text{ for }\; m = 0 \quad \text{and} \quad n = 2 \;\text{ for }\; m \neq 0 \tag{2.28}$$

to give the values that can be inserted into the model (2.27). Moreover, we see that the Earth's quadrupole moment $C_{20} = J_2$ has the largest influence. Therefore, we may further simplify our model to a quadrupolar gravity field described by Eq. (2.16).

Now, the gravity potential is axisymmetric; it depends only on the coordinates R and Θ, and all its level surfaces share this property. Since for a quadrupolar geoid we have

$$\mathrm{d}W\big|_{\mathrm{geoid}} = \partial_R W\,\mathrm{d}R + \partial_\Theta W\,\mathrm{d}\Theta\big|_{\mathrm{geoid}} = 0\,, \tag{2.29}$$

we obtain

$$\frac{\mathrm{d}R}{\mathrm{d}\Theta}\bigg|_{\mathrm{geoid}} = -\,\frac{\partial_\Theta W}{\partial_R W}\bigg|_{R=R(\Theta)}\,, \tag{2.30}$$

and integration yields the geoid surface in terms of $R = R(\Theta)$, provided an initial value $R_0 = R(\Theta_0)$ is given as a solution of $W(R_0, \Theta_0) = W_0$. We have calculated the Newtonian geoid and gravity on the geoid's surface in this quadrupolar model using the data in Tab. 2.3 for the EGM96 model. The results are shown in Figures 2.5 and 2.6. We clearly see the main features: the geoid has an oblate spheroidal shape and gravity is stronger at the poles, decreasing towards the equator. A best fit ellipsoid of revolution, see next section, for the geoid surface in this model gives the following

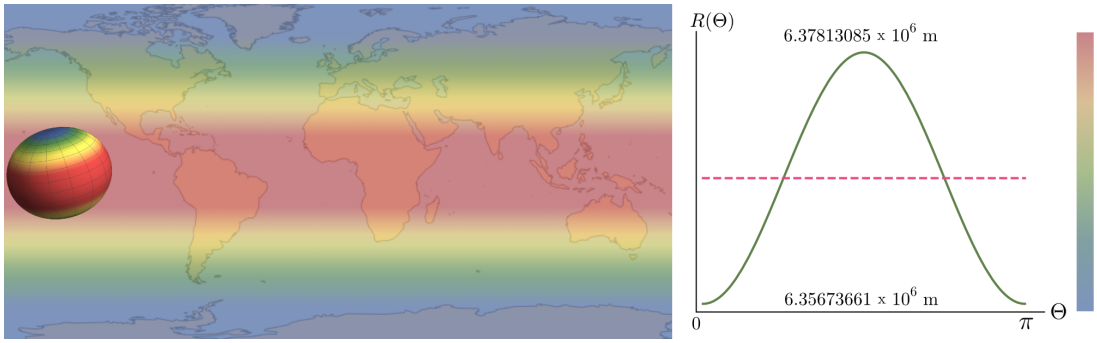

FIGURE 2.5: The Newtonian geoid in our simple quadrupolar model (2.16). We show the angular dependence in a color coded plot (left) and the plot $R(\Theta)$ (right). R is the geoid radius and Θ the polar angle in a spherical coordinate system centered at the Earth's COM. We have marked the minimal radius (at the poles) and maximal radius (in the equatorial plane). The mean value is $6.36742860 \times 10^6\,\mathrm{m}$ and it is marked by the dashed line. This quadrupolar geoid model will serve as a reference to obtain the magnitude of relativistic corrections later.

values:

$$a = 6.378\,139 \times 10^6\,\mathrm{m}\,, \quad b = 6.356\,745 \times 10^6\,\mathrm{m}\,, \quad 1/f = 298.125\,. \tag{2.31}$$

The values for the axes are only about $3 \times 10^{-5}\,\%$ off compared to the WGS84 values for the reference ellipsoid, see Ref. [100] and Tab. 2.4. The difference is due to the neglected influence of all higher moments. However, the error in the inverse flattening amounts to about $4 \times 10^{-2}\,\%$. Including higher order axially symmetric moments J_{n0} up to $n = 5$ improves the accuracy for the axes to about $6 \times 10^{-6}\,\%$ and for the flattening to about $1 \times 10^{-2}\,\%$ compared to WGS84 values.

Clearly, our simplified quadrupolar model for the gravitational field does not capture azimuthal and local structures, but it serves as a crude model to depict basic properties of the gravity field and its dominant behavior related to J_2. Relativistic generalizations of such a quadrupolar model will be discussed in later sections of this work.

2.2.4 The reference and level ellipsoid - Normal gravity

Since the geoid surface in general is enormously complex and can not be described by a simple mathematical surface model, the question of how this surface can be approximated in the best way arises naturally. "In the best way" means, of course, with respect to operational applicability for complicated observations as well as mathematical simplicity. It shall be as complex as necessary but as simple as possible at the same time.

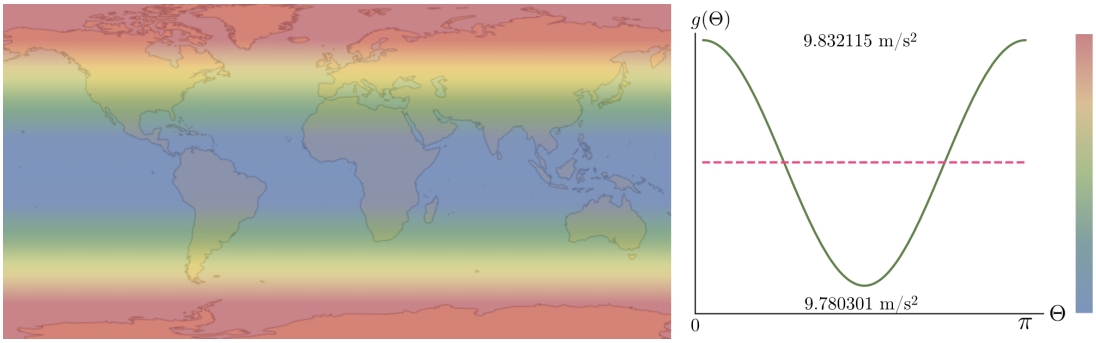

FIGURE 2.6: Gravity on the Newtonian geoid in our simple quadrupolar model (2.16). We show the angular dependence in a color coded plot (left) and the plot $g(\Theta)$ (right). Here, $g = ||\vec{\nabla} W||_2$ is gravity (magnitude) which Earth-fixed co-rotating observers experience, and Θ is the polar angle in a spherical coordinate system in $\mathbb{R}^3$, centered at the Earth's COM. We have marked the minimal value (in the equatorial plane) and maximal value (at the poles). The mean value is $9.806307\,\mathrm{m/s^2}$ and is marked by the dashed line.

The most simple approximation of the geoid surface is a sphere. This reference sphere can either be determined as the best fit to the geoid or as the sphere of which the radius is the mean geoid radius, or the sphere of which the area (or volume) coincides with the one of the geoid, respectively. However, this spherical model is still too simple; subtracting it from the full expression leaves large quadrupolar contributions, causing the flattening of the geoid, which dominate all other influences; see the last section.

The reference ellipsoid

The next approximation level, due to the features exhibited in the last section regarding the flattening of the geoid, is to introduce an ellipsoid of revolution. Such a geometric figure is uniquely determined by specification of two parameters, e.g., the semi-major and the semi-minor axes. The particular ellipsoid that fits best to the actual geoid is called the Earth's reference ellipsoid. It serves as the reference for coordinate systems related to angles measured from the axes and heights measured along the surface normal. Modern observations and space missions such as GPS are described in coordinate systems derived in this manner, e.g., using the GRS80 and WGS84 [100, 128]. See appendix A for details on ellipsoid coordinates and related quantities. Now, we make the following definition for the geometrical reference ellipsoid of the Earth:

The Earth's reference ellipsoid is a bi-axial ellipsoid of revolution that is a best fit to the Earth's geoid. It is a geometrical concept and conventionally defined by specification of any two defining parameters taken from the set $\{a, b, f, e\}$, where we have the semi-major axis a, the semi-minor axis b, the flattening f, and the eccentricity e.

Note, however, that also any other geometrical quantity for the description of an ellipsoid of revolution, derived from the set $\{a, b, f, e\}$, can be used for the definition. The main point is just to use two independent defining parameters and, in our understanding, the given set consists of the primary ones related to observations.

Points on the reference ellipsoid can be described by two angles. One of them is usually taken to be the geocentric longitude, which is called Φ in this work since it can be made to coincide with the azimuthal angle in spherical coordinates. Besides geocentric latitude, the geodetic latitude and the reduced latitude are commonly used, see, e.g., [95, 188] and appendix A for details. Introducing the height above the ellipsoid's surface in direction of the surface normal as a third coordinate, we obtain a suitable three-dimensional coordinate system adapted to the symmetry.

The level ellipsoid and normal potential

The reference ellipsoid defined above - a bi-axial ellipsoid of revolution, is a geometric concept, a best fit approximation of the geoid. Now, we proceed one step further to obtain a good approximative description of the gravity field itself. To do so, we introduce the level ellipsoid and the normal potential.

Let a reference ellipsoid be also a particular equipotential surface of an artificial gravity potential $W_N(\vec{X})$. Then, we call it a level ellipsoid and make the following definition.

The Earth's normal gravity potential $W_N(\vec{X})$ is uniquely defined by (i) postulating that the reference ellipsoid is also a level ellipsoid, i.e. that it is an equipotential surface of $W_N(\vec{X})$, and (ii) the parameters for GM and ω, where M is the total mass of the Earth and ω its angular velocity. The value of $|W_N|$ on the level ellipsoid is the geopotential value W_0.

Hence, we need four parameters to define the normal potential: two parameters for the geometry of the level ellipsoid as well as GM and ω. This is in agreement with the theorem of Stokes-Poincaré[5]. However, all other level surfaces of the normal potential, except the level ellipsoid, will not have the shape of ellipsoids of revolution and the actual mass distribution is unknown and far from being trivial - if even physically realizable. For obvious reasons, the normal gravity potential must be axisymmetric.

[5]The theorem of Stokes-Poincaré states that the exterior gravity field of an object with total mass M which rotates around a fixed rotation axis with constant angular velocity ω and a level surface S that encloses the entire mass is uniquely determined by the parameters defining S and the pair (M, ω). The proof involves Dirichlet's principle and can be found, e.g., in the textbook [95].

We can split it into gravitational parts $U_N(\vec{X})$ and centrifugal parts $V(\vec{X})$ according to

$$W_N(\vec{X}) = U_N(\vec{X}) + V(\vec{X}) = U_N(\vec{X}) - \frac{1}{2}\omega^2 R^2 \sin^2\Theta\,. \tag{2.32}$$

Hence, if we subtract it from the full gravity potential,

$$W(\vec{X}) - W_N(\vec{X}) = U(\vec{X}) - U_N(\vec{X}) =: T(\vec{X})\,, \tag{2.33}$$

the result does not contain centrifugal terms anymore and is known as the disturbing potential $T(\vec{X})$.

The normal potential can be expanded in a series of harmonic functions. The easiest representation is to use ellipsoidal harmonics, which are obviously adapted to the symmetry. Using coordinate transformations, we can also obtain a representation in terms of spherical harmonics; see, e.g., Refs. [95, 188]. In harmonic ellipsoidal coordinates (u, β, Φ) the gravitational part U_N of the normal potential is

$$U_N(u,\beta) = -\left(\frac{GM}{E}\tan^{-1}\frac{E}{u} + \frac{1}{3}\omega^2 a^2 \frac{q}{q_0} P_2(\sin\beta)\right)\,, \tag{2.34}$$

where a and b are the level ellipsoid's semi-major and semi-minor axes, respectively, and $E = \sqrt{a^2 - b^2}$ is the linear eccentricity. The abbreviations q and q_0 are defined by

$$q = \frac{1}{2}\left[\left(1 + 3\frac{u^2}{E^2}\right)\tan^{-1}\frac{E}{u} - 3\frac{u}{E}\right]\,, \tag{2.35a}$$

$$q_0 = q|_{u=b}\,. \tag{2.35b}$$

See the appendix A for definitions of the coordinate systems and relations of ellipsoid parameters.

We can also express the centrifugal potential in harmonic ellipsoidal coordinates

$$V(u,\beta) = -\frac{1}{2}\omega^2(u^2 + E^2)\cos^2\beta\,, \tag{2.36}$$

and use the second Legendre polynomial P_2 to finally obtain the normal gravity potential

$$W_N(u,\beta) = -\left(\frac{GM}{E}\tan^{-1}\frac{E}{u} + \frac{1}{2}\omega^2 a^2 \frac{q}{q_0}\left(\sin^2\beta - \frac{1}{3}\right) + \frac{1}{2}\omega^2(u^2 + E^2)\cos^2\beta\right)\,. \tag{2.37}$$

We can see that the normal potential is indeed axisymmetric since Eq. (2.37) does not depend on Φ. On the level ellipsoid ($u = b$), we have the relation

$$-W_N(b,\beta) = W_0 = \frac{GM}{E}\tan^{-1}\frac{E}{b} + \frac{1}{3}\omega^2 a^2\,. \tag{2.38}$$

In a spherical harmonic expansion we have

$$W_N(R,\Theta) = -\frac{GM}{R}\sum_{l=0}^{\infty} J_{2l}\left(\frac{a}{R}\right)^{2l} P_{2l}(\cos\Theta) - \frac{1}{2}\omega^2 R^2\sin^2(\Theta)\,, \tag{2.39}$$

where the multipole moments of the expansion of the normal gravity potential follow the scaling behavior

$$J_0 = 1\,,\quad J_{2l} = (-1)^l\frac{3(E/a)^{2l}}{(2l+1)(2l+3)}\left(1 - l - 5l\frac{a^2}{E^2}J_2\right)\,,\quad \forall\, l > 1\,. \tag{2.40}$$

Furthermore, the relation

$$J_2 = -\frac{1}{3}\frac{E^2}{a^2}\left(1 - \frac{2}{15}\frac{\omega^2 a^2 E}{GMq_0}\right) \tag{2.41}$$

can be derived. Thereupon, two parameters of the set

$$\{a, b, f, E, e, W_0, J_2\} \tag{2.42}$$

together with ω and GM uniquely determine the normal gravity potential. The choice can be made according to different philosophies. As can be seen in Tab. 2.4, the GRS80 and the WGS84 make different choices for the sets of defining parameters. A purely gravitationally inspired choice is, e.g., to take the set $\{\omega, GM, W_0, J_2\}$, which to our understanding is also discussed in the geodetic community. However, if W_0 is in fact derived from the defined constant L_g, then the set of parameters defining the normal gravity potential actually reads $\{\omega, GM, L_g, J_2\}$.

We close this section by defining normal gravity γ as the norm of the gradient of the normal potential, i.e.

$$\vec{\gamma} := -\vec{\nabla}W_N\,,\quad \gamma = ||\vec{\gamma}||_2\,. \tag{2.43}$$

2.2.5 Geodetic Reference Systems (GRS)

Geodetic Earth models are approximations of the geoid (in terms of a reference ellipsoid) as well as the exterior gravity field of the Earth (in terms of a normal potential). Geodetic reference systems are geodetic Earth models with a particular set of parameters that are assumed to be conventionally adapted as standards. They are geocentric

TABLE 2.4: A comparison of the geodetic reference frames GRS80 and WGS84 in terms of their respective defining parameters.

Quantity	**GRS80**	**WGS84**
GM	$3.986005 \times 10^{14}\,\mathrm{m}^3/\mathrm{s}^2$	$3.986004418 \times 10^{14}\,\mathrm{m}^3/\mathrm{s}^2$
a	$6.378137 \times 10^{6}\,\mathrm{m}$	$6.378137 \times 10^{6}\,\mathrm{m}$
J_2	-1.08263×10^{-3}	
ω	$7.292115 \times 10^{-5}\,\mathrm{rad/s}$	$7.292115 \times 10^{-5}\,\mathrm{rad/s}$
f		$1/298.257223563$

reference systems, co-rotating with the Earth, and provide a good approximation of the real gravity field of the Earth and the geoid. In other words, in our understanding geodetic reference systems comprise a geometrically defined and oriented reference ellipsoid and an associated normal potential, such that the reference ellipsoid is used as a level surface of the normal potential. Hence, we need in total four parameters to define a geodetic reference frame as a realization of the reference system: the two parameters defining the ellipsoid and two parameters to define the total mass and the angular velocity in the normal potential. Instead of the total mass M, usually the product GM, which can be measured more accurately, is used. The orientation and origin must be fixed by the definition of the respective reference system.

Examples of such geodetic reference systems are, e.g., the GRS80 [128] and the WGS84 [100], see also Ref. [95] for a clear explanation of these systems. The ellipsoid of WGS84 uses the geoid of the gravity field model EGM96 [117]. In Table 2.4, we list the defining parameters in the respective realization of both reference systems, the GRS80 reference frame and the WGS84 reference frame. For the GRS80, the four defining constant are (GM, a, J_2, ω), whereas for WGS84 in its most recent version the defining constants are (GM, a, f, ω).

In Ref. [161] and Ref. [102] defining constants for historically used reference ellipsoids can be found in an overview table.

2.3 Height measurements

2.3.1 Height concepts and common understanding

In geodesy, there are different concepts for the height of points on and above or below the Earth's surface; they differ on the reference surface with respect to which the height is measured and the direction of measurement (e.g., the normal direction w.r.t. the reference surface). Four height concepts, which are

- Orthometric height H (above the geoid)

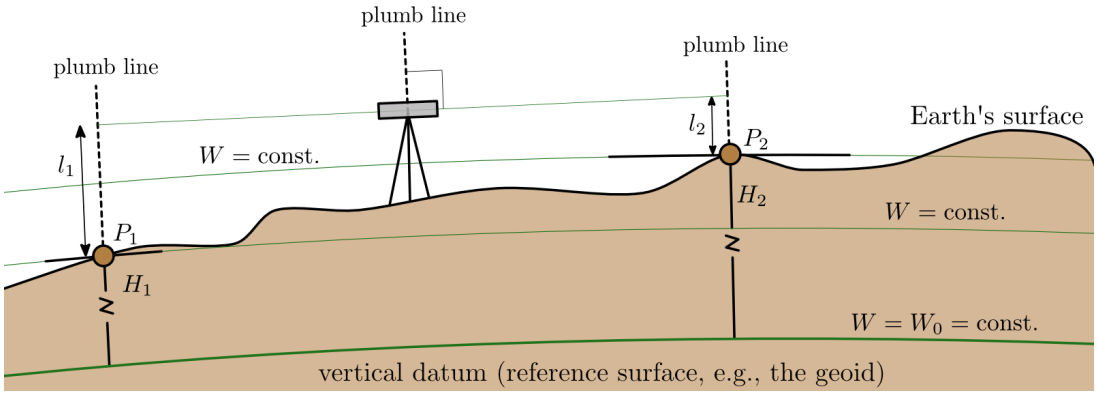

FIGURE 2.7: The principle idea of leveling to determine the height difference H_{12} between points P_1 and P_2.

- Ellipsoid height h (above the level ellipsoid)
- Normal height H_{N} (above the quasi-geoid)
- Dynamic height H_{D} (no geometric interpretation)

are of particular importance. These concepts will be explained briefly in the following, for details we refer to the standard literature, e.g., Refs. [95, 188].

The orthometric height H is the height above the geoid, measured along the true curved plumb line, and coincides with the common understanding of height above sea level. The ellipsoidal height h is the height above the level ellipsoid, measured along the ellipsoid's surface normal. Normal height H_{N} and dynamic height H_{D} are somewhat more abstract concepts and will be explained below.

Let us start by recalling the idea of classical leveling first. As shown in Fig. 2.7, the two rods are positioned vertically (in direction of the plumb line) and the leveling instrument is adjusted horizontally (perpendicular to the plumb line). The height differences $\delta H_{12} = l_1 - l_2$ between points P_1 and P_2 is to be determined. If the points are not close to each other, multiple leveling steps are performed in between and the height differences are summed up. However, if we were to measure in a closed leveling loop, i.e. returning to the point P_1 after several successive leveling measurements, the height will in general not be zero and we encounter the problem of misclosure - even if we had infinite accuracy at our disposal. This misclosure is due to the non-parallelism of the equipotential surfaces of the gravity field and becomes clear following the mathematical explanation below.

2.3.2 Geopotential numbers and height definitions

We know that for the gravity potential we have[6]

$$\mathrm{d}W = g\,\mathrm{d}n\,, \tag{2.44}$$

where n is the normal direction w.r.t. equipotential surfaces of W. Therefore, we have

$$\int_{P_1}^{P_2} \mathrm{d}W = W_2 - W_1 = \int_{P_1}^{P_2} g\,\mathrm{d}n\,. \tag{2.45}$$

We further have, of course,

$$\int_{P_1}^{P_1} g\,\mathrm{d}n = \oint g\,\mathrm{d}n = W_1 - W_1 = 0\,, \tag{2.46}$$

whilst

$$\oint \mathrm{d}n \neq 0\,. \tag{2.47}$$

The two equations above represent the problem of the misclosure of closed leveling loops which was mentioned above. The mathematical explanation is related to the differential $g\,\mathrm{d}n$, which is an exact form (or perfect differential), whereas $\mathrm{d}n$ is not. Hence, the misclosure is a property of the missing integrating factor g which makes $g\,\mathrm{d}n$ exact.

Now, let a point P_0 be positioned on the geoid, i.e. at zero orthometric height. Then, we have for a second point P above the geoid

$$\int_{P_0}^{P} g\,\mathrm{d}n = W_P - W_{P_0} = W_P + W_0 = W_0 - |W_P| =: C_P\,, \tag{2.48}$$

where C_P is called the geopotential number. It is assumed to be always positive, and we refer, again, to our (physical) sign convention which differs from common geodesy conventions. In the latter case, the order of the potential terms in (2.48) must be changed. We have also inserted the potential value on the geoid, where $W|_{\mathrm{geoid}} = -W_0$.

[6] Note that we follow the negative sign convention for the potential, i.e. W is negative everywhere outside the Earth with the limit $W \to 0$ at infinity.

The number C_P can, in principle, be calculated by integrating gravity g along the curved plumb line,

$$C_P = H_P \frac{1}{H_P} \int_0^{H_P} g \, \mathrm{d}H =: H_P \, \bar{g} \,, \tag{2.49}$$

where we define the average gravity $\bar{g}$ along the path of integration, i.e. the average gravity along the plumb line from P_0 to P. Hence, the orthometric height can finally be given by

$$H_P = \frac{C_P}{\bar{g}} \,, \tag{2.50}$$

and it can be determined if the geopotential number of the point P of interest as well as the average gravity along the plumb line from P_0 to P are known.

Approximating the true gravity field W by the normal gravity field W_N, an analog equation for the normal height H_N can be derived

$$H_\mathrm{N} = \frac{C}{\bar{\gamma}} \,, \tag{2.51}$$

where $\bar{\gamma}$ is the average of normal gravity,

$$\bar{\gamma} = \frac{1}{H_\mathrm{N}} \int_0^{H_\mathrm{N}} \gamma \mathrm{d}H_\mathrm{N} \,, \tag{2.52}$$

calculated along the plumb line of the normal gravity field. The normal height is the distance, measured along the plumb line of the normal gravity field, between a point Q associated to P and the level ellipsoid. The point Q is obtained by following the plumb line of the normal gravity field until a point where W_N at Q is W_P. The surface formed by all points Q_i associated in this way to all surface points P_i is called the telluroid. The reference surface of the normal heights is the quasi-geoid, it is obtained by subtracting the normal heights from all surface points.

Finally, dynamic height H_D is defined by

$$H_\mathrm{D} = \frac{C}{\gamma_0} \,, \tag{2.53}$$

where γ_0 is some conventionally chosen normal gravity, usually at 45 deg latitude, and can be calculated from the defining parameters of a geodetic reference system. The dynamic height has, however, no intuitive geometrical interpretation - but is the easiest to calculate.

2.3.3 Geoid undulations, deflection of the vertical, height anomalies

The geoid undulation (geoid height) N is the vertical distance between the geoid and the level ellipsoid,

$$N := h - H\,, \tag{2.54}$$

where H is the orthometric height and h the ellipsoid height. Effects due to the curvature of the plumb linke are neglected in this definition. The difference

$$\zeta := h - H_{\mathrm{N}} \tag{2.55}$$

between the ellipsoid height and the normal height is called the height anomaly. The angular difference between the direction of the normal gravity $\vec{\gamma} = -\vec{\nabla}W_N$ (normal plumb line) and the gravity vector $\vec{g} = -\vec{\nabla}W$ (true plumb line) is called the deflection of the vertical, see Fig. 2.8. It gives information about how accurate the gravitational Earth model in terms of the normal potential is.

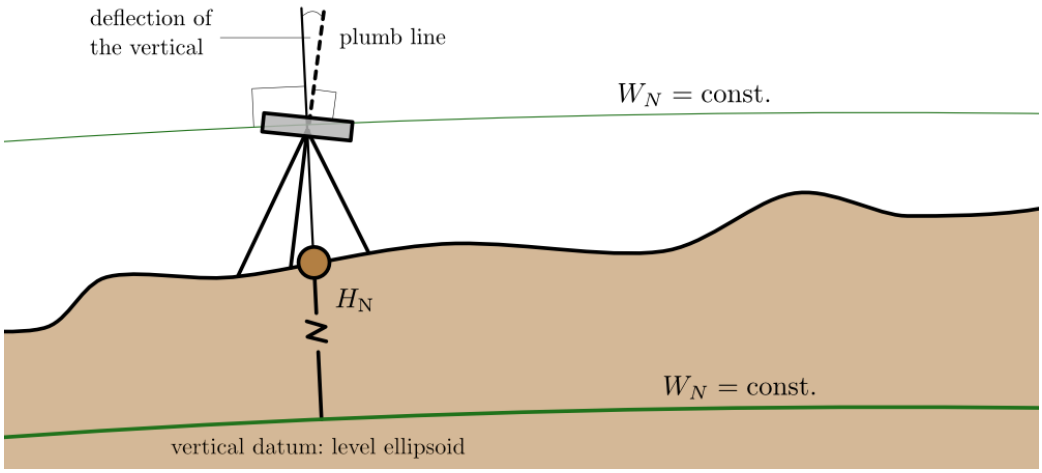

FIGURE 2.8: The deflection of the vertical: the angular difference between the normal plumb line and the gravity vector (true plumb line).

Chapter 3

General Relativity, Spacetime Models and Relativistic Concepts

3.1 Einstein's field equation and basic concepts

This section serves as a very brief introduction to General Relativity. However, it is actually more of a recapitulation of the most important concepts and its main purpose is to fix the notation. The focus lies on the introduction of some important exact solutions of Einstein's field equation that are of relevance for relativistic geodesy.

3.1.1 Spacetime

In contrast to Newtonian mechanics in Euclidean space $\mathbb{R}^3$, Special Relativity tells us that space and time merge to the concept of spacetime. Building on the principles of Special Relativity, which are still valid locally, General Relativity describes gravity as a curved spacetime geometry. Hence, the full apparatus of differential geometry is to be employed to obtain a clear mathematical formulation. Most of the following relations will be given without proof. We recommend the standard textbooks [127, 183, 165, 195] for details.

A general relativistic spacetime is a pair (M, g), consisting of a 4-dimensional manifold M and a Lorentzian metric g. The metric is a symmetric bilinear form and ensures that the spacetime is equipped with notions of length, volume, angles and so on. In a local chart, i.e. a locally valid coordinate system, the metric can be represented by its components $g_{\mu\nu}$. In a neighborhood of each event on spacetime, coordinates can be chosen such that the metric g becomes the Minkowski metric η,

$$(\eta_{\mu\nu}) = \mathrm{diag}(-1, 1, 1, 1)\,. \tag{3.1}$$

Here and in the following, we choose the signature convention $(-,+,+,+)$ for the metric. Greek indices are spacetime indices and take values 0 to 3, whereas Latin indices are spatial indices and take the values 1 to 3, and we employ Einstein's summation conventions throughout this work.

On spacetime, we have scalar fields, vector fields, covector fields, and general tensor fields of higher rank. We lower indices of contravariant tensor fields with the help of the metric

$$A_\mu = g_{\mu\nu} A^\nu \,, \tag{3.2}$$

and we raise indices of covariant tensor fields with the help of the inverse metric $g^{\mu\nu}$

$$B^\mu = g^{\mu\nu} B_\nu \,, \tag{3.3}$$

where the inverse metric is defined by

$$g_{\mu\nu} g^{\mu\sigma} = \delta^\sigma_\nu \,. \tag{3.4}$$

Here, δ^μ_ν is the Kronecker delta. Important examples of spacetime metrics and their respective properties are presented in the following sections.

3.1.2 The field equation

Einstein's field equation relates the geometry of spacetime to the sources of gravity. It reads

$$\mathcal{R}_{\mu\nu} - \frac{1}{2}\mathcal{R}\, g_{\mu\nu} + \Lambda g_{\mu\nu} = \kappa\, T_{\mu\nu} \,. \tag{3.5}$$

The field equation above contains all the necessary information to (i) calculate the curved spacetime geometry from the source distribution and (ii) to calculate to motion of the source elements in the curved spacetime. Here, $\kappa = 8\pi G/c^4$ is Einstein's gravitational constant, $\mathcal{R}_{\mu\nu}$ is the Ricci tensor, and its trace $\mathcal{R} = g^{\mu\nu} R_{\mu\nu}$ is the Ricci scalar. Λ is the cosmological constant. For the remainder of this work, we will ignore Λ since it is of no relevance for geodesy and local physics in the vicinity of the Earth. Its estimated value is $\Lambda \approx 10^{-52}\,\mathrm{m}^{-2}$ and, thus, it is not important on scales of about the size of the solar system. The Ricci tensor can be calculated by contraction of the Riemann curvature tensor

$$\mathcal{R}_{\mu\nu} = \mathcal{R}^\alpha{}_{\mu\alpha\nu} \,, \tag{3.6}$$

and the components of the curvature tensor $\mathcal{R}^{\mu}{}_{\nu\rho\sigma}$ in turn are given by non-linear combinations of first and second derivatives of the metric. In General Relativity, gravity is encoded and represented by the curvature of spacetime. Mathematically, curvature manifests itself in the change that a vector undergoes when it is parallel transported along a closed loop.

For vacuum, $T_{\mu\nu} = 0$ and the field equation (3.5) reduces to

$$R_{\mu\nu} = 0\,, \tag{3.7}$$

if we neglect the cosmological constant. This equation is particularly important since outside a central body such as the Earth, it must be fulfilled. In the next section, we will look at various examples of spacetime geometries, all of which solve the vacuum field equation above.

3.1.3 Important mathematical notation

In this section, we summarize the most important mathematical ingredients for this work, without proof or derivation.

Let an observer's worldline be described by $x^{\mu}(\tau)$, where proper time τ is defined by the normalization of the tangent vector to the observer's worldline,

$$g_{\mu\nu}\frac{\mathrm{d}x^{\mu}}{\mathrm{d}\tau}\frac{\mathrm{d}x^{\nu}}{\mathrm{d}\tau} = -c^2\,. \tag{3.8}$$

At any event P_0 in spacetime, the light cone can be constructed and yields a definition of the causal future and the causal past of P_0. With respect to P_0, other events can be characterized as being timelike, lightlike, or spacelike, i.e. they lie within the light cone, on the boundary of the light cone, or outside the light cone at P_0. We call a vector A^{μ} timelike if $g_{\mu\nu}A^{\mu}A^{\nu} < 0$, lightlike if $g_{\mu\nu}A^{\mu}A^{\nu} = 0$, or spacelike if $g_{\mu\nu}A^{\mu}A^{\nu} > 0$.

The scalar product of two vectors A^{μ} and B^{ν} with respect to the metric is denoted as

$$g(A,B) = g_{\mu\nu}A^{\mu}B^{\nu} = A^{\mu}B_{\mu} = A_{\nu}B^{\nu} =: \big\langle A, B\big\rangle\,. \tag{3.9}$$

In a local chart, the covariant derivative of a contravariant vector field is given by

$$A^{\mu}{}_{;\nu} := D_{\nu}A^{\mu} = \partial_{\nu}A^{\mu} + \Gamma^{\mu}{}_{\nu\sigma}A^{\sigma}\,, \tag{3.10}$$

and for a covector field we have

$$A_{\mu;\nu} := D_\nu A_\mu = \partial_\nu A_\mu - \Gamma^\sigma{}_{\mu\nu} A_\sigma \,, \tag{3.11}$$

where $\Gamma^\mu{}_{\nu\sigma}$ are the Christoffel symbols. In a local chart, they can be calculated from derivatives of the metric,

$$\Gamma^\mu{}_{\nu\sigma} = \frac{1}{2} g^{\mu\lambda} \left(\partial_\nu g_{\sigma\lambda} + \partial_\sigma g_{\nu\lambda} - \partial_\lambda g_{\nu\sigma} \right) . \tag{3.12}$$

For an arbitrary k-tensor $T_{\mu_1 \ldots \mu_k}$, the symmetrization and antisymmetrization are defined by

$$T_{(\mu_1 \ldots \mu_k)} := \frac{1}{k!} \sum_{I=1}^{k!} T_{\pi_I\{\mu_1 \ldots \mu_k\}}, \tag{3.13}$$

$$T_{[\mu_1 \ldots \mu_k]} := \frac{1}{k!} \sum_{I=1}^{k!} (-1)^{|\pi_I|} T_{\pi_I\{\mu_1 \ldots \mu_k\}}, \tag{3.14}$$

where the sum is taken over all possible permutations of the k indices, which we symbolically denote by $\pi_I\{\mu_1 \ldots \mu_k\}$.

3.1.4 Equation of motion

In General Relativity, the equation of motion for structureless test particles is given by the geodesic equation

$$\ddot{x}^\mu + \Gamma^\mu{}_{\nu\sigma} \dot{x}^\nu \dot{x}^\sigma = 0 \,, \tag{3.15}$$

where the overdot denotes the derivative with respect to some curve parameter, usually the proper time. For an overview of equations of motion in relativistic theories of gravity and involved concepts, we recommend Ref. [152]. The geodesic equation (3.15) is equivalent to the Euler-Lagrange equations for the Lagrangian

$$\mathcal{L} = \frac{1}{2} g_{\mu\nu} \dot{x}^\mu \dot{x}^\nu \,. \tag{3.16}$$

The canonical momenta are

$$p_\mu = \frac{\partial \mathcal{L}}{\partial \dot{x}^\mu} = g_{\mu\nu} \dot{x^\nu} \,, \tag{3.17}$$

and we can construct the Hamiltonian

$$\mathcal{H} = \frac{1}{2} g^{\mu\nu} p_\mu p_\nu \,, \tag{3.18}$$

which gives the geodesics as solutions to the well-known Hamilton equations of motion.

The trajectories of light rays can also be calculated by solving the geodesic equation (3.15) but with the normalization

$$g_{\mu\nu}\frac{\mathrm{d}x^\mu}{\mathrm{d}s}\frac{\mathrm{d}x^\nu}{\mathrm{d}s} = 0\,, \tag{3.19}$$

for an affine curve parameter s since the concept of proper time is meaningless for photons.

We denote the four-velocity of a particle (or photon) with worldline x^μ by

$$u^\mu = \dot{x}^\mu\,, \tag{3.20}$$

and the four-acceleration is

$$a^\mu = \ddot{x}^\mu = \dot{u}^\mu\,, \tag{3.21}$$

where the overdot denotes the derivative w.r.t. proper time for particles or, respectively, derivatives w.r.t. an affine curve parameter for photons.

3.2 Spacetime models

In this section, we introduce some important spacetime models and summarize their respective properties. These spacetimes will be used to apply relativistic geodetic notions in the respective geometry and serve as test scenarios to: (i) give some insight into how the developed concepts work and are to be applied explicitly, and (ii) yield estimates of relativistic effects as well as effective correction terms that are to be expected in observations.

In the following, we introduce the Schwarzschild spacetime [171], general static axisymmetric spacetimes [196], the particular example of the spacetime found be Erez and Rosen [48], the Kerr spacetime [107, 106], and the (parametrized) post-Newtonian spacetime [150]. We focus only on vacuum solutions of Einstein's field equation to approximate the spacetime outside a compact mass distribution, e.g., the Earth. We do not consider electrovacuum solution since a possible net charge is of no relevance for geodesy. However, spacetimes related to the exterior region of celestial objects should be matched to interior solutions at the physical surface of the respective object that is to be described. The search for interior solutions of well-known spacetimes has a long history since the presentation of the gravitational field equations. We do not consider this problem here; but refer in general to the standard reference on exact solutions [182].

3.2.1 Schwarzschild spacetime

The Schwarzschild spacetimes is the simplest, and probably best known, solution of Einstein's vacuum field equation. It was found by Karl Schwarzschild only shortly after the final form of the field equation was published. It describes the spacetime outside a spherically symmetry, and according to Birkhoff's theorem therefore also static, mass distribution. In the standard coordinates $(t, r, \vartheta, \varphi)$, the spacetime metric reads

$$g = -\left(1 - \frac{2m}{r}\right) c^2 \mathrm{d}t^2 + \left(1 - \frac{2m}{r}\right)^{-1} \mathrm{d}r^2 + r^2 \mathrm{d}\vartheta^2 + r^2 \sin^2\vartheta \mathrm{d}\varphi^2 \,. \tag{3.22}$$

Sometimes the angular part $\mathrm{d}\vartheta^2 + \sin^2\vartheta \mathrm{d}\varphi^2$, which is the Riemannian metric on a unit two-sphere, is abbreviated by $\mathrm{d}\Omega^2$. The parameter $2m$ is an abbreviation for the Schwarzschild radius $r_s := 2m$. The relation to the total mass of the source M, in SI-units, is given by

$$m = \frac{GM}{c^2} \,. \tag{3.23}$$

Hence, m is the mass of the source in geometric units. Note that the metric coefficients diverge at $r = r_s$ and a coordinate singularity is encountered. For stellar and planetary objects, the radius r_s lies in the interior and does not cause any problem at all since the metric (3.22) is not valid inside the body. For our sun, the Schwarzschild radius is about $(r_s)_\odot \approx 3 \times 10^3\,\mathrm{m}$, whereas for the Earth it is about $(r_s)_\oplus \approx 8.9 \times 10^{-3}\,\mathrm{m}$.

If, however, an object is compressed below the radius r_s, gravitational collapse leads to a black hole. In this case, the surface $r = r_s$ is an event horizon, separating the inner from the outer domain of communication and no signal can escape from regions $r < r_s$.

The radial coordinate r is called area-coordinate since spheres with coordinate radius $r = r_0$ have a surface area $4\pi r_0^2$. It should also be noted that the true distance L, measured with the metric, between two points r_1, r_2 on the radial line is not given by $r_2 - r_1$. One has to calculate this distance by

$$L = \int_{r_1}^{r_2} \sqrt{g_{rr}} \mathrm{d}r = \int_{r_1}^{r_2} \frac{1}{\sqrt{1 - 2m/r}} \mathrm{d}r \,. \tag{3.24}$$

The Schwarzschild spacetime has two important Killing vector fields ∂_t and ∂_φ. The latter is spacelike, whereas ∂_t is timelike and hypersurface-orthogonal everywhere. The geodesic equation, for test-particles and light rays in the Schwarzschild spacetime is, due to the spherical symmetry, solvable in terms of elliptic functions, see Refs. [54, 84, 32, 33]. The first analytic solution was presented by Forsyth in 1920 and in

Refs. [78, 80], a modern treatment extending the problem to include a cosmological constant[1] is found. Also the concept of the black hole shadow was investigated in the Schwarzschild spacetime. The shadow can be calculated analytically as shown in Ref. [71], and was also investigated for a black hole surrounded in a plasma [139]. The BlackHoleCam project is an exemplary collaboration looking for signatures of the shadow of our galaxy's black hole [64].

Analyzing the orbits and worldlines of light and test-particles, some particularly important relativistic effects can be calculated: the Shapiro-delay, the bending of light, and the perigee precession. Using the Schwarzschild spacetime as an approximation to describe the exterior geometry around the Earth, estimates for these relativistic effects are obtained. To do so, the gravity constant of the Earth GM must be used to calculate the parameter m in the metric (3.22).

3.2.2 General Weyl spacetimes

Weyl spacetimes[2] are a class of axisymmetric and static solutions to Einstein's field equation. Here, we only consider vacuum solutions and dismiss the case of electrovacuum since it is of little relevance for geodesy.

All axisymmetric static spacetime geometries that solve Einstein's vacuum field equation can be described by the Weyl metric

$$g_{\mu\nu}dx^\mu dx^\nu = -e^{2\psi}c^2dt^2 + e^{-2\psi}\rho^2 d\varphi^2 + e^{-2\psi}e^{2\gamma}(d\rho^2 + dz^2)\,, \tag{3.25}$$

where (t, ρ, z, φ) are Weyl's canonical coordinates, see the original article [196]. Both metric functions, ψ and γ, depend only on the coordinates ρ and z; axisymmetry is assured by φ-independence.

Some well-known examples of Weyl spacetimes are (i) the Schwarzschild metric, (ii) the Erez-Rosen metric [48], and (iii) the q-metric [160] (also known as the Zipoy-Voorhees metric [203, 194]).

For the metric (3.25), there are two important Killing vector fields ξ^μ associated with the coordinates t and φ. We have $\xi_1 = \partial_t$ and $\xi_2 = \partial_\varphi$, the former of which is timelike, the latter is spacelike. Note that also any linear combination of the two, as long as constant coefficients are used, is of course again a Killing vector field. In

[1] Including a cosmological constant, the corresponding spacetime is described by the Schwarzschild-de Sitter metric.

[2] Do not confuse the Weyl spacetimes considered here as solutions of Einstein's vacuum field equation (also called Weyl metrics or Weyl solutions) with Weyl's theory of gravity and notions therein.

total, we can consider two different kinds of timelike observer congruences of which the worldlines are given by integral curves of ξ_1, ξ_2, and combinations thereof. These congruences are isometric, and therefore serve to describe observers who determine the relativistic geoid, see chapter 4. We have

(1) Non-rotating congruences of which the worldlines are integral curves of the timelike Killing vector field $\xi_1 = \partial_t$,

(2) Rotating congruences formed by worldlines that are integral curves of the combination $\partial_t + \omega\,\partial_\varphi$, with $\omega \in \mathbb{R}$.

Since the integral curves shall describe the worldlines of observers, the domain for the choice of ω is bounded by some $\omega_{\max}$ for rigid rotation, i.e. for observers with fixed "central distance" ρ. In general, the combination is timelike on a cylindrical domain about the rotation axis. On the boundary of this domain, it becomes lightlike, and outside this domain, it is spacelike. For increasing values of ω, the size of the timelike domain decreases. Note that in natural units ω has the dimension of an inverse length, whereas in SI-units, it has the dimension of a frequency.

With applications to geodesy and measurements by Earth-bound observers in mind, we associate the first congruence, (1), with observers whose spatial coordinates remain constant and we think of them as being attached to the surface of a non-rotating central object. In contrast, the second congruence, (2), is associated with observers who are attached to the surface of a rotating central object with angular velocity ω, e.g., the Earth. However, the metric (3.25) is static and, therefore, the gravitomagnetic field of the Earth is not taken into account in this approach.

Einstein's vacuum field equation with the ansatz for the Weyl metric (3.25) is reduced to

$$\Delta\psi = 0\,, \tag{3.26a}$$

$$\partial_\rho\gamma - \rho\,(\partial_\rho\psi + \partial_z\psi)(\partial_\rho\psi - \partial_z\psi) = 0\,, \tag{3.26b}$$

$$\partial_z\gamma - 2\rho\,\partial_\rho\psi\,\partial_z\psi = 0\,, \tag{3.26c}$$

see, e.g., Refs. [196, 156]. Hence, we see that the metric function γ can be obtained by integration using the solution of the Laplace equation for ψ. Therefore, we regard ψ as the primary (and more important) metric function. It will also be important for the Newtonian limit of Weyl spacetime geometries, see below. The general solution for all static, axisymmetric, and furthermore asymptotically flat spacetimes can be obtained by solving the radial and angular parts of the decoupled vacuum field equation under

these conditions. Using a series expansion, this general solution reads [156, 182]

$$\psi = \sum_{l=0}^{\infty} c_l \frac{P_l(\cos\Upsilon)}{\chi^{l+1}}\,, \tag{3.27a}$$

$$\gamma = \sum_{l,i=0}^{\infty} \frac{(i+1)(l+1)}{i+l+2} c_i c_l \frac{P_{l+1}(\cos\Upsilon)P_{i+1}(\cos\Upsilon) - P_l(\cos\Upsilon)P_i(\cos\Upsilon)}{\chi^{l+i+2}}\,, \tag{3.27b}$$

where we define the abbreviations $\chi^2 = \rho^2 + z^2$ and $\cos\Upsilon = z/\chi$. The $P_l(\cos\Upsilon)$ are the Legendre polynomials of degree l, and the c_l are arbitrary expansion parameters, sometimes also called Weyl multipoles.

Unfortunately, the representation above involving the expansion coefficients c_l gives only little insight into the geometry and properties of the respective solution. Nevertheless, the representation is indeed useful for some specific applications. For the simplest member of the Weyl class of spacetimes, the Schwarzschild solution, we must choose infinitely many coefficients c_l in a non-obvious manner; for the choice [56]

$$c_{2l} = -\frac{1}{2l+1}\, m^{2l+1}\,, \tag{3.28a}$$

$$c_{2l+1} = 0\,, \tag{3.28b}$$

the series (3.27a) converges to

$$\psi = \frac{1}{2}\log\left(\frac{r_+ + r_- - 2m}{r_+ + r_- + 2m}\right)\,, \quad \text{where} \quad r_\pm^2 := \rho^2 + (z \pm m)^2\,. \tag{3.29}$$

Thereupon, the well-known Schwarzschild metric (3.22) follows after another coordinate transformation given by

$$\frac{r}{m} - 1 := \frac{r_+ + r_-}{2m}\,, \tag{3.30a}$$

$$\cos\vartheta := \frac{r_+ - r_-}{2m}\,. \tag{3.30b}$$

Now, we clearly see the disadvantages of the Weyl multipole moments c_l and the corresponding expansion (3.27a). The Schwarzschild solution, describing the spacetime around a spherically symmetric mass (distribution), should be characterized by only one number, i.e. a monopole moment related to the total mass. However, since the Weyl moments c_l are coordinate multipole moments, we happen to need infinitely many of them to describe the Schwarzschild solution. Therefore, it is recommendable to use coordinate invariant multipole moments, e.g., those defined by Geroch and Hansen [85, 63], see below.

An alternative approach that yields more physical insight is described in the following. Here, we follow the work of Quevedo [155] and recommend this reference for

any details and derivations. We start by introducing spheroidal coordinates x and y by the coordinate transformation

$$\rho^2 =: m^2(x^2-1)(1-y^2)\,, \tag{3.31a}$$
$$z =: mxy\,. \tag{3.31b}$$

We keep the angular coordinate φ and the time coordinate t unchanged. The transformation above can also be introduced in terms of r and ϑ

$$x := r/m - 1\,, \tag{3.32a}$$
$$y := \cos\vartheta\,. \tag{3.32b}$$

So far, the parameter m in (3.31) and (3.32) is just some factor with the dimension of a length. Its interpretation and relation to an invariantly defined monopole moment becomes clear below.

Written in the new spheroidal coordinates, the Weyl metric reads now

$$g_{\mu\nu}dx^\mu dx^\nu = -e^{2\psi}c^2dt^2 + m^2e^{-2\psi}(x^2-1)(1-y^2)d\varphi^2 + m^2e^{-2\psi}e^{2\gamma}(x^2-y^2)\left(\frac{dx^2}{x^2-1}+\frac{dy^2}{1-y^2}\right)\,. \tag{3.33}$$

Einstein's vacuum field equation for the transformed Weyl metric above can be found, e.g., in Refs. [156] and [182]. In Ref. [156], Quevedo has shown that the general asymptotically flat solution with elementary flatness on the axis for the primary metric function is given by

$$\psi = \sum_{l=0}^{\infty}(-1)^{l+1}q_l\,Q_l(x)\,P_l(y)\,. \tag{3.34}$$

Here, the Q_l are Legendre functions of the second kind; see, e.g., Ref. [6] for details. The first four functions are

$$Q_0(x) = \frac{1}{2}\log\frac{x-1}{x+1}\,, \tag{3.35a}$$
$$Q_1(x) = \frac{1}{2}x\log\frac{x-1}{x+1} - 1\,, \tag{3.35b}$$
$$Q_2(x) = \frac{1}{2}P_2(x)\log\frac{x-1}{x+1} - \frac{3}{2}x\,, \tag{3.35c}$$
$$Q_3(x) = \frac{1}{2}P_3(x)\log\frac{x-1}{x+1} - \frac{5}{2}x^2 + \frac{2}{3}\,, \tag{3.35d}$$
$$Q_l(x) = \frac{1}{2}P_l(x)\log\frac{x-1}{x+1} + \mathcal{P}_{l-1}(x)\,, \tag{3.35e}$$

where $\mathcal{P}_{l-1}(x)$ is a polynomial of degree $l-1$. The new expansion coefficients q_l are related to the Weyl moments c_l and might be called Quevedo multipoles.

In the new representation (3.34), the Schwarzschild metric is obtained by the choice $q_0 = 1$ and $q_l = 0 \; \forall \; l > 0$. For this choice of q_0, the parameter m involved in the coordinate transformation (3.30) is the usual mass parameter of the Schwarzschild solution and related to the Schwarzschild radius $r_s = 2m$.

In the next section, we discuss the Newtonian limit of the general solution (3.33) for Weyl spacetimes. Moreover, we investigate their invariant relativistic multipole moments[3] and link them to their Newtonian counterparts which we encountered in Section 2.

Newtonian limit

The following consideration is based on Refs. [44], [156], and the clarification of the limit procedure in [145]. We use Ehlers' definition of the Newtonian limit and apply it to a general Weyl spacetime described by the metric (3.25) and (3.33).

In Ref. [44] Ehlers defined the Newtonian limit of a general relativistic spacetime that allows us to read off the Newtonian multipole moments of the configuration. Let the metric function ψ depend on the parameter $\lambda := 1/c^2$. Then, the limit

$$U(\rho, z) = \lim_{\lambda \to 0} \frac{1}{\lambda} \psi(\rho, z, \lambda) \tag{3.36}$$

yields the Newtonian gravitational potential for the weak-field description of the spacetime at hand. The canonical coordinates ρ and z are kept fixed while the limit is taken. This approach is motivated by the fact that the Newtonian potential U satisfies the Laplace equation. This is also true for the metric function ψ in Weyl's canonical coordinates. Hence, we want this property to be preserved during the limit procedure. However, it becomes inevitable to assume that the spheroidal coordinates (x, y) depend on λ. This dependence becomes clear if we consider the Schwarzschild solution which involves λ in the coordinate transformation (3.31). In this case, the Newtonian limit leads to the gravitational potential

$$U = -\frac{GM}{R}, \quad R^2 = \rho^2 + z^2, \tag{3.37}$$

[3] For the relativistic moments, we use the coordinate invariant definition by Geroch [63] and Hansen [85].

since the mass parameter m depends on λ according to

$$m = \frac{GM}{c^2} = GM\lambda\,, \tag{3.38}$$

where M is the total mass of the source; G and M are, of course, independent of λ. Using the result in (3.31) now clarifies how the spheroidal coordinates x and y depend on λ.

Now, we explicitly calculate the Newtonian limit of (3.34) following Ref. [156][4]. We have to calculate

$$U = \lim_{\lambda\to 0}\frac{1}{\lambda}\sum_{l=0}^{\infty}(-1)^{l+1}q_l\,Q_l\left(\frac{r_+ + r_-}{2\lambda GM}\right)\,P_l\left(\frac{r_+ - r_-}{2\lambda GM}\right)\,. \tag{3.39}$$

The limit for the spheroidal coordinates x and y, expressed in terms of ρ and z, is

$$\lim_{\lambda\to 0} x = \lim_{\lambda\to 0}\frac{r_+ + r_-}{2\lambda GM} = \infty\,, \tag{3.40a}$$

$$\lim_{\lambda\to 0} y = \lim_{\lambda\to 0}\frac{r_+ - r_-}{2\lambda GM} = \frac{z}{\sqrt{\rho^2 + z^2}}\,, \tag{3.40b}$$

respectively. The Legendre polynomials are continuous and, therefore, we can pull the limit into the argument and get

$$\lim_{\lambda\to 0} P_l\,(y) = P_l\left(\lim_{\lambda\to 0} y\right) = P_l\left(\frac{z}{\sqrt{\rho^2 + z^2}}\right)\,. \tag{3.41}$$

Eq. (3.40a) shows that the limit $\lambda \to 0$ is equivalent to the limit $x \to \infty$. Hence, we can expand the function $Q_l(x)$ in inverse powers of x. The expansion yields

$$Q_l(x) = Q_l\left(\frac{r_+ + r_-}{2\lambda GM}\right) = \sum_{k=0}^{\infty} b^l_{l+2k+1}\left(\frac{2\lambda GM}{r_+ + r_-}\right)^{l+2k+1}\,, \tag{3.42}$$

where the expansion coefficients b_l are given by [6]

$$b^l_{l+2k+1} = \frac{(l+2k-1)(l+2k)}{2k(2l+2k+1)}b^l_{l+2k-1}\,, \tag{3.43a}$$

$$b^l_{l+1} = \frac{l!}{(2l+1)!!}\,. \tag{3.43b}$$

We observe that each summand of Eq. (3.39) has an existing finite limit. Moreover,

[4] We calculate the limit here again because in Ref. [156], there are some minor errors in the limit procedure as pointed out in [145].

absolute convergence allows to interchange the summation and the limit [156]. Inserting the expansion for the Legendre functions Q_l, we finally obtain the expression

$$U = \sum_{l=0}^{\infty}(-1)^{l+1}P_l\left(\frac{z}{\sqrt{\rho^2+z^2}}\right)\lim_{\lambda\to 0}\frac{1}{\lambda}q_l\sum_{k=0}^{\infty}b^l_{l+2k+1}\left(\frac{2\lambda GM}{r_+ + r_-}\right)^{l+2k+1}. \tag{3.44}$$

The limit exists and gives a non-zero result if and only if the dimensionless Quevedo multipoles q_l depend on dimensional coefficients $\bar{q}_l$ and the combination $G\lambda$ in the following way

$$q_l = (G\lambda)^{-l}\bar{q}_l\,. \tag{3.45}$$

These $\bar{q}_l$ have the dimension $[\bar{q}_l] = (\mathrm{m/kg})^l$. Now, only the lowest-order term, $k = 0$, gives a non-zero contribution to the limit and we finally obtain the Newtonian gravitational potential

$$\begin{aligned} U &= \sum_{l=0}^{\infty}(-1)^{l+1}b^l_{l+1}P_l\left(\frac{z}{\sqrt{\rho^2+z^2}}\right)\lim_{\lambda\to 0}q_l\lambda^l\left(\frac{2GM}{r_+ + r_-}\right)^{l+1} \\ &= G\sum_{l=0}^{\infty}(-1)^{l+1}b^l_{l+1}\bar{q}_l M^{l+1}P_l\left(\frac{z}{\sqrt{\rho^2+z^2}}\right)\times\lim_{\lambda\to 0}\left(\frac{2}{r_+ + r_-}\right)^{l+1} \\ &= -G\sum_{l=0}^{\infty}(-1)^l\bar{q}_l\frac{l!}{(2l+1)!!}M^{l+1}\frac{P_l(\cos\Upsilon)}{\chi^{l+1}}\,, \end{aligned} \tag{3.46}$$

where χ and Υ have been defined before.

Multipole moments

In chapter 2, we have defined dimensional Newtonian multipole moments $\tilde{J}_l$ for axisymmetric mass distributions, see Eqs. (2.12) and (2.14). Comparing the result to (3.46) and identifying the coordinates $\chi \mathrel{\widehat{=}} R$, $\Upsilon \mathrel{\widehat{=}} \Theta$ we read off the relation

$$\tilde{J}_l = (-1)^l\frac{l!}{(2l+1)!!}M^{l+1}\bar{q}_l \quad\Leftrightarrow\quad J_l = (-1)^l\frac{l!}{(2l+1)!!}\left(\frac{m}{R_{\mathrm{ref}}}\right)^l q_l\,. \tag{3.47}$$

Since $q_0 = 1 = \bar{q}_0$, the total mass of the source is given by M (in kg), which is the monopole moment $\tilde{J}_0 = M$. The dipole moment can always be eliminated by choosing the origin of the coordinate system to coincide with the center of mass, see chapter 2. The next higher-order moment is the quadrupole, which is given by

$$\tilde{J}_2 = \frac{2}{15}\bar{q}_2 M^3\,. \tag{3.48}$$

With the results above, we see that the parameters $\bar{q}_l$ determine the Newtonian multipoles of the central source of which the exterior spacetime is described by the Weyl metric (3.33). Or, the other way around, prescribing Newtonian moments $\tilde{J}_l$, obtained from various measurements, we know how to set up the best Weyl spacetime approximation of the configuration by calculating the corresponding $\bar{q}_l$.

On the other hand, also the relativistic Geroch-Hansen multipole moments $\mathcal{M}_l$ are uniquely determined by a choice of the parameters $\bar{q}_l$. The mass moments, which depend of course on $\lambda = c^{-2}$, can be written in the form

$$\mathcal{M}_l = \tilde{J}_l + C_l \,, \tag{3.49}$$

as a sum of the Newtonian moments and relativistic corrections C_l. The corrections can be calculated exactly, i.e. without any weak-field or far-field approximation. Following Quevedo [156], the first five correction terms are

$$C_0 = 0 \,, \; C_1 = 0 \,, \; C_2 = 0 \,, \tag{3.50a}$$

$$C_3 = -\frac{2}{5} m^2 \tilde{J}_1 \,, \tag{3.50b}$$

$$C_4 = -\frac{2}{7} m^2 \tilde{J}_2 - \frac{6}{7} m \frac{G}{c^2} \tilde{N}_1^2 \,. \tag{3.50c}$$

In general, the correction terms C_l are of the form $C_l = C_l(\tilde{J}_{l-2}, \tilde{J}_{l-3}, \ldots, \tilde{J}_0)$. Since $\tilde{J}_1$ can be set to zero, the octupole correction C_3 becomes irrelevant. Hence, a difference between the relativistic and the Newtonian multipoles sets in for the first time at the $l = 4$ level, which is a surprising result that was first derived in Ref. [156]. In Ref. [89], the authors show how Weyl multipole moments are operationally accessible via gyroscope measurements.

The laborious derivation of all the properties above pays off in the following sections. Using the results, it becomes easy to construct special examples of Weyl spacetimes such as the Erez-Rosen spacetime, see the next section. Also in chapter 4, where we define the relativistic normal gravity spacetime, we heavily rely on the results above regarding Weyl spacetimes, their Newtonian limits, and multipolar structure.

3.2.3 Erez-Rosen spacetime

The Schwarzschild solution was the simplest member of the Weyl class, involving only the expansion parameter q_0 in (3.34). Since a dipole moment related to q_1 is of no relevance, the next expansion term is proportional to q_2. Hence, for the choice $q_0 = 1$, $q_1 = 0$, $q_2 \neq 0$, and $q_l = 0 \; \forall l > 2$, we obtain a spacetime with monopole and

quadrupole moments according to

$$\mathcal{M}_0 = M\,, \tag{3.51a}$$

$$\mathcal{M}_2 = \frac{2}{15}\bar{q}_2\, M^3\,. \tag{3.51b}$$

The quadrupole moment also coincides with the Newtonian quadrupole $\tilde{J}_2$ of the configuration in the Newtonian limit. Higher order multipole moments $\mathcal{M}_{2n}$ exist for all $n > 1$ but are uniquely determined by $\mathcal{M}_0$ and $\mathcal{M}_2$.

The metric functions ψ and γ in Eq. (3.33) now become

$$2\psi_{\mathrm{ER}} = \log\left(\frac{x-1}{x+1}\right) + q_2(3y^2-1)\left(\frac{(3x^2-1)}{4}\log\left(\frac{x-1}{x+1}\right) + \frac{3}{2}x\right)\,, \tag{3.52}$$

and

$$\begin{aligned}\gamma_{\mathrm{ER}} = {}& \frac{1}{2}(1+q_2)^2\log\left(\frac{x^2-1}{x^2-y^2}\right) \\ & - \frac{3}{2}q_2(1-y^2)\left(x\log\left(\frac{x-1}{x+1}\right)+2\right) + \frac{9}{16}q_2^2(1-y^2) \\ & \times\left[x^2+4y^2-9x^2y^2-\frac{4}{3}+x\left(x^2+7y^2-9x^2y^2-\frac{5}{3}\right)\right. \\ & \left.\times\log\left(\frac{x-1}{x+1}\right)+\frac{1}{4}(x^2-1)(x^2+y^2-9x^2y^2-1)\times\log\left(\frac{x-1}{x+1}\right)^2\right]\,. \end{aligned} \tag{3.53}$$

This particular metric is indeed the vacuum solution found by Erez and Rosen [48] in 1959[5]. In the limit $q_2 \to 0$, we obtain again the Schwarzschild solution.

By the results of the previous section, we know the Erez-Rosen metric describes a spacetime of which the Newtonian limit yields a gravitational potential of a configuration with monopole $\tilde{J}_0 = M$ and quadrupole $\tilde{J}_2$ only; all $\tilde{J}_n$ are zero for $n > 2$. This is indeed also supported by the following consideration. We change to the coordinate (r, ϑ) using the transformation (3.32). Now, we can expand the metric component

[5] As pointed out in Ref. [202], the original work by Erez and Rosen contains some mistakes concerning numerical factors within the expression for the metric functions. A corrected version can be found, for example, in Ref. [202].

$g_{00} = -\exp(2\psi)$ in powers of the dimensionless quantity m/r. We obtain

$$\begin{aligned} -g_{00} = e^{2\psi} &= 1 - \frac{2m}{r} - \frac{2}{15} q_2 m^3 \frac{3\cos^2\vartheta - 1}{r^3} + \mathcal{O}(m^4/r^4) \\ &= 1 - \frac{2}{c^2}\left(\frac{GM}{r} + GMm^2 \frac{2}{15} q_2 \frac{3\cos^2\vartheta - 1}{2r^3}\right) + \mathcal{O}(m^4/r^4) \\ &= 1 - \frac{2}{c^2}\left(\frac{GM}{r} + G\tilde{J}_2 \frac{3\cos^2\vartheta - 1}{2r^3}\right) + \mathcal{O}(m^4/r^4)\,. \end{aligned} \tag{3.54}$$

We have used the relation

$$\tilde{J}_2 = \frac{2}{15} M m^2 q_2 = \frac{2}{15} \bar{q}_2 M^3\,, \tag{3.55}$$

and recognize the term in brackets as the Newtonian potential of a quadrupolar gravitational source, see chapter 2. Actually, we have just calculated a weak-field expansion of the Erez-Rosen metric in suitable coordinates; we know that in such a limit we have $-g_{00} \to (1 + 2U/c^2)$ which gives the first term in the post-Newtonian metric for a Newtonian quadrupolar potential. However, higher orders are different and we have to keep in mind that the coordinates do not have the same meaning as in Newtonian gravity in $\mathbb{R}^3$. On $t = \text{const.}$, $r = \text{const.}$ surfaces, the metric is not the standard metric on the 2-sphere S^2, and r is not an area coordinate as it was for the Schwarzschild spacetime.

Since the Erez-Rosen spacetime is a particular Weyl spacetime, we also have the two Killing vector field $\xi_1 = \partial_t$, $\xi_2 = \partial_\varphi$, the generators of time translations and rotations, respectively.

3.2.4 Higher-order static axisymmetric spacetimes with prescribed limits

As we have seen above, the Erez-Rosen metric describes a relativistic quadrupolar spacetime which possesses also all higher-order moments. However, these moments are uniquely determined by the first two. The Newtonian limit of this spacetime yields a quadrupolar gravitational potential, i.e. a potential involving only J_2 as the highest-order term and all other Newtonian moments are zero.

In the same spirit, we can construct a more general Weyl spacetime of which the weak-field limit is a prescribed Newtonian axisymmetric field. This means, we can prescribe l parameters $\tilde{J}_l$ which uniquely characterize the Newtonian field that shall be the weak field limit of our general relativistic spacetime. Thereupon, l parameters $\bar{q}_l$ are uniquely determined by Eq. (3.47) and a Weyl spacetime can be constructed according to Eq. (3.33).

This construction is limited to axisymmetric configurations but no exact general relativistic spacetimes that describes a static non-axisymmetric field related to a central source, such as a planet, is known so far. Thus, it might be argued that due to the Earth's non-axisymmetric gravity field, the outlined construction of exact spacetimes is of no, or only very little use [180]. However, we disagree at this point and we will give arguments for our position in later chapters. For instance, we will use an exact spacetime, constructed as shown above, to describe the relativistic normal gravity field of the Earth in chapter 4.

3.2.5 Stationary axisymmetric spacetimes - Kerr metric

The metric for any axisymmetric stationary solutions to Einstein's vacuum field equation can be given in the Weyl-Lewis-Papapetrou form

$$g = -e^{2\psi}(c\,\mathrm{d}t + \omega \mathrm{d}\varphi)^2 + e^{-2\psi}\sigma^2 e^{2\gamma}(x^2-y^2)\left(\frac{\mathrm{d}x^2}{x^2-1} + \frac{\mathrm{d}y^2}{1-y^2}\right) + e^{-2\psi}\sigma^2(x^2-1)(1-y^2)\mathrm{d}\varphi^2\,, \quad (3.56)$$

in which we use the spheroidal coordinates (x, y), which have proven to be very useful in the last section, see Refs. [155] and [182] for details. Here, the metric functions ψ, γ, and ω depend only on x and y, and σ is a constant with the dimension of a length.

We can define the Ernst potentials E and ϵ

$$E := e^{2\psi} + i\,\Sigma\,, \quad \epsilon := \frac{1-E}{1+E}\,, \quad (3.57)$$

which are complex functions in general. The new function Σ, which appears in the imaginary part, is given by a solution of

$$\sigma(x^2-1)\partial_x\Sigma = -e^{4\psi}\partial_y\omega\,, \quad (3.58a)$$

$$\sigma(1-y^2)\partial_y\Sigma = e^{4\psi}\partial_x\omega\,. \quad (3.58b)$$

Now, the vacuum field equation can be reduced to an equation for the complex Ernst potential, see, e.g., Ref. [158]. In the limit of static spacetimes, the Ernst potential becomes real and we recover all results of the previous section for Weyl spacetimes. Note that the equation of motion, i.e. the geodesic equation, can be solved analytically in such axisymmetric spacetimes; see, e.g., results and analytically derived observables in Refs. [81, 82, 83].

One particularly simple solution to the Ernst equation for the special case $\omega = 0$ is given by $\epsilon = 1/x$, which is the Schwarzschild spacetime in spheroidal coordinates. The probably best-known and most important stationary solution of the Ernst equation is

the Kerr solution. It is a two parameter family of spacetime metrics, since the Ernst potential depends on the two parameters mass m and spin a according to

$$\epsilon^{-1} = \frac{\sigma}{m}x + i\frac{a}{m}y\,, \quad \sigma = \sqrt{m^2 - a^2}\,, \tag{3.59}$$

and the Kerr metric functions in the Weyl-Lewis-Papapetrou form become

$$e^{2\psi} = \frac{\sigma^2x^2 + a^2y^2 - m^2}{(\sigma x + m)^2 + a^2y^2}\,, \tag{3.60a}$$

$$\omega = \frac{2am\,(\sigma x + m)(1 - y^2)}{\sigma^2x^2 + a^2y^2 - m^2}\,, \tag{3.60b}$$

$$\gamma = \frac{1}{2}\log\left(\frac{\sigma^2x^2 + a^2y^2 - m^2}{\sigma^2(x^2 - y^2)}\right)\,. \tag{3.60c}$$

The standard form of the Kerr metric in Boyer-Lindquist coordinates $(t, r, \vartheta, \varphi)$ is obtained after the coordinate transformation

$$\sigma x = r - m\,, \quad y = \cos\vartheta\,. \tag{3.61}$$

The metric becomes

$$\begin{aligned} g = &-\left(1 - \frac{2mr}{\rho^2}\right)c^2\mathrm{d}t^2 + \frac{\rho^2}{\Delta}\mathrm{d}r^2 + \rho^2\mathrm{d}\vartheta^2 + \sin^2\vartheta\left(r^2 + a^2 + \frac{2mra^2\sin^2\vartheta}{\rho^2}\right)\mathrm{d}\varphi^2 \\ &- \frac{4mra\sin^2\vartheta}{\rho^2}\,c\,\mathrm{d}t\mathrm{d}\varphi\,, \end{aligned} \tag{3.62}$$

and we introduce the abbreviations

$$\rho^2 = r^2 + a^2\cos^2\vartheta\,, \quad \Delta = r^2 + a^2 - 2mr\,. \tag{3.63}$$

The parameter $m = GM/c^2$ gives the total mass of the source in natural units, see below, and the Kerr parameter a is related to the spin angular momentum J by

$$a = \frac{J}{Mc}\,, \tag{3.64}$$

and has the dimension of a length.

The Kerr spacetime describes the geometry of a rotating black hole for $a < m$. The case $a > m$ describes a naked singularity and $a = m$ is the boundary corresponding to an extreme black hole. For the former case, there are two horizons given by the roots of Δ, and the outer solution is an event horizon. A curvature ring singularity is found at $r = 0$, $\vartheta = \pi/2$. For the case $a = 0$, the two horizons coincide at $r = 2m$ and the Schwarzschild spacetime is recovered. Another important surface is obtained by the roots of g_{00}. The region between the outer solution and the event horizon is called ergosphere. In this region, all observers have to rotate with the black hole. The

geodesic equation in the Kerr spacetime can be solved analytically in terms of elliptic functions, see Ref. [82, 83] and references therein. Also the shadow of Kerr black holes can be calculated analytically, even in the presence of a plasma [71, 138]. Observing a shadow of the black hole in the center of our galaxy will, hopefully, give information about the spin and verify the applicability of the Kerr metric for astrophysical compact objects. It is, therefore, also a test of General Relativity, or at least a test of a class of theories which admit trapped light orbits around central objects.

The Kerr metric has an interesting multipole structure; in natural units, the lowest-order moments are

$$\mathcal{M}_0 = m\,, \tag{3.65a}$$
$$\mathcal{S}_1 = ma\,, \tag{3.65b}$$
$$\mathcal{M}_2 = -ma^2\,, \tag{3.65c}$$

where $\mathcal{S}_1$ is the spin dipole. All higher-order mass moments $\mathcal{M}_n$ exist for even n and all spin moments $\mathcal{S}_n$ exist for odd n but are uniquely determined by a choice of m and a. We find the two Killing vector fields $\xi_1 = \partial_t$ (timelike) and $\xi_2 = \partial_\varphi$ (spacelike) related to stationarity and axisymmetry, respectively. The spacetime is stationary since ξ_1 is not hypersurface orthogonal in general.

The Kerr metric can not describe the actual spacetime outside an axisymmetric planetary object such as the Earth. Calculating the mass $m_\oplus \approx 0.44\,\mathrm{cm}$ and the Kerr parameter a for the angular momentum and mean surface radius of the Earth, we find $a_\oplus \approx 892m$ which clearly corresponds to an over-extreme solution. Moreover, the Kerr quadrupole moment is uniquely determined by m and a, whereas for the Earth it is independent and not even close to the Kerr value. However, the Kerr spacetime can be used to estimate so-called gravitomagnetic effects in the vicinity of the Earth due to the frame dragging of the spacetime geometry. Particular examples of such effects are the Lense-Thirring precession measured by Gravity Probe B [49, 50] and the gravitomagnetic clock effect, see [79] and references therein.

3.2.6 Parametrized post-Newtonian spacetime

Empirical evidence, supporting that the Einstein equivalence principle holds, suggests that in particular metric theories are viable theories of gravity. Following Ref. [200], we make three assumptions

- There exists a symmetric metric; in a local chart $g_{\mu\nu} = g_{\nu\mu}$.
- The worldlines of test-particles without internal structure are timelike geodesics of the metric.

- The laws of special relativity hold in a Local Lorentz Frame (LLF).

Metric theories of gravity can be described in the parametrized post-Newtonian formalism (ppN).

In the following, we neglect all time-dependencies and use a nearly globally Lorentz coordinates system with harmonic Cartesian ppN coordinates $(x^\mu) = (ct, x, y, z)$. Hence, for these coordinates, the harmonic gauge

$$\partial_\mu \left(\sqrt{-g} g^{\mu\nu}\right) \tag{3.66}$$

is fulfilled. This gauge condition can alternatively be written as $g^{\mu\nu}\Gamma^\lambda{}_{\mu\nu} = 0$.

For the sake of simplicity, we now construct a ppN spacetime model for the isolated, time-independent, and rigidly rotating Earth using only the two ppN parameters β and γ. In harmonic non-rotating GCRS coordinates, the metric components can be written as

$$g_{00}(\mathbf{x}) = -\left(1 + \frac{2U(x,y,z)}{c^2} + \frac{2\beta U(x,y,z)^2}{c^4}\right) + \mathcal{O}(c^{-6})\,, \tag{3.67a}$$

$$g_{0i}(\mathbf{x}) = -\frac{2(\gamma+1)\,|U^i(x,y,z)|}{c^3} + \mathcal{O}(c^{-5})\,, \tag{3.67b}$$

$$g_{ij}(\mathbf{x}) = \delta_{ij}\left(1 - \frac{2\gamma U(x,y,z)}{c^2}\right) + \mathcal{O}(c^{-4})\,. \tag{3.67c}$$

where $U(x,y,z)$ is the Newtonian gravitational potential and $U^i(x,y,z)$ is the vector potential in the post-Newtonian formalism. Note that $U < 0$ in our convention. For details, and more complicated ppN metrics including an extended set of parameters and potentials, see Refs. [200, 109, 35, 179, 112]. We also recommend the so-called DSX papers [28, 29, 30, 31] for very detailed considerations. The vector potential U^i causes frame dragging effects and might be called gravitomagnetic potential for this reason.

For our choice of the metric and the assumptions made above, the potentials U and U^i are to be determined from

$$\Delta U(\mathbf{x}) = 4\pi G\rho(\mathbf{x})\,, \tag{3.68a}$$

$$\Delta U^i(\mathbf{x}) = 4\pi G\rho^i(\mathbf{x}) = 4\pi G\rho(\mathbf{x})\, v^i(\mathbf{x})\,. \tag{3.68b}$$

The rest mass density ρ and its flux ρ^i are related to the energy-momentum tensor components of the Earth: $\rho = (T^{00} + T^{ii})/c^2$ and $\rho^i = T^{0i}/c$, and are measured in a locally comoving freely falling frame. By v^i we denote the matter's coordinate velocity

in the GCRS. In an integral representation, we obtain [23]

$$U(\mathbf{x}) = -G \int d^3X' \, \frac{\rho(\mathbf{x}')}{|\mathbf{x} - \mathbf{x}'|} \,, \tag{3.69a}$$

$$U^i(\mathbf{x}) = -G \int d^3X' \, \frac{\rho(\mathbf{x}') \, v^i(\mathbf{x}')}{|\mathbf{x} - \mathbf{x}'|} \,. \tag{3.69b}$$

Combining U and U^i to $(U^\mu) = (U, U^i)$ as well as ρ and ρ^i to $(\rho^\mu) = (\rho, \rho^i)$ allows to express the asymptotic behavior by

$$\lim_{|\mathbf{x}| \to \infty} U^\mu = 0 \,, \tag{3.70}$$

and the field equations become

$$U^\mu(\mathbf{x}) = - \int \frac{\rho^\mu(\mathbf{x})}{|\mathbf{x} - \mathbf{x}'|} \mathrm{d}^3x' \,. \tag{3.71}$$

The two ppN parameters have the following interpretation [200]: β describes the "amount of non-linearity" occurring in the (broken) superposition principle of the time-time component g_{00}. The parameter γ describes the "amount of spatial curvature" produced by a unit rest mass that is to be taken into account. Using only β and γ, theories contained in the framework are, e.g., General Relativity and scalar-tensor theories such as Brans-Dicke or general $f(\mathcal{R})$ theories. The ppN parameter γ is constrained to $|\gamma| \leq 2.3 \times 10^{-5}$ by measurements related to the Cassini spacecraft mission [7] and β is limited by $|\gamma| \leq 3 \times 10^{-5}$ thanks to planetary ephemeris [149].

Now, we introduce a rotating coordinate system (t, x', y', z'), rigidly co-rotating with the Earth. In spherical coordinates, this is done by the transformation of the azimuthal angle (longitude) according to

$$\phi \to \phi' = \phi - \omega t \,, \tag{3.72}$$

where ω is the Earth's angular velocity. We assume that the rotation axis coincides with the z-axis of the coordinate system, i.e. $z' = z$. All purely spatial metric components will formally not change but we have to calculate the new g'_{00} and g'_{0i} components. The result is

$$g'_{00}(\mathbf{x}') = - \left(1 + \frac{2W(x', y', z')}{c^2} + \frac{2\beta U(x', y', z')^2}{c^4} \right) + \mathcal{O}(c^{-6}) \,, \tag{3.73a}$$

$$g'_{0i}(\mathbf{x}') = - \frac{2(\gamma + 1) \, |U^i(x', y', z')|}{c^3} - \frac{\epsilon_{ijk} x'^j \omega^k}{c} + \mathcal{O}(c^{-5}) \,, \tag{3.73b}$$

$$g'_{ij}(\mathbf{x}') = \delta_{ij} \left(1 - \frac{2\gamma U(x', y', z')}{c^2} \right) + \mathcal{O}(c^{-4}) \,, \tag{3.73c}$$

where $W = U - \omega^2(x^2 + y^2)/2$ is the Earth's gravity potential including centrifugal effects, see chapter 2, and $(\omega^i) = (0, 0, \omega)$ is the Earth's angular velocity vector. Note that we can express $g'_{0i}(\mathbf{x}')$ also in the form

$$g'_{0i}(\mathbf{x}') = -\frac{\gamma + 1}{c^3} L_i - \frac{\epsilon_{ijk} x'^j \omega^k}{c} , \tag{3.74}$$

with the Earth's gravitomagnetic field [181, 199]

$$\vec{L}_\oplus = \frac{G\vec{J}_\oplus \times \vec{x}'}{r'^3} , \tag{3.75}$$

and the total angular momentum $\vec{J}_\oplus$ of the Earth. In the new coordinates, observers on the Earth's surface are described by $\mathrm{d}x'^i = 0$.

For a spherical central mass M with radius R_0, rotating around the x^3-axis with angular velocity ω, the gravitomagnetic vector potential can be evaluated easily and we obtain

$$g_{03} = -\frac{2(\gamma + 1)GM/R}{5c^3} \left(\frac{R_0}{R}\right)^2 \epsilon_{3ij} \omega^i x^j . \tag{3.76}$$

3.2.7 Post-Newtonian spacetime for the Earth

The post-Newtonian (pN) metric components, describing the spacetime outside the isolated time-independent rigidly rotating Earth in the GCRS, is obtained from the metric by assigning to the ppN parameters β and γ their values in General Relativity, i.e. $\beta = 1$ and $\gamma = 1$. The coordinates $(\mathbf{x})$ are non-rotating nearly global Cartesian coordinates. From , we now obtain the pN metric components

$$g_{00}(\mathbf{x}) = -\left(1 + \frac{2U(x, y, z)}{c^2} + \frac{2U(x, y, z)^2}{c^4}\right) + \mathcal{O}(c^{-6}) , \tag{3.77a}$$

$$g_{0i}(\mathbf{x}) = -\frac{4\,|U^i(x, y, z)|}{c^3} + \mathcal{O}(c^{-5}) , \tag{3.77b}$$

$$g_{ij}(\mathbf{x}) = \delta_{ij}\left(1 - \frac{2U(x, y, z)}{c^2}\right) + \mathcal{O}(c^{-4}) , \tag{3.77c}$$

see, e.g., the IAU conventions and corresponding explanations in Refs. [97, 103, 178] and references therein. In co-rotating non-inertial coordinates $(\mathbf{x}')$, the pN metric becomes

$$g'_{00}(\mathbf{x}') = -\left(1 + \frac{2W(x', y', z')}{c^2} + \frac{2U(x', y', z')^2}{c^4}\right) + \mathcal{O}(c^{-6})\,, \tag{3.78a}$$

$$g'_{0i}(\mathbf{x}') = -\frac{4\,|U^i(x', y', z')|}{c^3} - \frac{\epsilon_{ijk} x'^j \omega^k}{c} + \mathcal{O}(c^{-5})\,, \tag{3.78b}$$

$$g'_{ij}(\mathbf{x}') = \delta_{ij}\left(1 - \frac{2U(x', y', z')}{c^2}\right) + \mathcal{O}(c^{-4})\,. \tag{3.78c}$$

In the equations above, W is the Earth's gravity potential, U is its gravitational part, and U^i is the vector potential taking care of the Earth's gravitomagnetic field, see section 3.2.6.

We again remind the reader about our sign convention $W < 0$ and $U < 0$ when comparing the results above to other references.

Chapter 4

Geodetic Concepts in Relativistic Gravity - Potentials and Reference Surfaces

4.1 Why concepts and basic notions must be redefined

Since the structure of General Relativity is fundamentally different compared to linear Newtonian gravity, new basic concepts, fundamental notions, and observables appear. Moreover, familiar concepts used in conventional geodesy must be reconsidered and lifted to the framework of relativistic gravity. To do so, it becomes inevitable to redefine the most fundamental geodetic notions to consistently interpret measurements at the highest possible accuracy level. We shall point out here, that it is not the (gravitational) measurement which changes when switching to another underlying theory of gravity. We rather have to interpret the data and observables in a consistent way within the chosen theory. The measurement itself 'does not care' about the theoretical framework that we have chosen and it is an abuse of notions to speak of Newtonian or relativistic measurements.

4.1.1 Concepts that will be addressed - Methodology

Clocks are among the most fundamental and most precise measurement devices. Modern clocks with a stability approaching the 10^{-18} regime [11, 24, 126] will be off less than a second in the age of the universe. These clocks with an unprecedented and mind-blowing accuracy can be used to detect mutual redshifts which result from (small) position offsets at the order of centimeters. They build the experimental foundations of an entirely new field which is called chronometric geodesy; see Refs. [35, 38, 126, 130] for a modern overview. It is indeed possible to detect the spacetime geometry

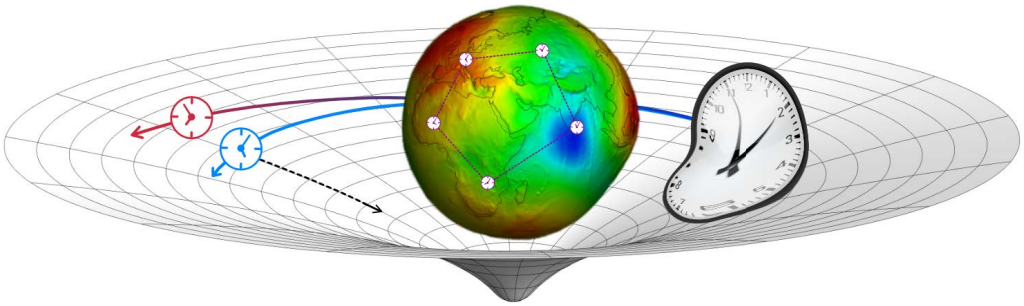

FIGURE 4.1: Methodology of chronometric measurements: We may consider two special kinds of observers, related to i) satellite measurements and therefore orbits around the Earth and ii) measurement stations fixed to the surface of the rotating Earth. These observers shall be equipped with standard clocks described in terms of timelike worldlines parametrized by the respective proper time.

and all components of the curvature tensor by a suitably prepared set of clocks. This construction is called the "clock compass", see Ref. [154].

Since we believe that chronometric measurements will be the main pillar of future relativistic geodesy, we base our considerations here on the analysis of clock comparison and redshift measurements. A relativistic definition of the geoid that is based on time and frequency measurements might be most convenient and operationally realizable with high accuracy.

After defining the redshift of two observers in General Relativity, we pass on to consider timelike congruences, which resemble a swarm of observers who can perform pairwise measurements. These measurements include, e.g., clock experiments, pairwise redshift measurements and the determination of relative accelerations. Using both, relative redshifts and accelerations, the curvature of spacetime can be determined point wise by the so-called "gravitational compass" and "clock compass", see Refs. [153, 154] and references therein.

Our approach eventually leads to the definition of a redshift potential, a scalar function on spacetime, which exists for special types of observer congruences. We show that this scalar function is also an acceleration potential for an isometric congruence of observers and that in the case of a time-independent redshift potential, the level sets are two-dimensional surfaces which foliate the three-dimensional space in a stationary spacetime geometry. We call these level surfaces isochronometric surfaces, and show how they can be determined by observers who co-rotate with the Earth and are equipped with standard clocks.

Thereupon, we use the redshift potential to define a relativistic gravity potential that is a generalization of the Newtonian function W. It gives rise to the definition of geodetic reference surfaces such as the relativistic geoid and the reference 'ellipsoid'. Moreover, we consider our definitions in the (post-)Newtonian limit and prove that well-known notions of conventional geodesy are recovered. In this chapter, we work out general relativistic definitions of

- the gravity potential,
- the geoid,
- the normal gravity field,
- and the level ellipsoid.

We shall note here already that our definitions are by no means restricted to describe only the gravitational field of the Earth. The concepts and notions presented in this chapter can be applied to a variety of astrophysical objects. Moreover, there is no restriction concerning the strength of the gravitational field since we do not employ any kind of (weak-field) approximation for the definitions.

The first approach towards the definition of a relativistic geoid was done by Bjerhammar [9, 10] in 1985. In his words:

> *The relativistic geoid is the surface nearest to mean sea level on which precise clocks run with the same speed.*

Inspired by Bjerhammar's approach, which, however, lacks some formal and mathematical clarity, we will work out a relativistic geoid definition based on clock comparison. Therefore, we need to translate Bjerhammar's definition into the language of mathematics: Firstly, we must specify what "precise clocks" are. Secondly, we have to interpret what is actually meant by saying that clocks "run at the same speed". In the formalism of General Relativity, without approximations, we suggest that "precise clocks" are standard clocks, i.e. clocks that measure proper time along their respective worldlines. Moreover, "clocks that run at the same speed" are to be identified by a vanishing mutual redshift. These identification, together with properties of special congruences of observer worldlines who co-rotate with the Earth, yields a new definition of the relativistic geoid in the end.

4.2 Redshift and acceleration potential, isochronometric surfaces

In the following section, we introduce the redshift of two observers in General Relativity. To avoid the discussion of the observers' nature and possible interactions with the

spacetime environment and other fields, we shall use an abstract concept that reduces the physical observer, or rather the measurement device taking care of the data reception and recording, to an infinitesimally small clock following a timelike worldline. Moreover, we demand that this clock measures its own proper time, i.e. we require it to be a standard clock. Note that the observers' worldlines do not need to be geodesics of the spacetime since they are, of course, allowed to move freely in an accelerated manner.

Once the notion of the redshift of two observers is defined, we pass on to investigate congruences. With applications to geodesy in mind, we necessarily need to consider a swarm of observers, who interact in a network and perform pairwise measurements. For Earth-bound measurements, we can think of rigidly co-rotating observers attached to the surface of the rotating Earth. Under certain conditions, we can define a time-independent redshift potential, a scalar function on spacetime which yields the redshift of any to worldlines in a congruence by evaluation on the respective paths. We will show that for isometric observer congruences, the redshift potential is an acceleration potential as well. This property leads to the fact that the so-called "u-geoid" and "a-geoid", defined in post-Newtonian gravity in Ref. [181], coincide genuinely in the framework of General Relativity.

4.2.1 Redshift in General Relativity

To operationally determine the redshift of observers, it is inevitable to compare two clocks. To do so, it is obviously necessary to send signals from one clock (emitter) to the other (receiver). This might also be done in a bidirectional way. In General Relativity, the natural choice for the signal transmission is to consider free light signals, which connect events on the emitter's worldline to events on the receiver's worldline. These light signals are, in the mathematical formalism, given by lightlike (null) geodesics.

In the following, we present the well-known definition of the redshift in General Relativity. Let γ and $\tilde{\gamma}$ be the worldlines of the emitter and the receiver, respectively. We parametrize the worldlines by the respective proper times τ and $\tilde{\tau}$. The tangent vectors to the worldlines (the four-velocity vectors) are then given by $u = \mathrm{d}\gamma/\mathrm{d}\tau$ and $\tilde{u} = \mathrm{d}\tilde{\gamma}/\mathrm{d}\tilde{\tau}$; $\gamma, \tilde{\gamma}$ are their integral curves, respectively. Proper time is defined by the normalization condition $g(u, u) = -c^2$.

Now, we assume that light rays are emitted at the two events $\gamma(\tau)$ and $\gamma(\tau + \Delta\tau)$ for an arbitrary time of emission τ. These signals are received at $\tilde{\gamma}(\tilde{\tau})$ and $\tilde{\gamma}(\tilde{\tau} + \Delta\tilde{\tau})$, respectively. A sketch of the situation is shown in Fig. 4.2. Let the worldlines of the light rays be $\lambda_n(s)$, where s is an affine parameter, and n labels the light rays. These light rays can be labeled, e.g., either by their emission time τ on γ or their reception time $\tilde{\tau}$ on $\tilde{\gamma}$ and, therefore, define a function $\tilde{\tau}(\tau)$. The redshift z is defined by the

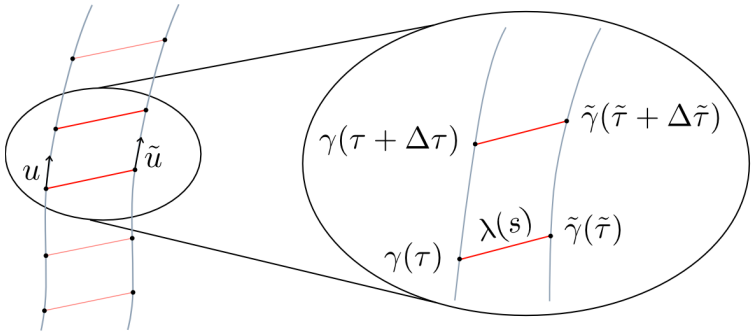

FIGURE 4.2: Definition of the redshift of observers in General Relativity: light signals are exchanged between two worldlines γ and $\tilde{\gamma}$ which are integral curves of the tangent vector fields u and $\tilde{u}$, respectively. Each worldline is parametrized by its respective proper time. Light signals (null geodesics) are emitted at a rate $\Delta\tau$ w.r.t. the emitter's clock and received with a rate $\Delta\tilde{\tau}$ w.r.t. the receiver's clock. In the limit $\Delta\tau \to 0$, their quotient defines the (momentary) redshift.

derivative of this function,

$$z + 1 := \frac{\nu}{\tilde{\nu}} = \frac{d\tilde{\tau}}{d\tau} = \lim_{\Delta\tau \to 0} \frac{\Delta\tilde{\tau}}{\Delta\tau}\,, \tag{4.1}$$

where ν and $\tilde{\nu}$ are the frequencies of the light, measured by the emitter and the receiver, respectively.

In General Relativity, there is a universal formula for the redshift z of two standard clocks,

$$z + 1 = \frac{\nu}{\tilde{\nu}} = \frac{\left(g_{\mu\nu} \dfrac{d\lambda^\mu}{ds} \dfrac{d\gamma^\nu}{d\tau} \right)\Big|_{\gamma(\tau)}}{\left(g_{\rho\sigma} \dfrac{d\lambda^\rho}{ds} \dfrac{d\tilde{\gamma}^\sigma}{d\tilde{\tau}} \right)\Big|_{\tilde{\gamma}(\tilde{\tau})}}\,. \tag{4.2}$$

It was derived first by Kermack et. *al.* [104]; also in the book of Synge [184], a derivation can be found. Other references that we recommend are the works of Brill [15] and Straumann [183], in which the redshift formula is derived in a simple way. Denoting the tangent to the light ray by $k := \mathrm{d}\lambda/\mathrm{d}s$, we may rewrite Eq. (4.2) in the following shorter way:

$$z + 1 = \frac{\nu}{\tilde{\nu}} = \frac{\langle k, u \rangle}{\langle k, \tilde{u} \rangle}\,, \quad \text{where } \langle a, b \rangle := g_{\mu\nu} a^\mu b^\nu = g(a, b)\,. \tag{4.3}$$

Note that we can label all points on the connecting null geodesics by the time of emission τ and the affine parameter s, which can always be rescaled to have the value $s = 0$ on γ and the value $s = 1$ on $\tilde{\gamma}$. Hence the pairs (τ, s) label all the points on the null geodesics λ_n. On the spacetime, $k = \partial_s$ and $l := \partial_\tau$ are vector fields. It is now

easy to show that (i): $\langle k, l \rangle$ is constant along null geodesics, and (ii): that $l(s=0) = u$ and $l(s=1) = (z+1)\,\tilde{u}$ [1]. Therefore, it follows that

$$\langle k, l \rangle_{s=0} = \langle k, u \rangle = (z+1)\langle k, \tilde{u} \rangle = \langle k, l \rangle_{s=1}\,, \tag{4.4}$$

and the redshift equations (4.2), (4.3) are immediate consequences.

In (4.2) and (4.3), we introduce the factor $z+1$ to define the redshift, instead of using only z as it is done by other authors. However, in the Newtonian limit our definition will yield a vanishing redshift $z = 0$ since the frequency ratio becomes one due to the nature of Newton's universal and absolute time.

4.2.2 Congruences of observer worldlines – redshift potential and isochronometric surfaces

Being interested in measurements related to the Earth's gravitational field and its properties, we are not satisfied with only two observers, which were described so far. We shall expand our considerations to describe an entire family of observers equipped with standard clocks and other measurement devices. These observers can be thought of as fixed ground stations on the Earth's surface, mobile measurement devices, or even satellites in orbits around the Earth.

In the theoretical framework of General Relativity, the notion of standard clocks is well-defined. We have to use the normalization condition, i.e. a worldline γ that is parametrized by proper time τ has a normalized tangent vector field $u = \mathrm{d}\gamma/\mathrm{d}\tau$ with $g(u,u) = -c^2$. Standard clocks can also be characterized operationally using light rays and freely falling particles as well as the notions of radar distance and radar time, see Perlick's work [140]. When comparing predictions from General Relativity with observations one always assumes that atomic clocks are standard clocks. This hypothesis is in agreement with all experiments to date.

To describe a swarm of observers, we now consider timelike congruences of worldlines and ask for the redshift of any pair of worldlines within a given congruence. Let such a congruence be defined by a four-velocity field u, which is normalized such that its integral curves are parametrized by the respective proper times. We introduce a scalar function ϕ that can be evaluated on all integral curves of u and that is used to calculate the redshift of any pair of observers within the congruence. We call such a

[1] The proof can be found in appendix B.

function ϕ a *redshift potential* for u if[2]

$$\log(z+1) = \phi\big(\tilde{\gamma}(\tilde{\tau})\big) - \phi\big(\gamma(\tau)\big) \tag{4.5}$$

for any two integral curves γ and $\tilde{\gamma}$ of u. In Ref. [86], it is shown that ϕ is a redshift potential for u if and only if

$$\exp(\phi)u =: \xi \tag{4.6}$$

is a conformal Killing vector field of the spacetime. Moreover, the redshift potential is also time-independent (i.e. it is constant along the integral curves of u) if and only if ξ is a Killing vector field. We call the worldlines of the congruence, the integral curves of u, Killing observers. Thus, we conclude that the existence of a time-independent redshift potential is guaranteed if and only if the spacetime is stationary because the Killing vector field must be timelike to describe observers in an operational sense.

We can introduce the general form of a stationary spacetime metric in coordinates (t, x^i), where the time coordinate is chosen such that $\partial_t := \xi$. The metric reads

$$g = e^{2\phi(x)}\left[-(c\,\mathrm{d}t + \alpha_a(x)\mathrm{d}x^a)^2 + \alpha_{ab}(x)\mathrm{d}x^a\mathrm{d}x^b\right], \tag{4.7}$$

where the metric functions ϕ, α_a, and α_{ab} depend on $(x^i) = (x^1, x^2, x^3)$ but not on the time coordinate t.

The spatial part of the spacetime is three-dimensional. The scalar redshift potential ϕ, or rather its level sets, foliate this 3d space into two-dimensional surfaces which we call isochronometric surfaces. Hence, any timelike congruence of Killing observers defines a foliation of the spatial part of the spacetime into isochronometric surfaces. The redshift of any two standard clocks, mathematically described by integral curves of the vector field $u = \exp(-\phi)\xi$, on the same isochronometric surface $\phi = \phi_0 = \text{const.}$ vanishes. Note that it can be shown that if any two clocks on integral curves of a vector field u have a constant redshift over time, then u must be proportional to a Killing vector field if its integral curves are complete, see Theorem 10 in Ref. [141]

For a metric in the form above, the redshift potential ϕ can be read off using

$$c^2 e^{2\phi} = -g_{\mu\nu}\xi^\mu\xi^\nu = -g_{tt}\,. \tag{4.8}$$

[2] Be careful with the order of γ and $\tilde{\gamma}$ to match the result in (4.2) for cases in which both formulae are applicable.

The redshift of any two stationary standard clocks in the congruence is then given by

$$z+1=\frac{\nu}{\tilde{\nu}}=e^{\phi|_{\tilde{\gamma}}-\phi|_{\gamma}}=\frac{e^{\phi}|_{\tilde{\gamma}}}{e^{\phi}|_{\gamma}}=\frac{\sqrt{-g_{tt}}|_{\tilde{\gamma}}}{\sqrt{-g_{tt}}|_{\gamma}}\,. \tag{4.9}$$

Note that the result (4.9) for the redshift is in agreement with (4.2) in all situations that allow the application of both formulae, i.e. in all stationary spacetimes for which we want to calculate the redshift of two Killing observers. This can easily be verified by evaluating the redshift equation (4.2) for the metric (4.7) and a congruence of worldlines that are integral curves of the vector field $u=\exp(-\phi)\,\partial_t$.

For the sake of clarity, we shall now briefly discuss the notion and limit of a redshift potential in (post-)Newtonian gravity. A detailed application to a (parametrized) post-Newtonian spacetime is given in chapter 5. For the weak-field limit, we have for a suitable coordinate system in which the time coordinate t is adapted to a timelike Killing vector field ∂_t:

$$-g_{00}=1+2W/c^2+\mathcal{O}\big(c^{-4}\big)\,, \tag{4.10}$$

where W is the Newtonian gravity potential. Thereupon, we obtain for the redshift potential ϕ

$$e^{\phi}=1+W/c^2+\mathcal{O}\big(c^{-4}\big)\,. \tag{4.11}$$

Note that we do only consider terms of $\mathcal{O}\big(c^{-2}\big)$ in the limit and the square root has been expanded accordingly. Thus, to lowest order the level surfaces of the redshift potential resemble the equipotential surfaces of the Newtonian gravity potential. This property is a very good starting point for a relativistic generalization of concepts based on W. Later in this chapter, we construct a relativistic gravity potential U^*, based on the redshift potential ϕ, which is used to investigate and redefine notions such as the relativistic geoid.

At the same approximation order, the redshift is determined by potential differences between the worldlines of the emitter and receiver of exchanged signals,

$$\frac{\nu_1}{\nu_2}=\frac{1+W_2/c^2}{1+W_1/c^2}\approx 1+\frac{W_2-W_1}{c^2}=:1+\frac{\Delta W}{c^2}\,. \tag{4.12}$$

The equation above is the very starting point for the field of chronometric geodesy in which redshift measurements of clocks at different positions (heights) are performed. The results of such measurements can verify the validity of the redshift equation and serve as a test of relativistic gravity. Close to the Earth's surface, a potential difference corresponds to a height difference. We can now easily calculate that the relative frequency change, i.e. the redshift, is about 10^{-16} per meter near the surface of the

TABLE 4.1: Index of refraction n for various materials.

Material	Index of refraction	% of vacuum speed of light
Vacuum	1	100
Air	1.0003	99.97
Water	1.33	75.19
Pure silica	1.44	69.44
Crown glass	1.52	65.79
Diamond	2.42	41.32

Earth. Hence, height differences at the centimeter level can be detected in the redshift signal by modern clocks with a stability in the 10^{-18} regime.

Clock comparison through optical fibers

So far, we have discussed the signal propagation on null geodesics which connect events on the clocks' worldlines. The general redshift formula (4.2) was derived and is only valid for such situations. We may now also consider light signals propagating through optical fiber links that physically connect the clocks and have a non-negligible extension as well as a specific profile for the index of refraction n. Clearly, light signals in these fibers do not propagate with the vacuum speed of light but rather with a modified speed c_n. The relation between c_n and c is given by

$$n = \frac{c}{c_n} \quad \Leftrightarrow \quad c_n = \frac{c}{n}\,. \tag{4.13}$$

Thus, an index of refraction larger than one leads to a reduced propagation velocity inside the material. Table 4.1 shows the index of refraction for various materials [87]. An optical fiber used for signal transmission between modern clocks has a distinct profile for the index of refraction in three spatial dimensions to ensure some optimal propagation and transmission properties. However, the index of refraction is approximately in the range of the value for silica. Thus, the speed of light inside such a fiber is approximately two thirds of the vacuum speed of light.

In the following, we will show that for a stationary spacetime Eq. (4.9) is also valid if the comparison is done with non-geodesic signals that move at the speed of light. These signals are not freely propagating but confined to a spacelike path established by the optical fiber. The important consequence is that redshift experiments can also be described in the framework of the redshift potential even if the signals are transmitted over long distances through optical fiber links.

For the following considerations, we assume that the fiber is at rest with respect to the congruence of Killing observers for which a time-independent redshift potential ϕ exists. The fiber is represented by a time-independent path in the geometry described

by the metric (4.7). A signal at the speed of light that propagates along this path has to satisfy the condition that its tangent is lightlike, i.e.

$$g_{\mu\nu}\dot{x}^\mu\dot{x}^\nu = 0\,, \tag{4.14}$$

where the overdot denotes the derivative taken with respect to an affine curve parameter s. The signal is, of course, future-directed and propagates on the emitter's future light cone. Hence, for the geometry (4.7) we obtain

$$c\,\mathrm{d}t + \alpha_a \mathrm{d}x^a = \sqrt{\alpha_{ab}\mathrm{d}x^a\mathrm{d}x^b}\,. \tag{4.15}$$

Thereupon, we can calculate the coordinate travel time of the signal by integration

$$\Delta t := t_2 - t_1 = \int_{t_1}^{t_2} dt = \frac{1}{c}\int_{s_1}^{s_2}\left(\sqrt{\alpha_{ab}\frac{\mathrm{d}x^a}{\mathrm{d}s}\frac{\mathrm{d}x^b}{ds}} - \alpha_c\frac{\mathrm{d}x^c}{ds}\right)\mathrm{d}s\,. \tag{4.16}$$

Since we have $\partial_t\alpha_a = 0$ and $\partial_t\alpha_{ab} = 0$, the travel time Δt is independent of the emission time t_1. It follows that for two signals that are emitted with a coordinate time difference Δt, the reception time difference is Δt as well. For the Killing observers in the congruence, the four-velocity is $u = \exp(-\phi)\partial_t$. The relation between the respective proper time τ and coordinate time t for each of these observers is given by

$$\frac{\mathrm{d}\tau}{\mathrm{d}t} = e^\phi\,. \tag{4.17}$$

Now, we can easily determine the redshift of a signal transmitted through an optical fiber between two observers in the congruence. We obtain

$$z + 1 = \frac{\nu}{\tilde{\nu}} = \frac{\mathrm{d}\tilde{\tau}}{\mathrm{d}\tau} = \frac{\mathrm{d}\tilde{\tau}}{\mathrm{d}t}\frac{\mathrm{d}t}{\mathrm{d}\tau} = \frac{e^\phi|_{\tilde{\gamma}}}{e^\phi|_\gamma}\,. \tag{4.18}$$

Hence, the correct frequency ratio and, therefore, the redshift is again obtained by the redshift formula (4.9) for the clock comparison via signal transmission through an arbitrarily shaped optical fiber. The only assumptions are the stationarity of the spacetime and a fiber at rest with respect to the observers. Both assumptions might be realized at least approximately for short time scales that cover the duration of the measurements.

The next step is to consider fiber links with an index of refraction different from one. In such fibers, the speed of a light signal is reduced compared to the situation before. We use the framework of optical metrics, see, e.g., Ref. [136]. The geometry is now to be described by the metric

$$g = e^{2\phi(x)}\left[-n(x)^{-2}(c\,\mathrm{d}t + \alpha_a(x)\mathrm{d}x^a)^2 + \alpha_{ab}(x)\mathrm{d}x^a\mathrm{d}x^b\right]\,, \tag{4.19}$$

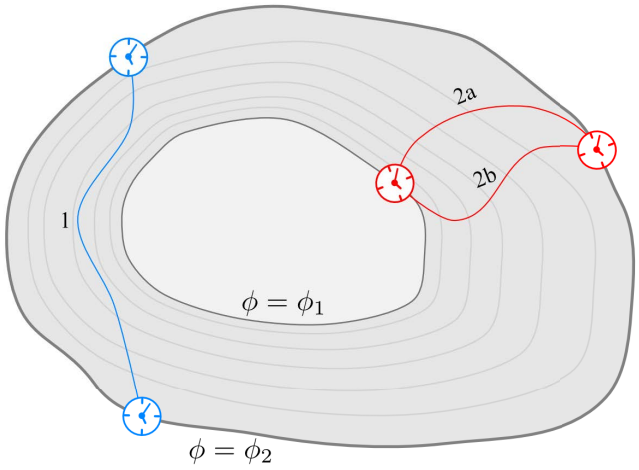

FIGURE 4.3: Sketch of surfaces of a constant redshift potential ϕ and optical fiber links connecting standard clocks on these surfaces. The redshift is independent of the spatial shape of the chosen fiber as long as the fibers are at rest with respect to the Killing observers which are indicated by the clocks' positions. The redshifts measured using fiber 2a and 2b will be identical, whereas the redshift measured using fiber 1 is zero.

instead of using (4.7). We assume again that the fiber is at rest with respect to the congruence of Killing observers. Hence, in particular emitter and receiver are spatially connected by the time-independent fiber path. The redshift of the two ends of the fiber now results in

$$z + 1 = \frac{\nu}{\tilde{\nu}} = \frac{e^{\phi}|_{\tilde{\gamma}}}{e^{\phi}|_{\gamma}} \frac{n|_{\gamma}}{n|_{\tilde{\gamma}}} \,. \tag{4.20}$$

Again, the redshift potential gives the correct redshift by evaluation on the emitter's receiver's worldlines, provided that the index of refraction is constant. Furthermore, the equation above shows that the redshift potential ϕ for the vacuum situation can be deduced from frequency comparisons using optical fiber links when the position-dependent index of refraction $n(x)$ of the particular fiber is known. However, this profile is known or can be determined by separate measurements. Figure 4.3 shows the principle idea of level surfaces of the redshift potential and clock comparison using optical fibers for different paths.

Comparison of optical clocks in fiber networks is actually performed nowadays at high accuracies, see, e.g., Ref. [118] and references therein.

4.2.3 Congruences of observer worldlines – acceleration potential

The introduction of a time-independent redshift potential requires the existence of a timelike Killing vector field, i.e. it requires the spacetime to be stationary. The congruence of observers who determine the redshift potential and its level surfaces must then be a timelike Killing congruence. In this section, we will recall some facts about general timelike congruences and show that the assumption of stationarity is naturally equivalent to a relativistic generalization of the requirements that we made for a time-independent Newtonian geoid, see chapter 2. The three assumptions have been:

(A1) The Earth is in rigid motion.

(A2) The Earth rotates with constant angular velocity about a fixed rotation axis.

(A3) There are no external forces acting on the Earth.

The relativistic generalization of these three assumptions leads to isometric (= Killing) observer congruences which can be described by an acceleration potential that coincides with the redshift potential defined above.

In the following, we consider a general timelike congruence of worldlines (see, e.g. Refs. [41, 42]). This congruence is a family of timelike curves which (i) do not intersect and (ii) fill a certain region of the four-dimensional spacetime. We use coordinates $(x^\mu) = (x^0, x^1, x^2, x^3)$ and we describe the worldlines of the congruence by integral curves of a timelike tangent vector field

$$u = u^\mu \partial_\mu \,, \quad (u^\mu) = (u^0, u^i) \,, \tag{4.21}$$

and we assume that u is normalized, i.e.

$$g(u,u) = g_{\mu\nu} u^\mu u^\nu = -c^2 \,. \tag{4.22}$$

One possible interpretation for u is to take it as the four-velocity field of a gravitating body. On the surface of the body at the other hand, u may also be interpreted as the four-velocity field of observers who are rigidly attached to the surface and equipped with standard clocks. Moreover, we can extend the vector field u into the exterior region where it may be interpreted as the four-velocity of observers hovering above the surface, e.g. clocks in satellites constellations. We will classify and characterize different cases that depend on the properties of u and, therefore, on the properties of the congruence. In the end, we outline the very special case in which u is proportional to a Killing vector field.

The observers in the congruence will perform mutual measurements, which may include the determination of distances, velocities, and redshifts. To describe such measurements and the kinematic decomposition of the congruence we need the projection onto the local rest space of the observers. This projection is given by the projection operator P^μ_ν, which in turn is given by

$$P^\mu_\nu = \delta^\mu_\nu + \frac{1}{c^2}\, u^\mu u_\nu \,. \tag{4.23}$$

The acceleration $a = a^\mu \partial_\mu$ of the congruence is defined by the covariant derivative of u in the direction of u. Hence, we have

$$a^\mu := \dot{u}^\mu = u^\nu D_\nu u^\mu \,. \tag{4.24}$$

Note that the acceleration a vanishes along a particular integral curve γ of u if and only if this curve is a geodesic of the spacetime. In the special case that the acceleration of the congruence vanishes, the integral curves of the vector field u describe a congruence of geodesics.

Kinematic decomposition of timelike congruences

As commonly done in nonrelativistic physics and continuum mechanics, a congruence of worldlines can be characterized by the kinematic quantities rotation $\omega_{\mu\nu}$, shear $\sigma_{\mu\nu}$, and expansion θ. For our timelike congruence of integral curves of u, these three kinematic quantities are calculated by projections of derivatives of u onto the rest space of the congruence. The rotation is described by projecting the anti-symmetric part, the shear is obtained by projecting the symmetric trace-free part, and the expansion is the remaining trace. We have

$$\omega_{\mu\nu} := P^\rho_\mu P^\sigma_\nu D_{[\sigma} u_{\rho]} = D_{[\nu} u_{\mu]} + \frac{1}{c^2}\, \dot{u}_{[\mu} u_{\nu]} \,, \tag{4.25a}$$

$$\sigma_{\mu\nu} := P^\rho_\mu P^\sigma_\nu D_{(\sigma} u_{\rho)} - \frac{1}{3}\theta P_{\mu\nu} = D_{(\nu} u_{\mu)} + \frac{1}{c^2}\, \dot{u}_{(\mu} u_{\nu)} - \frac{1}{3}\theta P_{\mu\nu} \,, \tag{4.25b}$$

$$\theta := D_\mu u^\mu \,. \tag{4.25c}$$

Therefore, the rotation tensor is antisymmetric $\omega_{\mu\nu} = -\omega_{\nu\mu}$, while the shear is symmetric and traceless $\sigma_{\mu\nu} = \sigma_{\nu\mu}$. The motion of neighboring worldlines with respect to a chosen worldline with tangent u is determined by the kinematic decomposition of the derivative

$$D_\nu u_\mu = \omega_{\mu\nu} + \sigma_{\mu\nu} + \frac{1}{3}\theta P_{\mu\nu} - \frac{1}{c^2}\, u_\nu a_\mu \,. \tag{4.26}$$

A congruence with vanishing expansion, $\theta = 0$, is called isochoric. For such a congruence, the volume of a comoving spatial region is constant and not changing

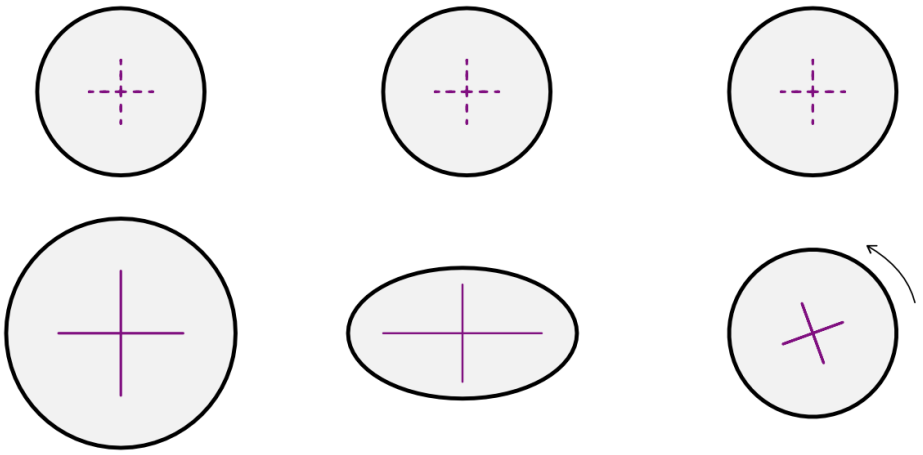

FIGURE 4.4: Sketch of different congruence properties. From left to right: expanding, shearing and rotating comoving area.

over time [41, 42]. An isochoric congruence with vanishing shear, $\sigma_{\mu\nu} = 0$, is called Born-rigid [12, 167]. Figure 4.4 schematically shows properties of different congruence flows. A comoving area that encloses a certain set of worldlines of the congruence is evolved over time with the flow of the wordlines. For an expanding congruence, the area increases in a symmetric way, for a congruence with shear, the area is deformed, and for a purely rotating flow the area and its shape remain constant.

A congruence is Born-rigid if and only if the spatial distance between any two infinitesimally neighboring integral curves of u remains constant over time. In this case, Eq. (4.26) simply reduces to

$$D_\nu u_\mu = \omega_{\mu\nu} - \frac{1}{c^2}\, u_\nu a_\mu \,. \tag{4.27}$$

In analogy to the Newtonian condition (A1) above, we require the congruence that describes the gravitating object to be Born-rigid. Hence, for our consideration Born-rigidity serves as the relativistic generalization of rigid motion in Newtonian physics. Thereupon, we translate the condition (A1) into

$$P^\rho_\mu\, P^\sigma_\nu\, D_{(\sigma} u_{\rho)} = 0 \,. \tag{A1"}$$

To define the analogs of the Newtonian conditions (A2) and (A3), we have to introduce some more derived quantities to characterize the congruence and restrict its properties even further. One important object is the rotation four-vector ω^μ defined by

$$\omega^\mu := \frac{1}{2c}\eta^{\mu\nu\sigma\lambda} u_\nu \omega_{\sigma\lambda} = \frac{1}{2c}\,\eta^{\mu\nu\sigma\lambda} u_\nu \partial_\lambda u_\sigma \,. \tag{4.28}$$

Since the rotation vector is orthogonal to the tangent vector of the congruence,

$$\omega^\mu u_\mu = 0\,, \tag{4.29}$$

the rotation vector ω^μ is spacelike. We can further decompose it into the form

$$\omega^\mu = \omega\, e^\mu\,, \tag{4.30}$$

where $e^\mu e_\mu = 1$. The unit vector e^μ gives the direction of the momentary rotation axis, and the scalar ω gives the magnitude of the momentary angular velocity.

We can now translate the Newtonian requirements (A2') and (A3') into the following relativistic conditions:

$$P^\mu_\nu \dot{\omega}^\nu = 0\,, \tag{A2"}$$
$$P^\mu_\nu \dot{a}^\nu = \omega^\mu{}_\nu a^\nu\,. \tag{A3"}$$

The new condition (A2") states that the unit vector of the rotation e^μ is Fermi-Walker transported and that the scalar ω is constant along each worldline of the congruence. This implies that the rotation axis and angular velocity are time-independent. The other condition (A3") means that any change of the acceleration, projected onto the rest space, along the congruence is only caused by the rotation. Moreover, if the acceleration vector a^μ initially points to one neighboring particle, it will always point to that very same neighbor for the entire evolution of the congruence.

Acceleration potential

In Ref. [41], Ehlers has shown that for a Born-rigid congruence the two requirements (A2") and (A3") together are equivalent to stating that

$$D_{[\nu} a_{\mu]} = 0\,. \tag{4.31}$$

The latter condition naturally means that there must exist a potential $\hat{\phi}$ for the acceleration such that

$$a_\mu = c^2 \partial_\mu \hat{\phi}\,. \tag{4.32}$$

This, in turn, is true for a Born-rigid congruence if and only if the tangent vector field u of the congruence is proportional to a timelike Killing vector field ξ [167, 5], such that the proportionality is given by the relation

$$\xi = e^{\hat{\phi}} u\,. \tag{4.33}$$

Clearly, we recognize that we must have

$$\hat{\phi} \equiv \phi \,, \tag{4.34}$$

which means that the acceleration potential $\hat{\phi}$ coincides with the time-independent redshift potential ϕ that was introduced before. Moreover, we have shown that stationarity, which is required for the existence of a time-independent redshift potential, is genuinely equivalent to the three relativistic conditions (A1"), (A2"), and (A3"). It is therefore very well motivated by the Newtonian analogs. A congruence that has the properties (A1") - (A3") is called isometric. The contravariant acceleration components can be calculated by

$$a^\mu = g^{\mu i} a_i = c^2 g^{\mu i} \partial_i \phi \,, \tag{4.35}$$

and the magnitude of the acceleration a is given by

$$a^2 = g^{\mu\nu} a_\mu a_\nu = c^4 g^{ij} \partial_i \phi \partial_j \phi \,. \tag{4.36}$$

It can be considered as relativistic gravity, the generalization of $g = ||-\vec{\nabla} W||_2$.

Integral curves of the Killing vector field defined by $\xi = \exp(\phi)\, u$ correspond to the worldlines of a co-rotating family of observers. However, note that ξ may be defined and timelike on a finite cylindrical neighborhood of the rotating body only. This neighborhood can be extended to infinity, covering all the exterior region, for a non-rotating and isolated central object. If extended outside of the neighborhood of a rotating object, the Killing vector field becomes spacelike. A rough estimate of the radius of the cylindrical region may be obtained by

$$R_\perp = \frac{c}{\omega} \,. \tag{4.37}$$

Finally, note that the accelerations of test particles as seen by observers in the congruence is given by $-a = -c^2 \mathrm{d}\phi$.

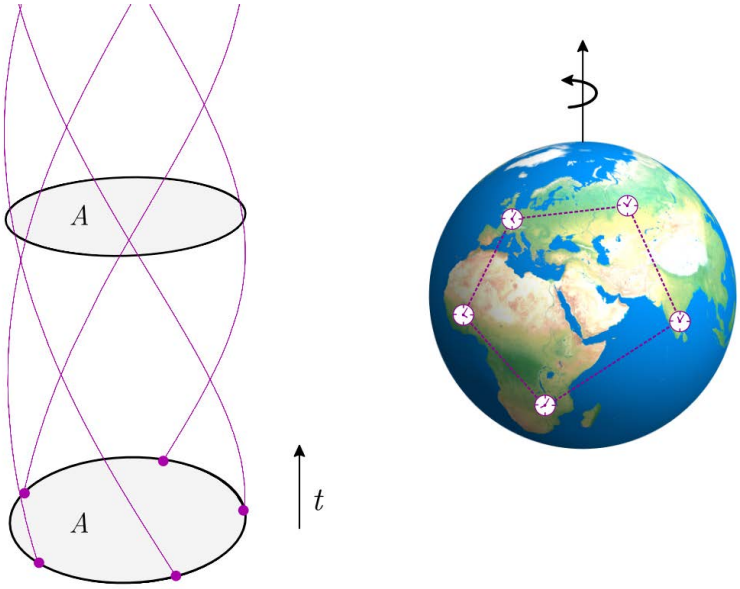

FIGURE 4.5: Sketch of the projection of a purely rotating flow that resembles the motion of the constituents of the central gravitating body or, equivalently, observers attached to the surface. A comoving area A, enclosed by a certain set of congruence worldlines, remains constant over time.

4.3 Relativistic gravity potential and geodetic reference surfaces

Now that we have collected all the ingredients to define relativistic generalizations of geodetic reference surfaces, we first define a new potential that replaces the Newtonian gravity potential in General Relativity. Afterwards, we proceed to show how redshift and acceleration measurements are described in terms of the new notion. Thereupon, we define the relativistic geoid in the theoretical framework of General Relativity.

For the following, we assume that the spacetime is stationary and described by the metric (4.7),

$$g = e^{2\phi(x)} \left[-(c\,\mathrm{d}t + \alpha_a(x)\mathrm{d}x^a)^2 + \alpha_{ab}(x)\mathrm{d}x^a\mathrm{d}x^b \right] , \tag{4.38}$$

where all metric functions are independent of the time coordinate t. We consider a timelike isometric congruence of observers of which the worldlines are integral curves of the vector field $u = \exp(-\phi)\partial_t$, where ϕ is the redshift (and acceleration) potential for these observers.

4.3.1 Relativistic gravity potential

Based on our considerations in the previous sections we now define a new artificial relativistic gravity potential U^* by the following relation

$$e^{\phi} =: 1 + \frac{U^*}{c^2} \quad \Leftrightarrow \quad U^* = c^2 \left(e^{\phi} - 1 \right) = c^2 \left(\sqrt{-g_{00}} - 1 \right) . \tag{4.39}$$

Observe that the dimension of the relativistic gravity potential U^* is the square of a velocity,

$$[U^*] = [c^2] = \mathrm{m}^2/\mathrm{s}^2 , \tag{4.40}$$

whereas the redshift potential itself is dimensionless. The intention of defining the new potential U^* as done above becomes clear in the Newtonian limit. Since the time coordinate t is associated with the timelike Killing vector field ∂_t, our potential U^* becomes the Newtonian gravity potential W in the weak field limit, i.e.

$$U^* \underset{c\to\infty}{\longrightarrow} W , \tag{4.41}$$

including centrifugal effects if the coordinates are adapted to a rotating congruence of observers. Note in particular that in our sign convention also $U^* < 0$.

In the first order post-Newtonian approximation, however, the leading order terms of the potential U^* become

$$U^*_{\mathrm{pN}} = W + \frac{1}{2}\frac{U^2}{c^2} , \tag{4.42}$$

as we will show later in more detail. Note that our definition of U^* does not involve any kind of (weak-field) approximation, and is valid in General Relativity for all stationary spacetimes.

Of course, a relativistic gravity potential based on the redshift potential ϕ can be defined in different ways and (4.39) is not the only possibility. In general, every monotonic function of the redshift potential serves the same purpose. However, our choice is natural and unique so some extent. We look for the simplest function U^* of ϕ for which the Newtonian limit (4.41) is valid. Moreover, U^* shall have the dimension of a potential, i.e. a squared velocity. And last but not least, we want the post-Newtonian limit of U^* to match the result of Soffel et. *al.* in Ref. [181]; see Eq. (4.42) but be reminded of the different sign convention of the authors. Taken into account these properties, we stand with our choice of U^*.

Redshift measurements

Redshift measurements of two observers who are members of the congruence of which the worldlines are integral curves of $u = \exp(-\phi)\partial_t$, i.e. the observers who determine the isochronometric surfaces, give the following result. Let the worldlines of the two observers be γ_1 and γ_2, respectively. The two observers shall measure their respective proper times, i.e. they carry standard clocks with them. We evaluate the redshift potential ϕ and the relativistic gravity potential U^* on their worldlines to have values

$$\phi_i := \phi|_{\gamma_i} \quad \text{and} \quad U_i^* := U^*|_{\gamma_i} \quad i = 1, 2\,, \tag{4.43}$$

The frequency ratio of their standard clocks is then given by

$$1 + z = \frac{\nu_1}{\nu_2} = e^{\phi_2 - \phi_1} = \frac{1 + U_2^*/c^2}{1 + U_1^*/c^2} = 1 + \frac{U_2^* - U_1^*}{c^2} + \mathcal{O}(c^4) =: 1 + \frac{\Delta U^*}{c^2} + \mathcal{O}(c^4)\,. \tag{4.44}$$

Hence, the relativistic gravity potential U^* also determines the redshift of two observers. To leading order, the redshift is given by the potential differences. The redshift vanishes in the Newtonian limit since Newton's universal time is absolute. But to first post-Newtonian order we obtain as the largest contribution

$$\frac{\nu_1}{\nu_2} = 1 + \frac{\Delta W}{c^2} + \mathcal{O}\big(c^{-3}\big)\,. \tag{4.45}$$

Note, however, that our definition of U^* is exact, i.e. without any approximation, and it is valid for an arbitrary stationary spacetime with a metric as given above. Thus, we have constructed a general relativistic generalization of the concept introduced by Soffel et *al.* in [181]. In this work, the authors derive a similar expression but investigate a first-order post-Newtonian spacetime only.

Acceleration measurements

The acceleration of freely falling objects w.r.t. comoving observers in the congruence of integral curves of $u = \exp(-\phi)\partial_t$, e.g., observers co-rotating with the Earth is given by

$$a = -c^2 \mathrm{d}\phi = -c^2 \frac{\partial \phi}{\partial U^*} \mathrm{d}U^* = \frac{-\mathrm{d}U^*}{1 + U^*/c^2}\,, \tag{4.46}$$

since the redshift potential ϕ is an acceleration potential as well. Hence, a as a 1-form is closed and exact. The components of the acceleration can be calculated by $a_\mu = c^2 \partial_\mu \phi$ and it is clear that $a_0 \equiv 0$ and $(a_\mu) = (0, a_1, a_2, a_3)$. Calculating the components leads

to

$$a_\mu = -c^2\partial_\mu\phi = -c^2 e^{-\phi}\partial_\mu e^{\phi} = \frac{-\partial_\mu U^*}{1+U^*/c^2}\,. \tag{4.47}$$

We notice that U^*, or rather its gradient, determines the acceleration of observers in the congruence. The surfaces $\phi = \text{const.}$, i.e. $U^* = \text{const.}$, are everywhere perpendicular to the acceleration.

In the Newtonian limit, $c \to \infty$, we do also recover the well known Newtonian formula[3]

$$\vec{g} = -\vec{\nabla}W\,, \tag{4.48}$$

according to which the acceleration is given by the gradient of the gravity potential. For the magnitude of the relativistic acceleration we obtain

$$\frac{a^2}{c^4} = \frac{g(a,a)}{c^4} = g^{ij}\partial_i\phi\,\partial_j\phi \quad \Rightarrow a^2 = g^{ij}\frac{\partial_i U^*\,\partial_j U^*}{(1+U^*/c^2)^2}\,, \tag{4.49a}$$

from which the Newtonian limit for $c \to \infty$ follows,

$$g^2 = (\vec{\nabla}W)^2 \quad \Leftrightarrow \quad g = ||\vec{\nabla}W||_2\,, \tag{4.50}$$

see chapter 2. In all the equations above, $\vec{\nabla}$ is the flat space operator.

4.3.2 The relativistic geoid

In analogy to the Newtonian understanding, we now define the relativistic geoid in terms of the level surfaces of the potential U^*:

> For a spacetime equipped with a metric in the form (4.7) and a congruence of observers of which the worldlines are integral curves of the vector field $u = e^{-\phi}\partial_t$, the relativistic geoid is a particularly chosen level surface of the relativistic gravity potential U^* such that $U^*\big|_{\text{geoid}} = U_0^* = \text{const.}$

The Newtonian limit of our relativistic definition is obvious: since the weak field limit of U^* is W, we obtain the Newtonian definition in terms of level surfaces of the gravity potential W such that on the geoid $W = -W_0$. Level surfaces of U^* are clearly level surfaces of ϕ and therefore they are isochronometric surfaces. The value U_0^*, which

[3] Note that in this limit the indices are raised and lowered with the Kronecker delta δ^μ_ν.

singles out one equipotential surfaces to be the relativistic geoid, must be given by some convention which is agreed upon. Two possible conventions are, e.g.,

(i) to fix the value by the conventional Newtonian gravity potential value on the geoid such that $U_0^* = -W_0$

(ii) to define a master clock which is, by definition, situated on the geoid surface and singles out one isochronometric surface (e.g., the one that passes through its center of mass).

Note that the choice (ii) is equivalent to just marking a point (possibly at the shore), representing the mean sea level, and therefore choosing a level surface for U^* in a geometric manner. In section 6.4.2, we outline a procedure by which a particular equipotential surface of U^* can be maintained over time by a point on this level surface that can be experimentally realized even though the topology of the Earth's surface underneath may change.

The relativistic gravity potential U^* can be used to define the relativistic geoid, to calculate the redshift of observers who determine the geoid, and to calculate the acceleration of co-moving observers and freely falling particles observed by them. In chapter 5 we apply the framework and concepts developed so far to various spacetime models such as exact relativistic vacuum spacetimes as well as a post-Newtonian approximation of General Relativity. Moreover, we quantitatively calculate the difference between the Newtonian geoid and the leading order relativistic contributions.

We shall at this point state an alternative definition of the relativistic geoid: the relativistic geoid for a congruence of observers of which the acceleration one form is exact, is given by a level surface of the acceleration potential. This definition yields a relativistic geoid related to acceleration measurements, the so-called a-geoid. However, as we have shown that the acceleration potential and the redshift potential coincide; this alternative definition is in fact equivalent to the definition of the so-called u-geoid given above.

As we will show in chapter 5, our definition of the relativistic geoid generalizes the definition by Soffel et. *al.* [181], which uses a first-order post-Newtonian framework. Our definition is valid to any order since neither do we involve any assumption about the strength of the gravitational field nor do we employ expansion schemes for large radii. Other definitions of the relativistic version of the Earth's geoid can be found in Refs. [114], [174], and [134]. In [114], the authors again use post-Newtonian concepts and the definition suffers slightly from some in-accurateness. In Ref. [134], the authors define an a-geoid on the basis of quasi-local frames, being interested only in the accelerations of these frames. Since we do believe that chronometric measurements offer the best future prospectives for relativistic geodesy on Earth, we base our definition of the relativistic

geoid on the relativistic gravity potential founded on the redshift potential for Killing observers. Moreover, we have demonstrated that the definitions of the u- and a-geoids coincide in General Relativity and that the definition can also be given in terms of the acceleration of an observer congruence, see above.

Stationarity is the main assumption for our definition. Of course, this is an idealization. But just as in conventional geodesy, in which the geoid is also defined in a stationary average, temporal variations can be taken into account by introducing time-dependent perturbations. To do so, one should consider a non-stationary metric $\Sigma_{\mu\nu}$ of the form

$$\Sigma_{\mu\nu} = g_{\mu\nu} + h_{\mu\nu} \tag{4.51}$$

such that $g_{\mu\nu}$ is stationary and the definition of the relativistic geoid is to be applied to it. This stationary part can be defined as an average over a sufficiently large time span. In this way, also permanent tidal effects due to external objects, such as the moon and the sun, can be included. The perturbations might be described by the time-dependent part $h_{\mu\nu}$, which shall be small compared to the stationary part with respect to some suitable measure. Examples for some perturbations are listed above. Here, we do not work out a relativistic theory of these perturbations. However, ignoring gravitational wave emission, our formalism applies also to irregularly shaped rotating astrophysical objects. In a strict sense, the spacetime is not stationary and gravitational wave emission slows down the rotation. Of course, this effect is completely negligible for the Earth and all other planets.

The extension of isochronometric surfaces and, therefore, the geoid into the interior of the gravitating body is also well defined if the assumption of Born-rigid rotation remains valid. Then, the four-velocity vector field u of the worldlines of the body's constituents is also well-defined and still proportional to a Killing vector field. An interior solution of the field equation must be matched to the exterior geometry at the surface and the level surface of the relativistic gravity potential U^* that defines the geoid will in general be continuous but not differentiable.

4.3.3 The relativistic normal potential and level surface

In chapter 2, we have given the definition of the normal potential W_N of the Earth. It is a special axisymmetric gravity field and a very good approximation to the true gravity potential W. The definition includes four parameters, two of which are for the geometry of the level ellipsoid and the other two are the Earth's gravity constant and the angular velocity of its rotational motion. We have seen that only even coefficients J_{2l} for $l \in \mathbb{N}_0$ contribute to the expansion in terms of Legendre polynomials. Therefore, the normal

gravity potential possesses also a $\mathbb{Z}_2$ symmetry, i.e. reflection symmetry with respect to the equatorial plane. Any axisymmetric gravitational potential can be expressed in the form (2.12) and for the normal potential the special relation (2.40) between the axisymmetric multipoles J_{2l} holds. Now, we use this relation and construct a relativistic spacetime that serves as the generalization of the Newtonian normal gravitational field. This spacetime is called normal gravity spacetime in the following. The construction is made such that in the Newtonian limit, all relations outlined in section 2.2.4 are recovered.

The normal gravity spacetime is assumed to be static (or stationary), asymptotically flat, axisymmetric, free of singularities in the exterior, it possess a reflection symmetry w.r.t. the equatorial plane, and is determined by four independent parameters. It is an exact general relativistic spacetime that, in the Newtonian limit, coincides with the normal gravity field of the Earth in the exterior region. It should be linked, however, to a source distribution and be matched to the interior solution at the boundary surface, if possible. The exhaustive derivation of properties of Weyl spacetimes in chapter 3 pays off now since an appropriately constructed Weyl spacetime possesses all these properties and is investigated below.

We start with the Newtonian normal gravity potential and use Eq. (2.40) for the coefficients J_{2l},

$$J_0 = 1\,, \quad J_{2l} = (-1)^l \frac{3(E/a)^{2l}}{(2l+1)(2l+3)} \left(1 - l - 5l\frac{a^2}{E^2}J_2\right)\,, \quad \forall\, l > 1\,, \tag{4.52}$$

and the relation (2.41) to calculate the dimensional multipoles $\tilde{J}_l = R_{\text{ref}}^l\, J_l\, M$ according to Eq. (2.14). Thereupon, we calculate the Quevedo moments $\bar{q}_l$ using (3.47) and obtain

$$\bar{q}_l = (-1)^l \frac{(2l+1)!!}{l!\, M^{l+1}} \tilde{J}_l = (-1)^l \frac{(2l+1)!!}{l!\, M^l}\, R_{\text{ref}}^l J_l\,. \tag{4.53}$$

Now, we construct a Weyl spacetime of which the main metric function ψ is given by

$$\begin{aligned}
\psi &= \sum_{l=0}^{\infty} (-1)^{l+1} q_l\, Q_l(x)\, P_l(y) = \sum_{l=0}^{\infty} (-1)^{l+1} \left(\frac{G}{c^2}\right)^{-l} \bar{q}_l\, Q_l(x)\, P_l(y) \\
&= -\sum_{l=0}^{\infty} \left(\frac{G}{c^2}\right)^{-l} \frac{(2l+1)!!}{l!\, M^{l+1}} \tilde{J}_l\, Q_l(x)\, P_l(y) \\
&= -\sum_{l=0}^{\infty} \left(\frac{G}{c^2}\right)^{-l} \frac{(2l+1)!!}{l!\, M^{l+1}} R_{\text{ref}}^l M J_l\, Q_l(x)\, P_l(y) \\
&= -\sum_{l=0}^{\infty} \frac{(2l+1)!!}{l!} \left(\frac{R_{\text{ref}}}{m}\right)^l J_l\, Q_l(x)\, P_l(y)\,,
\end{aligned} \tag{4.54}$$

with $m = GM/c^2$, see Eq. (3.34). Note that ψ is indeed dimensionless. Using only the even terms J_{2k} for the Newtonian normal gravity field, see above, we get

$$\begin{aligned}\psi_N &= -\sum_{k=0}^{\infty} \frac{(4k+1)!!}{(2k)!} \left(\frac{R_{\text{ref}}}{m}\right)^{2k} J_{2k}\, Q_{2k}(x)\, P_{2k}(y) \\ &= -Q_0(x) - \frac{15}{2}\left(\frac{R_{\text{ref}}}{m}\right)^{2} J_2 Q_2(x) P_2(y) - \sum_{k=2}^{\infty} \frac{(4k+1)!!}{(2k)!} \left(\frac{R_{\text{ref}}}{m}\right)^{2k} J_{2k}\, Q_{2k}(x) P_{2k}(y) \\ &\mathrel{\mathring{=}} \frac{1}{2}\log\left(\frac{x-1}{x+1}\right) + \frac{15}{2}\frac{R_{\text{ref}}^2}{m^2} J_2 \frac{(3y^2-1)}{2}\left(\frac{(3x^2-1)}{4}\log\left(\frac{x-1}{x+1}\right) + \frac{3}{2}x\right) + \dots .\end{aligned} \tag{4.55}$$

We can insert a series expansion for the Legendre functions $Q_l(x)$ [6] and write the exact result in terms of Legendre polynomials and simple logarithmic terms,

$$\begin{aligned}\psi_N = -\sum_{k=0}^{\infty} \Bigg[&\frac{(4k+1)!!}{(2k)!}\left(\frac{R_{\text{ref}}}{m}\right)^{2k} J_{2k}\, P_{2k}(y) \\ &\times \left(\log\left(\frac{x+1}{x-1}\right) P_{2k}(x) - 2\sum_{i=0}^{k-1} \frac{4k-4i-1}{(2k-i)(2i+1)} P_{2k-2i-1}(x)\right)\Bigg] ,\end{aligned} \tag{4.56}$$

and ψ_N can be evaluated to arbitrary order $k_{\max}$. The metric component g_{00} of the normal gravity spacetime becomes now

$$\begin{aligned}g_{00} &= -\exp(2\psi_N) = -\exp\left(-2\sum_{k=0}^{\infty} \frac{(4k+1)!!}{(2k)!}\left(\frac{R_{\text{ref}}}{m}\right)^{2k} J_{2k}\, Q_{2k}(x)\, P_{2k}(y)\right) \\ &= -\prod_{k=0}^{\infty} \exp\left(-2\frac{(4k+1)!!}{(2k)!}\left(\frac{R_{\text{ref}}}{m}\right)^{2k} J_{2k}\, Q_{2k}(x)\, P_{2k}(y)\right) \\ &\mathrel{\mathring{=}} -\left(\frac{x-1}{x+1}\right) \times \exp\left[J_2 \frac{15}{2}\frac{R_{\text{ref}}^2}{m^2}(3y^2-1)\left(\frac{(3x^2-1)}{4}\log\left(\frac{x-1}{x+1}\right) + \frac{3}{2}x\right)\right] \times \dots ,\end{aligned} \tag{4.57}$$

which is a product of terms according to the structure

$$g_{00} = -\left(\frac{x-1}{x+1}\right) \times \exp(\sim J_2) \times \exp(\sim J_4) \times \exp(\sim J_6) \times \dots . \tag{4.58}$$

Note that the sign of the x-dependent part in the exponent is always negative,

$$\operatorname{sign}\left[-J_{2k}\, Q_{2k}(x)\right] = -1 \quad \forall k \geq 1 , \tag{4.59}$$

when the proper values for J_{2k} are inserted.

The equations (4.55), (4.56), and (4.57) tell us that the 0-th order approximation of the normal gravity spacetime is a Schwarzschild spacetime, and the next order

approximation is an Erez-Rosen spacetime.

For Weyl spacetimes, it is true that for observers on integral curves of the Killing vector field $\xi_1 = \partial_t$, the redshift potential ϕ can be identified with the metric function ψ. However, we are interested in the description of concepts as measured by observers co-rotating with the Earth. Such observers move on integral curves of the Killing vector field $\xi_1 + \omega\,\xi_2 = \partial_t + \omega\,\partial_\varphi$, see chapter 3 and the section devoted to Weyl spacetimes therein. After a coordinate transformation

$$\varphi \to \varphi' = \varphi - \omega t \tag{4.60}$$

the redshift potential ϕ_N in the normal gravity spacetime for rigidly co-rotating observers on the Earth is to be read off from the new metric component g'_{00}, see Eq. (4.8) and Ref. [145]. We obtain

$$e^{\phi_N} = \sqrt{e^{2\psi_N} - \frac{\omega^2}{c^2} m^2 e^{-2\psi_N}(x^2-1)(1-y^2)}\,. \tag{4.61}$$

Thereupon, the relativistic normal gravity potential U_N^* can be constructed via Eq. (4.39),

$$U_N^* = c^2\left(e^{\phi_N} - 1\right)\,. \tag{4.62}$$

The relativistic level "ellipsoid" can now be defined in the following way:

The relativistic level "ellipsoid" is an isochronometric surface in the normal gravity spacetime. It is defined as the two-dimensional surface on which the following condition holds

$$U_N^*(x,y)\big|_{\text{ellipsoid}} = U_0^*\,, \tag{4.63}$$

where U_0^* is the value used in the definition of the relativistic geoid.

This surface will not have the shape of an ellipsoid of rotation and deviate slightly from the perfect bi-axial ellipsoid. However, it is axisymmetric by construction and coincides with the Newtonian level ellipsoid in the weak-field limit since for the relativistic normal gravity potential U_N^* we have

$$U_N^* \underset{c\to\infty}{\longrightarrow} W_N\,, \tag{4.64}$$

see the section on the Newtonian limit of Weyl spacetimes in chapter 3 for the proof. Expanding U_N^* around the Newtonian limit yields

$$U_N^* = W_N + \sum_{n=2}^{\infty} \frac{\kappa_n}{c^n} K_n \,, \tag{4.65}$$

where K_n might be successively defined at increasing post-Newtonian orders and κ_n are formal expansion coefficients. The first term in the expansion then becomes $K_2 = U_N$, the gravitational part of the Newtonian normal gravity field, see 2.2.4.

The relativistic normal gravity (vector) a_N, as a generalization of $\vec{\gamma}$, is constructed by the differential

$$a_N = -c^2 \mathrm{d}\phi_N \,, \quad (a_N)_i = -c^2 \partial_i \phi_N \,, \quad (a_N)^\mu = -c^2 g^{\mu j} \partial_j \phi_N \,, \tag{4.66}$$

where the index $i = 1$ corresponds to the x-component and $i = 2$ corresponds to the y-component in spheroidal coordinates. Note that the normal gravity spacetime is described by a symmetric metric. The magnitude, i.e. the relativistic normal gravity, is

$$(a_N)^2 = c^4 g^{ij}\, \partial_i \phi_N\, \partial_j \phi_N \,. \tag{4.67}$$

For the normal gravity spacetime, we have

$$g_{xx} = m^2 e^{-2\psi_N} e^{2\gamma_N} \frac{x^2 - y^2}{x^2 - 1} \,, \tag{4.68a}$$

$$g_{yy} = m^2 e^{-2\psi_N} e^{2\gamma_N} \frac{x^2 - y^2}{1 - y^2} \,, \tag{4.68b}$$

and the metric function γ_N can be calculated from ψ_N; see, e.g., Refs. [156, 182]. Hence, we have the explicit formula for the relativistic normal gravity

$$\frac{(a_N)^2}{c^4} = \frac{(\partial_x \phi_N)^2}{g_{xx}} + \frac{(\partial_y \phi_N)^2}{g_{yy}} \,, \tag{4.69}$$

which coincides with Eq. (2.43), i.e.

$$\gamma^2 = (\partial_R W_N)^2 + \frac{(\partial_\Theta W_N)^2}{R^2} \,, \tag{4.70}$$

in the Newtonian limit.

We shall note here that also other authors have developed notions of the relativistic normal gravity field. In Refs. [113, 114, 115], Kopeikin et. *al.* constructed a post-Newtonian framework and calculate the level ellipsoid as an equipotential surface of a rotating fluid source. Our construction here is only valid in the exterior and we have

no relations to an interior solution and to sources of the gravity field. However, a link between both notions should be established and, according to basic principles, the two approaches should be related.

4.3.4 On the true geometry of reference surfaces - isometric embedding of the relativistic geoid into Euclidean space

We have defined the relativistic geoid to be one particular level surface of the relativistic gravity potential $U^*|_{\text{geoid}} = U_0^* = \text{const.}$, which is defined for any stationary spacetime. This potential depends on the spatial coordinates x^i but is time-independent. The relativistic geoid is a two-dimensional surface in three dimensional curved space and it can be visualized in various ways but the apparent shape and geometry depends on the chosen coordinates.

However, we seek a way to show and analyze the intrinsic geometry of the geoid surface. Moreover, a comparison with the Newtonian geoid to calculate the differences is also of great interest, especially in the geodetic community. The Newtonian geoid is defined in Euclidean space $\mathbb{R}^3$. Therefore, we have decided to construct an isometric embedding of the relativistic geoid into $\mathbb{R}^3$ to directly compare both surfaces. Whenever such an embedding is possible, it allows to observe the true (intrinsic) geometry and enables us to directly compare two different geoid surfaces.

The same token holds for the geometry of the relativistic level "ellipsoid". Its intrinsic geometry can be analyzed after isometrically embedding the surface.

Details on the embedding procedure and involved equations can be found in the appendix C. We want to state here that the embedding is of great importance to calculate deviations from the well-known and commonly used Newtonian geoid. The order of magnitude of these differences decides, when compared to experimental accuracy for specific applications, which formalism and framework must be used to consistently interpret the measurement.

Chapter 5

Application to Spacetime Models

In this chapter, we apply the notions developed so far to the relativistic spacetimes of chapter 3. Using the results of this chapter enables us to investigate relativistic effects on geodetic measurements in the next one.

All the considered spacetime geometries provide two Killing vector fields which are the generators of time translations and rotations, respectively. In each case, suitable coordinates (t, φ) are adapted to these symmetries, and we can construct two different kinds of isometric observer congruences: (1) observers on $t-$lines, i.e. following the integral curves of ∂_t, and (2) observers of which the worldlines are integral curves of $\partial_t + \omega\partial_\varphi$, for suitable values of ω such that the combination is timelike. Quantities attributed to these two different families of observers are labeled by (1) and (2), respectively.

For stationary spacetimes, the redshift potential ϕ can in general be read off from the g_{00} metric component, see Eq. (4.8) in chapter 4. For the congruence (1) this is straight forwardly possible since the metrics in chapter 3 are given in suitable coordinates such that all considered cases have a metric of the form

$$g = g_{00}\, c^2 \mathrm{d}t^2 + 2g_{0\varphi}\, c\mathrm{d}t\, \mathrm{d}\varphi + g_{11}(\mathrm{d}x^1)^2 + g_{22}(\mathrm{d}x^2)^2 + g_{\varphi\varphi}\mathrm{d}\varphi^2\,, \tag{5.1}$$

where x^1 is some kind of radial coordinate and x^2 is an angle. It follows that

$$e^{2\phi_1} = -g_{00}\,. \tag{5.2}$$

For the congruence (2), we apply a coordinate transformation $x^\mu \to x'^\mu$ given by $\varphi \to \varphi' = \varphi - \omega t$. Thereupon, the metric is rewritten in the new coordinates. Then, the rotating observers are characterized by $\mathrm{d}x'^i = 0$ and the new metric component g'_{00} is used to read off the redshift potential. If the value of ω is interpreted as the Earth's angular velocity, the observers rigidly co-rotate with the Earth. The coordinate

transformation yields

$$g' = \left(g_{00} + 2\frac{\omega}{c}g_{0\varphi} + \frac{\omega^2}{c^2}g_{\varphi\varphi}\right) c^2\mathrm{d}t^2 + 2(g_{0\varphi} + \omega g_{\varphi\varphi})\, c\mathrm{d}t\, \mathrm{d}\varphi' + g_{11}\left(\mathrm{d}x'^1\right)^2 + g_{22}\left(\mathrm{d}x'^2\right)^2 + g_{\varphi\varphi}\mathrm{d}\varphi'^2\,, \tag{5.3}$$

such that

$$g'_{00} = g_{00} + 2\frac{\omega}{c}g_{0\varphi} + \frac{\omega^2}{c^2}g_{\varphi\varphi}\,, \quad \text{and} \quad g'_{0\varphi'} = g_{0\varphi} + \omega g_{\varphi\varphi}\,. \tag{5.4}$$

Note that two of the coordinates remain unchanged, $x'^1 = x^1$ and $x'^2 = x^2$. Now, we read off the redshift potential

$$e^{2\phi_2} = -g'_{00} = -\left(g_{00} + 2\frac{\omega}{c}g_{0\varphi} + \frac{\omega^2}{c^2}g_{\varphi\varphi}\right)\,, \tag{5.5}$$

for co-rotating observers.

5.1 Schwarzschild spacetime

To get started, we begin with the simplest spacetime, the Schwarzschild solution. The metric is given by (3.22) and in this spacetime model, the Earth is approximated by a spherically symmetric mass distribution with total mass M and surface radius $r_\oplus$. The mass parameter m for the metric is $m_\oplus = GM/c^2$, where GM is the Earth's gravity constant. Using the parameters of the EGM96 gravity field model, we obtain $m_\oplus = 0.004\,435\,03\,\mathrm{m}$ and $r_\oplus = 6.378\,136\,3 \times 10^6\,\mathrm{m}$. The Schwarzschild spacetime is the relativistic generalization of a monopolar Newtonian gravitational potential $U(R) = -GM/R$.

The redshift potential for observers on integral curves of the Killing vector field ∂_t is given by

$$e^{\phi_1(r)} = \sqrt{1 - \frac{2m}{r}}\,. \tag{5.6}$$

It can be used to calculate the redshift between two static observers at different radii,

$$z + 1 = \frac{\nu_1}{\nu_2} = \frac{e^{\phi_1(r_2)}}{e^{\phi_1(r_1)}} = \frac{\sqrt{1 - \dfrac{2m}{r_2}}}{\sqrt{1 - \dfrac{2m}{r_1}}}\,. \tag{5.7}$$

If $r_2 > r_1$, then we read off that $v_2 < v_1$ which means that a signal from clock 1 to clock 2 is redshifted. In an abuse of notion, one might say that a photon loses energy

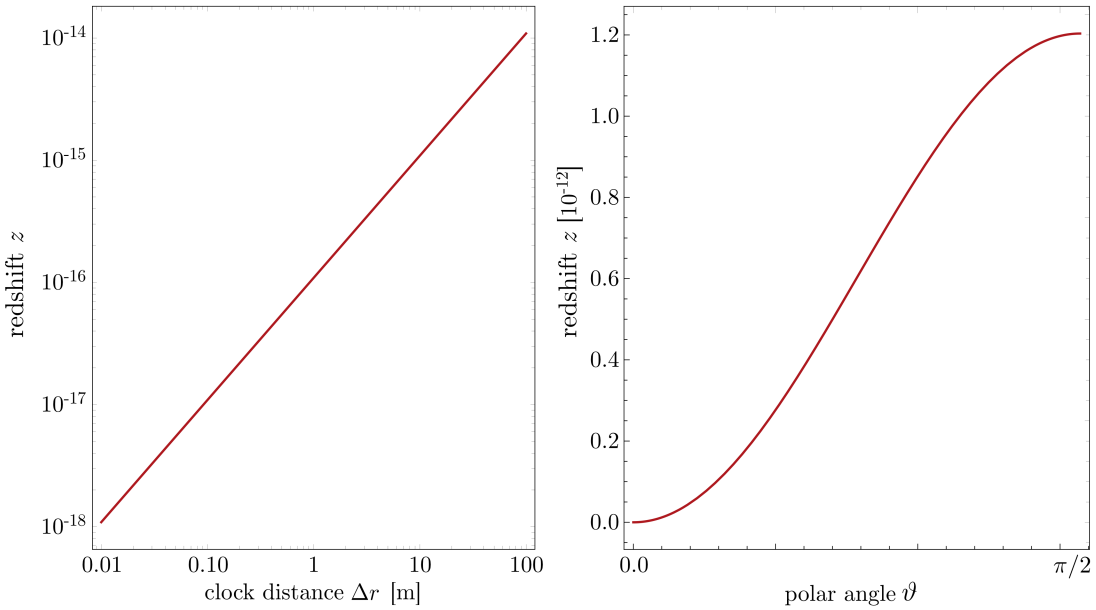

FIGURE 5.1: Gravitational redshift of two clocks at different radii (left) and Doppler induced Redshift of a clock on the Earth's surface separated by an angle ϑ from the pole (right). See Eqs. (5.7) and (5.10), respectively.

when escaping a gravitational field. To estimate the magnitude of the redshift, let one clock be positioned on the Earth's surface $r_1 = r_\oplus$ (emitter) and another clock a distance $r_2 = r_1 + \Delta r$ further away (receiver). The redshift of the signal is plotted in Fig. 5.1. A redshift of $z = 10^{-18}$ corresponds to a height difference of about 1 cm. Thus, accurate clock comparison can be used to determine height differences, see also [130]. In 2010, Chou et. *al.* [24] published results for redshift measurements by comparison of two clocks separated by less than one meter in height. Other similar experiments are described in Refs. [116, 185].

For observers on the Earth's surface, centrifugal effects must be included. This actually means to include Doppler terms in the redshift. We describe them by integral curves of $\partial_t + \omega\partial_\varphi$. These worldlines form an isometric congruence and can be thought of as observers rigidly co-rotating with the Earth or, equivalently, the integral curves can be considered as the worldlines of the Earth's constituents. For these observers, the redshift potential is given by

$$e^{\phi_2(r,\vartheta)} = \sqrt{-\big(g_{00}(r,\vartheta) + \omega^2 g_{\varphi\varphi}(r,\vartheta)/c^2\big)} = \sqrt{1 - \frac{2m}{r} - \frac{\omega^2}{c^2} r^2 \sin^2\vartheta}\,. \tag{5.8}$$

Hence, the redshift between two members of this congruence at positions (r_1, ϑ_1) and (r_2, ϑ_2), respectively, is

$$z+1 = \frac{\nu_1}{\nu_2} = \frac{e^{\phi_2(r_2,\vartheta_2)}}{e^{\phi_2(r_1,\vartheta_1)}} = \frac{\sqrt{1-\dfrac{2m}{r_2}-\dfrac{\omega^2}{c^2}r_2^2\sin^2\vartheta_2}}{\sqrt{1-\dfrac{2m}{r_1}-\dfrac{\omega^2}{c^2}r_1^2\sin^2\vartheta_1}}\,. \tag{5.9}$$

We can use the result to, e.g., compare a clock positioned at the equator (clock 1) to a clock at one of the poles (clock 2). The redshift of the two clocks is

$$z+1 = \frac{\nu_1}{\nu_2} = \frac{\sqrt{1-\dfrac{2m}{r_\oplus}}}{\sqrt{1-\dfrac{2m}{r_\oplus}-\dfrac{\omega^2}{c^2}r_\oplus^2}} = \frac{\sqrt{1-\dfrac{2m}{r_\oplus}}}{\sqrt{1-\dfrac{2m}{r_\oplus}-\dfrac{v^2}{c^2}}}\,, \tag{5.10}$$

where the relative velocity v was introduced. We see that for this constellation, z is positive and $\nu_1 > \nu_2$; a signal from clock 1 to clock 2 is redshifted due to transversal Doppler effects; this effect is well-known in Special Relativity and, therefore, necessarily included in the general relativistic framework. For a radius $r_\oplus = 6.378\,136\,3 \times 10^6\,\mathrm{m}$, see EGM96, we obtain a redshift of $z = 1.203\,437 \times 10^{-12}$. In Fig. 5.1, this redshift is shown as a function of the separation angle ϑ.

Co-rotating observers experience an acceleration given by (4.32)

$$a = c^2 \mathrm{d}\phi_2 \quad \Rightarrow \quad a_i = c^2 \partial_i \phi_2\,. \tag{5.11}$$

Since $(a_\mu) = (0, a_r, a_\vartheta, 0)$, we have only the two components

$$a_r = c^2\partial_r\phi_2 = e^{-2\phi_2}\frac{c^2}{2}\left(\frac{2m}{r^2} - 2\frac{\omega^2}{c^2}r\sin^2\vartheta\right) = e^{-2\phi_2}\left(\frac{GM}{r^2} - \omega^2 r\sin^2\vartheta\right)\,, \tag{5.12a}$$

$$a_\vartheta = c^2\partial_\vartheta\phi_2 = e^{-2\phi_2}\frac{c^2}{2}\left(-2\frac{\omega^2}{c^2}r^2\sin\vartheta\cos\vartheta\right) = e^{-2\phi_2}\left(-\omega^2 r^2\sin\vartheta\cos\vartheta\right)\,, \tag{5.12b}$$

and the magnitude of the acceleration becomes

$$\begin{aligned} a &= \sqrt{g^{rr}(a_r)^2 + g^{\vartheta\vartheta}(a_\vartheta)^2} \\ &= e^{-2\phi_2}\sqrt{\left(1-\frac{2m}{r}\right)\left(\frac{GM}{r^2} - \omega^2 r\sin^2\vartheta\right)^2 + \frac{1}{r^2}\left(\omega^2 r^2\sin\vartheta\cos\vartheta\right)^2}\,. \end{aligned} \tag{5.13}$$

In the Newtonian limit, this becomes

$$g = ||\vec{\nabla}W||_2\,, \quad W = -\frac{GM}{r} - \frac{1}{2}\omega^2 r^2\sin^2\vartheta\,, \tag{5.14}$$

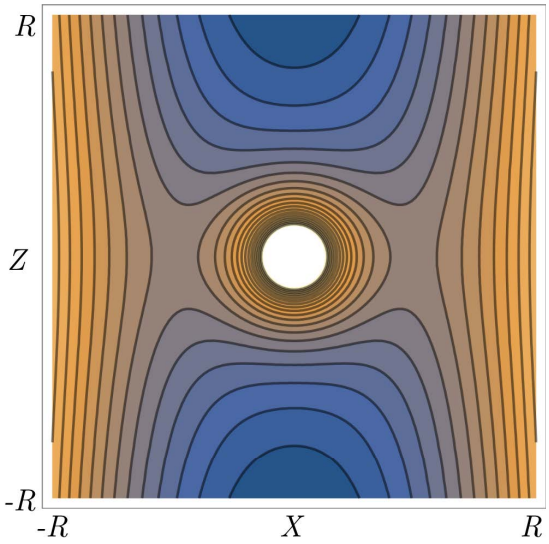

FIGURE 5.2: The shape of isochronometric surfaces in the Schwarzschild spacetime in pseudo-Cartesian coordinates (X, Z) in a meridional plane.

which is gravity in a spherically symmetric field.

For the rigidly rotating observers, isochronometric surfaces are the level surfaces of (5.8). Due to the influence of the rotation, these surface become oblate spheroids, see Fig. 5.2. The isochronometric surfaces are shown as a contour plot in pseudo-Cartesian coordinates (X, Z), constructed from the Schwarzschild coordinates (r, ϑ) in a meridional plane. There is a boundary, on which the tangent vector field to the observer congruence becomes lightlike and the level surfaces are not closed anymore but become deformed cylinders.

5.2 Erez-Rosen spacetime

The Erez-Rosen spacetime can be used to describe the spacetime outside a quadrupolar Earth. It is the natural relativistic generalization of a quadrupolar Newtonian gravitational potential (2.15),

$$U(R,\Theta) = -\frac{GM}{R}\left(1 + \frac{J_2 R_{\text{ref}}^2}{2R^2}\left(3\cos^2\Theta - 1\right)\right) . \tag{5.15}$$

This particular Newtonian potential will also be recovered in the weak-field limit, see the results for the Newtonian limit of Weyl spacetimes in the preceding chapter for a proof. We can choose the parameters m and q_2 in the Erez-Rosen metric functions (3.52) and (3.53) to let the relativistic monopole $\mathcal{M}_0$ and the quadrupole $\mathcal{M}_2$ coincide with the respective Newtonian moments of the Earth. To do so, we have to choose $m_\oplus = GM/c^2$, see above, and according to Eq. (3.47), q_2 must then be chosen such

that

$$q_2 = \frac{15}{2}\left(\frac{R_{\text{ref}}}{m}\right)^2 J_2\,. \tag{5.16}$$

Let us construct the isometric congruence of observers who rigidly co-rotating with the Earth. These observers move on integral curves of the Killing vector field $\partial_t + \omega\partial_\varphi$. For them, there exists the time-independent redshift potential

$$e^{\phi_2(x,y)} = \sqrt{e^{2\psi_{\text{ER}}(x,y)} - \frac{\omega^2}{c^2}m^2(x^2-1)(1-y^2)e^{-2\psi_{\text{ER}}(x,y)}}\,, \tag{5.17}$$

where the metric function ψ_{ER} is given by Eq. (3.52),

$$\psi_{\text{ER}(x,y)} = \frac{1}{2}\log\left(\frac{x-1}{x+1}\right) + q_2\frac{(3y^2-1)}{2}\left(\frac{(3x^2-1)}{4}\log\left(\frac{x-1}{x+1}\right) + \frac{3}{2}x\right)\,. \tag{5.18}$$

Isochronometric surfaces as seen by the rigidly rotating congruence of observers are given by the level surfaces of (5.17).

The redshift of two co-rotating observers at positions (x_1, y_1) and (x_2, y_2) is

$$\begin{aligned} z+1 = \frac{\nu_1}{\nu_2} &= e^{\phi_2(x_2,y_2)-\phi_2(x_1,y_1)} \\ &= \frac{\sqrt{e^{2\psi_{\text{ER}}(x_2,y_2)} - \frac{\omega^2}{c^2}m^2(x_2^2-1)(1-y_2^2)e^{-2\psi_{\text{ER}}(x_2,y_2)}}}{\sqrt{e^{2\psi_{\text{ER}}(x_1,y_1)} - \frac{\omega^2}{c^2}m^2(x_1^2-1)(1-y_1^2)e^{-2\psi_{\text{ER}}(x_1,y_1)}}}\,. \end{aligned} \tag{5.19}$$

For applications of this result, various scenarios are possible. For instance, we could repeat the calculation of the preceding section for the redshift of clocks at the equator and one of the poles. At the equator, we have $y = 0$, and at the north pole, we have $y = 1$. Moreover, different radii x_1 and x_2 can be introduced to account for the difference of polar and equatorial radius of the Earth.

We can estimate the influence of the quadrupole on the redshift by choosing two clocks on the radial line, separated by a distance Δx. Therefore, we choose radii according to $x_1 = x_\oplus = r_\oplus/m - 1$ and $x_2 = x_1 + \Delta x$, respectively; see the coordinate transformation (3.32). We let the clocks be positioned on the boundary of the same cone $y = \cos\vartheta = \text{const}$. The redshift then becomes

$$z+1 = \frac{\nu_1}{\nu_2} = e^{\phi_2(x_\oplus+\Delta x,y)-\phi_2(x_\oplus,y)}\,. \tag{5.20}$$

and depends on the value of y and the quadrupole moment. For $q_2 \to 0$, the previous result for the Schwarzschild spacetime is recovered. Subtracting this value gives an estimate on the redshift contribution due to the quadrupole, which is shown in Fig.

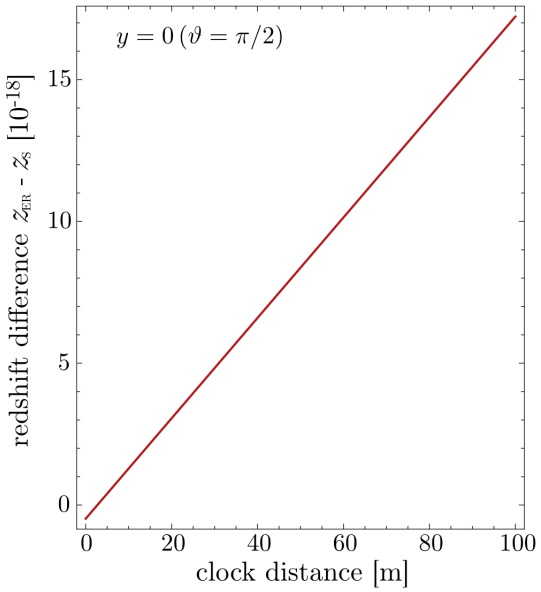

FIGURE 5.3: The influence of the relativistic quadrupole on the redshift between two clocks separated on a radial line. We show the difference between the Schwarzschild and Erez-Rosen redshift of two clocks in the equatorial plane as a function of the radial separation.

5.3. There are, however, some subtleties involved in this procedure. Firstly, the radial distance is a height distance only in the Schwarzschild spacetime but for the Erez-Rosen spacetime it is close to the actual main direction of the acceleration. Secondly, we have to translate the clock distance Δr in the Schwarzschild scenario to a distance $\Delta x = (\Delta r)/m - 1$ in the Erez-Rosen case. Moreover, these are only coordinate distances and not the real measured distances, i.e. distances determined with the metric measure. The difference between the coordinate distances and the true distance is also different in each of the two cases since we deal with different spacetimes. Luckily, the comparison still makes sense because in either case, the difference between coordinate distance and true distance for clocks on the Earth's surface and 100 m above is smaller than 100 nm, which corresponds to redshift corrections orders of magnitude below todays most accurate measurement capabilities. Hence, we are safe.

The acceleration of co-rotating observers can be calculated by the differential of the redshift potential, $a = c^2 \mathrm{d}\phi$, see Eq. (4.32). Thus,

$$a_x = c^2 e^{-\phi_2(x,y)}\, \partial_x e^{\phi_2(x,y)}\,, \tag{5.21a}$$

$$a_y = c^2 e^{-\phi_2(x,y)}\, \partial_y e^{\phi_2(x,y)}\,. \tag{5.21b}$$

and the magnitude becomes

$$a = \sqrt{g^{xx}(a_x)^2 + g^{yy}(a_y)^2} = c^2 e^{-\phi_2(x,y)} \sqrt{g^{xx}\left(\partial_x e^{\phi_2(x,y)}\right)^2 + g^{yy}\left(\partial_y e^{\phi_2(x,y)}\right)^2}\,. \tag{5.22}$$

Since the spatial part of the metric is diagonal, we have $g^{xx} = 1/g_{xx}$ and $g^{yy} = 1/g_{yy}$, see (3.52) and (3.53). In the Newtonian limit, we recover the acceleration for the quadrupolar gravity potential W,

$$g = ||\vec{\nabla} W||_2 \,, \quad \text{where} \quad W = -\frac{GM}{R}\left(1 + \frac{J_2 R_{\text{ref}}^2}{2R^2}\left(3\cos^2\Theta - 1\right)\right) - \frac{1}{2}\omega^2 R^2 \sin^2\Theta \,. \tag{5.23}$$

5.3 General Weyl spacetimes

A first example of how a special Weyl spacetime can be used for relativistic geodesy was discussed already in chapter 4 in great detail; we constructed the relativistic normal gravity spacetime as a generalization of the Earth's normal gravity field which was introduced in chapter 2.

For a general static, axisymmetric, and asymptotically flat spacetime which is free of singularities in the exterior, the metric is given by (3.33) with the metric function (3.34). This representation allows to calculate the redshift potential of static observers on integral curves of the Killing vector field $\xi_1 = \partial_t$, see (4.8),

$$e^{\phi_1(x,y)} = e^{\psi} \,. \tag{5.24}$$

Hence, the redshift potential ϕ_1 is Weyl's metric function ψ. We can insert the expansion of the Legendre functions Q_l and finally obtain the exact result

$$\begin{aligned} 2\phi_1(x,y) = &\sum_{l=0}^{n} (-1)^{l+1} q_l P_l(y) \\ &\times \left(\log\left(\frac{x+1}{x-1}\right) P_l(x) - 2 \sum_{k=0}^{[l/2-1/2]} \frac{2l-4k-1}{(l-k)(2k+1)} P_{l-2k-1}(x) \right) \,, \end{aligned} \tag{5.25}$$

where $[l/2 - 1/2]$ denotes the smallest integer that is closest to the expression. Isochronometric surfaces as seen by static observers in an asymptotically flat general Weyl spacetime are given by level surfaces of (5.25).

For rigidly rotating observers on integral curves of $\partial_t + \omega\partial_\varphi$, the redshift potential can be expressed in terms of the static potential ϕ_1,

$$e^{\phi_2(x,y)} = \sqrt{e^{2\phi_1(x,y)} - \frac{\omega^2}{c^2} m^2 (x^2-1)(1-y^2) e^{-2\phi_1(x,y)}} \,. \tag{5.26}$$

Note that if the sum is taken only up to $l = 2$, the results for the Erez-Rosen spacetime are recovered. Isochronometric surfaces as seen by the rotating observers are the level sets of (5.26).

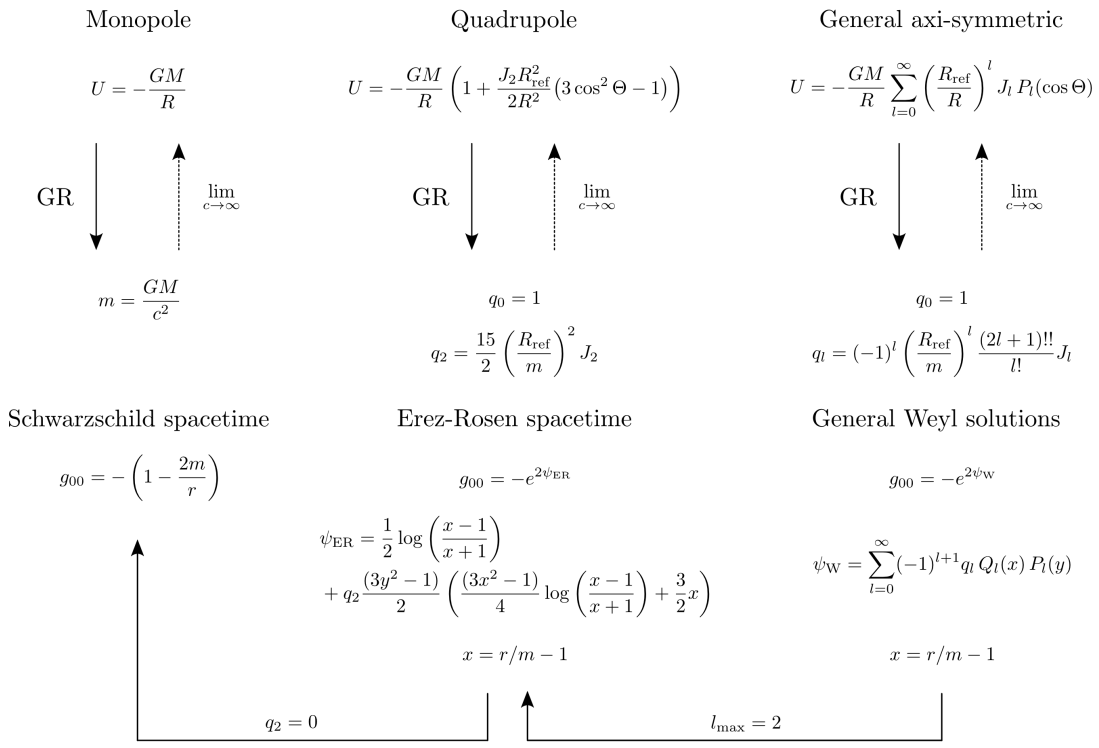

FIGURE 5.4: Overview of exact relativistic spacetimes that generalize Newtonian gravitational fields and their limits. Note that all results are exact, i.e. valid without approximation.

Such Weyl spacetimes are the natural relativistic generalization of axisymmetric Newtonian gravitational potentials of the form

$$U(R,\Theta) = -\frac{GM}{R}\sum_{l=0}^{\infty}\left(\frac{R_{\rm ref}}{R}\right)^l J_l\, P_l(\cos\Theta)\,, \tag{5.27}$$

which are recovered in the weak field limit for the choice

$$q_l = (-1)^l\frac{(2l+1)!!}{l!}\left(\frac{R_{\rm ref}}{m}\right)^2 J_l\,. \tag{5.28}$$

see section 3.2.2.

In Fig. 5.4 we summarize the results for the spacetimes that were consider so far and show an overview for relations between Newtonian gravitational fields and their generalizations in terms of exact spacetimes in General Relativity. Note that the relativistic normal gravity spacetime, see section 4.3.3, is a particular case of the situation on the right hand side of the figure such that a special relation between the J_{2l} holds.

5.4 Kerr spacetime

The Kerr metric in Boyer-Lindquist coordinates $(t, r, \vartheta, \varphi)$ is given by (3.62). As already mentioned in section 5.4, the Kerr spacetimes is not a good approximation of the spacetime outside the Earth, see also Ref. [180]. Moreover, it is not a generalization of any Newtonian gravitational potential. In fact, the weak field limit of a Kerr spacetime is not a purely Newtonian limit, see [44, 43]. However, it can still be used to model some crucial relativistic effects and their magnitude. The gravitomagnetic field of the Kerr spacetime approximates frame dragging effects in the Earth's vicinity very well, if parameters are chosen appropriately. The first multipole moments of the Kerr metric are

$$\text{Mass monopole} \quad \mathcal{M}_0 = m\,, \tag{5.29a}$$

$$\text{Spin dipole} \quad \mathcal{S}_1 = ma\,, \tag{5.29b}$$

$$\text{Mass quadrupole} \quad \mathcal{M}_2 = -ma^2\,, \tag{5.29c}$$

see Eq. (3.65). The Kerr parameter is related to the angular momentum by $a = J/(Mc)$. Hence, we can choose m such that the Kerr monopole is the total mass of the Earth, and a such that the spin dipole coincides with the Earth's angular momentum. To have this correspondence, we set $m_\oplus = GM/c^2$, as before. To calculate the Kerr parameter a we use the relation of the angular momentum to the moment of inertia I, $J = I\omega$. For a rigidly rotating sphere with radius $r_\oplus$, we have $I = 2/5 M r_\oplus^2$. Hence, the Kerr parameter for the Earth becomes

$$a_\oplus = \frac{2}{5}\frac{\omega}{c} r_\oplus^2\,. \tag{5.30}$$

Calculating the values, we obtain $m_\oplus = 0.004\,435\,03\,\mathrm{m}$ and $a_\oplus = 892.45\,m_\oplus$, where the radius and angular velocity as given by the EGM96 model are used.

The redshift potential for stationary observers on t-lines is given by

$$e^{\phi_1(r,\vartheta)} = \sqrt{1 - \frac{2mr}{\rho^2}} = \sqrt{1 - \frac{2mr}{r^2 + a^2\cos^2\vartheta}}\,. \tag{5.31}$$

Note that these observers have a non-zero angular momentum w.r.t. observers at spatial infinity. Observers on integral curves of $\partial_t + \omega\partial_\varphi$ rigidly co-rotate with the Earth. For

them, the redshift potential is

$$e^{\phi_2(r,\vartheta)} = \sqrt{-g_{00}(r,\vartheta) - 2\frac{\omega}{c}g_{0\varphi}(r,\vartheta) - \frac{\omega^2}{c^2}g_{\varphi\varphi}(r,\vartheta)}$$
$$= \sqrt{1 - \frac{2mr}{\rho(r,\vartheta)^2} + 4\frac{\omega}{c}\frac{amr\sin^2\vartheta}{\rho(r,\vartheta)^2} - \frac{\omega^2}{c^2}\sin^2\vartheta\left(r^2 + a^2 + \frac{2mra^2\sin^2\vartheta}{\rho(r,\vartheta)^2}\right)}, \tag{5.32}$$

see Eq. (3.62) for the Kerr metric functions. Two co-rotating observers measure a redshift between their standard clocks according to

$$z + 1 = \frac{\nu_1}{\nu_2}$$
$$= \frac{\sqrt{-g_{00}(r2,\vartheta_2) - 2\frac{\omega}{c}g_{0\varphi}(r_2,\vartheta_2) - \frac{\omega^2}{c^2}g_{\varphi\varphi}(r_2,\vartheta_2)}}{\sqrt{-g_{00}(r_1,\vartheta_1) - 2\frac{\omega}{c}g_{0\varphi}(r_1,\vartheta_1) - \frac{\omega^2}{c^2}g_{\varphi\varphi}(r_1,\vartheta_1)}}. \tag{5.33}$$

The influence of frame dragging on the redshift can be best analyzed by comparing a clock at one of the poles to a clock on the equator. For this constellation, the difference between the Kerr and Schwarzschild result becomes $z \approx 1 \times 10^{-21}$, which is attributed to the influence of frame dragging and only two orders of magnitude away from being measurable.

Isochronometric surfaces, as seen by rigidly rotating observers, of the Kerr spacetime are given by the level surfaces of (5.32). However, since the quadrupole moment of the Kerr spacetime is by no means a good approximation for the Earth's moment, the isochronometric surfaces deviate a lot; they do not show the necessary flattening. Thus, when gravitomagnetic contributions are to be estimated, the Kerr results can be used. When the geometry of isochronometric surfaces, i.e. the geoid or normal gravity field, is searched for, it is recommended to use the results of the previous section.

5.5 Parametrized post-Newtonian spacetime

Since $W(x,y,z)$ and $U^i(x,y,z)$ in (3.73) are independent of t, we have ∂_t as a timelike Killing vector field. The coordinates (x',y',z') used in (3.73) are co-rotating coordinates and observers on the Earth's surface are characterized by $\mathrm{d}x'^i = 0$. Hence, these observers move on t-lines. In the following, we omit the prime for the sake of readability. The metric (3.73) is of the form (4.7) and we can, thus, read off the ppN redshift

TABLE 5.1: Order of magnitude of the involved and related terms in the definition of the relativistic gravity potential U^* for a post-Newtonian spacetime close to the surface of the Earth.

Quantity in Eq. (5.35)	Magnitude $[\mathrm{m}^2/\mathrm{s}^2]$
W	$\approx 6 \cdot 10^{7}$
W^2/c^2	$\approx 4 \cdot 10^{-2}$
U^2/c^2	$\approx 4 \cdot 10^{-2}$
UV/c^2	$\approx 7 \cdot 10^{-5}$
V^2/c^2	$\approx 1 \cdot 10^{-7}$

potential ϕ_{ppN} from the g_{00} component,

$$\begin{aligned} e^{\phi_{\mathrm{ppN}}} = \sqrt{-g_{00}} &= \sqrt{1 + \frac{2W(x,y,z)}{c^2} + \frac{2\beta U(x,y,z)^2}{c^4}} \\ &= 1 + \frac{W(x,y,z)}{c^2} + \frac{U^2(x,y,z)(\beta - 1/2)}{c^4} \,. \end{aligned} \tag{5.34}$$

We know that ϕ_{ppN} is a time-independent redshift potential for a congruence of observers of which the worldlines are integral curves of $u = \exp(-\phi)\partial_t$, i.e. for the co-rotating observers fixed to the Earth's surface. Note that we need $\exp(\phi)$ to order $\mathcal{O}(c^{-4})$ since we want to calculate the relativistic gravity potential $U^* = c^2(\exp\phi - 1)$ to order $\mathcal{O}(c^{-2})$ in the next step.

The relativistic gravity potential U^*_{ppN} for the ppN metric (3.73) is consequently given by

$$U^*_{\mathrm{ppN}} = W + \frac{U^2(\beta - 1/2)}{c^2} \,, \tag{5.35}$$

and for the post-Newtonian approximation of General Relativity, we get

$$U^*_{\mathrm{pN}} = W + \frac{U^2}{2c^2} \,. \tag{5.36}$$

Hence, deviations from the Newtonian gravity potential are described by the second term in (5.35) which is proportional to U^2/c^2. Note that that this result coincides with the work of Soffel et. *al.* in Ref. [181]. However, the relativistic gravity potential U^* is defined in chapter 4 without any approximations regarding the strength of the gravitational field. In contrast to Ref. [181], in which the authors define this potential only in the first-order ppN framework. Thus, we have shown that our framework recovers the well-known notions in an appropriately constructed limit of General Relativity. Table 5.1 shows the magnitude of involved terms in (5.35).

5.5.1 The redshift in a ppN spacetime

Let us assume that we send signals from one observer on the worldline γ_1 to another observers on the worldline γ_2. Both observer worldlines shall be integral curves of $u = \exp(-\phi_{\rm pN})\partial_t$, i.e. the observers are members of the isometric congruence and co-rotate with the Earth. To the appropriate order $\mathcal{O}(c^{-2})$, the redshift is now given by

$$1 + z = \frac{\nu_1}{\nu_2} = \frac{1 + U_2^*/c^2}{1 + U_1^*/c^2} = 1 + \frac{W_2 - W_1}{c^2} + \mathcal{O}(c^{-4}) \,, \tag{5.37}$$

where $U_i^* = U^*|_{\gamma_i}$ and $W_i = W|_{\gamma_i}$ for $i = 1, 2$. We observe that to first-order in the ppN framework, i.e. including terms $\mathcal{O}(c^{-2})$ only, the redshift for the observers in the congruence is proportional to $\Delta W := W_2 - W_1$ and it is not sensitive to the ppN parameters β and γ. In fact, with (5.37) we have just derived the basic equation of chronometric geodesy. However, since we derived it in a top-down approach, we know how it is conceptually embedded in a broader theoretical framework; this gives some trust in its validity since it is not only an approximative result in the pN framework that could, in principle, become useless at the full theoretical level.

The leading order contribution to the redshift is due to the relativistic monopole moment and given by the redshift result for the Schwarzschild spacetime in the first section of this chapter. Close to the Earth's surface, we find the correspondence between a height difference of two clocks and the redshift signal: the redshift is roughly 10^{-16} per meter height distance, see below. For most application related to clock comparison close to the Earth's surface it will be sufficient to expand the gravity potential in Eq. (5.37) up to J_2.

For a small spatial distance between the two clocks, expanding the gravity potential W_2 around the value W_1 leads to

$$W_2 = W_1 + \vec{\nabla} W \cdot (\vec{X}_2 - \vec{X}_1) + \mathcal{O}\big(|\vec{X}_2 - \vec{X}_1|^2\big) \,. \tag{5.38}$$

Hence, we obtain

$$W_2 = W_1 - \bar{g}_{12} H_{12} + \mathcal{O}\big(H_{12}^2\big) \,, \tag{5.39}$$

in terms of the orthometric height H_{12} between both clock positions. Here, $\bar{g}_{12}$ denotes the averaged gravity between the clocks' positions along the plumb line. Therefore, the redshift becomes

$$z\big(H_{12}\big) \approx \bar{g}_{12} \frac{H_{12}}{c^2} \,. \tag{5.40}$$

Hence, redshift measurements are useful to determine the orthometric height, provided that they are supported by gravity measurements.

5.5.2 The relativistic geoid in a ppN spacetime

The relativistic geoid in the ppN formalism is given by one particular isochronometric surface; that is an equipotential surface of U^*_{ppN} such that

$$U^*_{\mathrm{ppN}}\big|_{\mathrm{geoid}} = W + \frac{U^2(\beta - 1/2)}{c^2}\bigg|_{\mathrm{geoid}} = U^*_0 = \mathrm{const.} \tag{5.41}$$

For the post-Newtonian approximation of General Relativity we obtain

$$U^*_{\mathrm{pN}}\big|_{\mathrm{geoid}} = W + \frac{U^2}{2c^2}\bigg|_{\mathrm{geoid}} = U^*_0 = \mathrm{const.} \tag{5.42}$$

This result will be used in the next chapter to access the leading-order relativistic corrections to the Newtonian geoid.

5.5.3 Acceleration measurements in a ppN spacetime

Using all the results of the chapters 4 and 3, we calculate the covariant acceleration components a_μ, the contravariant components a^μ, and the norm of the acceleration a at the level of $\mathcal{O}(1/c^2)$ accuracy[1]

$$a_{i,\mathrm{ppN}} = -\partial_i \left(W + \frac{U^2(\beta - 1)}{c^2} \right) , \tag{5.43a}$$

$$a^i_{\mathrm{ppN}} = -\delta^{ij}\, \partial_j \left(W + \frac{U^2(\beta + \gamma - 1)}{c^2} \right) \tag{5.43b}$$

$$\Leftrightarrow \vec{a}_{\mathrm{ppN}} = -\vec{\nabla} \left(W + \frac{U^2(\beta + \gamma - 1)}{c^2} \right) =: -\vec{\nabla}\bar{U}_{\mathrm{ppN}} \tag{5.43c}$$

$$a_{\mathrm{ppN}} = \left|\left| \vec{\nabla} \left(W + \frac{U^2(\beta + \gamma/2 - 1)}{c^2} \right) \right|\right|_2 =: ||\vec{\nabla}\tilde{U}_{\mathrm{ppN}}||_2 \,, \tag{5.43d}$$

where $\vec{\nabla}$ is the flat space operator such that $||\vec{\nabla}\tilde{U}||_2 = \delta^{ij}\, \partial_i\tilde{U}\partial_j\tilde{U}$ in Cartesian coordinates.

[1] Formally, the contravariant acceleration components can include a non-zero a^0. However, we have $a^0_{\mathrm{ppN}} = 0 + \mathcal{O}(c^{-3})$.

As shown above in Eq. (5.43), we define two new potentials: (i) the potential $\bar{U}_{\mathrm{ppN}}$, which determines the "acceleration vector" $\vec{a}_{\mathrm{ppN}}$, and (ii) the potential $\tilde{U}_{\mathrm{ppN}}$ of which the norm of the gradient gives the measured acceleration a_{ppN}.

Note that for the ppN parameter values of General Relativity, $\beta = 1, \gamma = 1$, we have[2]

$$\bar{U}_{\mathrm{pN}} = W + \frac{W^2}{c^2}\,, \tag{5.44a}$$

$$\tilde{U}_{\mathrm{pN}} = U^*_{\mathrm{pN}} = W + \frac{W^2}{2c^2}\,. \tag{5.44b}$$

However, measuring the acceleration of co-rotating observers on the Earth's surface yields bounds on the value of the combination $(\beta + \gamma/2 - 1)$.

In this section, we have recovered and generalized the results of Ref. [181] which was one of the major sources of inspiration for the development of our framework. In their work, the authors construct the notions of potentials and the relativistic geoid in a ppN spacetime approximation. Here, we have shown how their results fit into a more general structure: the general relativistic framework that allows to develop all notions without any approximation. We regard it as a good test for our definitions that we successfully recover the results in Ref. [181]; be reminded of our sign convention for the comparison of results.

[2] Actually the statement remains true for all ppN theories for which $\gamma = 1$ and β remains arbitrary.

Chapter 6

Relativity in Geodetic Measurements

6.1 Length and time scales

6.1.1 On metric length and coordinate distance

General Relativity describes gravity by a curved spacetime geometry. The set of all events is the base manifold. To have notions of distance, length, area, volume, and angles, a metric on this 4-dimensional manifold is essential. One of the main differences to flat space is that there are no global coordinate systems and length must be calculated using the metric components in a given local chart. Depending on the chosen coordinates, there might be a huge difference between the true measured length, w.r.t. the metric, and the coordinate length. Even though in most of the cases considered here we introduce spherical like coordinates of which the radius is called r, the coordinate difference $r_2 - r_1$ is never equal the measured distance. However, it might be sufficiently close such that we can neglect the differences in some applications.

Let us estimate this difference for the spacetime around the Earth (3.77). For some of the applications that follow, we evaluate distances close to the Earth's surface and up to some 10^3 m above. The leading-order relativistic correction can be calculated using the Schwarzschild result

$$l(r_1, r_2) := \int_{r_1}^{r_2} \frac{1}{\sqrt{1 - 2m/r}} \mathrm{d}r \,. \tag{6.1}$$

With the expression above, we can calculate the difference between the coordinate distance $\Delta r := r_2 - r_1$ and the true distance l. For r_1 being roughly the Earth's surface and $r_2 = r_1 + 10^3\,\mathrm{m}$, we obtain $l \approx (10^3 + 10^{-7})\,\mathrm{m}$. Hence, the difference between the Δr and l is less than $1\,\mu$m and negligible for, e.g., clock comparisons and redshift measurements over heights in the km-regime. However, there are cases in which the

difference matters. For instance, integrating up to satellite orbit heights of $10^4\,\mathrm{km}$ yields differences of about $4\,\mathrm{mm}$. Here, we start to enter the measurable regime and in such cases, first-order corrections should be applied.

6.1.2 Proper time on the geoid

Let us start with a general stationary metric of the form

$$g = e^{2\phi(x)}\left[-(c\,\mathrm{d}t + \alpha_a(x)\mathrm{d}x^a)^2 + \alpha_{ab}(x)\mathrm{d}x^a\mathrm{d}x^b\right], \tag{6.2}$$

where ϕ is the redshift potential for observers on integral curves of ∂_t. Hence for these observers we have $\mathrm{d}x^i = 0$. The relativistic geoid is a particular level surface of ϕ such that $\phi = \phi_0 = \text{const}$. Therefore, the proper time τ_g of these observers on the geoid is determined by

$$\mathrm{d}\tau_g = e^{\phi_0(x)}\mathrm{d}t =: \left(1 - L_g^*\right)\mathrm{d}t\,, \tag{6.3}$$

where we define the constant $L_g^* > 0$ as shown above. Between both time scales, the linear relation

$$\tau_g = \left(1 - L_g^*\right)t \tag{6.4}$$

holds. Now, we can use τ_g as a new time coordinate on the spacetime and rewrite the metric to obtain

$$\begin{aligned} g &= e^{2\phi(x)}\left[-\left(\frac{c\,\mathrm{d}\tau_g}{1 - L_g^*} + \alpha_a(x)\,\mathrm{d}x^a\right)^2 + \alpha_{ab}(x)\mathrm{d}x^a\mathrm{d}x^b\right] \\ &=: \frac{e^{2\phi(x)}}{(1 - L_g^*)^2}\left[-(c\,\mathrm{d}\tau_g + \bar{\alpha}_a(x)\mathrm{d}x^a)^2 + \bar{\alpha}_{ab}(x)\mathrm{d}x^a\mathrm{d}x^b\right]. \end{aligned} \tag{6.5}$$

In these coordinates, the geoid is determined by the condition $g_{\tau_g\tau_g} = g(\partial_{\tau_g}, \partial_{\tau_g}) = -1$.

If we were able to invert the equation $\phi = \phi(x^i)$ such that $x^1 = x^1(\phi, x^2, x^3)$ we could adapt the coordinate system even further to the geoid and use ϕ as a coordinate. In the next section, we apply the result to the general form of a stationary and axisymmetric spacetime metric we show how the induced geometry on the geoid can be described.

For later use, let us rewrite Eqs. (6.3) and (6.5) above using the relativistic gravity potential U^*, see section 4.3. We obtain for the relation between the proper time on

the geoid and coordinate time:

$$\mathrm{d}\tau_g = \left(1 + \frac{U^*}{c^2}\right)\Big|_{\text{geoid}} \mathrm{d}t = \left(1 + \frac{U_0^*}{c^2}\right) \mathrm{d}t\,, \tag{6.6}$$

where $U_0^* < 0$ is the value that chooses the particular isochronometric surface which is the relativistic geoid. A clock on the geoid 'runs slower' than a clock at infinity. We can read off that L_g^* and U_0^* are related by

$$L_g^* = \frac{|U_0^*|}{c^2}\,, \tag{6.7}$$

and the metric (6.5) now becomes

$$g = \left(\frac{1 + U^*/c^2}{1 + U_0^*/c^2}\right)^2 \left[-(c\,\mathrm{d}\tau_g + \bar{\alpha}_a(x)\mathrm{d}x^a)^2 + \bar{\alpha}_{ab}(x)\mathrm{d}x^a\mathrm{d}x^b\right]. \tag{6.8}$$

For the proper time τ of a clock at a point P which co-rotates with the Earth, above or below the geoid, we get

$$\frac{\mathrm{d}\tau}{\mathrm{d}\tau_g} = \frac{\nu_g}{\nu_P} = e^{\phi_P - \phi_0} = \frac{1 + U_P^*/c^2}{1 + U_0^*/c^2} = 1 + \frac{U_P^* - U_0^*}{c^2} + \mathcal{O}\big(c^{-4}\big)\,. \tag{6.9}$$

If the point P is above the geoid, then $U_P^* - U_0^*$ is positive and the clock 'runs faster' than a clock on the geoid, meaning that a signal send from the geoid to P is redshifted.

Stationary axisymmetric spacetimes

All exact solutions of Einstein's vacuum equation which we considered in the preceding chapter have a metric of the same form, see the introduction of chapter 5. Let us use the results of the preceding section and apply them to this form of the metric. We start with

$$g = g_{00}\,c^2\mathrm{d}t^2 + 2g_{0\varphi}\,c\mathrm{d}t\,\mathrm{d}\varphi + g_{11}(\mathrm{d}x^1)^2 + g_{22}(\mathrm{d}x^2)^2 + g_{\varphi\varphi}\mathrm{d}\varphi^2\,, \tag{6.10}$$

in non-rotating coordinates (t, x^1, x^2, φ), where x^1 is a radial coordinate and x^2 is an angle. We assume that all metric functions do not depend on t and φ, related to the Killing vector fields ∂_t and ∂_φ, which are generators of time translations and rotations, respectively. Now, we apply the coordinate transformation $\varphi \to \varphi' = \varphi - \omega t$ to rewrite the metric in the new coordinates. The value of ω shall be interpreted as the Earth's angular velocity such that co-rotating observers characterized by $\mathrm{d}x'^i = 0$ are rigidly rotating with the Earth. Note that $x'^1 = x^1$ and $x'^2 = x^2$. The coordinate

transformation yields

$$g' = \left(g_{00} + 2\frac{\omega}{c}g_{0\varphi} + \frac{\omega^2}{c^2}g_{\varphi\varphi}\right) c^2\mathrm{d}t^2 + 2(g_{0\varphi} + \omega g_{\varphi\varphi})\, c\mathrm{d}t\, \mathrm{d}\varphi' + g_{11}\left(\mathrm{d}x'^1\right)^2 + g_{22}\left(\mathrm{d}x'^2\right)^2 + g_{\varphi\varphi}\mathrm{d}\varphi'^2\,, \tag{6.11}$$

Hence, we read off the time-independent redshift potential ϕ for the co-rotating observers

$$e^{2\phi} = -g'_{00} = -\left(g_{00} + 2\frac{\omega}{c}g_{0\varphi} + \frac{\omega^2}{c^2}g_{\varphi\varphi}\right)\,, \tag{6.12}$$

and the relativistic geoid is given by a level surface $\phi = \text{const.}$ such that

$$e^{\phi}\Big|_{\text{geoid}} = \sqrt{-g_{00} - 2\frac{\omega}{c}g_{0\varphi} - \frac{\omega^2}{c^2}g_{\varphi\varphi}} =: 1 - L_g^* = \text{const.} \tag{6.13}$$

On the relativistic geoid, we have for the proper time τ_g of co-rotating observers

$$c^2\mathrm{d}\tau_g^2 = -\left(g_{00} + 2\frac{\omega}{c}g_{0\varphi} + \frac{\omega^2}{c^2}g_{\varphi\varphi}\right)\Big|_{\text{geoid}} c^2\mathrm{d}t^2 = \left(1 - L_g^*\right)^2 c^2\mathrm{d}t^2\,, \tag{6.14}$$

therefore

$$\frac{\mathrm{d}\tau_g}{\mathrm{d}t} = \sqrt{-g_{00} - 2\frac{\omega}{c}g_{0\varphi} - \frac{\omega^2}{c^2}g_{\varphi\varphi}} = \left(1 - L_g^*\right)\,. \tag{6.15}$$

Then, the linear relation between τ_g and coordinate time t is given by

$$\tau_g(t) = \left(1 - L_g^*\right)\, t\,, \quad \mathrm{d}\tau = (1 - L_g^*)\mathrm{d}t\,. \tag{6.16}$$

We now let τ_g be the new time coordinate in the non-rotating and the rotating metric. For the non-rotating case we get

$$g = \frac{g_{00}}{(1 - L_g^*)^2}\, c^2\mathrm{d}\tau^2 + \frac{2g_{0\varphi}}{1 - L_g^*}\, c\mathrm{d}\tau_g\, \mathrm{d}\varphi + g_{11}(\mathrm{d}x^1)^2 + g_{22}(\mathrm{d}x^2)^2 + g_{\varphi\varphi}\mathrm{d}\varphi^2\,, \tag{6.17}$$

and for the metric in co-rotating coordinates we have

$$g' = \frac{\left(g_{00} + 2\frac{\omega}{c}g_{0\varphi} + \frac{\omega^2}{c^2}g_{\varphi\varphi}\right)}{(1 - L_g^*)^2} c^2\mathrm{d}\tau_g^2 + \frac{2(g_{0\varphi} + \omega g_{\varphi\varphi})}{1 - L_g^*}\, c\mathrm{d}\tau_g\, \mathrm{d}\varphi' + g_{11}(\mathrm{d}x'^1)^2 + g_{22}(\mathrm{d}x'^2)^2 + g_{\varphi\varphi}\mathrm{d}\varphi'^2\,. \tag{6.18}$$

If the relations

$$\mathrm{d}\phi = \partial_1\phi \mathrm{d}x^1 + \partial_2\phi \mathrm{d}x^2 \quad \mathrm{d}x^1 = \frac{\mathrm{d}\phi - \partial_2\phi \mathrm{d}x^2}{\partial_1\phi}\,. \tag{6.19}$$

can be solved for $x^1 = x^1(\phi, x^2)$, we may use ϕ as a coordinate instead of x^1 and write the metric as

$$\begin{aligned} g' = &\frac{g_{00} + 2\frac{\omega}{c}g_{0\varphi} + \frac{\omega^2}{c^2}g_{\varphi\varphi}}{(1 - L_g^*)^2} c^2 \mathrm{d}\tau_g^2 + \frac{2(g_{0\varphi} + \omega g_{\varphi\varphi})}{(1 - L_g^*)}\, c\mathrm{d}\tau_g\, \mathrm{d}\varphi' \\ &+ \frac{g_{11}}{(\partial_1\phi)^2}\mathrm{d}\phi^2 - \frac{2g_{11}\partial_2\phi}{(\partial_1\phi)^2}\mathrm{d}\phi\mathrm{d}x^2 + \left(g_{22} + g_{11}\frac{(\partial_2\phi)^2}{(\partial_1\phi)^2}\right)(\mathrm{d}x^2)^2 + g_{\varphi\varphi}\mathrm{d}\varphi'^2\,. \end{aligned} \tag{6.20}$$

Hence, we label events on a stationary spacetime now by the proper time on the geoid τ_g, the number of the respective leaf of the foliation of space into isochronometric surfaces, and two angles (x^2, φ) on such a foliation leaf. All metric components are now functions of ϕ and x^2. The expression $\partial_1\phi$ must be evaluated for $x^1(\phi, x^2)$. Note that not in all cases ϕ is a good coordinate. This is true in particular close to compact objects such as black holes. However, for geodesy in the vicinity of the Earth, we do not encounter such problems.

On the geoid, it is true that $\mathrm{d}\phi = 0$ and $g_{\tau_g\tau_g} = -1$. Therefore,

$$g^{(2d)} = \left(g_{22} + g_{11}\frac{(\partial_2\phi)^2}{(\partial_1\phi)^2}\right)(\mathrm{d}x^2)^2 + g_{\varphi\varphi}\mathrm{d}\varphi'^2\,, \tag{6.21}$$

is the induced metric on the two-dimensional geoid surface. This metric is crucial for the embedding of isochronometric surfaces into the Euclidean space $\mathbb{R}^3$, see appendix C.

6.1.3 Time scales and the geopotential value W_0

In section 3.2.7, we introduced the post-Newtonian metric of the spacetime around the Earth in (i) nearly global inertial Cartesian and (ii) co-rotating Earth-fixed coordinates. In section 5.5, we constructed the relativistic geoid within the first-order pN framework. The coordinate time t is the same for both metrics: the geocentric coordinate time t_{TCG}. It is the time as measured by observers who are infinitely far away from the Earth. Using the results of the preceding sections, we will now introduce the proper time τ_g on the Earth's geoid as the new coordinate time of the post-Newtonian metric. This time is also called international atomic time t_{TAI} and it is a realization of terrestrial time, see [38, 130, 168] and references therein. Alongside of our considerations, we will shed some light on the definition of the geopotential value W_0 that defines the geoid.

From the last section, we know that the relation between the coordinate time $t = t_{\mathrm{TCG}}$ and the proper time on the geoid $\tau_g = t_{\mathrm{TAI}}$ is given by the defined constant L_g^*. Starting with the metric (3.78) we know that the redshift potential is given by (5.34),

$$e^{2\phi} = 1 + \frac{2W(x,y,z)}{c^2} + \frac{2U^2(x,y,z)}{c^4}\,. \tag{6.22}$$

For the pN spacetime in co-rotating coordinates, we explicitly have the relation between proper time on the geoid and coordinate time,

$$\frac{\mathrm{d}\tau_g}{\mathrm{d}t} = \frac{\mathrm{d}t_{\mathrm{TAI}}}{\mathrm{d}t_{\mathrm{TCG}}} = 1 - L_g^* = 1 - \frac{W_0}{c^2} + \mathcal{O}\big(c^{-4}\big) =: 1 - L_g + \mathcal{O}\big(c^{-4}\big)\,, \tag{6.23}$$

valid to $\mathcal{O}\big(c^{-2}\big)$ accuracy, where W_0 is the gravity potential value on the geoid. Note that in the last sections, we introduced the constant L_g^* as defined for a general relativistic spacetime without approximation. Here, L_g is defined accordingly at the first-order pN level. Hence, L_g is the pN approximation of L_g^*.

In the 2000, the IAU declared L_g to a defining constant (IAU 2000, Resolution B1.9), see Ref. [97]. Hence, the value of W_0 is effectively fixed by the relation above. This leads to the inconsistencies which are discussed in section 2.2.2.

A clock which is co-rotating with the Earth at a point P has a height H above the geoid. This clock's proper time is related to the proper time on the geoid according to

$$\frac{\mathrm{d}\tau}{\mathrm{d}\tau_g} = \frac{1 + U_P^*/c^2}{1 + U_0^*/c^2} = 1 + \frac{W_P + W_0}{c^2} + \mathcal{O}\big(c^{-4}\big)\,. \tag{6.24}$$

We may expand the potential W_P around the value W_0 according to

$$W_P = -\big(W_0 + \vec{\nabla}W \cdot (\vec{X}_P - \vec{X}_0)\big) + \mathcal{O}\big(|\vec{X}_P - \vec{X}_0|^2\big)\,. \tag{6.25}$$

In terms of the orthometric height H, we can reduce this result to

$$W_P = -(W_0 - \bar{g}H) + \mathcal{O}\big(H^2\big)\,, \tag{6.26}$$

where $\bar{g}$ is the averaged gravity between P and P_0. Hence we have

$$\frac{\mathrm{d}\tau}{\mathrm{d}\tau_g} \approx 1 + \frac{\bar{g}H}{c^2}\,. \tag{6.27}$$

6.2 Relativistic corrections to acceleration measurements

Let us now estimate the relativistic contributions to acceleration measurements based on the results in section 5.5.3. The acceleration of test particles on the Earth as seen by co-rotating observers is (5.43),

$$\vec{a}_{\mathrm{ppN}} = -\vec{\nabla}\left(W + \frac{U^2(\beta+\gamma-1)}{c^2}\right) =: \vec{\nabla}\bar{U}_{\mathrm{ppN}}\,. \tag{6.28}$$

Now, we assume that for the correction term, which is proportional to c^{-2}, only the two first expansion terms for U give measurable contributions, i.e. we calculate corrections due to the relativistic monopole and quadrupole. Hence, U is expanded as

$$U(r,\vartheta) = -\frac{GM}{r}\left(1 + \frac{J_2 R_{\mathrm{ref}}^2}{2r^2}\left(3\cos^2\vartheta - 1\right)\right) \tag{6.29}$$

in spherical coordinates, see Eq. (2.15). Therefore, we obtain the following leading order ppN corrections to the Newtonian acceleration $\vec{g} = -\vec{\nabla}W$

$$a^r_{\mathrm{ppN}} = (-\vec{\nabla}W)_r + \frac{(\beta+\gamma-1)}{c^2}\left[\frac{2(GM)^2}{r^3} + \frac{8\,(GM)^2\,J_2\,R_{\mathrm{ref}}^2 P_2(\cos\vartheta)}{r^5}\right] + \mathcal{O}\big(r^{-7}/c^2\big) \tag{6.30a}$$

$$a^{\vartheta}{}_{\mathrm{pN}} = (-\vec{\nabla}W)_\vartheta + \frac{(\beta+\gamma-1)}{c^2}\frac{6\,(GM)^2\,J_2\,R_{\mathrm{ref}}^2}{r^5}\cos\vartheta\sin\vartheta + \mathcal{O}\big(r^{-7}/c^2\big)\,. \tag{6.30b}$$

Using $\beta = 1$, $\gamma = 1$ for the pN approximation of the Earth, we obtain corrections to the Newtonian acceleration of $1.3627\times10^{-8} - 5.9\times10^{-11}P_2(\cos\vartheta)\,\mathrm{m/s^2}$ in the radial direction and $-4.4\times10^{-11}\cos\vartheta\sin\vartheta\,\mathrm{m/s^2}$ in the ϑ-direction, respectively, close to the Earth's surface[1]. Thus, at least a first-order post-Newtonian formalism needs to be employed to interpret high-precision Earth-bound acceleration measurements with state of the art instruments such as superconducting gravimeters, see, e.g., Refs. [65, 93].

6.3 Magnitudes of relativistic corrections to the geoid

In this section, we determine and quantify the magnitudes of relativistic corrections to the Earth's geoid at the leading order. Therefore, we study a simple quadrupolar Earth model, see (2.16), in the Newtonian theory and its relativistic generalization in the general relativistic framework. As we have seen in the preceding chapters, the best

[1] We use the EGM96 values for all involved quantities n the calculation. Note, in particular, that $J_2 < 0$.

relativistic generalization of such a model is given by an appropriately constructed Erez-Rosen spacetime, see section 5.2. The leading order effects are given by the first-order post-Newtonian approximation of the Erez-Rosen metric, which is the post-Newtonian metric (3.78) constructed for a quadrupolar potential (2.16).

The Earth's quadrupole moment, related to its flattening, gives the first (and by far the largest) non-trivial contribution to its gravitational field beyond the monopole. As can be seen in Figs. 2.5 and 2.6, the quadrupole causes gravity to change from the equator towards the poles with a $\sin^2\lambda$ like behavior, where λ is the geocentric latitude. Hence, we expect relativistic corrections due to influence of the relativistic monopole and quadrupole (i) to induce an overall spherical correction due to the monopole and (ii) to yield latitude-dependent corrections about three orders of magnitude smaller since $J_2/J_0 \approx 10^{-3}$ for the Earth.

The methodology of this section is as follows. We use the Newtonian gravity potential (2.16) for a quadrupolar configuration and, thereupon, construct the post-Newtonian approximation of this situation to access the first-order relativistic contributions. Then, we construct the Newtonian geoid and the relativistic geoid based on our relativistic gravity potential U^*. In either case, we obtain a two-dimensional surface given by some function $x^1(x^2)$, where x^1 is a radial coordinate and x^2 is, e.g., the polar angle.

The comparison of both results must be done in a way that eliminates coordinate ambiguities. We have decided to use an isometric embedding of the relativistic geoid surface into the three-dimensional Euclidean space $\mathbb{R}^3$. If such an embedding is possible, it is unique and allows to investigate the intrinsic geometry of the relativistic geoid by applying well-known methods for the analysis of curved two-dimensional surfaces. The Newtonian geoid generically "lives" in this Euclidean space, and a comparison of closed two-dimensional surfaces in $\mathbb{R}^3$ is possible, e.g., in terms of their radial distance in any angular direction. Therefore, once the relativistic geoid is embedded, we can calculate the difference to the Newtonian one. Not that such an embedding is in general only possible by numerical methods, even though the embedding equations can be given exactly, see appendix C.

However, we also have to overcome some conventional issues: in the Newtonian case, the geoid is defined by the level surface of the gravity potential such that $|W| = W_0$. Nowadays, W_0 is an agreed upon constant related to coordinate time transformations from TCG to TAI, see section 6.1.3. Already in the Newtonian case, there are conceptional difficulties with properties of the geoid being "a mean sea surface fit" and derived constant W_0 which is not at all directly related to the sea surface, see the remarks in section 2.2.2. Let us, therefore, assume that some value of W_0 is chosen, one way or another, that defines the geoid.

In the relativistic case, we define the geoid by one particular isochronometric surface, a level surface of the relativistic gravity potential U^* such that $U^*|_{\text{geoid}} = U_0^*$. Now, we need a clear prescription of how to choose U_0^*. Hence, some gauge freedom is left in the choice of the constant. In the following, we consider different possible approaches and calculate the differences between Newtonian and relativistic geoid in either case.

In approach (I), we choose $-U_0^* \equiv W_0$, which may be obvious regarding the Newtonian limit and is supported due to the results of the previous section regarding the proper time on the geoid, the defining constant L_g and its relation to W_0. In approach (II), we choose the value of U^* such that after the isometric embedding into $\mathbb{R}^3$ and comparison to the Newtonian geoid, the difference vanishes in the equatorial plane and is globally as small as possible. This means, we choose the gauge freedom in the comparison such that the relativistic geoid is as close as possible to the Newtonian geoid. In approach (III), we choose the value of U_0^* such that in its post-Newtonian expansion $W \to W_0$ and $U \to U_0$. Finally, we also consider approach (IV), which is analoge to approach (I) but without embedding the relativistic geoid into $\mathbb{R}^3$. Instead, we identify the global coordinates, which are used for the Newtonian geoid, and the pN coordinates. This approach enables us to judge of whether or not the embedding is really necessary at the leading order.

6.3.1 Geoid models

The Newtonian gravity potential of the quadrupolar gravitational field is (2.16),

$$W(R,\Theta) = -G\left(\frac{M}{R} + \frac{N_2 P_2(\cos\Theta)}{r^3}\right) - \frac{1}{2}R^2\omega^2\cos^2 . \tag{6.31}$$

Note that $N_2 = J_2 R_\oplus^2 M_\oplus$. We use spherical coordinates (R,Θ,Φ) for the $\mathbb{R}^3$, and $R_\oplus$, $M_\oplus$ are the Earth's radius and mass, respectively. Its angular velocity is ω. The geoid determined by observers on the rotating Earth, i.e. including centrifugal effects, in this model is the level surface of W such that

$$-W(R,\Theta)|_{\text{geoid}} = W_0 = 6.2636856 \times 10^7 . \tag{6.32}$$

For the post-Newtonian approximation of this configuration we have to use

$$\begin{aligned} U^*(r,\theta) &= U(r,\theta) - \frac{1}{2}r^2\omega^2\sin^2\theta + \frac{1}{2}\frac{U(r,\theta)^2}{c^2} \\ &= W(r,\theta) + \frac{1}{2}\frac{U(r,\theta)^2}{c^2} . \end{aligned} \tag{6.33}$$

The relativistic geoid is given by one chosen level surface of $U^*(r,\theta)$ such that

$$U^*(r,\theta)|_{\text{geoid}} = U_0^* \,. \tag{6.34}$$

We choose spherical coordinates (r,θ,φ) for the post-Newtonian spacetime and the flat space coordinates (R,Θ,Φ) are their 0-th order approximations.

6.3.2 Geoid comparison approach (I)

Using the comparison method I, we choose

$$U_0^* = -W_0 \tag{6.35}$$

and construct the relativistic geoid for the post-Newtonian configuration. The result is a two-surface described by $r(\theta)$. After embedding this surface into $\mathbb{R}^3$, we determine the radial distance, at any polar angle, to the Newtonian geoid, which is generically given in $\mathbb{R}^3$ as function $R(\Theta)$. The result is shown in Fig. 6.1. We find the mean difference between both geoids to be about 2.21 mm with some small angular deviations that are three orders of magnitude smaller due to the quadrupolar influence. Hence, we exactly find what we predicted at the beginning: the relativistic monopole causes a global deviation and the relativistic quadrupole induces some angular variation.

In a nutshell: the result is that the first order corrections to the Earth's geoid due to General Relativity are about 2.21 mm with latitudinal variations of 1 μm.

6.3.3 Geoid comparison approach (II)

For the second approach, we choose the value U_0^* such that in the embedding space both geoids coincide in the equatorial plane. This choice can be easily translated into the structure of the embedding equations, see appendix C. However, in general it is not possible to deduce properties or parameter values in spacetime from requirements which shall be fulfilled after an embedding.

The result of this approach is show in Fig. 6.2. We see that the overall modulation is removed and only the latitudinal variation of about 8 μm remains. By this choice, we have fitted the relativistic geoid to the Newtonian one in the best possible way. The remaining difference is due to the relativistic quadrupole.

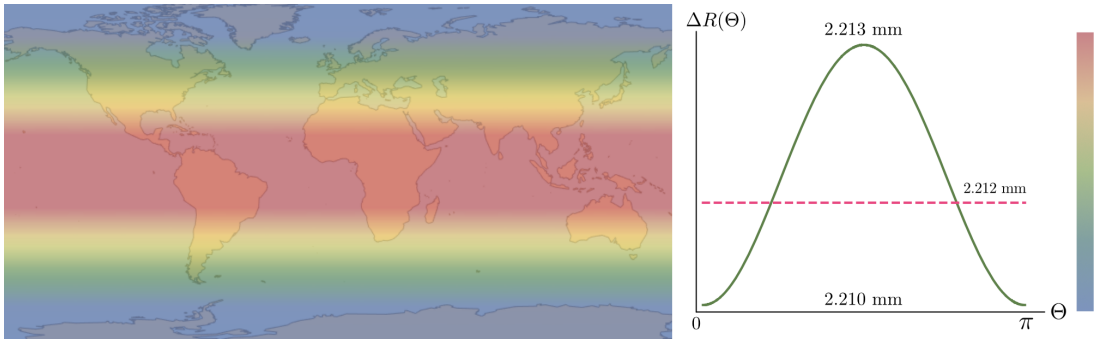

FIGURE 6.1: Comparison of the relativistic and Newtonian geoid at leading order for approach (I). We show the geoid radii differences $\Delta R(\Theta) = R_{\mathrm{PN}}(\Theta) - R_{\mathrm{N}}(\Theta)$ in the embedding space $\mathbb{R}^3$ as a function of Θ. The maximal, minimal, and mean differences are indicated respectively.

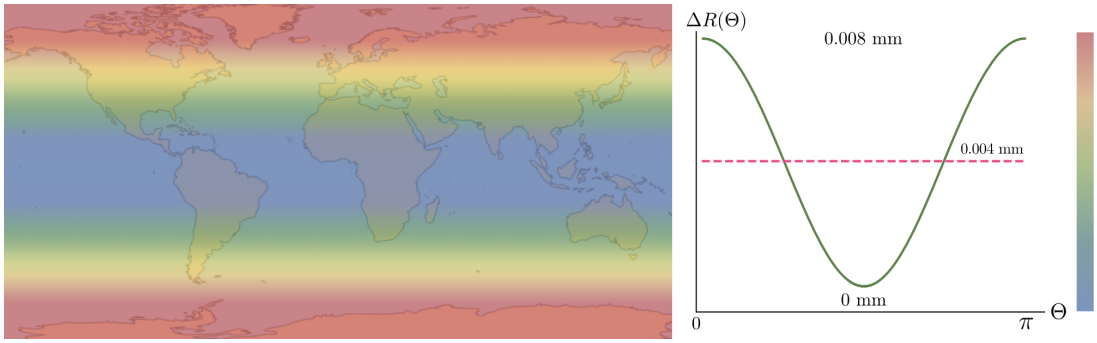

FIGURE 6.2: Comparison of the relativistic and Newtonian geoid at leading order for approach (II). We show the geoid radii differences $\Delta R(\Theta) = R_{\mathrm{PN}}(\Theta) - R_{\mathrm{N}}(\Theta)$ in the embedding space $\mathbb{R}^3$ as a function of Θ. The maximal, minimal, and mean differences are indicated respectively.

6.3.4 Geoid comparison approach (III)

For the third approach, we choose the value U_0^* such that

$$U_0^* = U^*\big|_{\mathrm{geoid}} = U_{\mathrm{pN}}^*\big|_{W\to -W_0, U\to U_0} = W_0 + \frac{U_0^2}{2c^2}\,, \tag{6.36}$$

and the result is shown in Fig. 6.3. For this choice, the difference between Newtonian and relativistic geoid in the embedding space is about 4 mm with latitudinal variation of 0.015 mm between the poles and the equatorial plane. The disadvantage of this choice is that the value of U^* varies for each post-Newtonian order. Hence, we may exclude choices like the above from further analysis.

6.3.5 Geoid comparison approach (IV)

To emphasize the importance of the embedding, we compare the relativistic and Newtonian geoid also using approach (IV). The result is quite remarkable and shown in

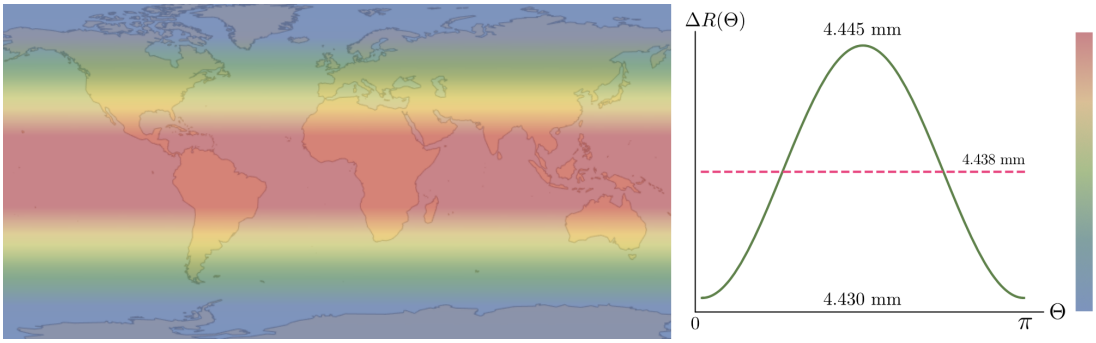

FIGURE 6.3: Comparison of the relativistic and Newtonian geoid at leading order for approach (III). We show the geoid radii differences $\Delta R(\Theta) = R_{\mathrm{PN}}(\Theta) - R_{\mathrm{N}}(\Theta)$ in the embedding space $\mathbb{R}^3$ as a function of Θ. The maximal, minimal, and mean differences are indicated respectively.

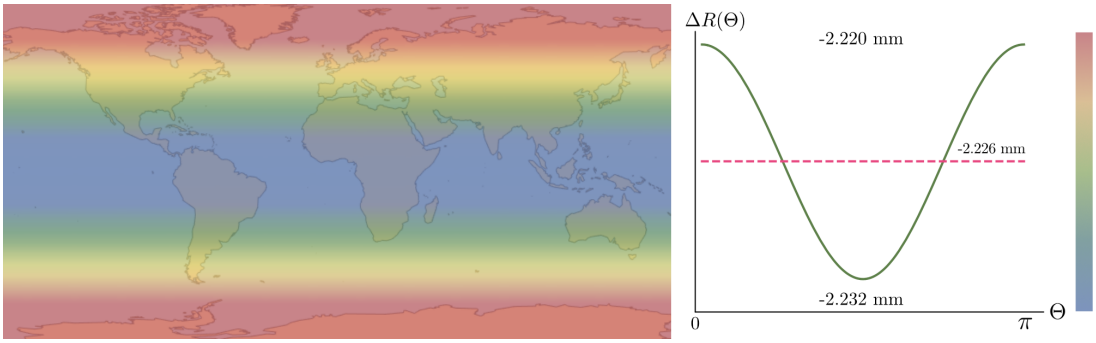

FIGURE 6.4: Comparison of the relativistic and Newtonian geoid at leading order for approach (IV), which is the same as approach one but without embedding. We show the geoid radii differences $\Delta R(\Theta) = R_{\mathrm{PN}}(\Theta) - R_{\mathrm{N}}(\Theta)$, for which Newtonian and pN coordinates are identified, as a function of Θ. The maximal, minimal, and mean differences are indicated respectively.

Fig. 6.4. We clearly see that, w.r.t. approach (I), the sign of the difference changes. As we can read off from Fig. 6.1 for approach (I), the radius of the relativistic geoid is globally about 2.2 mm larger than the radius of the Newtonian geoid. For approach (IV) it is vice versa. The "effect" appears due to the mismatch of the coordinates which is of the order of 4 mm such that pN radii are smaller than Newtonian radii. Hence, the embedding is not only a theorists pedantism but really has an important influence on the result. It is, however, a mere coincidence that +2 mm become −2 mm by coordinate and embedding effects. Therefore statements on the magnitude of "2 mm difference" between the geoids, as communicated in the geodetic community, remain correct; but signs do matter!

6.4 Chronometric Geodesy and height measurements

In chapter 2, different height measures were introduced. Among them, there is the orthometric height, the normal height, the dynamical height, and the ellipsoid height.

The first three height notions are constructed in the same conceptual way. Gravity potential numbers C are defined as the difference $W_0 - |W_P|$ for a point P in space or on the surface and a point P_0 on the geoid. Then, the potential number is divided by either the true averaged gravity between the geoid and P along the true plumb line (orthometric height) or the averaged normal gravity along the normal plumb line between the level ellipsoid an P (normal height).

Chronometric geodesy offers an entirely new perspective and new observables for height determination. Since the redshift is, to first order, sensitive to gravity potential differences, see Eq. (5.37) in section 5.5, we have

$$z + 1 = \frac{\nu_0}{\nu_P} = 1 + \frac{W_P + W_0}{c^2} + \mathcal{O}\big(c^{-4}\big) =: 1 + \frac{\Delta W}{c^2} + \mathcal{O}\big(c^{-4}\big)\,. \tag{6.37}$$

Here, ν_0 is the frequency of a clock on the geoid and ν_P is the frequency of a clock at point P. Since $W_P + W_0 = W_0 - |W_P| =: \Delta W$ is positive for points above the geoid[2], a signal from the geoid to P is redshifted; the photon has "to fight against gravity" and loses energy. Now, geopotential numbers

$$C_P = W_P + W_0 = c^2 z - \mathcal{O}(c^{-2}) \tag{6.38}$$

can be obtained by clock comparison, see also Refs. [34, 38, 130, 174] for detailed explanations. Moreover, using only the leading order term, the defining equation (2.50) for orthometric heights can be rewritten in terms of the redshift to define the orthometric height H of a point P above the geoid,

$$H = c^2\,\frac{z}{\bar{g}}\,. \tag{6.39}$$

Here, z is the redshift of a signal which is emitted from a clock on the geoid and received by a clock at P. If P is above the geoid, the redshift is positive and so is the height of P are positive. For points below the geoid, the height becomes negative since the signal is blue-shifted.

However, calculating orthometric or normal heights by geopotential numbers obtained from clock comparison is a kind of semi-relativistic approach. The respective

[2] W_0 is a positive value, defined as shown in chapter 2. W_P is the gravity potential at P and negative in our sign convention.

notion of height is still defined in a completely Newtonian framework and only an approximation of the "true height". Also, the Newtonian limit of a height defined by (6.39) is not obvious. Therefore, a general relativistic definition of heights, using the notions developed here, is preferred even though deviations are below present accuracy. Luckily, such a generalization can be done in a straight forward approach, analog to the definition of orthometric height in section 2.3.2.

6.4.1 Chronometric height

Let ϕ be the redshift potential for co-rotating observers on the Earth's surface in the stationary spacetime that describes the exterior of the Earth. Then, the acceleration of such observers is $a = c^2 \mathrm{d}\phi$ and we define the redshift potential number for a point P on the Earth's surface

$$C_P^* := c^2 \left(e^{\phi_P} - e^{\phi_0} \right) = U_P^* - U_0^* \,, \tag{6.40}$$

using U_0^* and U_P^*, the value of the relativistic gravity potential on the relativistic geoid and at point P, respectively. Note that the definition is exact, no approximation is involved, and $C^* > 0$ for points above the geoid. C_P^* can be determined from redshift measurements since

$$C_P^* = c^2 e^{\phi_0} \left(e^{\phi_P - \phi_0} - 1 \right) = c^2 e^{\phi_0} \left(\frac{\nu_0}{\nu_P} - 1 \right) = c^2 e^{\phi_0} z \,, \tag{6.41}$$

where z is the redshift of signal send from a point on the geoid to the point P and $e^{\phi_0} = 1 + U_0^*/c^2$ is a constant given by the geoid value U_0^*, which might be chosen by $U_0^* = -W_0$ with W_0 as in chapter 2. Thereupon, we define the chronometric height H^* of P by

$$H_P^* = \frac{C_P^*}{\bar{a}} \tag{6.42}$$

using the average acceleration between the relativistic geoid and P, calculated along the normal direction of the isochronometric surfaces. At any point, the normal direction is given by the acceleration vector of the co-rotating congruence and we can normalize the acceleration to define the unit normal

$$n_\mu = \frac{a_\mu}{\sqrt{g^{\rho\sigma} a_\rho a_\sigma}} = \frac{\partial_\mu \phi}{\sqrt{g^{\rho\sigma} \partial_\rho \phi \partial_\sigma \phi}} = \frac{\partial_\mu U^*}{\sqrt{g^{\rho\sigma} \partial_\rho U^* \, \partial_\sigma U^*}} \,, \tag{6.43a}$$

$$n^\mu = \frac{g^{\mu\nu} a_\nu}{\sqrt{g^{\rho\sigma} a_\rho a_\sigma}} = \frac{g^{\mu\nu} \partial_\nu \phi}{\sqrt{g^{\rho\sigma} \partial_\rho \phi \partial_\sigma \phi}} = \frac{g^{\mu\nu} \partial_\nu U^*}{\sqrt{g^{\rho\sigma} \partial_\rho U^* \, \partial_\sigma U^*}} \,. \tag{6.43b}$$

In the Newtonian limit we have $U^* \to W$ and $C_P^* \to C_P$. The unit surface normal becomes the normalized gradient of the gravity potential and the chronometric height

H^* yields the orthometric height H.

We shall emphasize that the chronometric height H^* is defined in General Relativity without approximations or Newtonian concepts, i.e. in a completely relativistic framework. It makes sense for any stationary spacetime.

6.4.2 On height reference surface determination and preservation

In this section, we show how a particular isochronometric surface can be operationally determined and maintained over time spans, even though the topography underneath may change due to dynamical phenomena such as, e.g., land uplift. This procedure enables the determination of an absolute height reference point that single out one level surface of the relativistic gravity potential U^*.

In the following, we assume that the spacetime is stationary and that surface topography changes do, to first order, not change the multipole moment structure of the gravity field. Using two clocks as emitter and receiver of a signal, respectively, redshift measurements give information about the relative height difference, see the preceding section. We assume that both clocks are at rest w.r.t. the rotating Earth. Hence, their worldlines are members of an isometric congruence and there is a time-independent redshift potential ϕ which is the fundamental ingredient to construct the relativistic gravity potential U^*.

Now we find ourselves with the task to operationally distinguish a particular level surface of the relativistic gravity potential. In principle, one clock can be declared as the master clock, being on the geoid by definition. Then, the geoid is the isochronometric surface that intersects (the center of mass of) this master clock. This particular level surface is well defined and the second clock at a point P can be used to test if P lies on the geoid. This is true if and only if the redshift of both clocks vanishes.

However, the master clock is somehow mounted on the Earth's surface and topography changes might lift it to a new height. Actually, by definition, the height of the master clock would not change since it is situated on the reference surface for height measurements. Hence, the clock would always be at height zero. One solution might be to distribute a set of master clocks and to take some statistical average to define the zero height surface. Another approach is outlined below.

Let neither of the two clocks be the master clock, but both have an equal status. Furthermore, assume that the clocks are rigidly connected such that they have a fixed proper distance L, which might be determined precisely by interferometric methods. Now, we introduce spherical-like coordinates such that the spatial part of the metric is diagonal and align the rigidly connected clocks with the r-direction. Let the clocks' radial positions be given by r_1 and $r_2 = r_1 + l$, respectively. Then, for the proper

distance of the clocks we have

$$L = \int_{r_1}^{r_2+l} \sqrt{g_{rr}} \mathrm{d}r \,, \tag{6.44}$$

which is an equation for the coordinate separation l.

The clocks shall be positioned in some kind of tower such that they can be moved in the radial direction. Depending on the (initial) positions of the clocks and the length l, there will be an (initial) redshift z_0 which is measured and recorded to the highest possible accuracy. We may now define the relativistic geoid as the particular isochronometric surface that intersects the (center of mass of) the lower clock. Alternatively, also the upper clock can be chosen for the definition, or some point can be marked on the rigid connection. As another choice, and this is the most elegant and expensive version, a third clock can be positioned at the center (geometric center) of the whole system and define the geoid by the particular isochronometric that it intersects. Then all clocks in the exterior can be compared to this third clock and arranged on the geoid by the vanishing redshift condition.

Now, due to dynamics of the Earth, the surface topography at the clock tower's position changes over time. This change causes a proper height offset H, related to a coordinate offset h by

$$H = \int_{r_1}^{r_1+h} \sqrt{g_{rr}} \mathrm{d}r \,, \tag{6.45}$$

such that the clocks are now at positions $r_1' = r_1 + h$ and $r_2' = r_1' + l' = r_1 + h + l'$, respectively. We must have

$$L = \int_{r_1'}^{r_2'} \sqrt{g_{grr}} \mathrm{d}r = \int_{r_1+h}^{r_1+h+l'} \sqrt{g_{grr}} \mathrm{d}r \,, \tag{6.46}$$

since the clocks are rigidly connected. This is an equation for l'. Thus, given an initial value for r_1 and a proper separation length L, the values for l, l', and h can be calculated from the proper height change H. It can be calculated that for redshift observations close to the Earth's surface, the difference between L, l, and l' as well as the difference between H and h can be safely ignored. Due to the height shift H of the rigidly connected clocks, their redshift will change to a value z'. The change of the redshift,

$$\Delta z := z' - z_0 \,, \tag{6.47}$$

is a monotonic function of the Height shift H. The entire rigid system is now to be moved up or down until the initial redshift is restored. Then, the third clock in the

center is again positioned at the initially chosen isochronometric surface. In Fig. 6.5, we have sketched the situation and basic idea of this "isochronometric surface maintainer". To have more sensitive directions, the shape of the device can be improved to be a tetrahedron, with clocks at all edges and a central clock in the geometric center.

Let us now apply the idea to the first-order pN metric of the Earth to estimate the size of the system as a function of the desired accuracy. We have the pN redshift equation (5.37)

$$1 + z = 1 + \frac{W_2 - W_1}{c^2} + \mathcal{O}\big(c^{-4}\big)\,. \tag{6.48}$$

The change of the redshift becomes

$$\Delta z = z' - z_0 = \frac{1}{c^2}(W_{2'} - W_2 + W_1 - W_{1'})\,. \tag{6.49}$$

For a height change in the radial direction this becomes

$$\Delta z \approx \frac{1}{c^2}(W(r_1 + h + l) - W(r_1 + l) + W(r_1) - W(r_1 + h))\,, \tag{6.50}$$

where we assume that the angular positions of clocks remain constant at their initial values. In Fig. 6.5, the plot for relation of the redshift change and the height sensitivity is shown. A redshift change of about 10^{-19} correspond to a height change $H \approx 29\,\mathrm{m}$ for a separation of about 100 m. The centimeter accuracy regime is reached for $\Delta z \approx 4 \times 10^{-23}$. Therefore, we conclude that the method works in general, but the expected accuracy for the geoid determination using state of the art clock comparison at the 10^{-19} level is orders of magnitude below other approaches.

We conclude by the following remarks. The redshift, given by potential difference, is sensitive to the gradient of the gravitational field. Thus, the change of the redshift is sensitive to the change of the gradient, i.e. the curvature. We have constructed a very simple and rudimentary version of a "clock compass", see Ref. [154].

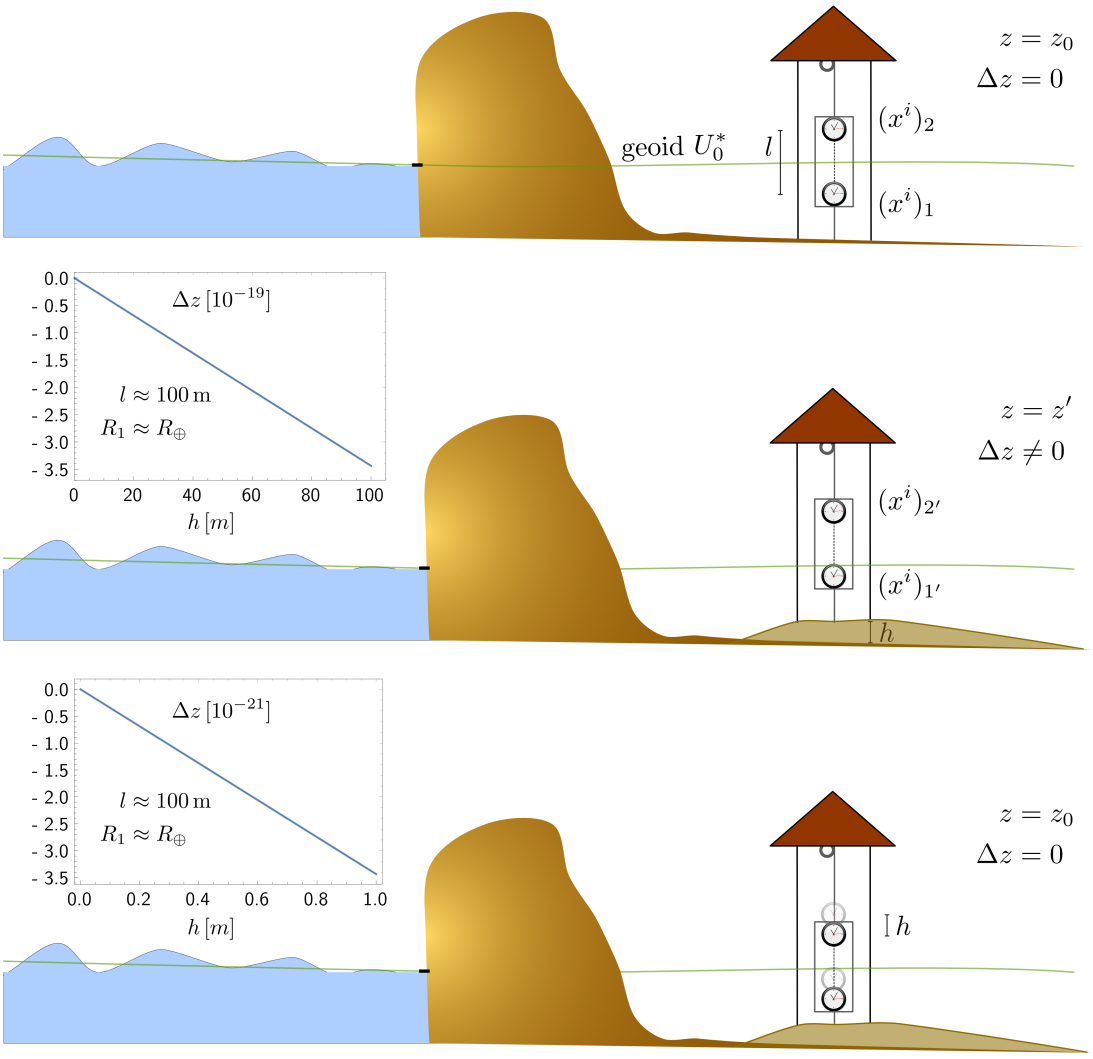

FIGURE 6.5: Isochronometric surface maintenance with rigidly connected clocks, sketch of the general idea and results for the relation between height resolution and accuracy for the redshift change.

6.5 Relativistic effects on satellite orbits

In this section, we investigate relativistic effects along satellite orbits. In the first part, an overview of important effects on satellite orbits and signal propagation is given. Then, we compare relativistic effects in a post-Newtonian framework to various non-gravitational orbit perturbations due to the space environment. As an example, a real GRACE orbit is studied and accelerations due to the dominant effects are calculated along a full orbital arc. In the last part, we analyze relativistic gravity gradiometry and the time development of nearby free fall orbits, i.e. of two geodesics, to relate their deviation to the curvature of spacetime by the well-known Jacobi equation.

6.5.1 Overview of relativistic effects

A list of the most prominent relativistic effects on satellite orbits and signal propagation in space between observers is given below.

- Perihelion precession
- Light bending
- Gravitational and Doppler redshift of signals
- Shapiro delay
- de Sitter precession (geodetic precession)
- Schiff effect
- Lense-Thirring precession
- Gravitomagnetic clock effects

At least some of these effects must be considered for geodetic missions in space. Accurate orbit modeling and determination needs to take into account, at least at a post-Newtonian order, that the spacetime curvature influences satellite orbits and signal propagation.

The first three effects are known as the classical tests of General Relativity [127, 169]. For an overview and the "confrontation of General Relativity and experiment" see Ref. [200, 199].

The unexplained perihelion precession of mercury was one of the mysteries at Einstein's time. A new theory of gravity was needed to explain the "anomalous" 43" per century in the perihelion advance of mercury's orbit. General Relativity is able to successfully explain the precession of elliptical orbits and an estimate of the precession of the perihelion for satellite orbits can be obtained by solving the equations of motion in

the Schwarzschild spacetime, which can be done exactly in terms of elliptical functions, see [81]. The weak-field approximation yields a shift

$$\Delta\alpha = \frac{6\pi\, GM}{c^2 a(1-e^2)}\,, \tag{6.51}$$

with the semi-major axis a and eccentricity e of an elliptical bound orbit. The result was already calculated by Einstein [45] and used to test his preliminary versions of the theory.

The second classical test of General Relativity is the bending of light rays close to gravitating bodies; the light has to propagate on the curved spacetime geometry. In 1919, Eddington verified the general relativistic prediction by observing stars during a solar eclipse. The deflection angle for light bending due to the relativistic monopole is given by

$$\delta = \frac{4GM}{c^2 r_{\min}}\,, \tag{6.52}$$

where $r_{\min}$ is the distance of closest approach. Based on the motion of light in curved spacetime, nowadays, gravitational lensing is used as a standard tool in astrophysics, see Refs. [136, 137].

Gravitational and Doppler redshifts have been explained to a great extent in this work. The first measurement of the gravitational redshift on Earth, but not with clocks, was done by Pound and Rebka, see [151]. The first space experiment to test the relativistic redshift was Gravity Probe A, see [191, 192, 193]. The results coincide with the predictions of general relativity within 1.4×10^{-4}. Modern optical clocks allow to measure their mutual redshifts in Earth-bound experiments and are the basis of chronometric geodesy, see Refs. [24, 129, 38, 34] and references therein. Also, the DLR-ESA funded project RELAGAL evaluates the clock data of the errant Galileo satellites GSAT0201 and GSAT0202 to test the general relativistic redshift. ACES, a clock ensemble in space will be used to achieve unprecedented accuracy in testing the equivalence principle and predictions of General Relativity with clocks [91].

The Shapiro delay is the time delay of a signal due to the increased propagation time on the curved spacetime geometry, see [172]. Geodetic precession, described first by de Sitter [177] is the precession of, e.g., the spin axis of an orbiting gyroscope. The difference between geodetic precession and the Lense-Thirring effect is the respective relativistic multipole moment which is responsible for the effect. The de Sitter precession occurs in the presence of a pure mass monopole, whereas frame dragging effects and the Lense-Thirring effect are due to the presence of a spin dipole moment and, therefore, a mass quadrupole. The total precession of a gyroscope's spin axis is calculated as the combined effect and was tested by the famous space mission Gravity Probe

B, see [49, 50]. Also satellite laser ranging with the LARES and LAGEOS satellites provides results for the Lense-Thirring effect in the vicinity of the Earth [26, 27].

Gravitomagnetic clock effects are also frame dragging effects in the presence of a rotating central source. Assume that two clocks are on a circular orbit in the equatorial plane of a Kerr spacetime with the Kerr parameter adapted to the angular momentum of the Earth, see section 5.4. Then, let the clocks orbit in opposite directions. After a full revolution of 2π in the azimuthal angle, they show a difference in elapsed proper times of about 100 ns, see Ref. [79] and references therein. As shown by the authors of Ref. [79], the effect can be generalized to arbitrary orbits and the result is given analytically without approximations. However, due to experimental constraints and error budgets, this effect has never been measured so far, even though a principle mission study termed Gravity Probe C was proposed about 20 years ago [72].

6.5.2 Relativistic effects and orbital perturbations

In this section, we are interested in the magnitudes of accelerations due to relativistic effects along satellite orbits and we compare these to non-gravitational orbital perturbation due to the space environment. The section is based on the results presented in Ref. [146].

The geodesic equation (3.15) for the motion of test particles is usually parametrized by the proper time. However, the equations of motion can also be given w.r.t. the coordinate time of the spacetime model. Using a first-order post-Newtonian metric (3.77) with GCRS coordinates, we expand the geodesic equation up to $\mathcal{O}(c^{-2})$ and obtain

$$\begin{aligned}\overset{\circ\circ}{\mathbf{x}} &= -\nabla U + c^{-2}\big(- 4U\nabla U + 4\big(\nabla U \cdot \overset{\circ}{\mathbf{x}}\big)\overset{\circ}{\mathbf{x}} - \big(\overset{\circ}{\mathbf{x}} \cdot \overset{\circ}{\mathbf{x}}\big)\nabla U + 4\overset{\circ}{\mathbf{x}} \times (\nabla \times \mathbf{U})\big) \\ &=: \mathbf{a}_{\mathrm{N}} + \mathbf{a}_{\mathrm{pN}}\,, \end{aligned} \tag{6.53}$$

where

$$\overset{\circ}{\mathbf{x}} := \frac{\mathrm{d}\mathbf{x}}{\mathrm{d}t} \tag{6.54}$$

is the coordinate time derivative, see also Refs. [16, 111] but note that in our convention, we have $U < 0$ and therefore, consequently, $\nabla U > 0$. Here, U is the gravitational potential of the Earth, and the vector potential $\mathbf{U}$ takes care of gravitomagnetic effects. The vector $\mathbf{x} = (X, Y, Z)$ is the three component Cartesian position vector in the GCRS and $\overset{\circ}{\mathbf{x}}$ its coordinate time derivative. The acceleration is denoted by $\mathbf{a}$. This equation formally looks like the Newtonian equation of motion supplemented with a relativistic correction term $\mathbf{a}_{\mathrm{pN}}$ proportional to c^{-2}. The leading order pN correction term due to

the monopole of the gravitational field is

$$\mathbf{a}^0_{\mathrm{pN}} = \frac{GM}{c^2R^2}\left[\left(\frac{4GM}{R} - \mathring{\mathbf{x}}\cdot\mathring{\mathbf{x}}\right)\mathbf{x} + 4\left(\mathbf{x}\cdot\mathring{\mathbf{x}}\right)\mathring{\mathbf{x}}\right] . \tag{6.55}$$

To estimate relativistic effects and their magnitude in comparison to other orbital perturbation we apply the following strategy. We set up a model for the satellite's motion, including the Newtonian acceleration $\mathbf{a}_{\mathrm{N}}$, the pN acceleration $\mathbf{a}_{\mathrm{pN}}$, and accelerations due to other space environmental effects summarized by $\mathbf{a}_{\mathrm{env}}$. Hence,

$$\mathbf{a} = \mathbf{a}_{\mathrm{N}} + \mathbf{a}_{\mathrm{pN}} + \mathbf{a}_{\mathrm{env}} . \tag{6.56}$$

The force models for various space environmental perturbations are implemented in the eXtended High Performance Satellite dynamics Simulator (XHPS) [201] developed at ZARM, University of Bremen. The XHPS uses the framework of Newtonian mechanics and allows to accurately simulate multi-satellite missions with an arbitrary gravity field as well as non-gravitational perturbations of the satellite orbit. Simulations at all levels of detail can be constructed, due to the modular design of the simulator, and different numerical integration schemes can be chosen. In principle, arbitrary high numerical accuracy can be achieved since the GNU MPFR library [55] allows to employ variable-precision. The reference systems used for the XHPS are the ICRS [3], and the ITRS [13]. They are Cartesian coordinate systems derived from the BCRS and GCRS, respectively. These systems are realized by reference frames according to the latest IERS conventions [142].

The equations of motion are integrated using the XHPS. The solar radiation pressure (SRP) [119], effects related to the Earth's albedo, atmospheric drag, and thermal radiation pressure (TRP) [164] are taken into account. These effects are among the dominant influences on many satellite orbits. All considered orbital perturbation models are based on a finite element model of the satellite, which allows to consider orientation, material properties, and shadowing to great detail [119]. The Albedo model is based on hourly CERES data [198]. TRP is computed with a transient temperature model for each element of the satellite taking into account radiation from Sun, albedo and infrared. Atmospheric effects are modeled by a basic atmospheric drag model with constant drag coefficient and the atmosphere's density is determined by the empirical JB2008 model [14].

Two different satellite orbits are considered: (i) a slightly elliptical low Earth orbit with semi-major axis $a = 8.5 \times 10^6$ m and eccentricity $e = 0.2$ in the equatorial plane, and (ii) the real 24h GRACE orbit from 2008-04-15, see Ref. [146]. For the satellite, a GRACE-like model is used together with Nadir pointing. In Fig. 6.7, the results for the first orbit are shown. We plot the accelerations due to the respective influences in

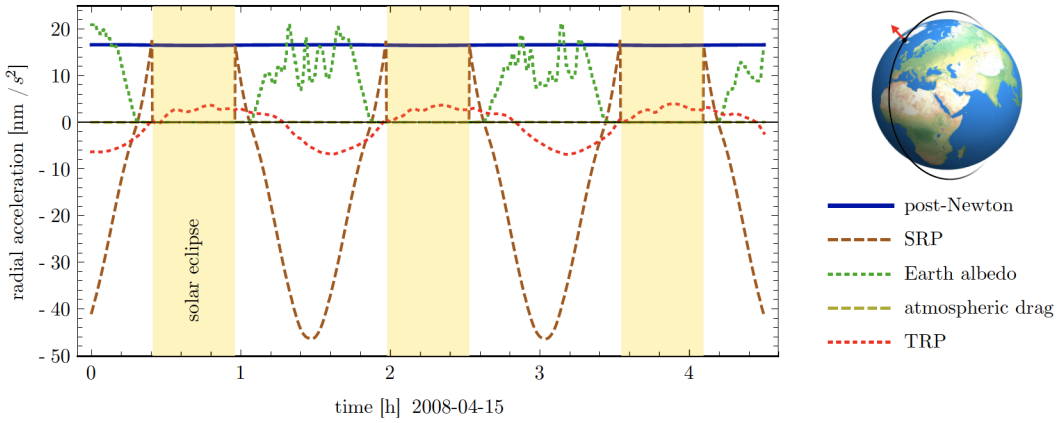

FIGURE 6.6: Relativistic and space environmental effects on a GRACE satellite orbit from 2008-04-15. Figure taken from Ref. [146].

a local Cartesian coordinate system attached to the satellite. For the GRACE orbit, we show the accelerations in the radial direction in Fig. 6.6.

Accelerations due to the first order relativistic correction in the radial direction reach a maximum of about $20\,\mathrm{nm/s^2}$ in both cases. As we can see, they are comparable to the non-gravitational perturbations and we conclude that at least first-order relativistic effects must be taken into account for high-precision space missions. These results do agree with results in Ref. [180], table 3. In their paper, the authors estimated magnitudes of several orbital effects for the LAGEOS mission. At this point I wish to express my gratitude to Florian Woeske for contributing the XHPS calculations to our joint work.

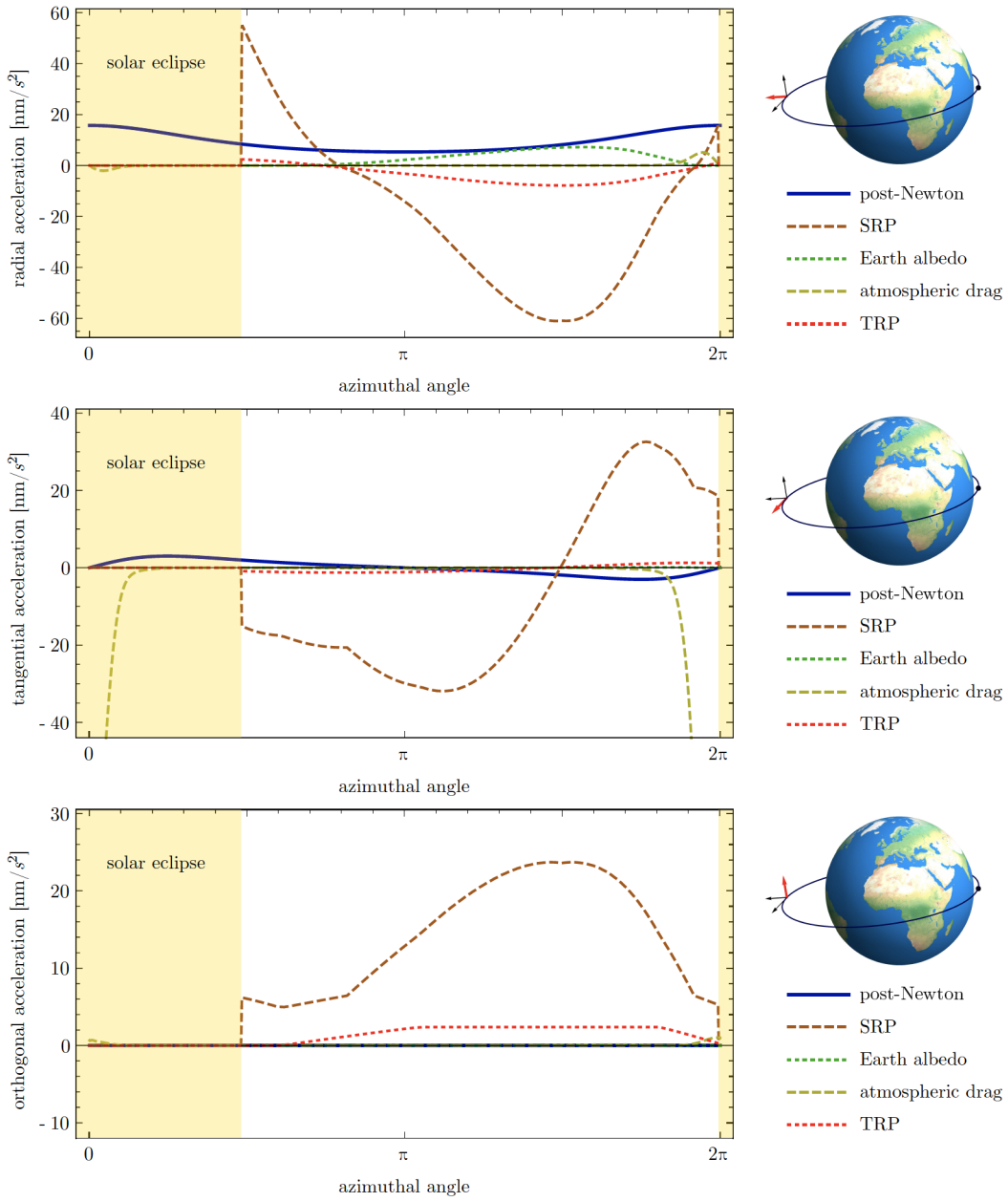

FIGURE 6.7: Relativistic and space environmental effects on a elliptic low Earth satellite orbit (LEO) with semi-major axis $a = 8.5 \times 10^6$ m and eccentricity $e = 0.2$. Figure taken from Ref. [146].

6.6 Relativistic gravity gradiometry

Gravity gradiometry is the study of variations in the acceleration of (test) particles due to gravity. The central object of interest is the gravity gradient. Test masses separated by some distance will in general experience different accelerations and their worldlines will deviate if they are allowed to move in free fall.

An intuitive simple example is the difference in the vertical acceleration at two points which are separated by a distance $2l$. The two accelerations can be measured using accelerometers, and we assume for this example that the gravity vector $\vec{g} = -\vec{\nabla}W$ in a Cartesian coordinate system has a z-component only. Then, we have the vertical gravity gradient

$$\partial_z g_z = -\partial_z(\vec{\nabla}W)_z =: -K_{zz} \approx \frac{g_z(z+l) - g_z(z-l)}{2l} \,. \tag{6.57}$$

Hence, the gravity gradient is given by second derivatives of the potential. In General Relativity, this concepts needs to be overworked since there is not just a single potential anymore, but a metric tensor that can be regarded as 10 potentials in total. Derivatives of the potential are then combined into the Christoffel symbols $\Gamma^{\mu}_{\nu\sigma}$ and derivatives of the $\Gamma^{\mu}_{\nu\sigma}$ are used to calculate the curvature tensor $\mathcal{R}^{\mu}{}_{\nu\sigma\rho}$. Thus, relativistic gravity gradients are curvature tensor components, and relativistic gravity gradiometry can measure spacetime curvature, see [153].

In the following, we study the deviation of particle worldlines and generalize the Newtonian solution of the gradiometer equation for a spherically symmetric potential to the solution of the geodesic deviation equation in the Schwarzschild spacetime.

6.6.1 Newtonian gradiometry

Let us start by briefly recalling how the deviation of two free fall orbits is constructed in the Newtonian theory, see, e.g., Refs. [147, 144, 143].

Let $Y^i(t)$ be a solution of the Newtonian equation of motion $\ddot{\vec{Y}} = -\vec{\nabla}U$. This curve is called the reference in the following. Now, assume that $X^{\mu}(t) = Y^a(t) + \eta^a(t)$ also solves $\ddot{\vec{X}} = -\vec{\nabla}U$, which defines the deviation η^a. Thus, we have

$$\ddot{X}^i = \ddot{Y}^i + \ddot{\eta}^i = -\partial^i U(X) = -\partial^i U(Y+\eta) \,. \tag{6.58}$$

If the deviation is small, we can linearize the potential at $\vec{X}$ in a Taylor series around the reference $\vec{Y}$,

$$U(X) = U(Y+\eta) = U(Y) + \eta^i \partial_i U(Y) + \mathcal{O}(\eta^2) \,. \tag{6.59}$$

Neglecting terms of order $\mathcal{O}(\eta^2)$ gives the first-order deviation equation

$$\ddot{\eta}^i = -[\partial^i \partial_j U(Y)]\,\eta^j =: -K^i{}_j \eta^i \,. \tag{6.60}$$

The deviation has a trivial linear time dependence if either the gravitational field is homogeneous, ($\partial_\nu U \equiv 0$), or vanishing. Then, we have $\eta^\mu(t) = A^\mu t + B^\mu$. In contrast, a non-linear time dependence is caused by second derivatives of the Newtonian gravitational potential $K^i{}_j \neq 0$. The matrix $K^i{}_j$ is also known as the tidal matrix.

For a monopolar Newtonian potential in a spherical coordinate system, a straightforward but rather lengthy calculation yields [144, 143]

$$\ddot{\eta}^\vartheta = -\frac{\dot{R}}{R}\dot{\eta}^\vartheta - \left(\frac{GM}{R^3} + \frac{\ddot{R}}{R}\right)\eta^\vartheta \,, \tag{6.61a}$$

$$\ddot{\eta}^r = \left(\dot{\Phi}^2 + \frac{2GM}{R^3}\right)\eta^r + \left(2\dot{R}\dot{\Phi} + R\ddot{\Phi}\right)\eta^\varphi + 2R\dot{\Phi}\,\dot{\eta}^\varphi \,, \tag{6.61b}$$

$$\ddot{\eta}^\varphi = -\frac{2\dot{R}}{R}\,\dot{\eta}^\varphi - \frac{2\dot{\Phi}}{R}\dot{\eta}^r - \left(\frac{\ddot{R}}{R} + \frac{GM}{R^3} - \dot{\Phi}^2\right)\eta^\varphi - \frac{\ddot{\Phi}}{R}\eta^r \,, \tag{6.61c}$$

which is a system of couple differential equations. Quantities in capital letters $R = R(t)$ and $\Phi = \Phi(t)$ are functions of the absolute time t and describe the reference path. Above, we introduced the matrix $K^i{}_j$ which is known very well in the framework of gradiometry as the tidal matrix.

A particular application of the result above is the deviation from a circular reference orbit with fixed radius R. In Ref. [69], the oscillating solution is derived and in Ref. [147], the full solution can be found. The reference motion is described by the Keplerian orbital frequency Ω_K such that

$$\dot{\Phi} = \Omega_K = \sqrt{\frac{GM}{R^3}} \;\Rightarrow\; \Phi(t) = \Omega_K\, t \,, \tag{6.62}$$

and the deviation equation (6.60) now has the general solution

$$R\eta^\vartheta(t) = C_{(5)} \cos\Omega_K t + C_{(6)} \sin\Omega_K t \,, \tag{6.63a}$$

$$\eta^r(t) = C_{(1)} + C_{(2)} \sin\Omega_K t + C_{(3)} \cos\Omega_K t \,, \tag{6.63b}$$

$$R\,\eta^\varphi(t) = 2\left(C_{(2)} \cos\Omega_K t - C_{(3)} \sin\Omega_K t\right) - \frac{3}{2}\,\Omega_K C_{(1)} t + C_{(4)} \,. \tag{6.63c}$$

Here, $C_{(5)}$ and $C_{(6)}$ are the normalized amplitudes of the two fundamental solutions and the deviation component η^ϑ oscillates with the Keplerian frequency Ω_K. There is a variety of possible perturbations of the reference curve. The integration constants $C_{(a)}, a = 1 \ldots 6$ define the initial phase space position (or, equivalently, the orbital elements) of the perturbed motion. Their impact on the perturbed orbit will be studied in

the next section for the general relativistic result. Finally, note that only the Keplerian frequency Ω_K appears such that orbits are closed and there is no perigee precession or similar effects.

6.6.2 Relativistic gradiometry

In General Relativity, the equation of motion for structureless test bodies is the geodesic equation (3.15), see Refs. [39, 133] for reviews of methods to derive this equation as well as higher order equations of motion by means of multipolar techniques.

In analogy to the Newtonian case, we consider two solutions of the geodesic equation, X^μ and Y^μ to define their deviation

$$\eta^a(s) := X^a(s) - Y^a(s)\,. \tag{6.64}$$

Here, s a parameter along the reference worldline Y. It can be, e.g., the proper time or coordinate time, and used to parametrize all worldlines. $\dot{Y}^\mu = \mathrm{d}Y^\mu/\mathrm{d}s$ is the four-velocity of the reference curve. Linearizing the geodesic equation for X w.r.t. the deviation and its first derivative, we obtain

$$\frac{\mathrm{D}^2\eta^\mu(s)}{\mathrm{d}s^2} = -\mathcal{R}^\mu{}_{\nu\rho\sigma}(Y)\,\dot{Y}^\nu\eta^\rho\dot{Y}^\sigma + \mathcal{O}(\eta^2,\dot{\eta}^2)\,, \tag{6.65}$$

which is the well-known geodesic deviation or Jacobi equation that relates the second covariant derivative of the deviation along the reference curve, i.e. the relative acceleration, to the curvature of spacetime $R^\mu{}_{\nu\rho\sigma}$. Thus, the curvature determines the time evolution of the deviation and generalizes the Newtonian tidal matrix $K^i{}_j$. Equation (6.60) is the Newtonian limit of Eq. (6.65). The deviation η will have a linear time dependence if and only if the spacetime curvature vanishes, that is, in flat space without any gravity field. For more details on the systematic derivation of the deviation equation and its possible generalizations as well as an overview of the literature we recommend Ref. [153].

Eq. (6.65) allows to determine the curvature tensor components pointwise in a local chart if the relative accelerations between the two worldlines X and Y are measured. In Ref. [153], the authors show that in vacuum a set of at least six suitably prepared objects is needed to determine all curvature components outside a gravitating body; this is a realization of the curvature compass, see [184].

Assume that a gradiometer is placed inside a satellite which is in free fall around the Earth, and the satellites worldline is taken to be the reference curve Y. Then, the gradiometer measures the relative acceleration of, e.g., two test masses, described by the perturbed worldline X, in the local satellite-attached coordinate system.

Therefore, we now project equation (6.65) into a comoving (with the reference orbit) proper reference frame, i.e. an orthonormal tetrad. Four mutually orthonormal tetrad vectors can be written as

$$e_{(\alpha)} = E^{\beta}_{(\alpha)}\partial_\beta \quad \text{with} \quad g(e_\alpha, e_{(\beta)}) = \eta_{(\alpha\beta)} = \eta_{(\alpha\beta)}\,. \tag{6.66}$$

Tetrad components (α) are denoted in brackets. We raise and lower a tetrad index $(\alpha, \beta, \dots)$ with the Minkowski metric $\eta_{(\alpha\beta)}$, whereas spacetime indices $\mu, \nu, \dots$ are raised and lowered with the metric $g_{\mu\nu}$. Now, we can project vectors, covectors, and tensors onto the tetrad basis. The deviation equation (6.65) in the tetrad frame becomes [184]

$$\frac{d^2\eta^{(\alpha)}}{\mathrm{d}s^2} = -\eta^{(\alpha\beta)}\mathcal{R}_{(\gamma\delta\rho\beta)}\dot{Y}^{(\gamma)}\eta^{(\delta)}\dot{Y}^{(\rho)}\,, \tag{6.67}$$

where $\eta^{(\alpha)} = \eta^\mu e^{(\alpha)}_\mu$ and the components of the curvature tensor are

$$\mathcal{R}_{(\alpha\beta\gamma\delta)} = \mathcal{R}_{\mu\nu\sigma\tau}e^{\mu}_{(\alpha)}e^{\nu}_{(\beta)}e^{\sigma}_{(\gamma)}e^{\tau}_{(\delta)}\,. \tag{6.68}$$

The gradiometer is at rest w.r.t. the satellite. We choose the tetrad such that $e_{(0)} = \dot{Y}$. Therefore, all components $\dot{Y}^{(i)}$ are zero. Hence, we have [173]

$$\frac{d^2\eta_{(\alpha)}}{\mathrm{d}s^2} = -\mathcal{R}_{(0\beta0\alpha)}\eta^{(\beta)}\,, \tag{6.69}$$

which is actually separable into temporal and spatial parts. We can orient the axes of the tetrad along the principle axes of $R_{(0i0j)}$ such that [173, 127]

$$\frac{d^2\eta_{(0)}}{\mathrm{d}s^2} = 0\,, \tag{6.70}$$

$$\frac{d^2\eta_{(i)}}{\mathrm{d}s^2} = -\mathcal{R}_{(0i0i)}\eta^{(i)} \quad \Rightarrow \quad \mathcal{R}_{(0i0i)} = -\frac{\dfrac{d^2\eta_{(i)}}{\mathrm{d}s^2}}{\eta^{(i)}}\,, \tag{6.71}$$

and all $R_{(0i0j)}$ are zero for $i \neq j$. The last equation tells us how to determine the tetrad components of the curvature from measurements of the gradiometer test-mass acceleration. A projection onto the spacetime coordinate reference frame yields the desired information about the Riemann tensor.

Application to a Schwarzschild spacetime

In the following, we investigate the geodesic deviation equation in a Schwarzschild spacetime model and obtain the relativistic generalization of (6.63).

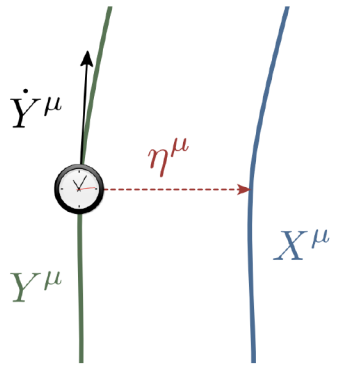

FIGURE 6.8: A sketch of the deviation of the two geodesics X^μ and Y^μ.

For the calculations, we choose an orthogonal parametrization such that $\eta_\mu \dot{Y}^\mu = 0$, see section III in Ref. [153] and Fig. 6.8 for a sketch. The overdot now denotes the derivative w.r.t. the proper time τ of an observer on the worldline Y^μ.

The metric of a spherically symmetric static spacetime can written in the form

$$g = -A(r)\mathrm{d}t^2 + B(r)\mathrm{d}r^2 + r^2(\mathrm{d}\vartheta^2 + \sin^2\vartheta \mathrm{d}\varphi^2)\,, \tag{6.72}$$

where $(t, r, \vartheta, \varphi)$ are spherical coordinates and we choose geometric units such that $c = 1$ and $G = 1$ to simplify calculations A circular reference geodesic Y^μ in the equatorial plane is described by $\big(Y^\mu(\tau)\big) = (T(\tau), R, \pi/2, \Phi(\tau))$. Since the metric above has two Killing vector fields which are generators of time translations and rotations, the energy E and angular momentum L are conserved,

$$E := A(r)\,\dot{t} = \text{const.}\,, \quad L := r^2\,\dot{\varphi} = \text{const.}\,, \tag{6.73}$$

see, e.g., Ref. [58]. Thus, the worldline Y^μ is described by

$$\Phi(\tau) = \dot{\Phi}\,\tau = \frac{L}{R^2}\,\tau =: \Omega_\Phi\,\tau\,, \tag{6.74a}$$

$$T(\tau) = \dot{T}\,\tau = \frac{E}{A(R)}\,\tau\,. \tag{6.74b}$$

In Ref. [60], Fuchs gave the first solution of the deviation equation (6.65) in the spacetime (6.72) in terms of first integrals. However, this solution is not applicable to circular reference geodesics since the condition $\dot{R} = 0$ causes divergencies. Shirokov [175] gave the first periodic solutions for the deviation from such circular geodesics in a Schwarzschild spacetime, see also [59]. The equation can also be solved in terms of relativistic epicycles, see [105, 110].

In a parallel propagated tetrad basis, the solution of the deviation equation can be found in [59]. This method is of direct relevance for relativistic geodesy. The results

allow to describe the deviation as observed in the comoving local frame, i.e. in particular by a gradiometer at rest w.r.t. a satellite in free fall.

The solution of the deviation in the tetrad basis is given by[3] [59]

$$\eta^{(1)} = g(\tau)\cos\Omega\tau - f(\tau)\sin\Omega\tau\,, \tag{6.75a}$$
$$\eta^{(3)} = g(\tau)\cos\Omega\tau + f(\tau)\sin\Omega\tau\,, \tag{6.75b}$$
$$\eta^{(2)} = C_{(5)}\cos\Omega_\Phi\tau + C_{(6)}\sin\Omega_\Phi\tau\,, \tag{6.75c}$$

where

$$g(\tau) = C_{(1)} + C_{(2)}\sin k\tau + C_{(3)}\cos k\tau\,, \tag{6.76a}$$
$$f(\tau) = \sqrt{\frac{\Delta}{k^2}}(C_{(2)}\cos k\tau - C_{(3)}\sin k\tau) + \frac{(k^2-\Delta)}{\sqrt{\Delta}}C_{(1)}\tau + C_{(4)}\,, \tag{6.76b}$$
$$k^2 = \frac{2A''A - A'^2}{2AB(2A - A'R)} + \frac{3A'}{2AB\,R}\,, \quad \Delta := \frac{2A'}{AB\,R}\,, \quad \Omega^2 = \frac{A'}{2A\,B\,R}\,. \tag{6.76c}$$

The constants of motion E, L of the reference orbit are given by

$$E^2 = \frac{2A^2}{2A - A'R}\,, \quad L^2 = \frac{R^3A'}{2A - A'R}\,. \tag{6.77}$$

In the equations above, the prime denotes derivatives w.r.t. r and the metric functions $A(r)$, $B(r)$ must be evaluated at the reference radius R. The integration constants $C_{(i)}$ characterize the type of perturbation and are related to the initial conditions in the phase space. The spacetime components of the deviation η^μ are then given by projecting the result on the coordinate basis, see [59, 143].

For the Schwarzschild spacetime, the metric functions are $A(r) = 1 - 2m/r$ and $B(r) = 1/A(r)$. Therefore, the constants of motion and parameters k, Δ simplify to

$$\Delta = \frac{4m}{R^3}\,, \qquad k^2 = \frac{m(R-6m)}{R^3(R-3m)}\,, \tag{6.78a}$$
$$E^2 = \frac{(R-2m)^2}{R(R-3m)}\,, \qquad L^2 = \frac{mR^2}{R-3m}\,. \tag{6.78b}$$

[3] Note that we solved the equation with different conventions for the integration constants $C_{(i)}$ which are related to the constants in Ref. [59] by constant factors.

such that the spacetime components of the deviation become [143]

$$\eta^t(\tau) = \frac{\sqrt{mR}}{R-2m}\bar{f}(\tau)\,, \tag{6.79a}$$

$$\eta^r(\tau) = \bar{g}(\tau)\,, \tag{6.79b}$$

$$\eta^\vartheta(\tau) = \frac{\bar{C}_{(5)}}{R}\cos\Omega_\Phi\tau + \frac{\bar{C}_{(6)}}{R}\sin\Omega_\Phi\tau\,, \tag{6.79c}$$

$$\eta^\varphi(\tau) = \frac{\bar{f}(\tau)}{R}\,, \tag{6.79d}$$

with

$$\bar{f}(\tau) = 2\sqrt{\frac{R}{R-6m}}\left(\bar{C}_{(2)}\cos k\tau - \bar{C}_{(3)}\sin k\tau\right) - \frac{3}{2}\Omega_\Phi\frac{R-2m}{R-3m}\bar{C}_{(1)}\,\tau + \bar{C}_{(4)}\,, \tag{6.80a}$$

$$\bar{g}(\tau) = \bar{C}_{(1)} + \bar{C}_{(2)}\sin ks + \bar{C}_{(3)}\cos ks\,. \tag{6.80b}$$

The coefficients $\bar{C}_{(i)}$ are slightly redefined versions of the $C_{(i)}$ which make the equations to appear simpler. The transformation is done using only constant factors. Two frequencies Ω_Φ and k appear in the solution. In SI-units, they are given by

$$k = \sqrt{\frac{GM}{R^3}}\sqrt{\frac{R-6m}{R-3m}} = \Omega_K\sqrt{\frac{R-6m}{R-3m}}\,, \tag{6.81a}$$

$$\Omega_\Phi = \sqrt{\frac{GM}{R^3}}\sqrt{\frac{R}{R-3m}} = \Omega_K\sqrt{\frac{R}{R-3m}}\,. \tag{6.81b}$$

In the Newtonian limit, both frequencies coincide and are equal to the Keplerian frequency Ω_K. Having two frequencies at hand, allows to describe precessing orbits; the radial and azimuthal motion are out of phase such that the perihelion of the orbit shifts. The Newtonian limit of the solution (6.79) is clearly given by (6.63), which is obtained for $m \to 0$, i.e. $c \to \infty$. This property was actually the reason why rescaled integration constants $\bar{C}_{(i)}$ have been introduced before.

In Ref. [143], it is shown how a variety of orbits can be constructed using the solution of the geodesic deviation equation and the integration constants $\bar{C}_{(i)}$ are related to the orbital elements of the perturbed orbit and the initial state vector. Moreover, the error in such an approximative description of orbits is investigated. Physical effects, such as perigee precession, in the solution as well as unphysical effects as an artifact of the linearization are studied in detail. In Fig. 6.9 we pick two examples of possible orbits which were constructed using the solution of the deviation equation. We show (i) elliptical orbits in the equatorial plane and (ii) pendulum orbits as off-equatorial perturbations. Both sets of orbits are calculated by perturbing a circular reference geodesic in the equatorial plane, respectively. We conclude this section by emphasizing again the importance of the relativistic deviation (or gradiometer) equation (6.65). It is of dual use: on the one hand, it relates acceleration measurements to

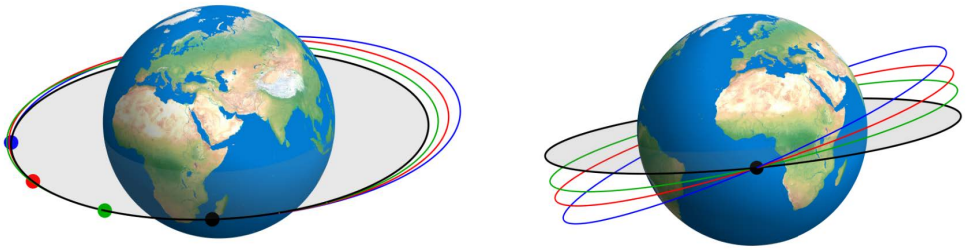

FIGURE 6.9: Perturbations of a circular equatorial reference geodesic. We show two different sets of orbits which are constructed as perturbations of a prescribed circular reference geodesic in the equatorial plane, respectively. On the left: elliptical orbits that show perigee precession. On the right: pendulum orbits as off-equatorial perturbations.

curvature components that are searched for. Thus, establishing an operational basis to determine the relativistic gravity field in full detail. On the other hand, in a given spacetime more complicated orbits can be constructed from simple reference geodesics. This will become useful when the geodesic equation admits no exact solutions or only highly symmetric ones. Then, besides numerical methods the analytically constructed deviation orbits may turn out as a useful tool.

Chapter 7

Conclusions and Outlook

In this work, we have shown how fundamental geodetic notions can be defined within a general relativistic framework. We have considered the relativistic gravity potential, the relativistic geoid, the normal gravity spacetime, the relativistic normal gravity potential, and a genuinely relativistic definition of the chronometric height. Moreover, we have outlined a simple procedure for the operational preservation of a chosen isochronometric surface.

For all these concepts the respective Newtonian notions in conventional geodesy are recovered in the weak-field limit. Furthermore, in the first-order (parametrized) post-Newtonian expansion we recover the results previously published in the literature and we have shown how the well-known results are embedded into the framework which is presented here. Therefore, we regard our definitions in a top-down approach, from the most fundamental to the approximative level, as the most general which are available to date. However, some - actually a lot - open questions and issues remain to be solved and are discussed briefly below in a non-exhaustive list.

A clear conceptual understanding of how the relativistic gravity potential value on the geoid is chosen and what its relation to the geopotential value W_0 is needs to be worked out. Also, the relation to the proper time on the geoid and the defining constant L_g in the IAU resolution must be clarified to overcome inconsistencies in the geoid definition.

A next step is to include gravitomagnetic contributions at the general relativistic level into all definitions. Here, we have mainly worked with static axisymmetric spacetimes and considered the Kerr metric as the only stationary example. However, as we have pointed out, the Kerr spacetime can be used to estimate gravitomagnetic effects in the Earth's vicinity but it is by no means a good description of the Earth's relativistic gravity field; the quadrupole moments are in utter disagreement. Thus, spacetimes that include more free parameters such as general Quevedo-Mashhoon spacetimes, see [159, 155, 157, 57], should be considered in our framework. Then, it is clear what the next step in defining an even better normal gravity spacetime is: the stationary

generalizations of Weyl spacetimes allows to choose a spin dipole independently from l mass moments. Hence, the issue related to the Kerr metric can be overcome and gravitomagnetic as well as quadrupolar effects can be described in the right way at the same time.

Another research perspective is to look for non-axisymmetric spacetimes as exact solution of Einstein's vacuum field equation. At least a static version of such spacetimes should exist. If the radiation of gravitational waves due to the rotation is ignored, also stationary versions should be possible. For geodesy on the Earth, this is a very good approximation. Related to such spacetimes is the question of how to define suitable multipole moments of the Earth's relativistic spacetime beyond the notions of, e.g. Geroch and Hansen, without introducing post-Newtonian approximations.

Regarding redshift and clock measurements, it must be critically analyzed if GRACE-like constellations equipped with highly accurate clocks allow to determine gravity field from redshift measurements at competitive accuracy. Therefore, the clock comparison between satellites and from satellites to ground stations is possible. This requires a relativistic model for exact timing and signal propagation in the curved spacetime, intimately related to the emitter-observer problem in General Relativity. However, a post-Newtonian framework for light propagation already exists and might be used as a very good approximation, see [204]. The error budget for clock measurements in space must be analyzed in particular w.r.t. the satellites' velocities. Doppler terms dominate the redshift signal and, thus, very accurate state vector information is needed.

For space measurements, swarms of satellites should be analyzed in a general relativistic framework to derive optimal configurations and use data fusion including clock and acceleration measurements as well as velocities and laser-ranged positions to determine the Earth's gravity field and the relativistic geoid from satellite measurements. Maybe a realization of the gravitational and clock compass is feasible with near-future technology, establishing the ultimate curvature detector.

For chronometric measurements on the Earth, the present time is very exiting. First results for clock comparison over long distances and height measurements via redshift detections have just started. Within the framework of General Relativity, optimal clock network topologies should be studied, taking into account also classical effects such as the Sagnac effect. With global clock networks, a realization of the relativistic geoid becomes available. Then, height determination might employ redshift measurements and miniaturized high-precision clocks as the standard tool. Maybe in the (far) future, we will not ask questions such as "What is the height of that building?" anymore but we will rather ask "What is the redshift up there?".

Developing the next generation of general relativistic positioning systems for navigation will also become inevitable at a certain accuracy threshold.

Last but not least, high-precision geodesy, astronomy, and related sciences offer endless possibilities to test the predictions of Special and General Relativity.

As one can see by this list, there are a lot of open questions and research directions - the field of relativistic geodesy has just started to be explored and there is a lot more to come!

Appendix A

Important Relations for Coordinate Systems and Ellipsoids of Rotation

Spherical coordinates

Starting from a Cartesian coordinate system (X, Y, Z) we introduce spherical coordinates (R, Θ, Φ) by the transformation

$$X = R \sin\Theta \cos\Phi \,, \tag{A.1a}$$

$$Y = R \sin\Theta \sin\Phi \,, \tag{A.1b}$$

$$Z = R \cos\Theta \,, \tag{A.1c}$$

where R is called the radius, Θ is the polar angle measured with respect to the Z-axis, and Φ is the azimuthal angle (geodetic longitude) measured with respect to the X-axis, see Fig. A.1. The angle Θ is measured positive southwards, whereas Φ is positive towards the East. We can also introduce the (geocentric) latitude λ by

$$\lambda = \frac{\pi}{2} - \Theta \,. \tag{A.2}$$

Note, however, that we employ conventions which are commonly used in physics. Hence, there is a difference between our notation above and the notation usually used in geodesy, where, e.g., λ is used for the geodetic longitude.

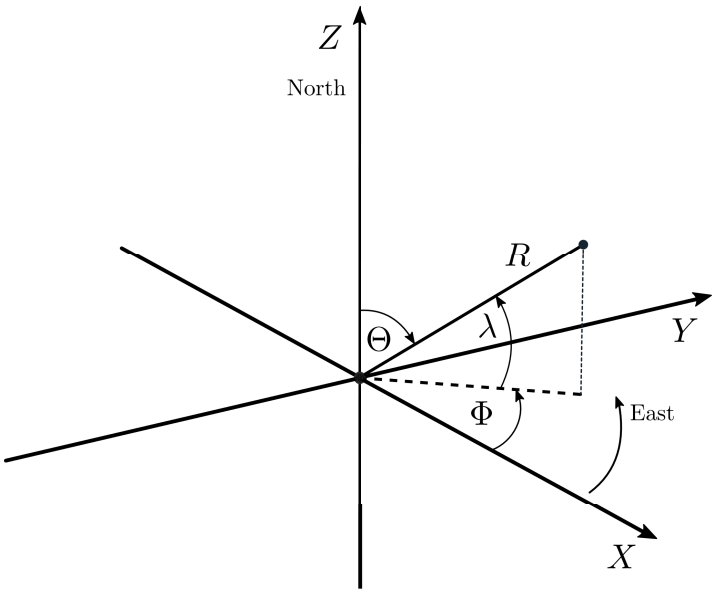

FIGURE A.1: Spherical coordinates and their relations to Cartesian coordinate axes.

Parameters and relations for ellipsoids

An ellipsoid of rotation is a two-surface in $\mathbb{R}^3$ and it is obtained by rotating an ellipse around one of the symmetry axes. For an oblate ellipsoid, which is used for a geodetic Earth model, the ellipse is rotated around the minor axis. The semi-major axis shall be denoted by a, whereas the semi-minor axis is b in the following.

The linear eccentricity E is the distance between the origin $\mathcal{O}$ and one of the two Foci F_i, $i = 1, 2$. It is given by

$$E = \sqrt{a^2 - b^2}\,. \tag{A.3}$$

Thereupon, the first and second eccentricity e and e' are defined by

$$e = \frac{E}{a}\,, \tag{A.4a}$$

$$e' = \frac{E}{b}\,, \tag{A.4b}$$

respectively. The flattening f is

$$f = 1 - \frac{b}{a}\,. \tag{A.5}$$

At a given point P on the ellipsoid, we call $\vec{n}$ the normal direction with respect to the surface.

Ellipsoidal and geodetic coordinates

We introduce ellipsoidal surface coordinates as shown in Fig. A.2. To a point P_0 on an ellipsoid we assign:

- The geodetic longitude Φ, measured in the equatorial plane between the X-axis and the meridional plane at P_0
- The geodetic latitude Λ

The meridional plane at P_0 is defined by the Z-axis and the surface normal at P_0. In this meridional plane, we also define the geocentric latitude λ, as done for spherical coordinates, and the reduced latitude β.

For a point P in $\mathbb{R}^3$, we supplement the ellipsoidal surface coordinates by the height h above a reference ellipsoid in the direction of the surface normal, see Fig. A.3. The sets of coordinates $\{h, \Phi, \Lambda\}$ and $\{h, \Phi, \lambda\}$ are called ellipsoidal coordinates. The set $\{h, \Phi, \Lambda\}$ is also known as geodetic coordinates.

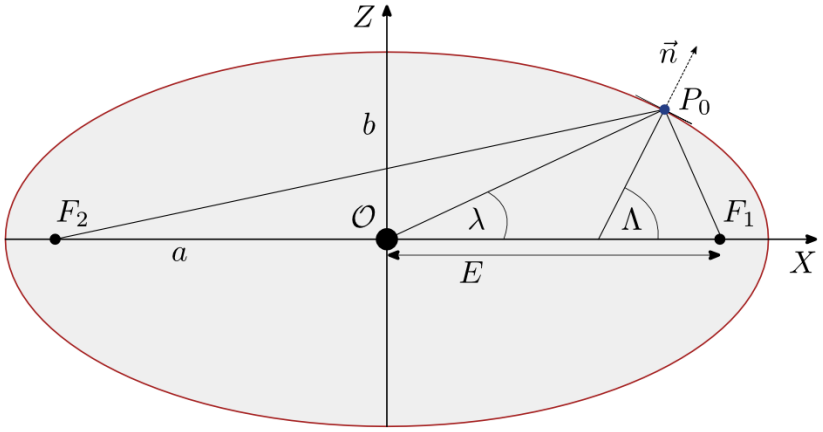

FIGURE A.2: Geometry and properties of ellipses I.

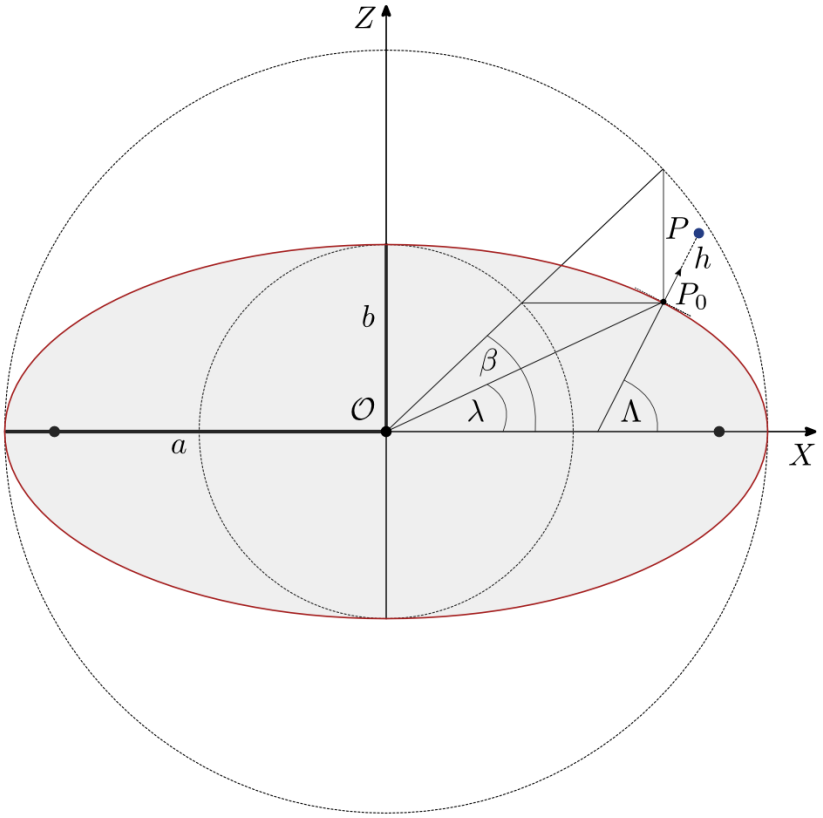

FIGURE A.3: Geometry and properties of ellipses II.

Ellipsoidal-harmonic coordinates

Ellipsoidal-harmonic coordinates allow to simplify the calculation of the normal potential of the Earth.

Let a and b be the semi-major and semi-minor axis of the reference ellipsoid, respectively, and E its linear eccentricity. Now, to assign coordinates to a point P in $\mathbb{R}^3$, we introduce a new "height" coordinate u as the semi-minor axis of the ellipsoid with the same linear eccentricity E of which P is a point on the surface. This ellipsoid is oriented such that its axes are aligned with the axes of the reference ellipsoid. The semi-major axis of this ellipsoid through P is then given by $\sqrt{u^2 + E^2}$. Moreover, we use the geodetic longitude Φ and the reduced latitude β as surface coordinates and call the set $\{h, \Phi, \beta\}$ ellipsoidal-harmonic coordinates, see Fig. A.4.

The relation to Cartesian coordinates is of particular importance. We have

$$X = u\sqrt{1 + E^2/u^2}\cos\beta\cos\Phi \tag{A.6a}$$

$$Y = u\sqrt{1 + E^2/u^2}\cos\beta\sin\Phi \tag{A.6b}$$

$$Z = u\sin\beta\,. \tag{A.6c}$$

Thereupon, we find the transformation to spherical coordinates

$$R = \sqrt{u^2/\cos^2\beta + E^2}\cos\beta\,, \tag{A.7a}$$

$$\cot\Theta = \frac{u}{\sqrt{u^2 + E^2}}\tan\beta\,, \tag{A.7b}$$

and the longitude Φ is the same in both coordinate systems.

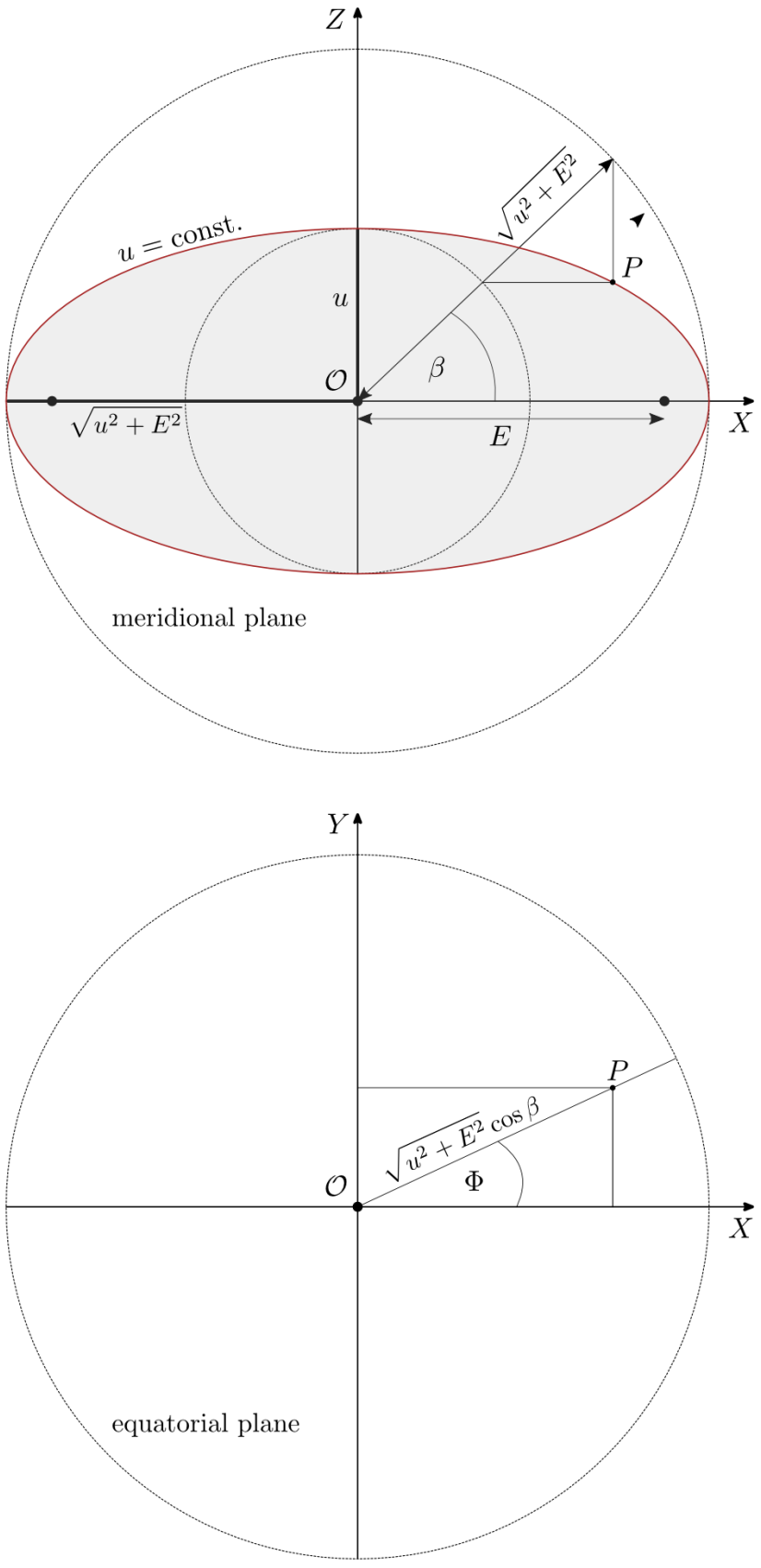

FIGURE A.4: Definition of ellipsoidal-harmonic coordinates; front view of the meridional plane (top) and top view of the equatorial plane (bottom).

Appendix B

Derivation of the Redshift Formula in General Relativity

Derivation of the redshift formula

We reconsider the situation outlined in section 4.2.1. Emitter and receiver of light signals (null geodesics) move on worldlines γ and $\tilde{\gamma}$ with four-velocities u and $\tilde{u}$, respectively. The two vector fields on spacetime that we use in the following are $k = \partial_s$ and $l = \partial_\tau$, where s is an affine parameter on the null geodesics between emitter and observer and τ is the proper time of the emitter, see Fig. 4.2. All points on the null geodesics can be labeled by the pairs (τ, s).

The affine parameter s is rescaled such that $s = 0$ on γ and $s = 1$ on $\tilde{\gamma}$. Then,

$$l(s=0) = u\,, \quad \text{and} \quad l(s=1) = \partial_\tau\big|_{s=1} = \frac{\mathrm{d}\tilde{\tau}}{\mathrm{d}\tau}\,\partial_{\tilde{\tau}} = \frac{\nu}{\tilde{\nu}}\,\partial_{\tilde{\tau}} = (z+1)\,\partial_{\tilde{\tau}}\,, \tag{B.1}$$

where $\tilde{\tau}$ is the proper time of the receiver. We now follow the derivation by Brill [15] to proof that $\langle l, k\rangle := g_{\mu\nu} l^\mu k^\nu$ is constant along null geodesics and that the redshift formula follows immediately. Since the integral curves of k are null geodesics, we have

$$\langle k, k\rangle = 0 \quad \text{(lightlike)}\,, \tag{B.2}$$

$$D_k k = 0 \quad \text{(geodesic)}\,. \tag{B.3}$$

Furthermore, we use $A\langle B, C\rangle = \langle D_A\, B, C\rangle + \langle B, D_A\, C\rangle$ and $[A, B] = D_A\, B - D_B\, A$, which hold for the Levi-Civita connection and vector fields A, B, C, to obtain

$$\partial_s\langle l, k\rangle = k\,\langle l, k\rangle = \langle D_k\, l, k\rangle + \langle l, \underbrace{D_k\, k}_{=0}\rangle = \langle D_k\, l, k\rangle\,. \tag{B.4}$$

Since $[k,l]=0$, we have $\langle D_k\, l, k\rangle = \langle D_l\, k, k\rangle$, and therefore

$$\partial_s\langle l,k\rangle = \langle D_l\, k, k\rangle = \frac{1}{2} l\, \langle k,k\rangle = 0\,, \tag{B.5}$$

which proves that $\langle l,k\rangle$ is constant along the null geodesics. Hence the redshift equation follows,

$$\begin{aligned} &\langle k,l\rangle_{s=0} = \langle k,u\rangle = (z+1)\langle k,\tilde{u}\rangle = \langle k,l\rangle_{s=1} \\ &\Rightarrow z+1 = \frac{\nu}{\tilde{\nu}} = \frac{\langle k,u\rangle}{\langle k,\tilde{u}\rangle}\,. \end{aligned} \tag{B.6}$$

Appendix C

Isometric Embedding and Geometric Properties of Isochronometric Surfaces

Isometric embedding

To investigate and visualize the intrinsic geometry of the relativistic geoid, which is described by a particular isochronometric surface, i.e. a level surface of the relativistic gravity potential $U^*|_{\text{geoid}} = U_0^* = \text{const.}$, we isometrically embed this surface into Euclidean space $\mathbb{R}^3$. If such an embedding is possible, the embedded surface shows the intrinsic geometry of the geoid.

In all our axisymmetric models, the relativistic geoid is a level surface

$$U^*(x,y)|_{\text{geoid}} = U_0^* = \text{const.}\,, \tag{C.1}$$

where x and y are the two spatial coordinates, related to a radius measure and the polar angle, respectively.

For any such two-dimensional surface defined by Eq. (C.1), the following is true everywhere on the surface

$$0 = \mathrm{d}U^* = \partial_x U^*(x,y)\,\mathrm{d}x + \partial_y U^*(x,y)\,\mathrm{d}y\,. \tag{C.2}$$

Hence, we have on the geoid surface

$$\mathrm{d}x = -\left(\frac{\partial_y U^*(x,y)}{\partial_x U^*(x,y)}\right)\mathrm{d}y\,, \tag{C.3}$$

which yields a relation $x = x(y)$ that describes this surface.

On the surface $U^*(x,y) = U_0^*$ there is a two-dimensional Riemannian metric defined according to

$$g^{(2)} = \left(g_{xx}(x,y)\,x'(y)^2 + g_{yy}(x,y)\right)\mathrm{d}y^2 + g_{\varphi\varphi}(x,y)\,\mathrm{d}\varphi^2\,, \tag{C.4}$$

where φ is the azimuthal angle related to the axisymmetry of the spacetime model.

We want to isometrically embed the surface $U^*(x,y) = U_0^*$ into Euclidean 3-space $\mathbb{R}^3$ with cylindrical coordinates (Λ, φ, Z), where Z is the height, Λ is the radius in the $Z = 0$ plane, and φ is the azimuthal angle. The Riemannian metric in $\mathbb{R}^3$ can then be written as

$$g_E^{(3)} = dZ^2 + d\Lambda^2 + \Lambda^2 d\varphi^2\,. \tag{C.5}$$

The embedding functions $Z(y)$ and $\Lambda(y)$ are to be determined from the equation

$$\begin{aligned}&\left[g_{xx}(x(y),y)\,x'(y)^2 + g_{yy}(x(y),y)\right]\mathrm{d}y^2 + g_{\varphi\varphi}(x(y),y)\,\mathrm{d}\varphi^2 &\text{(C.6)}\\ &= \left(Z'(y)^2 + \Lambda'(y)^2\right)\,dy^2 + \Lambda^2(y)d\varphi^2\,. &\text{(C.7)}\end{aligned}$$

If Eq. (C.3) can be explicitly solved for $x = x(y)$, we may insert this expression into (C.6). Comparing coefficients results in

$$\Lambda(y) = \sqrt{g_{\varphi\varphi}(x,y)}\Big|_{x=x(y)}\,, \tag{C.8a}$$

$$Z(y) = \pm\int_0^y dy\,\left(g_{xx}(x,y)\left(\frac{\partial_y U^*(x,y)}{\partial_x U^*(x,y)}\right)^2 + g_{yy}(x,y) - \frac{g'_{\varphi\varphi}(x,y)^2}{4g_{\varphi\varphi}(x,y)}\right)^{1/2}_{x=x(y)}\,. \tag{C.8b}$$

In Eq. (C.8b), the expression $g'_{\varphi\varphi}$, by abuse of notation, is understood to mean that first $x(y)$ is to be inserted and then the derivative with respect to y is to be taken. The integral in Eq. (C.8b) has to be calculated either analytically, if this is possible, or numerically.

Equations (C.8a) and (C.8b) give us the cylindrical radius coordinate Λ and the cylindrical height coordinate Z in Euclidean 3-space as functions of the parameter y of which the allowed range is given by $y \in [-1,1]$, corresponding to a polar angle $\vartheta \in [0,\pi]$. In this way, we get a meridional section of the embedded surface in parametrized form; by letting this figure rotate about the axis, we get the entire embedded surface. The embedding is possible near all y values for which

$$g_{xx}(x,y)\left(\frac{\partial_y U^*(x,y)}{\partial_x U^*(x,y)}\right)^2 + g_{yy}(x,y) > \frac{g'_{\varphi\varphi}(x,y)^2}{4g_{\varphi\varphi}(x,y)}\,. \tag{C.9}$$

If this condition is violated, the surface cannot be isometrically embedded into Euclidean 3-space, which means that its intrinsic geometry is hard to visualize.

This direct construction of the embedded surface in parametrized form is possible if Eq. (C.3) can be explicitly solved for $x = x(y)$. If this cannot be done, we have at least an expression for the derivative of this function, as Eq. (C.2) implies that

$$x'(y) = \frac{dx}{dy} = -\frac{\partial_y U^*(x,y)}{\partial_x U^*(x,y)}\,. \tag{C.10}$$

Using Eq. (C.8b), we obtain a coupled system of differential equations,

$$x'(y) = -\left.\frac{\partial_y U^*(x,y)}{\partial_x U^*(x,y)}\right|_{x=x(y)}\,, \tag{C.11a}$$

$$\Lambda(y) = \sqrt{g_{\varphi\varphi}(x(y),y)}\,, \tag{C.11b}$$

$$Z'(y) = \pm\left(g_{xx}(x(y),y)\left(x'(y)\right)^2 + g_{yy}(x(y),y) - \Lambda'(y)^2\right)^{1/2}\,, \tag{C.11c}$$

for the functions $x(y)$, $\Lambda(y)$, and $Z(y)$, which is to be solved numerically with initial conditions $x(0) = x_0$, $Z(0) = 0$. Of course, this is possible only if an embedding exists. If $x(y)$ has been obtained, the functions $\Lambda(y)$ and $Z(y)$ can be determined as well.

Gaussian curvature

We can introduce spherical coordinates (R, Θ, Φ) in the embedding space. Then, we can derive an equation for the Gaussian curvature $\mathcal{G}$ of any axisymmetric surface that is parametrically described by $R(\Theta)$:

$$\mathcal{G}(\Theta) = \frac{\big(R(\Theta) - \cot\Theta R'(\Theta)\big)\big(R^2(\Theta) + 2R'^2(\Theta) - R(\Theta)R''(\Theta)\big)}{R(\Theta)\big(R^2(\Theta) + R'^2(\Theta)\big)^2} \tag{C.12}$$

Using this result, the Gaussian curvature of the embedded geoids in the quadrupolar model can be calculated and analyzed.

Appendix D

Calculation of Relativistic Multipole Moments

Geroch-Hansen mass multipoles

For relativistic multipole moments, we use the definition given by Geroch and Hansen [63, 85] in terms of expansions of tensor fields around a point after a conformal mapping. In Refs. [157, 77] it is shown how these moments are related to other multipole definition by, e.g., Thorne [187] and Beig and Simon [176].

The Geroch-Hansen moments are defined for any stationary axisymmetric spacetime. Since their calculation can be quite difficult using the original definition, easier schemes have been developed.

Static axisymmetric spacetimes

For the multipole moments of static spacetimes, a relation between the Ernst potential and the multipole moments can be used. This relation was found by the authors of Ref. [53]. The method allows to calculate the multipole moments from values of the Ernst potential on the symmetry axis. It works as follows: for static axisymmetric spacetimes, the Ernst potential is

$$\epsilon(x, y) = \frac{1 - e^{2\psi}}{1 + e^{2\psi}} \tag{D.1}$$

where ψ is Weyl's metric function. Now, we introduce the inverse z-coordinate on the symmetry axis ζ by

$$\zeta = \frac{1}{z} = \frac{1}{mx}\,, \tag{D.2}$$

see equation (3.31) for $y = 1$. Thereupon, the inverse Ernst potential on the symmetry axis is constructed according to

$$\bar{\epsilon}(\zeta) = \frac{1}{\zeta}\,\epsilon(\zeta, 1). \tag{D.3}$$

The mass multipole moments $\mathcal{M}_l$ can now be read off from

$$\mathcal{M}_l = m_l + d_l\,, \tag{D.4a}$$

$$m_l = \frac{1}{l!}\frac{\mathrm{d}^l\bar{\epsilon}(\zeta)}{\mathrm{d}\zeta^l}\Big|_{\zeta=0}\,. \tag{D.4b}$$

At order l, the m_l are given by the l-th derivative of the inverse Ernst potential. The d_l are given by lower order derivatives and can be expressed in terms of the m_l. However, it can be shown that all d_l for $l < 4$ vanish identically. In Ref. [56], the authors calculated the d_l up to $l = 10$ in terms of the m_l.

Stationary axisymmetric spacetimes

To calculate the mass and spin moments of stationary axisymmetric spacetimes, various attempts lead to the same results, see, e.g., Refs. [53, 77, 94, 157]. One possible strategy is to construct a Taylor expansion of the inverse Ernst potential evaluated on the symmetry axis and for the inverse z-coordinate $\zeta = 1/z = 1/(\sigma x)$, see (3.56). Then, the FHP equations [53] are used to obtain the multipole moments. In Ref. [57], the authors calculate quite a few mass and spin moments for some exemplary spacetimes.

Bibliography

[1] Zuheir Altamimi, Xavier Collilieux, and Laurent Métivier. "ITRF2008: an improved solution of the international terrestrial reference frame". In: *Journal of Geodesy* 85.8 (2011), pp. 457–473. ISSN: 1432-1394. DOI: 10.1007/s00190-011-0444-4. URL: https://doi.org/10.1007/s00190-011-0444-4.

[2] B.A. Archinal et al. *The Unified Lunar Control Network 2005: U.S. Geological Survey Open-File Report 2006-1367*. 2006. URL: http://pubs.usgs.gov/of/2006/1367/.

[3] E. F. Arias et al. "The extragalactic reference system of the International Earth Rotation Service, ICRS." In: *Astron. Astrophys.* 303 (1995), pp. 604–608.

[4] Neil Ashby. "Relativity in the Global Positioning System". In: *Living Reviews in Relativity* 6.1 (2003), p. 1. ISSN: 1433-8351. DOI: 10.12942/lrr-2003-1. URL: https://doi.org/10.12942/lrr-2003-1.

[5] J. Audretsch and C. Lämmerzahl. "Neutron interference: general theory of the influence of gravity, inertia and space-time torsion". In: *Journal of Physics A: Mathematical and General* 16.11 (1983), p. 2457. DOI: 10.1088/0305-4470/16/11/017.

[6] H. Bateman and A. Erdélyi. *Higher Transcendental Functions*. Vol. 1. Higher Transcendental Functions. McGraw-Hill, New York, 1955.

[7] B. Bertotti, L. Iess, and P. Tortora. "A test of general relativity using radio links with the Cassini spacecraft". In: *Nature* 425 (), pp. 374–376. DOI: 0.1038/nature01997. URL: https://doi.org/10.1038/nature01997.

[8] Bruce G. Bills. "Planetary geodesy". In: *Geophysics*. Boston, MA: Springer US, 1989, pp. 931–938. ISBN: 978-0-387-30752-7. DOI: 10.1007/0-387-30752-4_113. URL: https://doi.org/10.1007/0-387-30752-4_113.

[9] Arne Bjerhammar. "On a relativistic geodesy". In: *Bull. Géodésique* 59.3 (1985), pp. 207–220.

[10] Arne Bjerhammar. *Relativistic Geodesy*. Tech. rep. NOS 118 NGS 36. 1986.

[11] Bloom, B. J. and Nicholson, T. L. and Williams, J. R. and Campbell, S. L. and Bishof, M. and Zhang, X. and Zhang, W. and Bromley, S. L. and Ye, J. "An optical lattice clock with accuracy and stability at the 10^{-18} level". In: *Nature* 506.7486 (2014), pp. 71–75. DOI: 10.1038/nature12941.

[12] Max Born. "Die Theorie des starren Elektrons in der Kinematik des Relativitätsprinzips". In: *Annalen der Physik* 335.11 (), pp. 1–56. DOI: 10.1002/andp.19093351102. URL: {https://onlinelibrary.wiley.com/doi/abs/10.1002/andp.19093351102}.

[13] C. Boucher. "Terrestrial Coordinate Systems and Frames". In: *Encyclopedia of Astronomy and Astrophysics*. Ed. by P. Murdin. 2000, p. 1906. DOI: 10.1888/0333750888/1906.

[14] Bruce Bowman et al. "A New Empirical Thermospheric Density Model JB2008 Using New Solar and Geomagnetic Indices". In: *AIAA/AAS Astrodynamics Specialist Conference and Exhibit* 2008-6438 (2008). DOI: doi:10.2514/6.2008-6438.

[15] Brill, Dieter R. "A simple derivation of the general redshift formula". In: *Methods of Local and Global Differential Geometry in General Relativity*. Ed. by Farnsworth, D. and Fink, J. and Porter, J. and Thompson, A. Berlin, Heidelberg: Springer Berlin Heidelberg, 1972, pp. 45–47. ISBN: 978-3-540-37434-3.

[16] V. A. Brumberg and Sergei M. Kopejkin. "Relativistic reference systems and motion of test bodies in the vicinity of the earth". In: *Il Nuovo Cimento B (1971-1996)* 103.1 (1989), pp. 63–98. ISSN: 1826-9877. DOI: 10.1007/BF02888894.

[17] Milan Burša. "Report of the International Association of Geodesy Special Commission SC3: fundamental constants. XXI IAG General Assembly Boulder CO, USA". In: (1995).

[18] Milan Burša, Zdislav Šíma, and Jan Kostelecký. "Determination of the geopotential scale factor from satellite altimetry". In: *Studia Geophysica et Geodaetica* 36.2 (1992), pp. 101–108. ISSN: 1573-1626. DOI: 10.1007/BF01614122. URL: https://doi.org/10.1007/BF01614122.

[19] Milan Burša et al. "Mean Earth'S Equipotential Surface From Topex/Poseidon Altimetry". In: *Studia Geophysica et Geodaetica* 42.4 (1998), pp. 459–466. ISSN: 1573-1626. DOI: 10.1023/A:1023356803773. URL: https://doi.org/10.1023/A:1023356803773.

[20] Milan Burša et al. "The geopotential value W0 for specifying the relativistic atomic time scale and a global vertical reference system". In: *Journal of Geodesy* 81.2 (2007), pp. 103–110. ISSN: 1432-1394. DOI: 10.1007/s00190-006-0091-3. URL: https://doi.org/10.1007/s00190-006-0091-3.

[21] M. Burša. "Primary and Derived Parameters of Common Relevance of Astronomy, Geodesy, and Geodynamics". In: *Earth Moon and Planets* 69 (1995), pp. 51–63. DOI: 10.1007/BF00627769.

[22] L. Cacciapuoti and Ch. Salomon. "Space clocks and fundamental tests: The ACES experiment". In: *The European Physical Journal Special Topics* 172.1 (2009), pp. 57–68. ISSN: 1951-6401. DOI: 10.1140/epjst/e2009-01041-7. URL: https://doi.org/10.1140/epjst/e2009-01041-7.

[23] S. Chandrasekhar. "The Post-Newtonian Equations of Hydrodynamics in General Relativity." In: *Astrophysical Journal* 142 (1965), p. 1488. DOI: 10.1086/148432.

[24] C. W. Chou et al. "Optical Clocks and Relativity". In: *Science* 329.5999 (2010), pp. 1630–1633. ISSN: 0036-8075. DOI: 10.1126/science.1192720. URL: http://science.sciencemag.org/content/329/5999/1630.

[25] B. H. Chovitz. "Parameters of common relevance of astronomy, geodesy, and geodynamics". In: *Bulletin géodésique* 62.3 (1988), pp. 359–367. ISSN: 1432-1394. DOI: 10.1007/BF02520723. URL: https://doi.org/10.1007/BF02520723.

[26] I. Ciufolini et al. "A test of general relativity using the LARES and LAGEOS satellites and a GRACE Earth gravity model. Measurement of Earth's dragging of inertial frames". In: *European Physical Journal C* 76 (2016), p. 120. DOI: 10.1140/epjc/s10052-016-3961-8.

[27] Ignazio Ciufolini. "The lageos lense-thirring precession and the LAGEOS non-gravitational nodal perturbations — I". In: *Celestial mechanics* 40.1 (1987), pp. 19–33. ISSN: 1572-9478. DOI: 10.1007/BF01232322.

[28] Thibault Damour, Michael Soffel, and Chongming Xu. "General-relativistic celestial mechanics. I. Method and definition of reference systems". In: *Phys. Rev. D* 43 (10 1991), pp. 3273–3307. DOI: 10.1103/PhysRevD.43.3273. URL: https://link.aps.org/doi/10.1103/PhysRevD.43.3273.

[29] Thibault Damour, Michael Soffel, and Chongming Xu. "General-relativistic celestial mechanics II. Translational equations of motion". In: *Phys. Rev. D* 45 (4 1992), pp. 1017–1044. DOI: 10.1103/PhysRevD.45.1017. URL: https://link.aps.org/doi/10.1103/PhysRevD.45.1017.

[30] Thibault Damour, Michael Soffel, and Chongming Xu. "General-relativistic celestial mechanics. III. Rotational equations of motion". In: *Phys. Rev. D* 47 (8 1993), pp. 3124–3135. DOI: 10.1103/PhysRevD.47.3124. URL: https://link.aps.org/doi/10.1103/PhysRevD.47.3124.

[31] Thibault Damour, Michael Soffel, and Chongming Xu. "General-relativistic celestial mechanics. IV. Theory of satellite motion". In: *Phys. Rev. D* 49 (2 1994), pp. 618–635. DOI: 10.1103/PhysRevD.49.618. URL: https://link.aps.org/doi/10.1103/PhysRevD.49.618.

[32] C. Darwin. "The gravity field of a particle". In: *Proc. R. Soc. London A* 249 (1959), p. 180.

[33] C. Darwin. "The gravity field of a particle II". In: *Proc. R. Soc. London A* 263 (1961), p. 39.

[34] P. Delva, H. Denker, and G. Lion. "Chronometric geodesy: methods and applications". In: *Relativistic Geodesy: Foundations and Applications*. Springer, to appear 2018.

[35] P. Delva and J. Geršl. "Theoretical Tools for Relativistic Gravimetry, Gradiometry and Chronometric Geodesy and Application to a Parameterized Post-Newtonian Metric". In: *Universe* 3.1 (2017), p. 24. ISSN: 2218-1997. DOI: 10.3390/universe3010024.

[36] P. Delva et al. "Test of Special Relativity Using a Fiber Network of Optical Clocks". In: *Phys. Rev. Lett.* 118 (22 2017), p. 221102. DOI: 10.1103/PhysRevLett.118.221102. URL: https://link.aps.org/doi/10.1103/PhysRevLett.118.221102.

[37] P. Delva et al. "Test of the gravitational redshift with stable clocks in eccentric orbits: application to Galileo satellites 5 and 6". In: *Classical and Quantum Gravity* 32.23 (2015), p. 232003. URL: http://stacks.iop.org/0264-9381/32/i=23/a=232003.

[38] Heiner Denker et al. "Geodetic methods to determine the relativistic redshift at the level of 10^{-18} in the context of international timescales: a review and practical results". In: *Journal of Geodesy* 92.5 (2018), pp. 487–516. ISSN: 1432-1394. DOI: 10.1007/s00190-017-1075-1. URL: https://doi.org/10.1007/s00190-017-1075-1.

[39] W. G. Dixon. "The New Mechanics of Myron Mathisson and Its Subsequent Development". In: *"Equations of Motion in Relativistic Gravity", D. Puetzfeld et. al. (eds.), Fundamental theories of Physics, Springer* 179 (2015), p. 1.

[40] S. Droste et al. "Optical-Frequency Transfer over a Single-Span 1840 km Fiber Link". In: *Phys. Rev. Lett.* 111 (11 2013), p. 110801. DOI: 10.1103/PhysRevLett.111.110801. URL: https://link.aps.org/doi/10.1103/PhysRevLett.111.110801.

[41] Jürgen Ehlers. "Beiträge zur relativistischen Mechanik kontinuierlicher Medien". In: *Abhandlungen der Mathmatisch-Naturwissenschaftlichen Klasse* 11 (1961). URL: http://hdl.handle.net/11858/00-001M-0000-0013-5F19-F.

[42] Jürgen Ehlers. "Contributions to the Relativistic-Mechanics of Continuous Media". In: *Gen. Relativ. Gravit.* 25.12 (1993), pp. 1225–1266. DOI: 10.1007/BF00759031.

[43] Jürgen Ehlers. "Examples of Newtonian limits of relativistic spacetimes". In: *Class. Quantum Grav.* 14.1A (1997), A119–A126. DOI: 10.1088/0264-9381/14/1A/010. URL: http://stacks.iop.org/0264-9381/14/i=1A/a=010.

[44] Jürgen Ehlers. "Über den Newtonschen Grenzwert der Einsteinschen Gravitationstheorie". In: *Grundlagenprobleme der modernen Physik*. Ed. by J Nitsch, J Pfarr, and E W Stachov. Mannheim: BI-Verlag Mannheim, 1981, pp. 65–84.

[45] A. Einstein. "Die Grundlage der allgemeinen Relativitätstheorie". In: *Annalen der Physik* 354 (1916), p. 769.

[46] Martin Ekman. "Impacts of geodynamic phenomena on systems for height and gravity". In: *Bulletin Géodésique* 63.3 (1989), pp. 281–296. ISSN: 1432-1394. DOI: 10.1007/BF02520477. URL: https://doi.org/10.1007/BF02520477.

[47] Martin Ekmann. "What Is the Geoid?" In: *Coordinate Systems, GPS, and the Geoid*. Ed. by M. Vermeer. Vol. 95. Reports of the Finnish Geodetic Institute 4. 1995, pp. 49–51.

[48] G. Erez and N. Rosen. "The gravitational field of a particle possessing a multipole moment". In: *Bull. Res. Coun. Isr.* 8F.47 (1959), pp. 47–50.

[49] C. W. F. Everitt et al. "Gravity Probe B: Final Results of a Space Experiment to Test General Relativity". In: *Phys. Rev. Lett.* 106 (22 2011), p. 221101. DOI: 10.1103/PhysRevLett.106.221101. URL: https://link.aps.org/doi/10.1103/PhysRevLett.106.221101.

[50] C. W. F. Everitt et al. "The Gravity Probe B test of general relativity". In: *Classical and Quantum Gravity* 32.22 (), p. 224001. DOI: 10.1088/0264-9381/32/22/224001. URL: http://stacks.iop.org/0264-9381/32/i=22/a=224001.

[51] Alan L. Fey, David Gordon, and Christopher S. (eds.) Jacobs. *The Second Realization of the International Celestial Reference Frame by Very Long Baseline Interferometry*. Tech. rep. IERS Technical Note No. 35. International Earth Rotation and Reference Systems Service (IERS), 2009. URL: https://www.iers.org/IERS/EN/Publications/TechnicalNotes/tn35.html.

[52] Frank Flechtner et al. "What Can be Expected from the GRACE-FO Laser Ranging Interferometer for Earth Science Applications?" In: *Surv. Geophys.* 37.2 (2016), pp. 453–470. DOI: 10.1007/s10712-015-9338-y. URL: http://dx.doi.org/10.1007/s10712-015-9338-y.

[53] C. Fodor G.and Hoenselaers and Z. Perjés. "Multipole moments of axisymmetric systems in relativity". In: *Journal of Mathematical Physics* 30.10 (1989), pp. 2252–2257. DOI: 10.1063/1.528551. eprint: https://doi.org/10.1063/1.528551. URL: https://doi.org/10.1063/1.528551.

[54] A. R. Forsyth. "Note on the central differential equation in the relativity theory of gravitation". In: *Proceedings of the Royal Society of London A: Mathematical, Physical and Engineering Sciences* 97.682 (1920), pp. 145–151. DOI: 10.1098/rspa.1920.0019.

[55] L. Fousse et al. "MPFR: A Multiple-Precision Binary Floating-Point Library With Correct Rounding". In: *ACM Transactions on Mathematical Software (TOMS)* 33 (2007). DOI: 10.1145/1236463.1236468.

[56] Francisco Frutos-Alfaro, Hernando Quevedo, and Pedro A. Sanchez. "Comparison of vacuum static quadrupolar metrics". In: *Royal Society Open Science* 5.5 (2018). DOI: 10.1098/rsos.170826. URL: http://rsos.royalsocietypublishing.org/content/5/5/170826.

[57] Francisco Frutos-Alfaro and Michael Soffel. "On relativistic multipole moments of stationary space–times". In: *Royal Society Open Science* 5.7 (2018). DOI: 10.1098/rsos.180640. URL: http://rsos.royalsocietypublishing.org/content/5/7/180640.

[58] H. Fuchs. "Conservation laws for test particles with internal structure". In: *Annalen der Physik* 34 (1977), p. 159.

[59] H. Fuchs. "Deviation of circular geodesics in static spherically symmetric space-times". In: *Astron. Nachr.* 311 (1990), p. 271.

[60] H. Fuchs. "Solutions of the Equations of Geodesic Deviation for Static Spherical Symmetric Space-times". In: *Annalen der Physik* 40 (1983), p. 231.

[61] T. Fukushima. "Time ephemeris". In: *Astron Astrophys* 294 (1995), pp. 895–906. URL: http://adsabs.harvard.edu/abs/1995A%26A...294..895F.

[62] Carl Friedrich Gauss. *Bestimmung des Breitenunterschiedes zwischen den Sternwarten von Göttingen und Altona: durch Beobachtungen am Ramsdenschen Zenithsector*. Bei Vandenhoeck und Ruprecht, Göttingen, 1828.

[63] Robert P. Geroch. "Multipole Moments. II. Curved space". In: *J. Math. Phys.* 11.8 (1970), pp. 2580–2588. DOI: 10.1063/1.1665427. URL: http://dx.doi.org/10.1063/1.1665427.

[64] C. Goddi et al. "BlackHoleCam: Fundamental physics of the galactic center". In: *International Journal of Modern Physics D* 26.02 (2017), p. 1730001. DOI: 10.1142/S0218271817300014. URL: https://doi.org/10.1142/S0218271817300014.

[65] John M. Goodkind. "The superconducting gravimeter". In: *Review of Scientific Instruments* 70.11 (1999), pp. 4131–4152. DOI: 10.1063/1.1150092. URL: https://doi.org/10.1063/1.1150092.

[66] *Gravity Recovery and Climate Experiment GRACE*. electronic. Accessed: 2018-11-11. URL: {https://grace.jpl.nasa.gov}.

[67] *Gravity Recovery and Climate Experiment GRACE*. electronic. Accessed: 2018-11-11. URL: {https://grace.jpl.nasa.gov/mission/grace-fo/}.

[68] Christian Grebing et al. "Realization of a timescale with an accurate optical lattice clock". In: *Optica* 3.6 (2016), pp. 563–569. DOI: 10.1364/OPTICA.3.000563.

[69] P. J. Greenberg. "The equation of geodesic deviation in Newtonian theory and the oblateness of the earth". In: *Nuovo Cimento* 24 B (1974), p. 272. DOI: 10.1007/BF02725960.

[70] *Greenland ice mass loss*. electronic. Accessed: 2018-11-11. URL: {https://gracefo.jpl.nasa.gov/resources/33/greenland-ice-loss-2002-2016/}.

[71] Arne Grenzebach, Volker Perlick, and Claus Lämmerzahl. "Photon regions and shadows of Kerr-Newman-NUT black holes with a cosmological constant". In: *Phys. Rev. D* 89 (12 2014), p. 124004. DOI: 10.1103/PhysRevD.89.124004. URL: https://link.aps.org/doi/10.1103/PhysRevD.89.124004.

[72] F. Gronwald et al. "Gravity Probe C(lock) - Probing the gravitomagnetic field of the Earth by means of a clock experiment". In: *ArXiv General Relativity and Quantum Cosmology e-prints* (1997). eprint: gr-qc/9712054.

[73] E. Groten. "Fundamental Parameters and Current (2004) Best Estimates of the Parameters of Common Relevance to Astronomy, Geodesy, and Geodynamics by Erwin Groten, IPGD, Darmstadt". In: *Journal of Geodesy* 77.10 (2004), pp. 724–797. ISSN: 1432-1394. DOI: 10.1007/s00190-003-0373-y. URL: https://doi.org/10.1007/s00190-003-0373-y.

[74] Erwin Groten. "Report of Special Commission 3 of IAG". In: *International Astronomical Union Colloquium* 180 (2000), 337–352. DOI: 10.1017/S0252921100000488.

[75] J. Grotti et al. "Geodesy and metrology with a transportable optical clock". In: *Nature Physics* 14 (May 2018), pp. 437–441. DOI: 10.1038/s41567-017-0042-3.

[76] J. Guéna et al. "First international comparison of fountain primary frequency standards via a long distance optical fiber link". In: *Metrologia* 54.3 (2017), p. 348. DOI: 10.1088/1681-7575/aa65fe. URL: http://stacks.iop.org/0026-1394/54/i=3/a=348.

[77] Yekta Gürsel. "Multipole moments for stationary systems: The equivalence of the Geroch-Hansen formulation and the Thorne formulation". In: *General Relativity and Gravitation* 15.8 (1983), pp. 737–754. ISSN: 1572-9532. DOI: 10.1007/BF01031881. URL: https://doi.org/10.1007/BF01031881.

[78] Eva Hackmann and Claus Lämmerzahl. "Complete Analytic Solution of the Geodesic Equation in Schwarzschild (Anti-)de Sitter Spacetimes". In: *Phys. Rev. Let.* 100 (2008), p. 171101. DOI: 10.1103/PhysRevLett.100.171101.

[79] Eva Hackmann and Claus Lämmerzahl. "Generalized gravitomagnetic clock effect". In: *Phys. Rev. D* 90.4 (2014), p. 044059. DOI: 10.1103/PhysRevD.90.044059. URL: http://link.aps.org/doi/10.1103/PhysRevD.90.044059.

[80] Eva Hackmann and Claus Lämmerzahl. "Geodesic equation in Schwarzschild-(anti-)de Sitter space-times: Analytical solutions and applications". In: *Phys. Rev. D* 78, 024035 (2008), p. 024035. DOI: 10.1103/PhysRevD.78.024035.

[81] Eva Hackmann and Claus Lämmerzahl. "Observables for bound orbital motion in axially symmetric space-times". In: *Phys. Rev. D* 85 (4 2012), p. 044049. DOI: 10.1103/PhysRevD.85.044049. URL: https://link.aps.org/doi/10.1103/PhysRevD.85.044049.

[82] Eva Hackmann et al. "Analytic solutions of the geodesic equation in axially symmetric space–times". In: *Europhys. Lett.* 88 (2009), p. 30008.

[83] Eva Hackmann et al. "Analytical solution of the geodesic equation in Kerr-(anti-) de Sitter space-times". In: *Phys. Rev. D* 81 (4 2010), p. 044020. DOI: 10.1103/PhysRevD.81.044020. URL: https://link.aps.org/doi/10.1103/PhysRevD.81.044020.

[84] Y. Hagihara. "Theory of the Relativistic Trajectories in a Gravitational Field of Schwarzschild". In: *Japanese Journal of Astronomy and Geophysics* 8 (1930), p. 67.

[85] R. O. Hansen. "Multipole moments of stationary space-times". In: *J. Math. Phys.* 15.1 (1974), pp. 46–52. DOI: 10.1063/1.1666501. URL: http://dx.doi.org/10.1063/1.1666501.

[86] Hasse, Wolfgang and Perlick, Volker. "Geometrical and kinematical characterization of parallax-free world models". In: *J. Math. Phys.* 29.9 (1988), pp. 2064–2068. DOI: 10.1063/1.527863. URL: http://dx.doi.org/10.1063/1.527863.

[87] W.M. Haynes. *CRC Handbook of Chemistry and Physics*. CRC Press, 2016. ISBN: 9781498754293.

[88] F.R. Helmert. *Die mathematischen und physikalischen Theorien der höheren Geodäsie: Die mathematischen Theorien*. Bd. 1. Teubner, Leipzig, 1880.

[89] L. Herrera and J. L. Hernández Pastora. "Measuring multipole moments of Weyl metrics by means of gyroscopes". In: *Journal of Mathematical Physics* 41.11 (2000), pp. 7544–7555. DOI: 10.1063/1.1319517. eprint: https://doi.org/10.1063/1.1319517. URL: https://doi.org/10.1063/1.1319517.

[90] Sven Herrmann et al. "Test of the Gravitational Redshift with Galileo Satellites in an Eccentric Orbit". In: *Phys. Rev. Lett.* 121 (23 2018), p. 231102. DOI: 10.1103/PhysRevLett.121.231102. URL: https://link.aps.org/doi/10.1103/PhysRevLett.121.231102.

[91] M. P. Heß et al. "The ACES mission: System development and test status". In: *Acta Astronautica* 69 (Dec. 2011), pp. 929–938. DOI: 10.1016/j.actaastro.2011.07.002.

[92] M.P. Heß et al. "The ACES mission: System development and test status". In: *Acta Astronautica* 69.11 (2011), pp. 929–938. ISSN: 0094-5765. DOI: https://doi.org/10.1016/j.actaastro.2011.07.002. URL: http://www.sciencedirect.com/science/article/pii/S0094576511001913.

[93] J. Hinderer, D. Crossley, and R.J. Warburton. "3.04 - Gravimetric Methods – Superconducting Gravity Meters". In: *Treatise on Geophysics*. Ed. by Gerald Schubert. Amsterdam: Elsevier, 2007, pp. 65 –122. ISBN: 978-0-444-52748-6. DOI: https://doi.org/10.1016/B978-044452748-6.00172-3. URL: http://www.sciencedirect.com/science/article/pii/B9780444527486001723.

[94] C. Hoenselaers and Z. Perjes. "Multipole moments of axisymmetric electrovacuum spacetimes". In: *Classical and Quantum Gravity* 7.10 (1990), p. 1819. DOI: 10.1088/0264-9381/7/10/012. URL: http://stacks.iop.org/0264-9381/7/i=10/a=012.

[95] B. Hofmann-Wellenhof and H. Moritz. *Physical Geodesy*. Springer Wien, 2005. ISBN: 9783211235843.

[96] *IAU (1991) Resolutions of the International Astronomical Union, XXI General Assembly, Buenos Aires, Argentina.* URL: https://www.iau.org/administration/resolutions/general_assemblies/.

[97] *IAU (2000) Resolutions of the International Astronomical Union, XXIV General Assembly, Manchester, United Kingdom.* URL: https://www.iau.org/administration/resolutions/general_assemblies/.

[98] *ICGEM calculation service.* URL: http://icgem.gfz-potsdam.de/vis3d/longtime.

[99] Johannes Ihde et al. "Definition and Proposed Realization of the International Height Reference System (IHRS)". In: *Surveys in Geophysics* 38.3 (2017), pp. 549–570. ISSN: 1573-0956. DOI: 10.1007/s10712-017-9409-3. URL: https://doi.org/10.1007/s10712-017-9409-3.

[100] National Imagery and Mapping Agency. *Department of Defense World Geodetic System 1984 Its Definition and Relationships with Local Geodetic Systems.* Tech. rep. NIMA TR 8350.2. 2004.

[101] *International Timescales with Optical Clocks (ITOC).* electronic. Accessed: 2018-11-11. URL: http://projects.npl.co.uk/itoc/.

[102] Christopher Jekeli. *Geometric reference systems in geodesy.* Division of Geodesy and Geospatial Science, School of Earth Sciences, Ohio State University 25, 2006.

[103] George H. Kaplan. *The IAU Resolutions on Astronomical Reference Systems, Time Scales, and Earth Rotation Models - Explanation and Implementation.* U.S. Naval Observatory, CIRCULAR NO. 179, Washington, D.C. 2005. URL: https://arxiv.org/abs/astro-ph/0602086.

[104] Kermack, W. O. and McCrea, W. H. and Whittaker, E. T. "On Properties of Null Geodesics, and their Application to the Theory of Radiation". In: *Proc. R. Soc. Edinburgh* 53 (1934), pp. 31–47. DOI: 10.1017/S0370164600015479.

[105] R. Kerner, J. W. van Holten, and R. Colistete Jr. "Relativistic epicycles: another approach to geodesic deviations". In: *Class. Quant. Grav.* 18 (2001), p. 4725. DOI: 10.1088/0264-9381/18/22/302.

[106] Roy P. Kerr. "Discovering the Kerr and Kerr-Schild metrics". In: *ArXiv e-prints* (June 2007). arXiv: 0706.1109 [gr-qc].

[107] Roy P. Kerr. "Gravitational Field of a Spinning Mass as an Example of Algebraically Special Metrics". In: *Phys. Rev. Lett.* 11 (5 1963), pp. 237–238. DOI: 10.1103/PhysRevLett.11.237. URL: https://link.aps.org/doi/10.1103/PhysRevLett.11.237.

[108] S. A. Klioner, P. K. Seidelmann, and M. H. Soffel, eds. *Relativity in Fundamental Astronomy: Dynamics, Reference Frames, and Data Analysis.* Vol. 261. IAU Symposium. 2010.

[109] Sergei A. Klioner and Michael H. Soffel. "Relativistic celestial mechanics with PPN parameters". In: *Phys. Rev. D* 62 (2 2000), p. 024019. DOI: 10.1103/PhysRevD.62.024019. URL: https://link.aps.org/doi/10.1103/PhysRevD.62.024019.

[110] G. Koekoek and J. W. van Holten. "Epicycles and Poincaré resonances in general relativity". In: *Phys. Rev. D* 83 (2011), p. 064041. DOI: 10.1103/PhysRevD.83.064041. URL: https://link.aps.org/doi/10.1103/PhysRevD.83.064041.

[111] R. Koop. *Global gravity field modelling using satellite gravity gradiometry*. Nr. 38. Delft, The Netherlands: Nederlandse Commissie voor Geodesie, 1993. ISBN: 9789061322467.

[112] Sergei M. Kopeikin, Michael Efroimsky, and George Kaplan. *Relativistic Celestial Mechanics of the Solar System*. Wiley-VCH, Weinheim, Germany, 2011. ISBN: 9783527634569. DOI: 10.1002/9783527634569.fmatter. URL: http://dx.doi.org/10.1002/9783527634569.fmatter.

[113] Sergei M. Kopeikin, Wenbiao Han, and Elena Mazurova. "Post-Newtonian reference ellipsoid for relativistic geodesy". In: *Phys. Rev. D* 93 (4 2016), p. 044069. DOI: 10.1103/PhysRevD.93.044069. URL: http://link.aps.org/doi/10.1103/PhysRevD.93.044069.

[114] Sergei M. Kopeikin, Elena M. Mazurova, and Alexander P. Karpik. "Towards an exact relativistic theory of Earth's geoid undulation". In: *Phys. Lett. A* 379.26-27 (2015), pp. 1555–1562. URL: https://doi.org/10.1016/j.physleta.2015.02.046.

[115] Sergei M. Kopeikin, Igor Vlasov, and Wen-Biao Han. "Normal gravity field in relativistic geodesy". In: *Phys. Rev. D* 97 (4 2018), p. 045020. DOI: 10.1103/PhysRevD.97.045020. URL: https://link.aps.org/doi/10.1103/PhysRevD.97.045020.

[116] Sergei M. Kopeikin et al. "Chronometric measurement of orthometric height differences by means of atomic clocks". In: *Gravitation and Cosmology* 22.3 (2016), pp. 234–244. ISSN: 1995-0721. DOI: 10.1134/S0202289316030099. URL: https://doi.org/10.1134/S0202289316030099.

[117] F.G. Lemoine et al. *The development of the joint NASA GSFC and the National Imagery and Mapping Agency (NIMA) Geopotential Model EGM96*. English. National Aeronautics and Space Administration, Goddard Space Flight Center, 1998, 575 p. in various pagings : URL: https://nla.gov.au/nla.cat-vn4135167.

[118] Christian Lisdat et al. "A clock network for geodesy and fundamental science". In: *Nature Communications* 7, 12443 (Aug. 2016), p. 12443. DOI: 10.1038/ncomms12443.

[119] Maike List et al. "Modelling of Solar Radiation Pressure Effects: Parameter Analysis for the MICROSCOPE Mission". In: *International Journal of Aerospace Engineering* 2015 (2015), p. 14. DOI: 10.1155/2015/928206.

[120] J. B. Listing. "Über unsere jetzige Kenntnis der Gestalt und Grösse der Erde". In: *Nachr. d. Kgl. Gesellsch. d. Wiss. der Georg-August-Univ.* (1873), pp. 33–98.

[121] D.A. Litvinov et al. "Probing the gravitational redshift with an Earth-orbiting satellite". In: *Physics Letters A* 382.33 (2018). Special Issue in memory of Professor V.B. Braginsky, pp. 2192 –2198. ISSN: 0375-9601. DOI: 10.1016/j.physleta.2017.09.014. URL: http://www.sciencedirect.com/science/article/pii/S0375960117304553.

[122] Bryant D. Loomis, R. S. Nerem, and S. B. Luthcke. "Simulation study of a follow-on gravity mission to GRACE". In: *J. Geod.* 86.5 (2012), pp. 319–335. DOI: 10.1007/s00190-011-0521-8. URL: http://dx.doi.org/10.1007/s00190-011-0521-8.

[123] C. Ma and M. (eds.) Feissel. *Definition and realization of the International Celestial Reference System by VLBI astrometry of extragalactic objects*. Tech. rep. IERS Technical Note No. 23. International Earth Rotation and Reference Systems Service (IERS), 1997. URL: https://www.iers.org/IERS/EN/Publications/TechnicalNotes/tn23.html.

[124] T. Mayer-Gürr et al. *The combined satellite gravity field model GOCO05s*. Presentation at EGU 2015, Vienna, April 2015. 2015.

[125] Dennis D. McCarthy. *IERS Conventions (1996). (IERS Technical Note ; 21) Paris: Central Bureau of IERS - Observatoire de Paris, 1996. [ii], ii, 97 p.* 1996. URL: https://www.iers.org/IERS/EN/Publications/TechnicalNotes/tn21.html.

[126] Tanja E. Mehlstäubler et al. "Atomic clocks for geodesy". In: *Reports on Progress in Physics* 81.6 (2018), p. 064401. DOI: 10.1088/1361-6633/aab409. URL: http://stacks.iop.org/0034-4885/81/i=6/a=064401.

[127] Charles W. Misner, Kip S. Thorne, and John A. Wheeler. *Gravitation*. San Francisco : W. H. Freeman, 1973. ISBN: 0716703343.

[128] H. Moritz. "Geodetic reference system 1980". In: *Bulletin Geodesique* 54 (Sept. 1980), pp. 395–405. DOI: 10.1007/BF02521480.

[129] Jürgen Müller, Michael H Soffel, and Sergei A Klioner. "Geodesy and relativity". In: *J. Geod.* 82.3 (2008), pp. 133–145. DOI: 10.1007/s00190-007-0168-7. URL: http://dx.doi.org/10.1007/s00190-007-0168-7.

[130] Jürgen Müller et al. "High Performance Clocks and Gravity Field Determination". In: *Space Science Reviews* 214.1 (2017), p. 5. ISSN: 1572-9672. DOI: 10.1007/s11214-017-0431-z. URL: https://doi.org/10.1007/s11214-017-0431-z.

[131] Isaac Newton. *Philosophiae naturalis principia mathematica*. J. Societatis Regiae ac Typis J. Streater, 1687.

[132] A. Nothnagel et al. "Space-Time Reference Systems for Monitoring Global Change and for Precise Navigation". In: *Mitteilungen des Bundesamtes für Kartographie und Geodäsie* 44 (2010).

[133] Yuri . N. Obukhov and Dirk Puetzfeld. "Multipolar test body equations of motion in generalized gravity theories". In: *"Equations of Motion in Relativistic Gravity", D. Puetzfeld et. al. (eds.), Fundamental theories of Physics, Springer* 179 (2015), p. 67.

[134] Marius Oltean et al. "Geoids in general relativity: geoid quasilocal frames". In: *Classical Quantum Grav.* 33.10 (2016). URL: http://stacks.iop.org/0264-9381/33/i=10/a=105001.

[135] R. Pail et al. "Combined satellite gravity field model GOCO01S derived from GOCE and GRACE". In: *Geophysical Research Letters* 37.20 (2010). DOI: 10.1029/2010GL044906. URL: https://agupubs.onlinelibrary.wiley.com/doi/abs/10.1029/2010GL044906.

[136] V. Perlick. *Ray Optics, Fermat's Principle, and Applications to General Relativity*. Vol. 61. Lecture Notes in Physics Monographs. Springer, 2000. ISBN: 9783540668985.

[137] Volker Perlick. "Gravitational Lensing from a Spacetime Perspective". In: *Living Reviews in Relativity* 7.1 (2004), p. 9. ISSN: 1433-8351. DOI: 10.12942/lrr-2004-9. URL: https://doi.org/10.12942/lrr-2004-9.

[138] Volker Perlick and Oleg Yu. Tsupko. "Light propagation in a plasma on Kerr spacetime: Separation of the Hamilton-Jacobi equation and calculation of the shadow". In: *Phys. Rev. D* 95 (10 2017), p. 104003. DOI: 10.1103/PhysRevD.95.104003. URL: https://link.aps.org/doi/10.1103/PhysRevD.95.104003.

[139] Volker Perlick, Oleg Yu. Tsupko, and Gennady S. Bisnovatyi-Kogan. "Influence of a plasma on the shadow of a spherically symmetric black hole". In: *Phys. Rev. D* 92 (10 2015), p. 104031. DOI: 10.1103/PhysRevD.92.104031. URL: https://link.aps.org/doi/10.1103/PhysRevD.92.104031.

[140] Perlick, Volker. "Characterization of standard clocks by means of light rays and freely falling particles". In: *Gen. Relativ. Gravit.* 19.11 (1987), pp. 1059–1073. DOI: 10.1007/BF00759142. URL: http://dx.doi.org/10.1007/BF00759142.

[141] Perlick, Volker. "On redshift and parallaxes in general relativistic kinematical world models". In: *J. Math. Phys.* 31.8 (1990), pp. 1962–1971. DOI: 10.1063/1.528645. URL: http://dx.doi.org/10.1063/1.528645.

[142] Gérard Petit and Brian Luzum. *IERS Conventions*. Tech. rep. 36. International Earth Rotation and Reference Systems Service (IERS), 2010.

[143] D. Philipp, D. Puetzfeld, and C. Lämmerzahl. "On the Applicability of the Geodesic Deviation Equation in General Relativity". In: *Relativistic Geodesy,*

Fundamental Theories of Physics. Ed. by D. Puetzfeld and C. Lämmerzahl. 2019, p. 419. DOI: 10.1007/978-3-030-11500-5_13.

[144] Dennis Philipp, Dirk Puetzfeld, and Claus Lämmerzahl. "On geodesic deviation in static spherically symmetric situations". In: *The Fourteenth Marcel Grossmann Meeting*, pp. 3731–3736. DOI: 10.1142/9789813226609_0489. URL: https://www.worldscientific.com/doi/abs/10.1142/9789813226609_0489.

[145] Dennis Philipp et al. "Definition of the relativistic geoid in terms of isochronometric surfaces". In: *Phys. Rev. D* 95 (10 2017), p. 104037. DOI: 10.1103/PhysRevD.95.104037. URL: https://link.aps.org/doi/10.1103/PhysRevD.95.104037.

[146] Dennis Philipp et al. "Modeling approaches for precise relativistic orbits: Analytical, Lie-series, and pN approximation". In: *Advances in Space Research* 62.4 (2018), pp. 921 –934. ISSN: 0273-1177. DOI: 10.1016/j.asr.2018.05.020. URL: http://www.sciencedirect.com/science/article/pii/S0273117718304162.

[147] Dennis Philipp et al. "On geodesic deviation in Schwarzschild spacetime". In: *2015 IEEE Metrology for Aerospace (MetroAeroSpace)*. 2015, pp. 198–203. DOI: 10.1109/MetroAeroSpace.2015.7180653.

[148] Dennis Philipp et al. "The relativistic geoid". In: *2017 IEEE International Workshop on Metrology for AeroSpace (MetroAeroSpace)*. 2017, pp. 114–119. DOI: 10.1109/MetroAeroSpace.2017.7999549.

[149] E. V. Pitjeva and N. P. Pitjev. "Relativistic effects and dark matter in the Solar system from observations of planets and spacecraft". In: *Monthly Notices of the Royal Astronomical Society* 432.4 (2013), pp. 3431–3437. DOI: 10.1093/mnras/stt695. URL: http://dx.doi.org/10.1093/mnras/stt695.

[150] E. Poisson and C. M. Will. *Gravity: Newtonian, Post-Newtonian, Relativistic*. Cambridge University Press, 2014. ISBN: 9781107032866.

[151] R. V. Pound and G. A. Rebka. "Apparent Weight of Photons". In: *Phys. Rev. Lett.* 4 (7 1960), pp. 337–341. DOI: 10.1103/PhysRevLett.4.337. URL: https://link.aps.org/doi/10.1103/PhysRevLett.4.337.

[152] Dirk Puetzfeld, Claus Lämmerzahl, and Bernard Schutz. *Equations of Motion in Relativistic Gravity*. Vol. 179. Fundamental Theories of Physics. Springer International Publishing, 2015. ISBN: 9783319183350. DOI: 10.1007/978-3-319-18335-0.

[153] Dirk Puetzfeld and Yuri N. Obukhov. "Generalized deviation equation and determination of the curvature in general relativity". In: *Phys. Rev. D* 93 (4 2016), p. 044073. DOI: 10.1103/PhysRevD.93.044073. URL: https://link.aps.org/doi/10.1103/PhysRevD.93.044073.

[154] Dirk Puetzfeld, Yuri N. Obukhov, and Claus Lämmerzahl. "Gravitational clock compass in general relativity". In: *Phys. Rev. D* 98 (2 2018), p. 024032. DOI: 10.1103/PhysRevD.98.024032. URL: https://link.aps.org/doi/10.1103/PhysRevD.98.024032.

[155] Hernando Quevedo. "Class of stationary axisymmetric solutions of Einstein's equations in empty space". In: *Phys. Rev. D* 33.2 (1986), pp. 324–327. DOI: 10.1103/PhysRevD.33.324. URL: http://link.aps.org/doi/10.1103/PhysRevD.33.324.

[156] Hernando Quevedo. "General static axisymmetric solution of Einstein's vacuum field equations in prolate spheroidal coordinates". In: *Phys. Rev. D* 39 (1989), pp. 2904–2911. DOI: 10.1103/PhysRevD.39.2904. URL: http://link.aps.org/doi/10.1103/PhysRevD.39.2904.

[157] Hernando Quevedo. "Multipole Moments in General-Relativity - Static and Stationary Vacuum Solutions". In: *Fortschr. Phys.* 38.10 (1990), pp. 733–840. DOI: 10.1002/prop.2190381002. URL: http://dx.doi.org/10.1002/prop.2190381002.

[158] Hernando Quevedo. "Quadrupolar metrics". In: (2016). arXiv: 1606.09361 [gr-qc].

[159] Hernando Quevedo and Bahram Mashhoon. "Exterior gravitational field of a rotating deformed mass". In: *Physics Letters A* 109.1 (1985), pp. 13 –18. ISSN: 0375-9601. DOI: https://doi.org/10.1016/0375-9601(85)90381-0. URL: http://www.sciencedirect.com/science/article/pii/0375960185903810.

[160] Hernando Quevedo, Saken Toktarbay, and Aimuratov Yerlan. "Quadrupolar gravitational fields described by the q-metric". In: *Int. J. Math. Phys.* 3.133 (2012).

[161] Richard H. Rapp. *Geometric geodesy*. Vol. 1. Division of Geodesy and Geospatial Science, School of Earth Sciences, Ohio State University 25, 1991.

[162] Sebastian M. F. Raupach, Andreas Koczwara, and Gesine Grosche. "Brillouin amplification supports 10^{-20} uncertainty in optical frequency transfer over 1400 km of underground fiber". In: *Phys. Rev. A* 92 (2 2015), p. 021801. DOI: 10.1103/PhysRevA.92.021801. URL: https://link.aps.org/doi/10.1103/PhysRevA.92.021801.

[163] *Relativistic Geodesy and Gravimetry with Quantum Sensors (geo-Q)*. electronic. Accessed: 2018-11-11. URL: https://www.geoq.uni-hannover.de.

[164] Benny Rievers, Maike List, and Stefanie Bremer. "Advanced Thermal Radiation Pressure modeling and its benefits for the MICROSCOPE mission". In: *Adv Astr Sci* 158 (2016), pp. 2997–3012.

[165] W. Rindler. *Relativity: Special, General, and Cosmological*. OUP Oxford, 2006. ISBN: 9780198567318.

[166] R. Rummel. "Gravity And Topography Of Moon And Planets". In: *Future Satellite Gravimetry and Earth Dynamics*. Ed. by Jakob Flury and Reiner Rummel.

New York, NY: Springer New York, 2005, pp. 103–111. ISBN: 978-0-387-33185-0. DOI: 10.1007/0-387-33185-9_9. URL: https://doi.org/10.1007/0-387-33185-9_9.

[167] G. Salzman and A. H. Taub. "Born-Type Rigid Motion in Relativity". In: *Phys. Rev.* 95.6 (1954), pp. 1659–1669. DOI: 10.1103/PhysRev.95.1659. URL: http://link.aps.org/doi/10.1103/PhysRev.95.1659.

[168] L. Sánchez et al. "A conventional value for the geoid reference potential W0". In: *Journal of Geodesy* 90.9 (2016), pp. 815–835. ISSN: 1432-1394. DOI: 10.1007/s00190-016-0913-x. URL: https://doi.org/10.1007/s00190-016-0913-x.

[169] L. I. Schiff. "On Experimental Tests of the General Theory of Relativity". In: *American Journal of Physics* 28.4 (1960), pp. 340–343. DOI: 10.1119/1.1935800. URL: https://doi.org/10.1119/1.1935800.

[170] B.F. Schutz. *A First Course in General Relativity*. Series in physics. Cambridge University Press, 1985. ISBN: 9780521277037.

[171] Karl Schwarzschild. "Über das Gravitationsfeld eines Massenpunktes nach der Einsteinschen Theorie". In: *Sitzungsber.Preuss.Akad.Wiss.Berlin (Math.Phys.)* (1916), pp. 189–196.

[172] Irwin I. Shapiro. "Fourth Test of General Relativity". In: *Phys. Rev. Lett.* 13 (26 1964), pp. 789–791. DOI: 10.1103/PhysRevLett.13.789. URL: https://link.aps.org/doi/10.1103/PhysRevLett.13.789.

[173] Wenbin Shen and Helmut Moritz. "On the separation of gravitation and inertia and the determination of the relativistic gravity field in the case of free motion". In: *Journal of Geodesy* 70.10 (1996), pp. 633–644. ISSN: 1432-1394. DOI: 10.1007/BF00868225. URL: https://doi.org/10.1007/BF00868225.

[174] Wenbin Shen et al. "Determination of the geopotential and orthometric height based on frequency shift equation". In: *Natural Science* 03.05 (2011), pp. 388–396. DOI: 10.4236/ns.2011.35052.

[175] M. F. Shirokov. "On one new effect of the Einsteinian theory of gravitation". In: *Gen. Rel. Grav.* 4 (1973), p. 131.

[176] Walter Simon and Robert Beig. "The multipole structure of stationary space-times". In: *Journal of Mathematical Physics* 24.5 (1983), pp. 1163–1171. DOI: 10.1063/1.525846. URL: https://aip.scitation.org/doi/abs/10.1063/1.525846.

[177] W. de Sitter. "On Einstein's Theory of Gravitation and its Astronomical Consequences. Second Paper." In: *Monthly Notices of the Royal Astronomical Society* 77.2 (1916), pp. 155–184. DOI: 10.1093/mnras/77.2.155. URL: http://dx.doi.org/10.1093/mnras/77.2.155.

[178] M. Soffel et al. "The IAU 2000 Resolutions for Astrometry, Celestial Mechanics, and Metrology in the Relativistic Framework: Explanatory Supplement". In:

Astron. J. 126 (2003), p. 2687. URL: http://stacks.iop.org/1538-3881/126/i=6/a=2687.

[179] M. H. Soffel. *Relativity in Astrometry, Celestial Mechanics and Geodesy*. Astronomy and Astrophysics Library. Berlin Heidelberg: Springer, 1989. ISBN: 9783642734069.

[180] Michael Soffel and F. Frutos. "On the usefulness of relativistic space-times for the description of the Earth's gravitational field". In: *J. Geod.* 90.12 (2016), pp. 1345–1357. DOI: 10.1007/s00190-016-0927-4. URL: http://dx.doi.org/10.1007/s00190-016-0927-4.

[181] Michael H. Soffel et al. "Relativistic theory of gravimetric measurements and definition of the geoid". In: *Manuscripta Geodaetica* 13 (1988), pp. 143–146.

[182] Hans Stephani et al. *Exact Solutions of Einstein's Field Equations*. Second. Cambridge University Press, Cambridge, England, 2003.

[183] Straumann, Norbert. *General relativity and relativistic astrophysics*. Springer, Berlin, 1984. ISBN: 978-3-642-84439-3.

[184] J.L. Synge. *Relativity: the general theory*. Series in physics. North-Holland, 1960.

[185] T. Takano et al. "Geopotential measurements with synchronously linked optical lattice clocks". In: *Nature Photonics* 10 (2016), pp. 662–666. DOI: 10.1038/nphoton.2016.159.

[186] Byron D. Tapley et al. "GRACE Measurements of Mass Variability in the Earth System". In: *Science* 305.5683 (2004), pp. 503–505. DOI: 10.1126/science.1099192.

[187] Kip S. Thorne. "Multipole expansions of gravitational radiation". In: *Rev. Mod. Phys.* 52 (2 1980), pp. 299–339. DOI: 10.1103/RevModPhys.52.299. URL: https://link.aps.org/doi/10.1103/RevModPhys.52.299.

[188] Wolfgang Torge and Jürgen Müller. *Geodesy*. Berlin: De Gruyter, 2012. ISBN: 978-3110207187.

[189] P. Tregoning and C. Rizos. *Dynamic Planet: Monitoring and Understanding a Dynamic Planet with Geodetic and Oceanographic Tools*. International Association of Geodesy Symposia. Springer Berlin Heidelberg, 2008. ISBN: 9783540493501.

[190] P. Vanicek and N.T. Christou. *Geoid and its Geophysical Interpretations*. CRC Press, 1993. ISBN: 9780849342271.

[191] R. F. C. Vessot. "Clocks and spaceborne tests of relativistic gravitation". In: *Advances in Space Research* 9 (1989), pp. 21–28. DOI: 10.1016/0273-1177(89)90004-5.

[192] R. F. C. Vessot and M. W. Levine. "A test of the equivalence principle using a space-borne clock". In: *General Relativity and Gravitation* 10.3 (1979), pp. 181–204. ISSN: 1572-9532. DOI: 10.1007/BF00759854. URL: https://doi.org/10.1007/BF00759854.

[193] R. F. C. Vessot et al. "Test of Relativistic Gravitation with a Space-Borne Hydrogen Maser". In: *Phys. Rev. Lett.* 45 (26 1980), pp. 2081–2084. DOI: 10.1103/PhysRevLett.45.2081. URL: https://link.aps.org/doi/10.1103/PhysRevLett.45.2081.

[194] B. H. Voorhees. "Static Axially Symmetric Gravitational Fields". In: *Phys. Rev. D* 2 (10 1970), pp. 2119–2122. DOI: 10.1103/PhysRevD.2.2119. URL: http://link.aps.org/doi/10.1103/PhysRevD.2.2119.

[195] R.M. Wald. *General Relativity*. University of Chicago Press, 2010. ISBN: 9780-226-870-373.

[196] Hermann Weyl. "Zur Gravitationstheorie". In: *Ann. Phys.* 359.18 (1917), pp. 117–145. DOI: 10.1002/andp.19173591804. URL: http://dx.doi.org/10.1002/andp.19173591804.

[197] M. A. Wieczorek. "10.05 - Gravity and Topography of the Terrestrial Planets". In: *Treatise on Geophysics*. Ed. by Gerald Schubert. Amsterdam: Elsevier, 2007, pp. 165 –206. ISBN: 978-0-444-52748-6. DOI: 10.1016/B978-044452748-6.00156-5. URL: http://www.sciencedirect.com/science/article/pii/B9780444527486001565.

[198] Bruce A. Wielicki et al. "Clouds and the Earth's Radiant Energy System (CERES): An Earth Observing System Experiment". In: *Bulletin of the American Meteorological Society* 77.5 (1996), pp. 853–868. URL: https://doi.org/10.1175/1520-0477(1996)077<0853:CATERE>2.0.CO;2.

[199] C. M. Will. *Theory and Experiment in Gravitational Physics*. Cambridge University Press, 1993. ISBN: 9780521439732.

[200] Clifford M. Will. "The Confrontation between General Relativity and Experiment". In: *Living Reviews in Relativity* 17.1 (2014), p. 4. ISSN: 1433-8351. DOI: 10.12942/lrr-2014-4. URL: https://doi.org/10.12942/lrr-2014-4.

[201] Florian Wöske et al. "Development of a high precision simulation tool for gravity recovery missions like GRACE". In: *Adv Astr Sci* 158 (2016), pp. 2445–2457.

[202] John H. Young and C. Alton Coulter. "Exact Metric for a Nonrotating Mass with a Quadrupole Moment". In: *Phys. Rev.* 184 (5 1969), pp. 1313–1315. DOI: 10.1103/PhysRev.184.1313. URL: http://link.aps.org/doi/10.1103/PhysRev.184.1313.

[203] D. M. Zipoy. "Topology of Some Spheroidal Metrics". In: *J. Math. Phys.* 7.6 (1966), pp. 1137–1143. DOI: 10.1063/1.1705005. URL: http://dx.doi.org/10.1063/1.1705005.

[204] Sven Zschocke. "Light propagation in the gravitational field of N arbitrarily moving bodies in the 1.5PN approximation for high-precision astrometry". In: *Phys. Rev. D* 93 (10 2016), p. 103010. DOI: 10.1103/PhysRevD.93.103010. URL: https://link.aps.org/doi/10.1103/PhysRevD.93.103010.